The fate of engineered nanomaterials in sediments and their route to bioaccumulation

Richard Kynaston Cross

University of Exeter

Submitted by Richard Kynaston Cross, to the University of Exeter as a thesis for the degree of Doctor of Philosophy in Biological Sciences, September 2017

This thesis is available for Library use on the understanding that it is copyright material and that no quotation from the thesis may be published without proper acknowledgement.

I certify that all material in this thesis which is not my own work has been identified and that no material has previously been submitted and approved for the award of a degree by this or any other University.

(Signature) …………………………………………

Abstract

The production of engineered nanomaterials is an emerging and rapidly expanding industry. It exploits the capacity for materials to be manufactured to present particular properties distinct from the bulk material, through tailoring of the particle size and surface functionality. This ability to fine tune particle properties at the nanoscale is responsible for the explosion in uses of engineered nanomaterials in industries as diverse as cosmetics and medicine, to "green" technologies and manufacturing. However, this increased reactivity at the nanoscale, defined as having at least one dimension<100 nm in size, is also responsible for the increasing concern over their environmental safety.

Material flows of engineered nanoparticles into the aquatic environmenthave been identified throughout their production, use and disposal, putting these ecosystems at potential risk of contamination. In particular, sediments are a likely sink of engineered nanomaterials in the aquatic environment due to their propensity to destabilise and settle out of suspension in natural freshwaters. An emerging body of literature has demonstrated toxicity of nanomaterials to aquatic species. In this thesis, the case is presented for using bioaccumulation as a first indicator of risk to aquatic organisms exposed toengineered nanomaterials. Using the sediment dwelling freshwater worm, *Lumbriculus variegatus*, this work investigates the factors which govern the bioaccumulation of cerium oxide and silver nanomaterials. It is hypothesised that the fate of these materials in sediments will be determined by their core composition, primary particle size and surface coating.

A novel approach is presented to measure two biologically relevant fate parameters (persistence of particles and dissolved species in the sediment pore waters) and how particle properties affect the distribution of the nanomaterials between these phases of the sediment. This provides the context within which to interpret biological exposures assessing both the extent of uptake and how they are accumulated, whether through dietary uptake or across the skin. Understanding this route to uptake is important as the mechanism of toxicity may depend upon the point of contact of a material at the nano-bio interface. For example, a nanoparticle which comes into contact with biological material in the gut may exert a different effect upon an organism than one which is translocated directly across the skin.

It isdemonstrated that sediment properties determine the fate of engineered nano cerium oxide and silver to a greater extent than stabilising surfactants, with the majority of particles aggregating or associating with the solid constituents of the sediment >200 nm in size. The dissolved fraction of the metal present in the pore waters was a better predictor of bioavailability than the persistence of particulate material <200 nm in size, with partially soluble nanosilver being more available than insoluble cerium oxide. The route to metal nanoparticle uptake also differed with particle core, with electrostatically stabilised citrate and sterically stabilised polyethylene glycol (PEG) coated ceria available only through dietary uptake, whilst citrate and PEG coated silver was accumulated through transdermal uptake. Dynamic changes in the fate of silver nanoparticles were also observed for sterically stabilised polyvinylpyrrolidone (PVP) coated silver, resulting in the emergence of a colloidal pore water fraction of silver after 3 months aging in sediments. However, this colloidal silver was still not considered accumulated, indicating that low molecular weight species of silver, dissolving from the particle surface either during the exposure or upon contact with the worms' surfaces was responsible for uptake of silver from the sediments.

In conclusion, this work contributes towards our understanding of the factors which determine both the route and extent of biological uptake of engineered nanomaterials. It presents a novel combination of methods which allow for understanding bioaccumulation of these materials in the context of their fate and behaviour within sediments.

Contents

List of Tables

List of Figures

Author's Declaration

My thesis is presented as five chapters, including a method development chapter, three experimental chapters for publication (under submission)and a final chapter discussing my work in the context of traditional silver toxicity and how we can prioritise engineered nanomaterials of concern, using silver as an example. I am the lead author of each article published or in the process of submission. All biological exposures and material characterisation was planned, organised and executed by myself in consultation with my supervisors. Published material (Appendix 1) was reformatted to provide a unified editorial and referencing style throughout, with figures embedded within the text. References are presented at the end of each chapter whilst supplementary files are compiled into a separate section at the end of the thesis.

Acknowledgements

Everyone you encounter throughout a PhD plays a part in making you the person you are when you come out the other end. First of all, I thank my supervisors ProfessorsTamara Galloway and Charles Tyler for their guidance and ability to inspire me to the cause after every meeting. Thank you. In this vein, I would also like to thank all those in the GUIDEnano project and at FENAC in Birmingham, who have funded my work and made this possible. Not only this, you have demonstrated to me the best face of science, one that is daring, open speaking and intellectually stimulating. In particular, RuteDomingos and Geert Cornelis, your frankness and rigor I hope one day to match.

To my colleagues, first the BioGaldem. You know who you are,you dragged me into the modern world with your Whatsitapp. A wonderful bunch. In particular Katie and Kat, you bring a dose of sanity and fun, wherever we have been. A cascade of thanks to the Piznizzle, latterly Uncle Tonz, most recently Dr Baker.To my friend and flat mate, Amy: keep on singing. We have rocked our way through this together with many a bad (read brilliant) rendition of some of the greatest songs known to human kind. For this, there can be no replacement. It's been a joy. Of course family must also get a mention. First my Grandparents, thank you both for being so proud. You were also the first to suggest I go to university, so, there lies the blame. To Sara and Andrew, no-one I know works harder or is so devoted to their work and their life. I hope that I can match the pleasure you get from the farm in whatever I do. Phil and Si. Nothing is the same as brothers. And Charlotte. No-one challenges me more, knows me so well, or drives me to be better like you. Cheers to you all.

Glossary of terms

Agglomerate: a loose collection of individual particles bound through physical interactions for example entanglement of surfactants or loose adhesion to neighbouring particles. As such the total surface area of an agglomerate may not differ appreciably from that of the sum of the individual particles that constitute the agglomerate. These agglomerates are dynamic and may both grow in size through the incorporation of additional primary particles, agglomerates or aggregates. They may also be disagglomerated into their constituent primary particles or into smaller agglomerates.

Aggregate: a collection of nanoparticles which have irreversibly bound to one another e.g. through sintering at the nanoparticle surface. The total surface area of an aggregate is thus reduced compared to the sum of surface areas of its constituent particles.

Benthos: the community of species living in the benthic zone, the ecological region at the lowest level of a water body. The benthic zone includesthe sediment surface and some sub-surface layers of the sediment.

Bioaccumulation: occurs when the uptake of a contaminant occurs at a faster rate than its breakdown and elimination from an organism.

Bioaccumulation factor: is the ratio between the internal concentration of a contaminant within an organism (the body burden) and the external concentration of the contaminant in the surrounding media (the exposure concentration) at any point during an exposure. As such it is a relative measure of bioaccumulation, useful for comparisons between similar exposures and experimental designs.

Bioaccessible: the fraction of acontaminant which can be taken up by an organism, but where potential for cellular internalisation may be physically or temporally constrained. This fraction can be measured in the abiotic environment, for example in soil sciences, the bioaccessible or bioavailable fraction of a contaminant is often defined as the soluble concentration of a contaminant in the aqueous phase of a soil or sediment.

Bioavailable: describesthe bioaccessible fraction of a contaminant actually bioaccumulated within a living organism. Definitions and measurements of the bioavailable fraction of a contaminant are not harmonised across disciplines. For the purpose of this thesis, we define a nanomaterial as having a bioavailable fraction if we observe bioaccumulation of the material within a living organism. During this thesis, examination of the partitioning of nanomaterials between different fractions of the sediment aims to provide context for how these materials present as bioavailable to the organism.

Bioconcentration: is the increase in concentration of the test substance in or on an organism, resulting exclusively from uptake via the body surface, relative to the concentration of the test substance in the surrounding medium.

Nanomaterial: a class of materials with at least one dimension under 100 nm in size. This includes nanoparticles where all three dimensions are <100 nm, and nano rods and nano-sheets where one or two dimensions are <100 nm. The European Commission's current working definition of a nanomaterial containing product is one "containing particles, in an unbound state or as an aggregate or as an agglomerate and where, for 50% or more of the particles in the number size distribution, one or more external dimensions is in the size range 1-100 nm"

Partitioning: attachment of nanoparticles to other particles or surfaces is not driven by equilibrium partitioning based upon thermodynamic principles as is the case for dissolved molecules. Equilibrium partition coefficients are therefore inappropriate for describing nanoparticle behaviour within sediments. Therefore, this thesis has not attempted to quantify generic partitioning of nanomaterials within sediments, but rather has used separation techniques to define different fractions of the sediment system and the concentration of nanomaterials "partitioned" to these fractions. This is to provide the context with which to understand the route to uptake and bioaccumulation of these nanomaterials in fulfilment of the aims of the thesis.

Transdermal uptake: uptake of a contaminant across the epidermis of an organism. In this thesis, this is operationally defined as nanoparticles which are accumulated by organisms which may not experience dietary uptake and so includes potential surface associations of nanomaterials to the organism and cellular uptake in the epidermis. Distinguishing between transcellular uptake (passing through cells of the epidermis) and intercellular uptake (traversing the epidermis through spaces between cells) was not within the scope of this thesis.

Risk: environmental risk is the likelihood of an adverse outcome in the environment. For a nanomaterial this is based both the possible adverse outcomes that material may elicit within the environment (acute/chronic toxic effects, biomagnification etc.) adjusted for the likelihood of these effects occurring in the environment (based upon expected concentrations in that environment). As such, risk is a function of both the properties of the nanomaterial, but also the emissions into and conditions within the environmental compartment under investigation.

General introduction

Engineered nanomaterials present a particular challenge for regulators and the scientific community at large. The unique properties and behaviours that materials exhibit at the nano scale (generally considered<100 nm) has led to a rapidly expanding global industry with an expected worth by 2020 of US$3 trillion[1]. Their versatility has led to an expansion in use in commercial applications as varied as manufacturing, cosmetics and the textiles industry. Not only this, but nanomaterials have found uses in many emerging sustainable technologies and "green" initiatives. These include ceria nanoparticles used as a catalyst in diesel fuels to improve efficiency [2] or iron oxides used in environmental remediation of polluted ground waters [3]. A strong societal case can be made for the use of such emerging products and technologies based upon their many benefits.

This explains the rapid uptake of these nanoparticle technologies by industry and commercial sectors. However, this must be balanced with the need for this industry to develop sustainably. An emerging body of scientific literature has found the potential for engineered nanomaterials to have toxic effects upon a wide range of terrestrial[4], marine [5] and freshwater aquatic species[6]. This is largely linked to properties such as increased photo-reactivity which can be designed into the material, differentiating engineered nanomaterials from incidental nanoscale particles in the environment.As such, efforts to understand the environmental exposure, fate and hazards that nanoparticles may present to the environment during their production, use or disposal must be carefully evaluated.Due to the unique properties of nanomaterials as compared with other known anthropogenic contaminants, an approach using a combination of both standard established methods and novel techniques and endpoints to test the specific risks that nanoparticles pose to the wider environment is called for [7].

Cerium oxide and silver nanoparticles as model nanomaterial contaminants

The work undertaken for this thesis contributes towards the wider FP7 funded European Union funded consortium, the GUIDEnano project (under grant

agreement no. 604387). The aims of this project were to create a web based tool for risk assessment of engineered nanomaterials throughout their lifecycle, and to validate the use of this tool with a number of nanoparticle case studies provided by industrial partners within the consortium. From the available materials, this thesis examines two widely used and commercially important nanoparticles, cerium oxide (CeO_2 NPs)used in ceramics and paints, and silver nanoparticles (Ag NPs) utilised increasingly for their antimicrobial properties. CeO_2 NPs potential toxicity stems from their capacity to generate reactive oxygen species under certain conditions, the extent of which is largely determined by the nature of surrounding anions [8]. Whilst the exact mechanism is unclear, one proposal is that CeO_2 may undergo Fenton-like reactions at the nanoparticle surface, where in the presence of H_2O_2, redox cycling of Ce generates reactive oxygen species [9]. Production of these reactive oxygen species has been implicated in the sub-lethal genotoxic and cytotoxic effects of CeO_2 NPs observed for the marine amphipod *Corophiumvolutator*[10].

The exact mechanism of toxicity of Ag NPs on the other hand is still disputed within the literature. In some cases the release of soluble silver from the surface of Ag NPs during exposures has been implicated in the resultant toxicity in *Daphnia magna* by Ag NPs coated with lactate, polyvinylpyrrolidone, and sodium dodecylbenzene sulfonate[11]. However, other studies have demonstrated that Ag NPs can induce greater genotoxicity than particles in the micron size range or soluble forms of silver,for example in the sediment dwelling worm *Nereisdiversicolor*[12].Full transcriptome studies in the earthworm *Eiseniafetida* and in the nematode *Caenorhabditis elegans* have identified different molecular mechanisms of toxicity for silver nanoparticles, silver sulphide nanoparticles (Ag_2S) and silver nitrate ($AgNO_3$). For example, the main differences between Ag NPs and $AgNO_3$ in *E. fetida* were associated with potential effects related to cellular uptake and internalisation [13] whilst processes affected in *C. elegans*differed, with nanoparticles affecting metabolism, Ag_2S affecting processes involved in moulting whilst $AgNO_3$ mainly affected stress related processes [14]. As such understanding behaviours of nanoparticles such as their dissolution during exposures is essential for interpreting their effects in the environment.

Whilst much of the nanotoxicology literature had focused upon the human and environmental hazards of pristine nanoparticles using a host of chemical assays, *in vitro* techniques[15] and simplified water exposures*in vivo* to identify nanoparticle effects, there is a need for more environmentally relevant scenarios to be tested. This canbuild upon our collective knowledge to properly quantify the risk that engineered nanomaterials pose to the wider environment at a range of scales from the subcellular to the population and community level [16]. The first step of this is to identify environmental compartments and classes of species which are most relevant both in terms of their likelihood of exposure[17], and the functional role they play in their respective ecosystems[18]. This provides context for selecting model organisms to utilise when exploring the risk of engineered nanoparticles to the environment.

Sediments as an important environmental sink of nanomaterials

Sediments will act as a major sink for engineered nanoparticles in both marine and freshwater aquatic environments. Aggregation drives the fate of nanomaterials in water, and this behaviour is a product of attractive van der Waals forces and repulsive electrostatic forces. The balance of these opposing forces is highly dependent on the physical and chemical properties of the materialas well as the physicochemical properties of their immediate environment[19]. Increasing salinity facilitates not only homoaggregation (aggregation between like particles) but also heteroaggregation (between nanoparticles and other naturally occurring colloids). This process of heteroaggregation has been demonstrated as the main cause of sedimentation of nanoparticles in river waters[20]. Both CeO_2 and Ag NPs have been observed to heteroaggregate in this way and experience faster sedimentation under more saline conditions[21] making them likely candidates for accumulation in aquatic sediments. Predicted environmental nanomaterials in sediments are oftenmany times higher than their counterparts in the water column. Ag NPs are expected at average concentrations of 0.66 ngL^{-1} in surface waters across the European Union [22] but in the µgkg^{-1} range in sediments [23]. Indeed, as material flows into the environment increase with the expansion of the industry, nanomaterials are likely to accumulate in sediments, with estimates of yearly increases of nanomaterials such as Ag NPs of 2.3 µgkg^{-1}year^{-1}[22].

The wide application of Ag NPsinantibacterial agents also makes them of particular concern for sediments, as bacterial communities are essential for ecosystem functioning such as nutrient cycling and providing the structural integrity of sediments[24]. For example, the impact of Ag NPs on benthic microbial communities has been demonstrated for an estuarine system.Following exposure to a single pulse of Ag NPs, utilisation of carbon substrates was inhibited in bacterial communities in the sediment and their functional diversity was altered [25]. Therefore, understanding the uptake and effects of Ag NPs in lower trophic level sediment dwelling organisms is of great importance.

Within sediments, nanoparticles may undergo a range of transformations. In soils and sediments, nanoparticles may persist bound to the solid fraction [26], associated with mobile colloidal constituents of the pore waters [27] and as dissolved species of silver [28]. These different behaviours of nanomaterials may alter the way in which they interact at the nano-bio interface with organisms, and the implications of such behaviours in sediments upon their uptake and toxicity is poorly understood. This thesis aims to address this gap in our knowledge concerning the fate and effects of nanomaterials within sediment environments, as althoughsediments are at risk of contamination by nanomaterials a dearth exists in research into these important ecosystems.

Bioaccumulation of nanomaterials within the sediment environment

Whilst nanomaterial concentrations in sediments may increase over time through sedimentationof particles from water column above, we know little of whether these particles may accumulate in biota within sediments. Such bioaccumulation is an important element in the risk assessment of engineered nanomaterials as materials which can bioaccumulate may be available for trophic transfer or even biomagnification through food webs. The published critical review into the transformations that affect the fate form and bioavailability of nanoparticles in sediments[18] is included in Appendix 1. This identified exemplar species for use in toxicity testing, grouped according to their role in ecosystem functioning and chosen for their wide application in the literature or the existence of standard test guidelines for the use of these organisms as model species. This informed the choice of species for this thesis, the sediment dwelling oligochaete worm *Lumbriculus variegatus*, for use in

subsequent experimental chapters within this thesis. These worms are a freshwater oligochaete worm, common across North America and Europe which feed upon detritus within the sediments. Typically the worm feeds with its anterior buried beneath the sediment surface, whilst the posterior remains in the overlying water for respiration, egesting material onto the sediment surface. Therefore these worms may be exposed to nanoparticlesfrom a variety of sources including contact with sediment bound particles, particles in the pore waters, particles in the overlying water and particles associated with food material within the sediments.

An important factor influencing the bioavailability of a nanomaterial will be its route to uptake into species within the contaminated sediment. Dietary uptake and transdermal uptake provide two distinct pathways for nanomaterial internalisation in organisms. These two distinct routes to uptake could lead to different rates of bioaccumulation or different toxic outcomes. For example, nanomaterials accumulated through dietary uptake may indirectly lead to a reduction in fitness of a species if the particles are eliminated slowly, or reduce the quality of the food source with which they are associated[29], whilst nanomaterials associating with external surfaces could elicit responses directly at the point of contact. Such toxicity has been observed for citrate coated Ag NPs interacting with the surface of the nematode *Caenorhabditiselegans* which caused severe epidemic endema, necrosis and secondary infections through broken skin [30].

L. variegatus reproduce through architomy, a process involving the fragmentation and regeneration of lost body parts though a combination of morphalaxis and epimorphosis [31]. During this regrowth phase worms cannot feed. Therefore, careful manipulation of this mode of reproduction allows for the generation of two life stages of the organisms: feeding and non-feeding worms. This method has been used to explore the relative importance of dietary and transdermal uptake of organic hydrophobic contaminants such as pyrene[32], however, it has never been used to assess the route to uptake of nanoparticles. Therefore, the objective of this thesis is to address this important gap in our understanding of the fate and bioaccumulation of nanomaterials from sediments, using a novel combination of biological and characterisation

techniques to examine the route to uptake of nanomaterials in the context of their fate within sediments.

Aims and objectives

Improved understanding of the bioavailability of nanoparticles to organisms in the environment is of key importance to tailornanotoxicity test designs to have greater environmental relevance. The fate and behaviour of nanoparticles is determined by the characteristics of the surrounding media[19]. The fate processes which dictate nanoparticle behaviour in the aquatic environment and in sediments in particular will determine the bioavailability of these particles to organisms.Understanding the effect that nanomaterial transformations may have upon bioavailability should be the first screening step for risk assessment of engineered nanomaterials to the aquatic environment. If particles are unavailable for uptake by organisms or cannot come into close enough proximity to elicit a toxicological effect, then although nanoparticles may be classified as hazardous, the research community could prioritise risk management and protection efforts for ecosystems at risk of exposure where these effects would actually be possible.

To help address this, a series of experiments were conducted using a combination of biological exposures and characterisation techniques to examine the route and extent of uptake of model CeO_2 and Ag NPs by the worm *L. variegatus* in the context of the fate of these particles during sediment exposures.

Chapter 1

Chapter 1identifies fate parameters of biological importance and develops methods to systematically follow nanoparticle behaviours alongside biological exposures.Methods and materials common throughout the thesis are presented. The rationale behind novel approaches to characterisation and subsequent optimisation of techniques are also presented in this chapter. Partitioning between the solid, colloidal (<200 nm) and dissolved (<1kDa) fractions of the sediment is characterised to provide the context of nanomaterial fate necessary to interpret biological exposures assessing the bioaccumulation of CeO_2 and Ag NPs from sediments.

Chapter 2

To examine the role nanoparticle core and surface properties play in the bioavailability of nanoparticles in sediments, we validate a model system using the aquatic worm *L. variegatus* to investigate the route of uptake for soluble and insoluble forms of cerium in Chapter 2. Inducing splitting in the worms allows for two life stages to be generated: feeding and non-feeding worms. In doing so, the relative importance of ingestion and transdermal uptake for bioaccumulation of CeO_2 NPs is investigated.

Using CeO_2 and its soluble salt cerium nitrate ($Ce(NO_3)_3$), the relative contribution of ingestion and transdermal uptake of Ce is examined along-side the fate of these two contaminants, based on the techniques developed in Chapter 1. This assesses the sensitivity of the model system in identifying different routes to uptake based on nanoparticle fate within sediments. This experimental chapter tests the hypothesis that changing properties such as particle size and surface coating willresult in differences in total accumulation and the route to uptake of CeO_2,either though dietary or transdermal uptake. These results are examined in the context of the persistence of cerium in the colloidal and dissolved fractions of the sediment.

Chapter 3

This work is expanded uponin Chapter 3to assess the route to uptake of silver nanoparticles, which can undergo dissolution under environmental conditions. This work examines the role of dissolution products upon total metal uptake during nanoparticle exposures. The role of different mechanisms of nanoparticle stabilisation is also addressed through the use of either electrostatic citrate or steric PEG stabilisers. Experiments were performed to investigate the impact of these surfactants upon the fate of Ag in sedimentsand how this relates to their relative accumulation through ingestion or transdermal uptake in the model system developed in Chapter2. The hypothesis tested was that different mechanisms of stabilisation would alter the extent of dissolution of silver nanoparticles within sediments, and that this would determine the route and extent of uptake of silver in sediment dwelling worms.

Chapter 4

25

A final series of experiments(Chapter4) address the dynamic nature of nanoparticle exposures over time and assesses the implications of different life cycle histories upon bioavailability. Three potential scenarios or case studies are compared, the first being exposure to "fresh" Ag nanoparticles, representing the immediate aftermath of accidental spillage events or single spikes of nanomaterials to the environment. A second scenario is that of exposure of organisms to a historically contaminated site, with particles "aged" for three months in sediment before *L. variegatus* were exposed to the contaminated sediments. A final scenario is that of Ag nanomaterials which had passed through waste water treatment processes before entering the aquatic environment. These "transformed" Ag nanoparticles were silver sulphide (Ag_2S) nanoparticles with the same characteristics as the "fresh" and "aged" (same primary particle size and coatings) but were sulfurized as this is the predicted main physicochemical transformation that silver will undergo during waste water treatment[33, 34]. Chapter4 presents the kinetic uptake and elimination dynamics of silver under these three exposure scenarios as well as comparing the route to uptake and the fate of silver within the sediments. These exposures are also compared with a dissolved form of silver, silver nitrate ($AgNO_3$) to assess the potential for nanoparticle specific bioaccumulation. Several hypotheses were addressed in this work. First, that insoluble Ag_2S would not be available for transdermal uptake, whilst partially soluble fresh and aged silver and soluble $AgNO_3$ would. Secondly, that aging silver would result in the release of dissolved species of silver available for transdermal uptake and that this would be observed through an increase in uptake of aged silver. We hypothesised that these different "exposure scenarios" would alter the fate of these particles within the sediment and so translate to observable differences in the kinetic uptake and elimination of silver in *L. variegatus*.

The results from the experimental chapters are then discussed in Chapter5in the context of the wider literature concerning silverbioavailability and ecotoxicity to identify areas of divergence between traditional silver ion toxicity and our understanding of nanoparticulate specific effects and behaviours in the environment. This is used to provide a structure for prioritising future research, recommendations based upon the findings of this thesis.

Summary

To summarise, the work presented within this thesis aims to address several major concerns that are raised in attempts to assess the risk that engineerednanoparticles present to sediment environments:

1. Identifying biologically relevant fate parameters and the development of simple and practical methods for quantifying these parameters.
2. Determining the route to uptake of nanoparticles into sediment dwelling organisms to provide better understanding of bioavailability from a whole organism perspective.
3. Assessing the role of particle core and surface properties upon the route and extent of nanomaterial bioaccumulation.
4. Examine the effect of different exposure scenarios upon the bioaccumulation of nanoparticles using silveras a case study.

References

1   M. C. Roco, C. A. Mirkin and M. C. Hersam, *J. Nanoparticle Res.*, 2011, **13**, 897–919.

2   B. Van Devener and S. L. Anderson, *Energy and Fuels*, 2006, **20**, 1886–1894.

3   A. B. Cundy, L. Hopkinson and R. L. D. Whitby, *Sci. Total Environ.*, 2008, **400**, 42–51.

4   J. Il Kwak and Y. J. An, *Hum. Ecol. Risk Assess.*, 2015, **21**, 1566–1575.

5   T. J. Baker, C. R. Tyler and T. S. Galloway, *Environ. Pollut.*, 2014, **186**, 257–271.

6   G. Vale, K. Mehennaoui, S. Cambier, G. Libralato, S. Jomini and R. F. Domingos, *Aquat. Toxicol.*, 2016, **170**, 162–174.

7   M. J. B. Amorim, *Int. J. Environ. Res. Public Health*, 2016, **13**, 10–12.

8   S. Singh, T. Dosani, A. S. Karakoti, A. Kumar, S. Seal and W. T. Self, *Biomaterials*, 2011, **32**, 6745–6753.

9   E. G. Heckert, S. Seal and W. T. Self, *Environ. Sci. Technol.*, 2008, **42**, 5014–5019.

10 Y. Dogra, K. P. Arkill, C. Elgy, B. Stolpe, J. Lead, E. Valsami-Jones, C. R. Tyler and T. S. Galloway, *Nanotoxicology*, 2016, **10**, 480–487.

11 C. M. Zhao and W. X. Wang, *Nanotoxicology*, 2012, **6**, 361–370.

12 Y. Cong, G. T. Banta, H. Selck, D. Berhanu, E. Valsami-Jones and V. E. Forbes, *Aquat. Toxicol.*, 2011, **105**, 403–411.

13 M. Novo, E. Lahive, M. Díez-Ortiz, M. Matzke, A. J. Morgan, D. J. Spurgeon, C. Svendsen and P. Kille, *Environ. Pollut.*, 2015, **205**, 385–393.

14 D. L. Starnes, S. S. Lichtenberg, J. M. Unrine, C. P. Starnes, E. K. Oostveen, G. V. Lowry, P. M. Bertsch and O. V. Tsyusko, *Environ. Pollut.*, 2016, **213**, 314–321.

15 H. M. Braakhuis, S. K. Kloet, S. Kezic, F. Kuper, M. V. D. Z. Park, S. Bellmann, M. van der Zande, S. Le Gac, P. Krystek, R. J. B. Peters, I. M. C. M. Rietjens and H. Bouwmeester, *Arch. Toxicol.*, 2015, **89**, 1469–1495.

16 P. A. Holden, R. M. Nisbet, H. S. Lenihan, R. J. Miller, G. N. Cherr, J. P. Schimel and J. L. Gardea-Torresdey, *Acc. Chem. Res.*, 2013, **46**, 813–822.

17 P. A. Holden, J. L. Gardea-Torresdey, F. Klaessig, R. F. Turco, M. Mortimer, K. Hund-Rinke, E. A. Cohen Hubal, D. Avery, D. Barceló, R. Behra, Y. Cohen, L. Deydier-Stephan, P. L. Ferguson, T. F. Fernandes, B. Herr Harthorn, W. M. Henderson, R. A. Hoke, D. Hristozov, J. M. Johnston, A. B. Kane, L. Kapustka, A. A. Keller, H. S. Lenihan, W. Lovell, C. J. Murphy, R. M. Nisbet, E. J. Petersen, E. R. Salinas, M. Scheringer, M. Sharma, D. E. Speed, Y. Sultan, P. Westerhoff, J. C. White, M. R. Wiesner, E. M. Wong, B. Xing, M. Steele Horan, H. A. Godwin and A. E. Nel, *Environ. Sci. Technol.*, 2016, **50**, 6124–6145.

18 R. K. Cross, C. Tyler and T. S. Galloway, *Environ. Chem.*, 2015, **12**, 627.

19 G. V. Lowry, K. B. Gregory, S. C. Apte and J. R. Lead, *Environ. Sci. Technol.*, 2012, **46**, 6893–6899.

20   J. T. K. Quik, M. C. Stuart, M. Wouterse, W. Peijnenburg, A. J. Hendriks and D. van de Meent, *Environ. Toxicol. Chem.*, 2012, **31**, 1019–1022.

21   J. T. K. Quik, I. Velzeboer, M. Wouterse, A. A. Koelmans and D. van de Meent, *Water Res.*, 2014, **48**, 269–279.

22   T. Y. Sun, F. Gottschalk, K. Hungerbühler and B. Nowack, *Environ. Pollut.*, 2014, **185**, 69–76.

23   F. Gottschalk, T. Sun and B. Nowack, *Environ. Pollut.*, 2013, **181**, 287–300.

24   S. U. Gerbersdorf and S. Wieprecht, *Geobiology*, 2015, **13**, 68–97.

25   V. Echavarri-Bravo, L. Paterson, T. J. Aspray, J. S. Porter, M. K. Winson, B. Thornton and M. G. J. Hartl, *Environ. Pollut.*, 2015, **201**, 91–99.

26   X. Liu, G. Chen and C. Su, *Environ. Sci. Technol.*, 2012, **46**, 6681–6688.

27   G. Cornelis, L. Pang, C. Doolette, J. K. Kirby and M. J. McLaughlin, *Sci. Total Environ.*, 2013, **463**–**464**, 120–130.

28   G. Cornelis, C. DooletteMadeleine Thomas, M. J. McLaughlin, J. K. Kirby, D. G. Beak and D. Chittleborough, *Soil Sci. Soc. Am. J.*, 2012, **76**, 891.

29   C.-M. Zhao and W.-X. Wang, *Environ. Toxicol. Chem.*, 2011, **30**, 885–892.

30   S. W. Kim, S. H. Nam and Y. J. An, *Ecotoxicol. Environ. Saf.*, 2012, **77**, 64–70.

31   V. G. Martinez, P. K. Reddy and M. J. Zoran, *Hydrobiologia*, 2006, **564**, 73–86.

32   M. T. Leppänen and J. V. K. Kukkonen, *Environ. Sci. Technol.*, 1998, **32**, 1503–1508.

33   B. Kim, C.-S. Park, M. Murayama and M. F. Hochella, *Environ. Sci. Technol.*, 2010, **44**, 7509–7514.

34   C. Doolette, M. McLaughlin, J. Kirby, D. Batstone, H. Harris, H. Ge and G. Cornelis, *Chem. Cent. J.*, 2013, **7**, 46–52.

Chapter 1

General methods and characterisation of the nanoparticle fate and behaviour in sediment

Abstract

This chapter outlines the methodology developed to characterise biologically relevant nanoparticle fate and behaviours in both freshwater and sediments. The rationale for characterisation and the choice of techniques alongside method development and validation will be presented. Generation of feeding and non-feeding life stages of the worm *Lumbriculus variegatus* and their application in sediment exposures is also detailed. These methods will be used throughout the thesis and will be referred to accordingly.

Contents

1.1. Introduction

The environment can be thought of as a global reactor for nanoparticles upon their release. Similar to a reactor, biotic and abiotic conditions will alter nanoparticle properties, resulting in dynamic transformations. These will evolve both temporally and spatially as nanomaterials are transported between different environmental compartments and along gradients of physicochemical conditions. Such transformations can be categorised as physical, chemical and biologically mediated transformations [1]. These transformations will be distinct within different environments, and as such the biological implicationsof nanoparticle transformations will also be specific to the environmental compartment under examination. For example aggregation of nanoparticles in the water column may lead to instability and sedimentation. On the one hand this would reduce bioavailability of these nanoparticles for pelagic species, whilst on the other it would increase nanoparticle exposure for benthic dwelling organisms. Therefore it is important to consider not only the transformations which are likely to occur within a test system, but also to balance this with a focus upon the transformations that will be biologically relevant.

Within sediments, dynamic processes of heteroaggregation and dissolution are likely to dominate the fate and behaviour of nanoparticles [2]. The focus of this thesis is to assess how these factors may influence nanoparticle bioaccumulation. There has been much discussion of the limitations of using Bioaccumulation Factors (BAFs) to interpret the bioavailability of metals in aquatic environments. This is due to several factors,principal of which is that metal uptake is often an active process and so body burdens can reach saturation leading to an inverse relationship between BAF and exposure concentration[3]. This means it is difficult to ascribe hazard to any particular value of BAF. The same is likely to apply for metal engineered nanomaterials. As such there is an emerging consensus calling for a deeper understanding of the routes to uptake of contaminants into organisms in order to interpret results correctly[4, 5]. This is particularly true of nanoparticles, where knowledge of the route to uptake would also improve our understanding of the pathways of toxicityfor these materials under environmental conditions[6]. Within sediments two major routes to uptake are available for nanoparticles: transdermal uptake across external membranes and uptake through ingestion. By examining the

route to uptake of nanoparticles within sediments alongside their fate and behaviour, bioaccumulation can be understood in the wider context of how environmental conditions and properties intrinsic to the nanoparticles themselves alter their fate and bioavailability. Such understanding would have implications for both ecotoxicology and the tailoring of nanoparticle production towards "safe by design" nanomaterials.

Characterisation of the pristine nanoparticles used in scientific studies has an important role in allowing researchers to replicate others studies or to build upon others work with comparable starting materials. However, it is also essential to examine them under the test conditions used in the study if any discussion of particle properties and the observed biological endpoints is desired. This is due to the myriad dynamic transformations that the pristine particles will undergo throughout the exposure period meaning biological effects often cannot be directly related to initial particle properties. Methods and standardised procedures are still under development for the routine characterisation of nanoparticles in the complex matrices often required for biological exposures. However, some structural and chemical characteristics of particular importance have been identified in recent literature [7], detailing the characterisation of nanoparticles required for research to be considered of good quality and of use for inter-study comparisons. This web based tool builds upon earlier work by Card and Magnuson, 2010, adapting their proposal to allow the systematic evaluation of the quality of peer reviewed research into the effects of nanoparticles in both human and ecotoxicology[8]. This includes mandatory requirements for characterisation of the sediment compartment and the engineered nanomaterials used in exposures. In particular, sediment organic carbon and pH of the sediment or overlying water are identified as mandatory sediment properties required for interpreting the results of research. The size or state of clustering of nanoparticles before, during or at the end of an exposure is also considered mandatory. This document has provided guidance in the choice and development of biologically relevant fate descriptors throughout this thesis.

1.1.2 Rationale for nanoparticle characterisation in media representative of sediment pore waters

To assess the size distribution of nanoparticles in water, a combination of dynamic light scattering (DLS), transmission electron microscopy (TEM) and

asymmetric flow field flow fractionation (AF4) can be employed. Each has its own strengths and weaknesses which have been reviewed extensively in the literature [9, 10]. Taking a multi-method approach to assessing the size of nanoparticles using a combination of these techniques allows for cross comparison between results and can be used to generate detailed information about the size, shape and distribution of nanoparticles in dispersion in water. These techniques however are limited at distinguishing between target engineered nanoparticles and other similar sized colloids. This is problematic when investigating the fate of nanoparticles within sediments themselves, where natural nano-sized colloids may outnumber the engineered nanoparticles by several orders of magnitude. Therefore, unless otherwise stated, this thesiswill use artificial freshwater as a proxy to represent the conditions experienced by nanoparticles in suspension in the sediment pore waters. DLS allows for time resolved analysis of the particles hydrodynamic diameter, aggregation state and stability of the particles in dispersion over the exposure period. AF4 can be used to confirm the primary particle size and distribution of particles within water samples alongside the DLS, whilst TEM can be used quantitatively to determine particle size distributions by number. TEM can also be used qualitatively to gather information concerning particle shape, uniformity and state of aggregation/agglomeration.

1.1.3 Defining biologically relevant fate parameters for nanoparticles in sediments

Within the sediments themselves, characterisation of nanoparticle properties such as size or surface potential is seriously limited by current analytical capabilities. Therefore, novel biologically relevant fate descriptors must be devised which are technically feasible whilst providing hypothesis driven endpoints that describe nanoparticle behaviours rather than direct properties of the materials themselves. Investigatingthe dynamic partitioning of nanoparticles between the solid and liquid fractions of the sediment would be an appropriate focus for this study to provide context to the biological uptake of nanoparticles from the sediment. I hypothesise that nanoparticles which preferentially associate with the solid fraction of the sediment will be available through ingestion (Figure 1.1 A), whilst those which persist in the pore waters may be available for accumulation through a combination of ingestion and transdermal uptake (Figure 1.1 C).

34
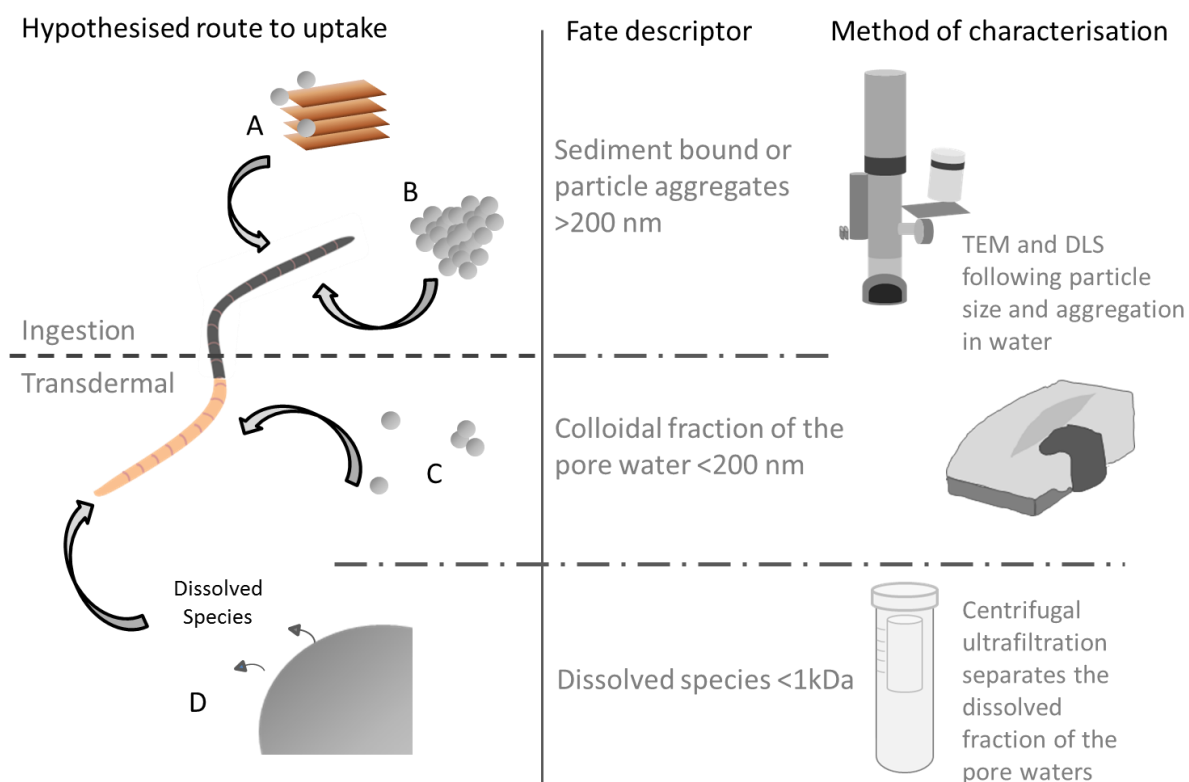
Figure1.1: Biologically relevant nanoparticle fate descriptors and the subsequent hypothesised routes to bioaccumulation. Methods of characterisation provided forA) Sediment bound fraction (e.g. nanoparticle-clay heteroaggregates), B) large homoaggregates, C) individual nanoparticles/clusters <200 nm, D) dissolved species from nanoparticles.

Therefore, nanoparticle partitioning into three fractions of the sediment is investigated: those bound to the solid fraction of the sediment, nanoparticles in the colloidal fraction of the sediment pore water <200 nm in sizeand those which persist as low molecular weight dissolution products of the nanoparticles in the sediment pore waters <1 kDa (Figure 1.1 D). A combination of centrifugation, microfiltration and centrifugal ultrafiltration is employed to separate these three fractions of the sediment to determine partitioning of nanoparticles by mass within the sediments during biological exposures.

1.2. Methods and materials:

1.2.1 Nanomaterials and reagents

Two commercially relevant nanomaterials are examined throughout this thesis: ceria nanoparticles (CeO_2 NPs) and silver nanoparticles (Ag NPs). Investigations utilised a combination of reference CeO_2 materials from the NM

series produced by the Joint Research Centre (JRC, Italy) and commercially available nanoparticles provided as part of the GUIDEnano project. To investigate the influence of primary particle size upon bioaccumulation, JRC NM series CeO_2 NPs were used:10 nm NM211, 33 nm NM212 and 615 nm NM213 particles. These particles were provided as dry powders. Three commercial CeO_2 NPs (PlasmaChem, Germany) of varying coatings were used to investigate the role of surface coatings upon bioaccumulation of CeO_2: uncoated CeO_2 dispersed in weak nitric acid to maintain dispersion (Uncoated-CeO_2), electrostatically stabilised citrate CeO_2 (Citrate-CeO_2) and sterically stabilised mono mPEGphosphonic acid ester CeO_2 (PEG-CeO_2). These particles were supplied in liquid dispersions. Each nanoparticle has a primary particle size of 4-8 nm according to the manufacturer (PlasmaChem, Germany).Ce(III)NO_3 salt (99.999% purity, Sigma Aldrich, UK) was used as a soluble source of Ce^{III} during experiments.

Silver nanoparticle (Ag NP) exposures used commercially available Ag NPs sourced from the GUIDEnano project. Two 10 nm Ag NPs were used to test the effect of surface functionalisation on the bioaccumulation of soluble Ag NPs. These wereelectrostatically stabilised citrate coated Ag (Cit-Ag) and sterically stabilised PEG-mercaptopropionic ether (molecular weight 550 Da) coated Ag (PEG-Ag), both provided in liquid dispersion (PlasmaChem, Germany). To investigate the effect of aging on Ag NP bioaccumulation, 50 nm polyvinylpyrrolidone (PVP-Ag) and 50 nm silver sulphide nanoparticles (Ag_2S NPs) also dispersed in 0.02 mM PVP were provided by the Catalan Institute of Nanoscience and Nanotechnology (ICN, Spain). To assess the contribution that dissolved low molecular weight Ag makes towards bioaccumulation, dissolved American Chemical Society (ACS) reagent grade silver nitrate, purity >99.0% ($AgNO_3$) was used as a representative ionic form of silver (Sigma Aldrich, UK).

Acid digestion of samples was performed in a*qua regia,*a 1:4 dilution of*Trace*SELECT® grade concentrated nitric acid (70% HNO_3) and hydrochloric acid (30% HCl) were used (Sigma-Aldrich, UK). Pre-conditioning of filters for pore water separations used 0.1 M $CuNO_3$ (copper nitrate, $Cu(NO_3)_2$約$3H_2O$, Sigma Aldrich, UK). All dilutions, suspensions and exposures were performed in either MilliQ "ultrapure" water (18 Ω cm-1, Millipore) or OECD reconstituted hard

water, ("freshwater", ionic strength of 13.4 mmol/L, pH 8, conductivity 760 μScm^{-1}) described in OECD test number 315 (DOI: 10.1787/2074577x).

1.2.2 Preparation of nanoparticle stocks and dispersions

Nanoparticles provided as dry powders were dispersed for stocks and experimental suspensions following the PROSPECT protocol for dispersal of dry nano-powders[11]. Briefly, nanoparticles were wetted drop wise to a paste with the dispersal media, either ultrapure water or freshwater. Composition of the freshwater can be found in Supplementary File 1. This paste was then slowly added to until the desired dilution is reached. This dispersion was then sonicated on ice for 2 minutes at 80% intensity to de-agglomerate the mixture using an Auto Tune Series, High Intensity Ultrasonic Processor (Sonics, USA).

Particles provided in dispersion by the manufacturer were homogenised before preparing stocks through gentle overhead mixing for 30 seconds. This low energy mixing was done rather than sonication to avoid damage to the nanoparticle coatings and subsequent destabilisation and sedimentation of the particles from dispersion. Stocks and working solutions for these nanoparticles were prepared by dilution in the relevant test water.

1.2.3 Characterisation of nanomaterials in test media

A suite of techniques were used to characterise different elements of nanoparticle properties and behaviours in both water and sediments. The technical details are presented below whilst optimisation and application of these techniques are presented in 1.3.

Analysis of particle size and stability

Primary particle size was measured using Transmission Electron Microscopy (TEM) using a Jeol 2100 200kV LaB6 TEM. The elemental composition of nanoparticles detected using TEM was confirmed using Energy-dispersive X-ray Spectroscopy (Oxford INCA EDS).

Dynamic Light Scattering (DLS, Malvern Instruments, Zetasizer nano Z-S) with a wavelength of 663 nm using Non-Invasive Backscatter optics and a scattering angle of 173˚ was used to characterise both thenanoparticle primary size and zeta-potential in MilliQ and freshwater. DLS was also used to assess the

stability and agglomeration state of particles over time in freshwater, details of which are presented in 1.3.1.

Ultraviolet-visible light spectrophotometry (UV-vis, Jenway 6800, UK) was used to assess the stability state of silver nanoparticles in ultrapure MilliQ and freshwater. The instrument was used in the absorbance mode with a scan speed of 400 nm minute^{-1} and a path length of 10 mm.

Analysis of metal concentrations using inductively coupled plasma mass spectrometry (ICP-MS)

A Thermo Scientific X Series 2 ICP-MS instrument (Hemel Hempstead, UK), housed in a Class 10000 clean room was used for the measurement of the Ce and Ag content in the digested exposure samples. Calibration standards were prepared from a 10000 mgL^{-1} Ag standard (VWR, UK) standard to produce calibration curves containing at least five data points. A secondary multi-element internal standard was prepared from a different 100 mgL^{-1} stock solution (QMX Laboratories, UK) from that used to prepare the calibration standards. All balances and pipettes and ICP based instruments used were calibrated and operated according to the relevant SOPs contained within the appropriate instrument Record Manual. The performance of the ICP-MS was checked against the manufacturers' specifications before the analysis of any samples began. The ICP-MS instrument was tuned and operated in collision/reaction cell mode, with 7% H_2 in He as the reaction/collision gas, to minimise the effect of any polyatomic species formed in the plasma or interface region. For analysis by ICP-MS In and Ir were added to all standards and samples for use as internal standards, to account for differences in nebulisation efficiency and any instrumental drift, with the latter also being monitored by the analysis of check standards every 10 – 15 samples. If instrumental drift was greater than 10% a fresh calibration series was acquired before sample analysis continued.

1.3. Method development and optimisation:

1.3.1 Assessing the stability of nanoparticles in model sediment pore waters using dynamic light scattering

To assess nanoparticle stability over time, DLS was used to measure the hydrodynamic size and zeta potential of nanoparticles across time periods equivalent to those experienced during the biological exposures presented in this thesis.Hydrodynamic size is often presented as either Z-average or primary peak size. The Z-average is calculated based upon the scattering intensity of nanoparticles, but this intensity is proportional to the square of the molecular weight of the particles. This can lead to overestimation of the hydrodynamic size of particles if there are larger aggregates in the sample or it is polydisperse, as larger particles have a proportionally far greater scattering intensity than smaller particles. As such, it is recommended that Z-averages are only comparable between samples if they are monodisperse and monomodal. The nature of the particles we are examining means we are assessing samples with multimodal size distributions and which are likely to be polydisperse when aggregating. Therefore, we present the average hydrodynamic particle size of the primary peak, as calculated from cumulants analysis of the intensity distributions of the samples. This primary peak is the largest peak by proportion of scattering intensity. By reporting this peak, we can compare particle size between samples whilst reducing the influence that a smaller peak of only a few individual but very large aggregates can have upon the Z-average. Unless stated otherwise, this exposure period totalled 6 days incubation of the nanoparticles in test media. This represents the full biological exposure period of 5 days plus 24 hours acclimation period of the test system before organisms were introduced.

Stability analysis:

To represent conditions experienced within the pore waters, nanoparticle dispersions were preparedat the same spiking concentrations as those usedfor biological exposures. Dispersions were incubated in the dark at 20 ºC in acid washed and rinsed 15 ml Greiner Bio-One polypropylene CELLSTAR tubes (Greiner Bio-One, UK) to limit losses of nanoparticles through adsorption to surfaces. Measurements at each time point were performed in one of two ways.The first is termed **"stability analysis"**. Aliquots of the nanoparticle dispersions were removed at each time point for DLS, with care taken to

prevent disturbance of the liquid to avoid re-suspension of any sedimented particles (Figure 1.2 A). This provided quantitative data concerning the size distribution of any particles which remained in suspension across the incubation period.These particles are considered those most likely to be representative of those which persist in suspension in the sediment pore waters.

Agglomeration analysis:

A secondary aim of this exposure was to generate both qualitative and quantitative measurements of the full size range and aggregation state of nanoparticles in waters representing the sediment pore waters. Preliminary trials found that some of the nanoparticles sedimented rapidly within the first few hours, resulting in count rates too low for reliable detection using DLS. We are interested in the size range of particles both remaining in dispersion in the water and those which had aggregated. To generate an idea of the overall state of agglomeration of particles in these waters, additional samples were prepared in which particles were gently re-suspended by overhead rotating of the sample tubes before sampling for DLS (Figure 1.2 B). This is referred to as the **"agglomeration analysis"**.
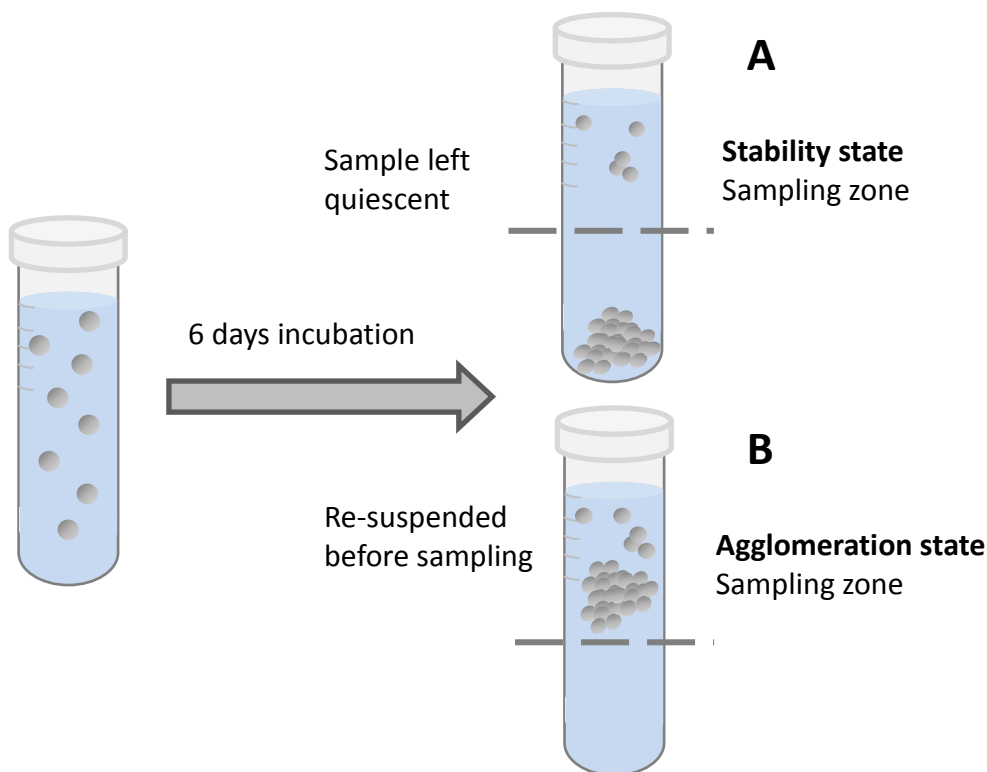
Figure 1.2: The two incubation and sampling regimes for examining the stability (A) and agglomeration (B) behaviour of nanoparticles dispersed in ultrapure and freshwater.

1.2.4 Ultraviolet-visible light spectrometry to assess nanoparticle stability

Alongside DLS measurements, UV-vis was used to assess the stability state of silver nanoparticles in ultrapure MilliQ and freshwater. Preliminary investigations found the peak absorbance wavelength to be between 400 and 450 nm depending upon the primary size of the particle. Therefore two measurement protocols were utilised. The first examined the initial loss of particles through aggregation and sedimentation in the first hour of dispersion, using a kinetic absorbance scan at a wavelength of 420 nm. 20 mgL^{-1} Ag samples were prepared to ensure sufficient signal for absorbance whilst being within the same order of magnitude concentration as that spiked to sediments during biological exposures (5.6 mgL^{-1}).

The second stability assessment was over the medium term, assessing the change in absorbance spectra over 24 hours after dispersion. This represents changes in the nanoparticle aggregations state (in the absence of solid constituents of the sediment) in the 24 hour settling period before organisms were introduced to the test systems and so is representative of nanoparticles at the start of the biological exposure. This spectrum scan was taken at 0, 1, 6 and 24 hours after dispersion. The spectrum scanned wavelengths between 350 and 550 nm with a sampling interval of 0.5 nm.

1.2.5 Optimisation and validation of quantitative size analysis using transmission electron microscopy

Nanoparticle diameter was calculated from TEM images assuming particles were spherical using the area of the particle to define the equivalent spherical diameter using equation 1:

$$d = 2^* \sqrt{\frac{a}{\pi}} \qquad \text{Eq. 1}$$

Where d is the equivalent diameter and a is the area.

Quantitative sizing of nanoparticles from TEM images was validated using NM300k (JRC, Italy), a reference silver nanomaterial using an adapted protocol from an interlaboratory case study by Rice et $al.$ 2013 [12]. Two methods for generating the TEM grids were trialled: a drop method and a floating grid method. The drop method involved placing a 15-30 µl drop of sample onto the TEM grid suspended from fine tweezers and allowing particles to diffuse onto

41

the grid for 1 hour. The drop was replenished if drying was apparent to prevent any artefacts in nanoparticle aggregation caused by drying on the grid. The second method, floating grid, involved placing the TEM grid face down to rest and "float" on top of a 30 µl drop of sample on a slide of Parafilm, allowing the nanoparticles to be drawn up onto the grid over the hour long incubation period. Samples prepared by both methods were then washed gently in a four step submersion wash of MilliQ water to remove excess nanoparticles not deposited onto the grid.Images were taken at random across transects from more than one "square" on the grid. Due to the low concentrations tested of ~5 µgml^{-1}, effort was made to measure a minimum of 100 particles for particle size distributions; however, this was not always possible.

Table 1.1: Comparison in calculated particle size for NM300k using two preparation methods for TEM grids.

Preparation method	Mean diameter (nm)	Standard deviation (nm)	Number of particles imaged
Drop method	19.9	6.3	310
Floating grid	22.5	5.9	177

The drop method was considered to generate a more representative population of particles, closer to the characterisation of NM300 particles (JRC, Italy). In particular, the drop method resulted in two distinct populations of particles (Figure 1.3 A), one with a peak ~20 nm in diameter, and the other ~5 nm. This bimodal population structure was observed in the JRC's characterisation of NM300 AgNPs, but this smaller sized population of particles ~5 nm in size was not observed when using the floating grid method, resulting in the larger average diameter of particles measured (Table 1.1). Therefore, all subsequent TEM analysis throughout this thesis uses the drop method of grid preparation.
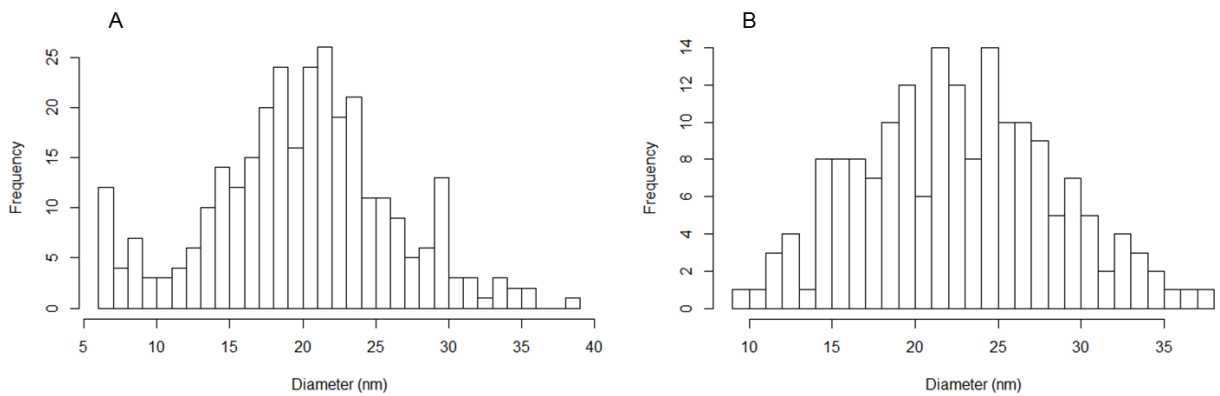
Figure 1.3: Comparison of size (diameter, nm) distributions by number of NM300k silver nanoparticles prepared using either A) the drop method or B) the floating grid method of grid preparation.

To assess the variability that could be introduced through human error in focusing the TEM to take the images, three images were taken of the same area of interest, one over-focused, one under-focused and a final image focused as if for image analysis. The standard deviation between particle diameters calculated for these images was compared to the resolution of the images. The standard deviation in diameter across the three focus levels was 0.26 nm whilst length per pixel of the image was 0.17 nm. Therefore, an approximation of the error attributable to variation in focusing of the image is close to the maximum resolution of the images and only ~1% of the particle sizes measured (~20 nm diameter) therefore could be considered negligible for our analysis.

1.2.6 Verifying the persistence of nanoparticles <100 nm in test media after aging using transmission electron microscopy

Thedrop methodwas used to prepare TEM grids of nanoparticles aged for 6 days in freshwater media. These represented the nanoparticle aggregation state at the end of the biological exposure, in the absence of sediment. Images were taken of the nanoparticle present on the grids and EDS used to verify the elemental composition of the particles.The aim of this was to verify the presence of the engineered nanoparticles after aging and to qualitatively assess the persistence of individual particles and any transformations they have undergone, including sintering to other nanoparticles or chemical transformations such as sulfidation.

43

1.2.7 Fate of nanoparticles in sediment matrices

Full characterisation of the sediment chemistry was not within the scope of this thesis. It should be noted that sediment chemistry including cation exchange capacity, redox potential through the sediment and chemical speciation or ions in the pore water will be important in determining the fate of nanoparticles. Future work aimed to develop models of particle behaviour within sediments will require such characterisation. However, for the purpose of this thesis, such analysis could not be performed. Instead, the work focus's upon the fate of nanoparticles under the specific conditions tested and the implications of these behaviours upon their uptake.

Preparation of samples for acid digestion and analysis:

All tissues and sediment material was freeze dried (Christ Freeze Dryer, Beta LD plus 2-8)and weighed to measure the dry mass before acid digestion.Water samples and freeze-dried tissues and sediments were microwave acid digested (Ethos EZ, Milestone, USA) following the Ethos EZ recommended procedures. Cerium and silver concentrations in acid digests were measured using ICP-MS.

Due to the presence of Cl ions in the freshwater media, all digests were performed in *aqua regia*, a 1:4 acid mix of concentrated nitric acid (HNO_3, ~70%) and hydrochloric acid(HCl, >30%). This was to ensure that after dilution for analysis by ICP-MS, the total concentration of HCl was >1%. At these chloride concentrations, silver chloride species persist in the dissolved $AgCl_2^-$ form, rather than as precipitates of $AgCl^0$, thus reducing losses of total silver in the digestions. For consistency, all digestions were performed in this *aqua regia* mix, before diluting in ultrapure MilliQ water to a final acid concentration of 5% v/v for analysis by ICP-MS. Recoveries for the various particles used throughout this thesis are provided in Table 1.2 where available. The generally high recoveries ranging between 90-110% suggest that error is more likely as a result of slight heterogeneity of dispersion rather than appreciable incomplete recovery of the metals, therefore no adjustment was made to the raw ICP-MS data.

Table 1.2: Digest recoveries for ceria (CeO$_2$) and silver (Ag) nanoparticles used throughout the thesis.

Nanoparticle	Coating	Media	Spike recovery (%)
CeO$_2$	Uncoated	Freshwater	111.8
		Sediment	99.7
	Citrate	Freshwater	103.0
		Sediment	109.9
	PEG	Freshwater	92.5
		Sediment	127.6
	Micron	Freshwater	-
		Sediment	87.6
	NM211	Freshwater	85.2
		Sediment	-
	NM212	Freshwater	86.2
		Sediment	-
	Ce^{III}	Freshwater	114.0
		Sediment	-
Ag	Citrate	Freshwater	-
		Sediment	93.2
	PEG	Freshwater	-
		Sediment	77.3
	PVP	Freshwater	95.6
		Sediment	87.6
	Ag$_2$S	Freshwater	93.7
		Sediment	-
	AgNO$_3$	Ultrapure water	110.1
		Sediment	97.8

Optimising separation of the colloidal fraction of the sediments

Three sediment fractions were considered of biological interest for this thesis: the sediment bound fraction, nanoparticles in the colloidal fraction of the pore water (<200 nm) and dissolved low molecular weight species (LWM). To define the colloidal fraction of the pore water, we optimised a method for the separation of water extractable nanoparticles, based upon the method outlined in Cornelis *et al.* 2010 [13]. To decide upon a size cut off for defining the colloidal fraction of the pore water we compared the extraction of Ce in fractions <1000, <500 and <200 nm from Citrate and PEG-CeO$_2$ spiked sediments. Separating these three fractions of the sediment was performed using centrifugation based upon the calculations in Plathe*et al.* 2010[14]. This allows for the centrifugation

speed and time to be calculated to separate particles of a desired size range based upon the density of the nanoparticle and the distance of the separation.

Table 1.3: Centrifuge operating parameters to separate three size fractions of pore water colloids.

Size fraction	g	Time (minutes)
<1000 nm	340	29
<500 nm	1360	29
<200 nm	4340	57

Centrifugation settings for the three fractions are presented in Table 1.3 whilst more information about the centrifugation method and theory can be found in Plathe*et al.* 2010 [14].
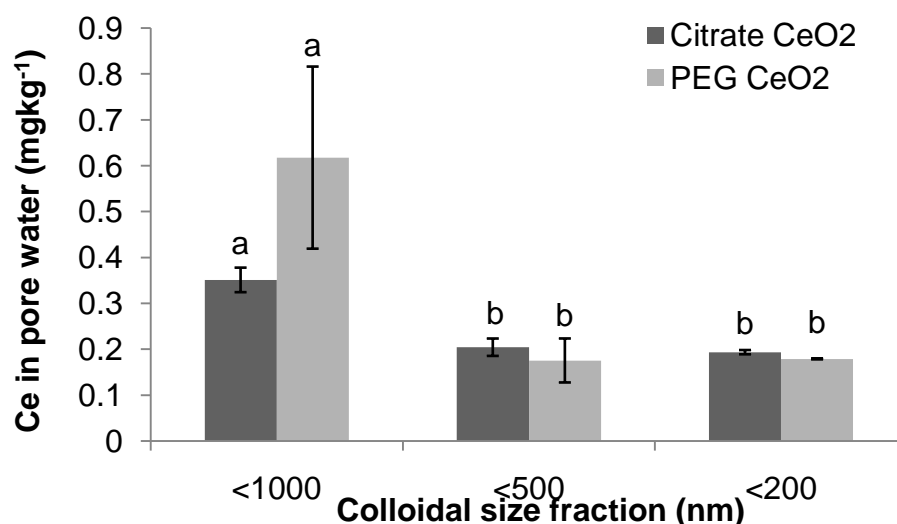
Figure 1.4: Comparison in partitioning of Citrate-CeO$_2$ and PEG-CeO$_2$ between three colloidal size fractions of sediment pore waters after 6 days. Like letters represent no statistically significant difference (α= 0.05).

Analysis of these results demonstrated that Ce in the pore waters persisted as a bi-modal size distribution with a significant peak of Ce between 500 and 1000 nm and a second peak <200 nm. No difference existed between <500 nm or <200 nm fractions suggesting that all Ce in these fractions was indeed below 200 nm in size (p=0.98, Tukey's HSD), with no difference between Citrate and PEG-CeO$_2$ (Figure 1.4). Therefore we decided to only separate this <200nm fraction to define our colloidal fraction of the pore waters, as this was both most

relevant in terms of capturing nanoparticles which may have increased reactivity due to their small size, whilst not losing information about the concentration of Ce in the sub-micron size range as the majority of these particles were <200 nm in any case. This also represented a practical method as 200 nm microfiltration units are readily available, allowing more consistent filtration than separation of fractions of mixed samples using centrifugation.

Separating biologically relevant fractions of the sediment

Based upon the optimisation of pore water separation methods detailed above, the pore water colloids and dissolved low molecular weight fraction were separated through a combination of centrifugation and micro/ultra-filtration techniques. Filters were preconditioned to limit losses of nanoparticles to the filtration membranes using 0.1 M $CuNO_3$ [13].Briefly, microfiltration units were preconditioned by filtering 2 ml of $CuNO_3$ then rinsing through with 4 ml of MilliQ before filtering the nanoparticles. The ultrafiltration units were preconditioned by centrifuging 2 ml of 0.1 M $CuNO_3$ at 2300g for 15 minutes followed by filtering 2 ml of MilliQ again at 2300g for 15 minutes to rinse the filter, before filtering the samples. Care was taken to minimise the time between preconditioning of the filters and filtering the samples to ensure that the filters did not dry. Preconditioning resulted in >90% recoveries of dissolved Ag.

Samples were prepared for fractionation in the following manner. Sediments were incubated for 6 days at 20 C under a light dark regime of 16:8 hours (Figure 1.5A). At the end of this incubation period, a slurry was formed with the overlying water resulting in a 1:10 dilution of sediment to freshwater. This slurry was mixed for 6 hours on an overhead rotating platform before centrifuging at 2300 g for 15 minutes (Figure 1.5 B and C). Two aliquots of the supernatant were then taken; the first was micro-filtrated using preconditioned Minisart0.2 µm syringefilters (Sartorius, Germany) and is defined as the pore water colloidal fraction of nanoparticles (Figure 1.5D). The second aliquot is separated to measure the dissolved LMW fraction (<1 kDa) of nanoparticles within the sediment by centrifugal ultrafiltration (Figure 1.5E).2 ml of the supernatant was centrifuged at 4000 g for 15 minutes. Filtered samples were acidified immediately to 1% HNO_3 to prevent losses to the storage vials (Polypropylene tubes) and stored for microwave digestion and metal analysis by ICP-MS.
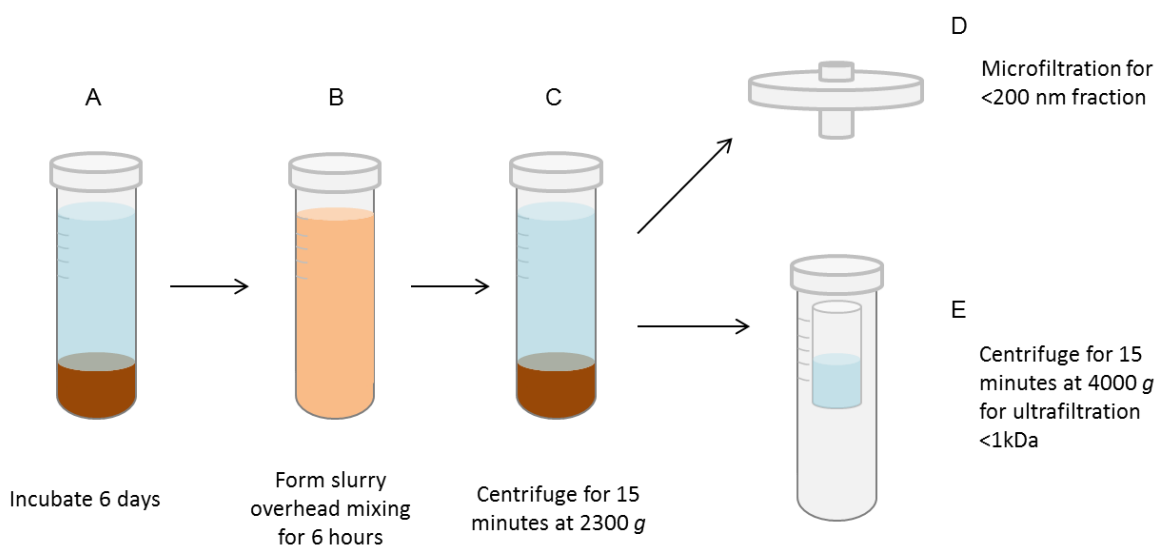
Figure 1.5: Methods used to separate three biologically relevant fractions of the sediment, the solid bound, pore water colloidal fraction (D) and dissolved low molecular weight species (E).

1.4. Generating feeding and non-feeding life stages of the worm *Lumbriculus variegatus*

All organisms experienced a 10 day acclimation period on clean sediment under freshwater (pH 7.6, conductivity 650 μScm^{-1}) before addition to the exposure units. Feeding organisms were synchronised at the start of this acclimation phase by inducing fractionation 10 days prior to exposure (Figure 1.6.a). This was to ensure that all feeding organisms were at the same life stage and that no natural splitting (and so cessation of feeding) would occur during the 5 day exposures. Non-feeding groups were acclimated for 10 days (Figure 1.6.b) and allowed to feed on clean sediments before synchronisation immediately prior to their addition to the exposure units (Figure 1.6.c).

Each static sediment exposure was carried out in acid washed and rinsed 50 ml Greiner Bio-One sterile and heavy metal free polypropylene CELLSTAR tubes (Greiner Bio-One, UK) to limit losses of nanoparticles through adsorption to surfaces, in accordance with Hammes, 2012 [15]. Each test unit comprised of a pool of 5 individuals within 10g of sediment spiked with engineered CeO$_2$ respective to thetreatment. 5 replicates were performed for each treatment. Particles were suspended in freshwater then wet spiked to the sediment to saturation point at a calculated loading of 50 mgkg^{-1} elemental Ce[16]. Exposure conditions and validity of the test was in accordance with OECD TG 315[17]. Sediments were settledfor 24 hours after spiking before commencement of the

5 day exposure. The overlying water was gently poured off and replaced after 24 hours avoiding resuspension of sediment to prevent a build-up of ammonia during the exposure. Negligible silver or cerium partitioned to the overlying water, with 0.01% of total spiked silver and 0.001 to 0.03% of cerium detected in the supernatant from this water change.

After 5 days, all organisms were removed from the sediment test units through gentle resuspension of the sediments with freshwater. Organisms without a clearance phase were rinsed in clean freshwater (Figure 1.6.d), snap frozen in liquid nitrogen (5 organisms per sample) and stored at -80 °C. The remaining organisms were allowed to evacuate their guts for 6 hours in clean TW (Figure 1.6.e), with three water changes to prevent re-ingestion of eliminated particles before snap freezing and storage at -80 °C. This is sufficient to remove >98% of the gut contents of the worms, whilst limiting depuration of contaminants from tissues [18]. All tissues and sediment samples from the exposures were then freeze dried (Christ Freeze Dryer, Beta LD plus 2-8) to measure the dry mass of each sample.
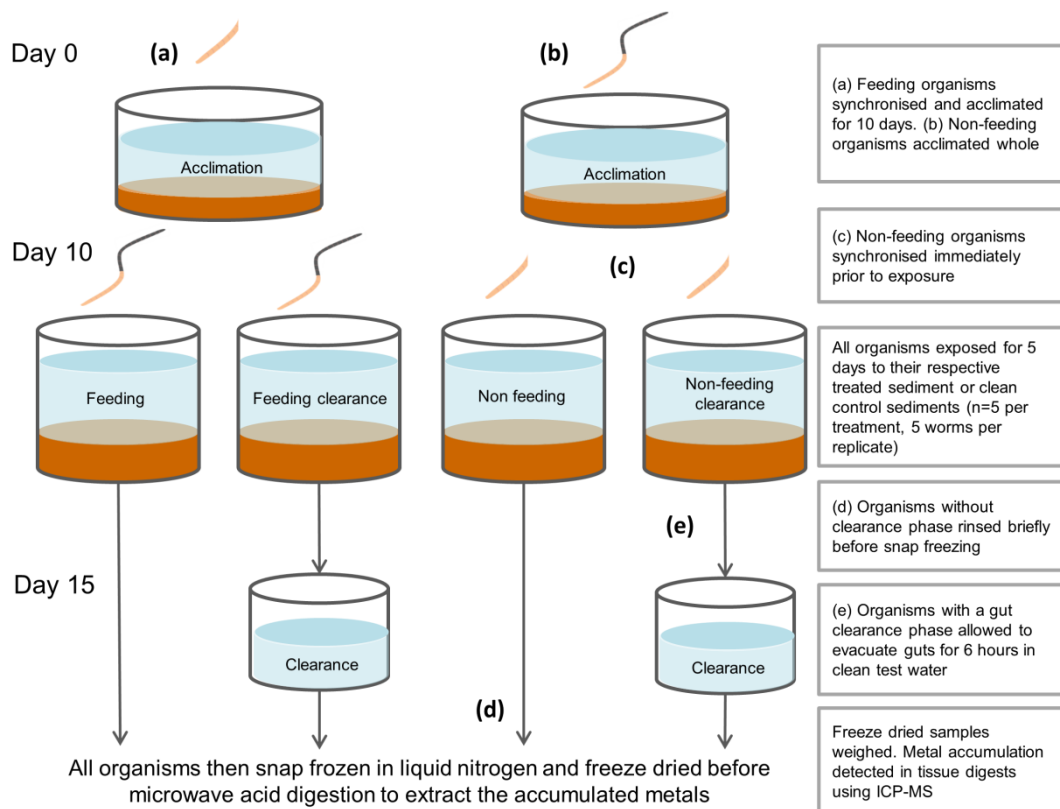
Figure 1.6: Experimental plan to investigate the relative importance of dietary versus transdermal uptake of nanoparticles through the generation of feeding and non-feeding phenotypes.

References

1   G. V. Lowry, K. B. Gregory, S. C. Apte and J. R. Lead, *Environ. Sci. Technol.*, 2012, **46**, 6893–6899.

2   R. K. Cross, C. Tyler and T. S. Galloway, *Environ. Chem.*, 2015, **12**, 627.

3   J. C. McGeer, K. V. Brix, J. M. Skeaff, D. K. Deforest, S. I. Brigham, W. J. Adams and A. Green, *Environ. Toxicol. Chem.*, 2003, **22**, 1017–1037.

4   N. J. Diepens, G. H. P. Arts, T. C. M. Brock, H. Smidt, P. J. Van Den Brink, M. J. Van Den Heuvel-Greve and A. A. Koelmans, *Crit. Rev. Environ. Sci. Technol.*, 2014, **44**, 255–302.

5   H. Selck, K. Drouillard, K. Eisenreich, A. A. Koelmans, A. Palmqvist, A. Ruus, D. Salvito, I. Schultz, R. Stewart, A. Weisbrod, N. W. van den Brink and M. van den Heuvel-Greve, *Integr. Environ. Assess. Manag.*, 2012, **8**, 42–63.

6   M. J. B. Amorim, C. P. Roca and J. J. Scott-Fordsmand, *Environ. Pollut.*, 2016, **218**, 1370–1375.

7   M. L. L. Fernandez-Cruz, D. Hernandez-Moreno, J. Catalan, R. Cross, H. Stockmann-Juvala, J. Cabellos, V. R. Lopes, M. Matzke, N. Ferraz, J. J. Izquierdo, J. M. Navas, M. V. Park, C. Svendsen and G. Janer, *Environ. Sci. Nano*, , DOI:10.1039/C7EN00716G.

8   J. W. Card and B. A. Magnuson, *Int. J. Toxicol.*, 2010, **29**, 402–410.

9   M. Baalousha, B. Stolpe and J. R. Lead, *J. Chromatogr. A*, 2011, **1218**, 4078–4103.

10   L. Calzolai, D. Gilliland and F. Rossi, *Food Addit. Contam. - Part A Chem. Anal. Control. Expo. Risk Assess.*, 2012, **29**, 1183–1193.

11   Prospect, *Protocol for Nanoparticle Dispersion*, 2010.

12   S. B. Rice, C. Chan, S. C. Brown, P. Eschbach, L. Han, D. S. Ensor, A. B. Stefaniak, J. Bonevich, A. E. Vladár, A. R. H. Walker, J. Zheng, C. Starnes, A. Stromberg, J. Ye and E. A. Grulke, *Metrologia*, 2013, **50**, 663–678.

13   G. Cornelis, J. K. Kirby, D. Beak, D. Chittleborough and M. J. McLaughlin, *Environ. Chem.*, 2010, **7**, 298–308.

14   K. L. Plathe, F. Von Der Kammer, M. Hassell, J. Moore, M. Murayama, T. Hofmann and M. F. Hochella, *Environ. Chem.*, 2010, **7**, 82–93.

15   J. Hammes, University of Trier, 2012.

16   OECD, *OECD Environment, Health and Safety Publications Series on the Safety of Manufactured Nanomaterials No 36. Guidance on Sample Preparation and Dosimetry for the Safety Testing of Manufactured Nanomaterials. Organization for Economic Cooperation and Develop*, 2012.

17   OECD, *OECD Guidelines for the Testing of Chemicals 315: Bioaccumulation in Sediment-dwelling Benthic Oligochaetes*, OECD Publishing, 2008.

18   D. R. Mount, T. D. Dawson and L. P. Burkhard, *Environ. Toxicol. Chem.*, 1999, **18**, 1244–1249.

Chapter 2

Using sediment dwelling worms to establish the relative importance of dietary versus transdermal routes to nanoparticle uptake

Abstract:

The relative importance of ingestion and transdermal uptake of nanomaterials is poorly understood, particularly in benthic organisms, where dietary uptake has the potential to contribute significantly towards particle accumulation. Nanoparticles may be bound to the solid fraction of the sediment, freely mobile in the pore water or experience dissolution if they are partially soluble. We hypothesise that the partitioning of cerium oxide nanoparticles (CeO_2) between these fractions of the sediment will present different routes to uptake to the sediment ingesting worm, *Lumbriculus variegatus*. Here, we exploited the regeneration capacity of this freshwater worm to generate feeding and non-feeding life stages to assess the relative contribution that dietary and transdermal uptake make towards CeO_2 bioaccumulation. We used this in combination with a series of separation techniques to explain differences in uptake in the context of the particles fate within the sediment.

We assess both the effect of differing particle size (10, 28 and 615 nm CeO_2) and stabilising surfactants (10 nm Citrate-CeO_2 and PEG-CeO_2) on the fate and bioaccumulation of CeO_2 from sediments. Soluble $Ce(III)NO_3$ was used as a source of dissolved cerium and was found to be accumulated across the skin. Sediments reduced the bioavailability of Ce^{III} by limiting dissolved species of cerium in the pore waters to <1% of the original dose. Of the nanoparticle treatments, only stabilised 10 nm CeO_2 were accumulated above the controls and this was solely through dietary uptake. Nanoparticulate CeO_2 did not dissolve in the sediments, indicating that transdermal uptake was likely only of dissolved species of cerium. Whilst Citrate and PEG-CeO_2 were accumulated significantly, the bioaccumulation factor was ~0.1 so CeO_2 was not deemed biomagnified. Neither particle size nor coatings altered the fate of these nanoparticles, with ~99% associated to the solid fraction of the sediment,

suggesting that sediment properties were more important for determining their partitioning between the solid, colloidal and dissolved phases of the sediment than properties intrinsic to the particles themselves.

Contents

2.1 Introduction

Understanding the biologically relevant fate processes of nanoparticles and the factors which determine bioaccumulation in different environmental compartments will be essential for determining the risk that nanoparticles pose to the environment[1]. Of particular importance are benthic dwelling species which are often lower trophic level organisms, integral for ecosystem functioning [2]. As sediments are predicted to be a major sink of nanoparticles when released into aquatic ecosystems, sediment dwelling organisms are also potentially most at risk to exposure from nanoparticles[3].

Sediments present two potential routes to nanoparticle uptake in benthic dwelling species: 1) through the ingestion of sediment bound nanoparticles and 2) via transdermal uptake from sediment pore waters and the overlying water [3]. The contributions these two routes make to nanoparticle uptake may vary both with nanoparticle core and the method of stabilisation. This is important as the route to uptake of nanoparticles in aquatic organisms may have profound implications for their bioavailability and toxicity. The point of contact with the organism at the nano-bio interface, whether at the organisms' surface or within the gastrointestinal tract, may fundamentally change the potential target sites and mechanisms of uptake and toxicity for the nanomaterial.

This chapter examines the application of a model system to test the relative contribution that these two routes to uptake make to bioaccumulation of nanoparticles, using the sediment dwelling worm, *Lumbriculus variegatus*. This aquatic worm is a useful model to study bioaccumulation as it is exposed to contaminant uptake both across the skin and through ingestion, and is widely used for regulatory toxicity testing (ENV/JM/MONO(2012)40) [4]. Its unusual method of reproduction through fragmentation (architomy) [5] leads to the generation of feeding and non-feeding individuals. This makes it an ideal model for investigating the extent and route of uptake of nanoparticles from contaminated sediments.

Inducing fragmentation with a scalpel incision to the mid-point of these worms can generate these two phenotypes. The worm tail fragment cannot feed for 7 to 10 days, but beyond this, fragments allowed to regrow the lost anterior body segments go on to recommence feeding within the sediment [6]. Regrown

individuals which we define as "feeding organisms" can experience both ingestion of sediment bound nanoparticles and transdermal uptake of nanoparticles through direct contact with external membranes,fromeitherthe overlying or interstitial pore water (Figure 2.1.1). The second group which are split immediately prior to the exposure form the "non-feeding organisms" and are exposed only totransdermal uptake of nanoparticles in contact with external membranes (Figure 2.1.2). This method has been used successfully to investigate the relative contribution of ingestion and transdermal uptake of pyrene [6] and ionisable pharmaceuticals including diclofenac and fluoxetine[7], but to our knowledge has never been used to examine the route to uptake of engineered metal nanoparticles.

Cerium oxide nanoparticles (CeO_2 NPs) are widely used as an additive in diesel fuels and in glass polishing. They remain in the particulate form in aquatic systems, undergoing negligible dissolution when examined in freshwater conditions [8]. We hypothesise that nanoparticles which do not undergo dissolution within sediments will experience markedly different uptake in comparison with those which do. This chapter will outline the successfulapplication of using *L. variegatus* as a model for investigating the route to uptake of nanoparticles from sediments. To do this a range of reference materials and commercially available CeO_2werestudied to examine the role of size and surface functionalisation upon the route and extent of nanoparticle uptake. Nanoparticles investigated in this study exhibited a range of primary particle sizes between 4 and 615 nm and various stabilisation mechanisms including uncoated, electrostatic and sterically stabilised nanoparticles. The relative importance of transdermal uptake versus ingestion as a route to accumulation for CeO_2 NPs was assessed by comparing bioaccumulation of insoluble nanoparticles with soluble Ce^{III} in feeding and non-feeding worms. The results are discussed in the context of the biologically relevant fate parameters investigated in Chapter 1, including persistence of the nanoparticles in the colloidal fraction of the pore waters (Figure 2.1.4) and as dissolved species (Figure 2.1.5). The aim is to bring together an understanding of the fate of CeO_2 NPs in sediments and the implication for bioaccumulation and the routes to nanomaterial uptake in a model sediment dwelling species.

To summarise, the three main experiments conducted in this study assessed:

1. The route and extent of uptake of dissolved Ce^{III} compared to CeO_2 NPs in waterborne exposures representing pore waters without solid constituents of the sediment

2. The role of nanoparticle size upon the route and extent of cerium uptake from sediments

3. The role of stabilising coatings on the route and extent of cerium uptake from sediments
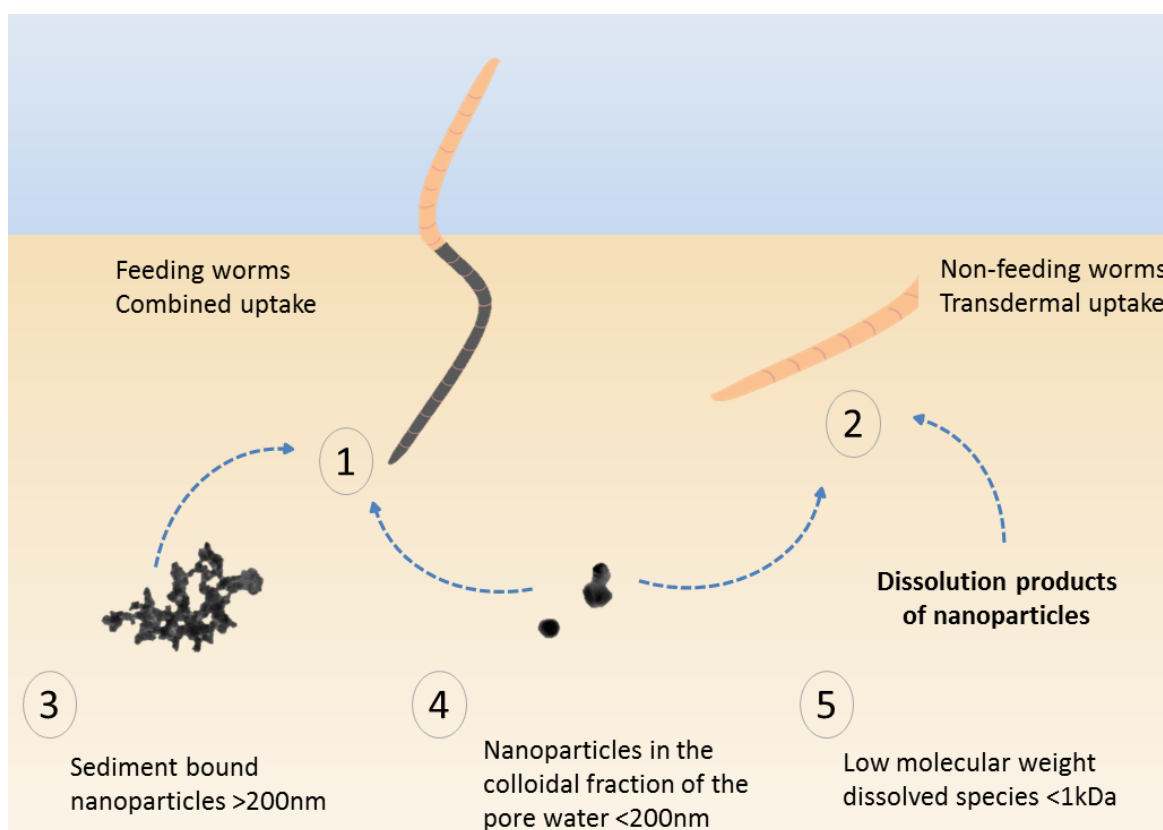
Figure 2.1: The different routes to uptake available for nanoparticles either in regrown worms feeding upon the sediment (1) exposed to a combination of dietary and transdermal uptake or non-feeding tails of worms (2) exposed to transdermal uptake only. Three separations were performed to examine the fate of nanoparticles within the sediment with those passing through a 1 kDa ultrafiltration process defined as low molecular weight species of the metal (5), the colloidal pore water fraction <200 nm (4) and the remainder which is bound to the solid fraction of the sediment (3). Hypothesised routes to uptake of these three fractions of the sediment are proposed through dotted arrows.

2.2 Methods

2.2.1 Materials and characterisation of pristine particles

This study examined the effect of particle size and stabilising coatings upon the route and extent of uptake of CeO_2 from sediments. Details of these particles are presented in Chapter 1. Materials tested in this experimental section are as follows: NM211 (10 nm), NM212 (28 nm), NM213 (micro-sized CeO_2), Ce(III)NO_3 (soluble form of Ce), Uncoated-CeO_2, Citrate-CeO_2 (electrostatically stabilised) and PEG-CeO_2 (sterically stabilised).

Characterisation consisted of a combination of Transmission Electron Microscopy (TEM), Scanning Electron Microscopy (SEM) and Dynamic Light Scattering (DLS), presented in Table 2.1. Freshwaterduring exposures had a measuredpH 7.75 ($^+$/- 0.03), conductivity 715 µScm^{-1} ($^+$/- 11.1) and a calculated ionic strength of 13.4 mmolL^{-1}. Concentration of Ce in various media (water, tissues and sediment) was measured using inductively coupled plasma mass spectrometry (ICP-MS) following the standard method (Chapter 1) for microwave digestion and analysis. The control exposures refer to the Ce naturally present in the standard soil LUFA Speyer 2.4 (LUFA Speyer, Germany).

Table 2.1: Size and stability of pristine CeO_2 NPs prior to exposure. NM-series nanoparticles were characterised by the Joint Research Council[9] (JRC, Italy DOI:10.2788/80203). The letter[a] refers to primary particle size calculated by the manufacturer from TEM images, whilst [b] refers to size measured using SEM.

Nanoparticle	Primary particle size (nm)	Z-average in MilliQ DLS (nm)	Zeta potential in MilliQ (mV)
NM 211	10-20 [a]	293	28
NM 212	28.4 [b]	213	33
NM 213	615.3 [b]	349	-7
Uncoated-CeO_2	4-8 [a]	912.3	12.2
Citrate-CeO_2	4-8 [a]	57.03	-37.9
PEG-CeO_2	4-8 [a]	86.99	-47.8

2.2.2 Fate of CeO$_2$ NPs in sediment during the biological exposures

The methodology and results for investigating the partitioning of Ce between the solid bound fraction of the sediment and the colloidal and low molecular weight (LMW) fraction of the pore waters is described in Chapter 1. Briefly, partitioning between these three fractions of the sediment was examined through centrifugation of a slurry of sediment in test water at the end of the 5 day biological exposure period. This supernatant was then micro-filtered to <200 nm to define the colloidal fraction of Ce in the pore waters, or centrifugal ultrafiltration was employed to separate Ce <1 kDa (~1nm filter pore size) in the sediment pore waters, which is defined as the LMW-Ce.

Methods to assess the stability and agglomeration state of CeO$_2$ NPs used in this study in two simple media are described in Chapter 1. Briefly, two populations of particles incubated in MilliQ and freshwater were assessed using DLS. The first population represents those particles which remained in suspension across the 5 day exposure period. This experiment is termed the "stability analysis". To assess the state of all particles (stable, aggregated/agglomerated and sedimented), "agglomeration analysis" was also performed, using DLS to examine the full range of particles formed by dynamic processes of aggregation during the exposure period. The total incubation time in MilliQ and freshwater was actually 6 days, so as to reflect the 24 hour settling period before organisms were introduced to the sediment and exposed for 5 further days.

Visual MINTEQ modelling (MINTEQ v3.1, Sweden) was also performed for the soluble Ce^{III} to assess the fate of this dissolved cerium in freshwater to act as a proxy for the sediment pore waters during exposure. The species distribution for this dissolved Ce in waterborne exposuresis presented in Table 2.2. Modelling of the chemical speciation of Ce(III)NO$_3$at a concentration of 113.4 mgL^{-1}in freshwater represents the Ce spiked to the sediment pore water resulting in a loading concentration of 50 mgkg^{-1}.

Table 2.2: Speciation of Ce(III)NO$_3$ spiked to freshwater at 113.4 mgL^{-1}, equivalent to 50 mgkg^{-1} in sediments, calculated by visual MINTEQ modelling.

Species	Concentration (µmol L^{-1})	Proportion of total Ce (%)
Ce^{+3}	435.330	53.801
CeSO$_4^+$	183.620	22.692
CeCO$_3^+$	0.707	18.192
CeNO$_3^{+2}$	19.529	2.413
CeHCO$_3^{+2}$	14.578	1.802
CeOH^{+2}	3.843	0.475
CeCl^{+2}	2.629	0.325
Ce(SO$_4$)$^{2-}$	1.723	0.213
Ce(CO$_3$)$^{2-}$	147.200	0.087

2.2.3 Generating two phenotypes for investigating the route and extent of nanoparticle uptake from sediments into *Lumbriculus variegatus*

Lumbriculus variegatus were purchased from Blades Biological UK Ltd. (Kent, UK) and housed on clean silica sand under an artificial freshwater flow through system (pH 7.6, conductivity 360 µScm^{-1}) which was constantly aerated. The organisms were fed twice weekly with 0.5 g of ground fish food (TetraMin, Blacksburg, USA).

Rationale for the use of induced fractionation of worms to generate feeding and non-feeding organisms is illustrated in Figure 2.1. The method for inducing fractionation and generating these two phenotypes is detailed in Figure 1.6 (Chapter 1). Examples of organisms at each life stage were imaged using a QIClick™ CCD Camera (Surrey, Canada) mounted to an LTSu-1000 light microscope (East Sussex, UK) and recorded using Q-capture Pro 7 software (Surrey, Canada).

2.2.4 The relative importance of transdermal and dietary uptake of cerium for dissolved Ce^{III} and nanoparticulate CeO$_2$

Exposures to nanoparticulate NM211 (10 nm CeO$_2$ NPs), NM212 (33 nm CeO$_2$ NPs) and micron sized NM213 (615 nm CeO$_2$ particles) aimed to assess the effect of particle size upon bioaccumulation, whilst exposure to Ce(III)NO$_3$ as a soluble form of Ce^{III} examined the potential for transdermal uptake of dissolved

forms of Ce. 24 hour static, water onlyexposures, represent simplified conditions within the sediment pore waters. This allowed the role of nanoparticle size upon bioaccumulation to be investigated in the absence of solid constituents of the sediment.

Each exposure was conducted in multiwall polystyrene culture plates (Grenier, Austria). NM-series nanoparticles were dispersed following the PROSPECT protocol for dispersal of dry nano-powders[10]. Briefly, nanoparticles were wetted drop wise to a paste in freshwater.This paste was then slowly added to until the desired dilution reached. This dispersion was then sonicated on ice for 2 minutes at 80% intensity to de-agglomerate the mixture using an Auto Tune Series, High Intensity Ultrasonic Processor (Sonics, USA). Nanoparticle exposures were randomised in 10 ml wells with a pool of 3 organisms randomly assigned to each exposure unit and3 replicate test units per data point. Spiking concentrations were based upon a compromise between being below expected effect concentrations (no observed effect of similar sized CeO_2 NPs on *Daphnia magna* after 96 hour exposures to 10 mgL^{-1}[11] and 48 hour EC50 of Ce^{III} for *D. magna* is 6.9 mgL^{-1}) but high enough for appreciable bioaccumulation to have occurred over the acute exposure period of 24 hours. Organisms were exposed to 11.3 mgL^{-1} Ce for nanoparticle exposures (equivalent to 5 mgkg^{-1} in sediment). Ce^{III} was spiked as cerium nitrate at two concentrations, a high concentration of 11.3 mgL^{-1} representing 5 mgkg^{-1} Ce^{III} in sediments and a low exposure of 11.3 µgL^{-1}. No mortality occurred in any of the treatments.

2.2.5 The role of particle size and surface coating on the route and extent of uptake of CeO_2 nanoparticles from sediments

The role of nanoparticle size and cerium solubility upon the route and extent of uptake of cerium from sediments was investigated using NM211, NM212 and Ce^{III}. Exposures were conducted as outlined in Figure 1.6 (Chapter 1), however, the Ce(III)NO$_3$ was spiked to the sediment in ultrapure water rather than freshwater in order to ensure a homogenous suspension and that Ce was in the dissolved Ce^{III} form before interacting with the sediment. Spike recoveries of the stock nanoparticle suspensions were performed to confirm loading rate of nanoparticles to sediments. Recoveries for $CeO_2$from sediments ranged from between 87.6% to ~100%.Uncoated, Citrate (electrostatic stabiliser) and PEG (steric stabiliser) coated CeO_2 NPswere used to assess the effect of

nanoparticle surface functionalisation upon the extent of uptake of commercial CeO_2 NPs from sediments.

Each test unit comprised of a pool of 5 individuals within 10g of sediment spiked with engineered CeO_2 respective to thetreatment. 5 replicates were performed for each treatment.Organisms were exposed for 5 days with a water change before exposure. Preliminary work found 0.001to 0.03% of the total spiked Ce in these overlying waters and so negligible amounts of the nanomaterialis lost from the system during this water change. After 5 days exposure, organisms without a clearance phase were rinsed in clean freshwater, snap frozen in liquid nitrogen (5 organisms per sample) and stored at -80 ^{o}C. The remaining organisms were allowed to evacuate their guts for 6 hours in clean freshwater, with three water changes to prevent re-ingestion of eliminated particles before snap freezing and storage at -80 ^{o}C. All tissues and sediment samples from the exposures were then freeze dried to measure the dry mass of each sample. Samples were prepared and analysed for cerium content as outlined in Chapter 1. Spike recoveries of the stock nanoparticle suspensions were performed to confirm loading rate of nanoparticles to sediments. Recoveries for $CeO_2$from sediments ranged from between 87.6% to ~100%.

2.2.6 Data handling and statistical analysis

Bioaccumulation factors after 5 days (BAF_5) were calculated for CeO_2 NPs of different size and coatings to make comparisons between nanoparticle treatments whilst taking into account any small differences in exposure concentrations. This was only done once accumulation of Ce to concentrations greater than those in the controls was confirmed through statistical analysis of the body burdens of Ce.BAF_5 was calculated as:

$$BAF_5 = \frac{C_{org}}{C_{sed}} \qquad (Eq.1)$$

C_{org} refers to the body burden or elemental concentration of Ce within the organism normalised to dry tissue mass (ngmg $^{-1}$) after 5 days exposure, whilst C_{sed} refers to the elemental concentration of Ce within the sediment normalised to dry sediment mass (ngmg $^{-1}$). It should be noted that C_{sed} is the combined concentration of background cerium and the additional spiked engineered nanoparticles. BAF_5 has the units of kg dry weight organism per kg dry weight

sediment ($kgkg^{-1}$). These BAF_5 do not represent accumulation at steady state, rather the accumulated cerium within worms in relation to the external concentration of the exposure under the specific conditions experienced during this study.

All statistical analysis was performed in R [15]. A minimum adequate model approach was taken for each data set on the uptake and bioaccumulation of nanoparticles in *L. variegatus* and appropriate *post hoc* tests chosen based upon the findings of factorial design two way analysis of variance and examination of normality and homogeneity of variance. Where the assumptions of ANOVA were not met, relevant transformations to the data were performed. Before analysis of BAF_5 was performed, mean body burdens of Ce in each of the cerium treatment groups were compared to the control body burdens using Dunnett's multiple comparisons test. For all cerium treatments, body burdens in feeding groups were at least double that of the controls.

For ANOVA which were significant, Tukey's HSD *post hoc* was used where either body burdens or BAF_5 differed significantly between cerium treatments (treatment effect) or where nanoparticles were accumulated through different routes to uptake, for example uptake was greater in feeding organisms than non-feeding organisms (organism group effect). In some cases the route to uptake was significantly different between cerium treatments (interaction effect). Where this interaction effect between nanoparticle treatment and route to uptake was statistically significant, pairwise contrasts were performed using the least-squares means approach with Tukey's method for p value adjustment (LSM Tukey's method). This examines the significance of differences between different levels of each factor in the model, allowing us to investigate how the route to uptake differed between different cerium treatments. This approach is advantageous as it also adjusts for unbalanced factorial design, where loss of samples through deletion of outliers can result in an imbalance in the data. LSM contrasts calculate the overall mean from the mean at each level of the data. This means that if there are missing values within a level (for example if a sample was an outlier and so discounted from the analysis), this has less influence upon the contrasts and so gives more statistical power for analysing factorial design data setswhich are unbalanced. Graphs present means,

standard errors and statistically significant differences, with significance taken as $p < 0.05$.

2.3. Results

2.3.1 Fate and characterisation of CeO_2 in sediments

Table 2.3: Partitioning of CeO_2 NPs between the solid, colloidal and low molecular weight fraction of the sediment at the end of the 5 day biological exposure period.

Dissolved species of Ce

Treatment	Sediment Ce mgkg^{-1}	Colloidal fraction <200 nm mgkg^{-1} (s.e.)	LMW-Ce<1kDa mgkg^{-1}
NM 211 (10-20 nm)	34.86	0.0255 (0.013)	<LOD
NM 212 (33 nm)	31.66	0.0851 (0.035)	<LOD
Micron-CeO_2 (615.3 nm)	19.33	0.2178 (0.138)	<LOD
Uncoated-CeO_2 (4-8 nm)	55.75	0.0823 (0.0132)	<LOD
Citrate-CeO_2 (4-8 nm)	56.57	0.674 (0.058)	<LOD
PEG-CeO_2 (4-8 nm)	59.03	0.075 (0.005)	<LOD
$Ce(NO_3)_3$	43.62	0.0106 (0.0001)	0.00087
Control	43.59	0.0051 (0.003)	<LOD

For all CeO_2 exposures, the low molecular weight fraction (LMW) was below the limit of detection (LOD) of ICP-MS (0.035 ngml^{-1} for coated CeO_2, 0.002 ngml^{-1} for NM-series and Ce^{III}), indicating that there was no dissolution of Ce from the nanoparticles during these exposures (Table 2.3). LMW-Ce was only detected in Ce^{III} treatments at a very low concentration of 0.87 µgkg^{-1} (~0.002% of total Ce). All nanoparticle treatments experienced elevated Ce in the colloidal fraction of the pore waters compared to the control sediments ($p < 0.05$, Dunnett's test). Citrate-CeO_2 had significantly higher colloidal pore water concentrations than all other Ce treatments ($p < 0.05$, Tukey's HSD) but this was still low compared with the sediment bound fraction of ~99% of spiked Ce.

2.3.2 Stability and agglomeration of CeO_2 nanoparticles over time
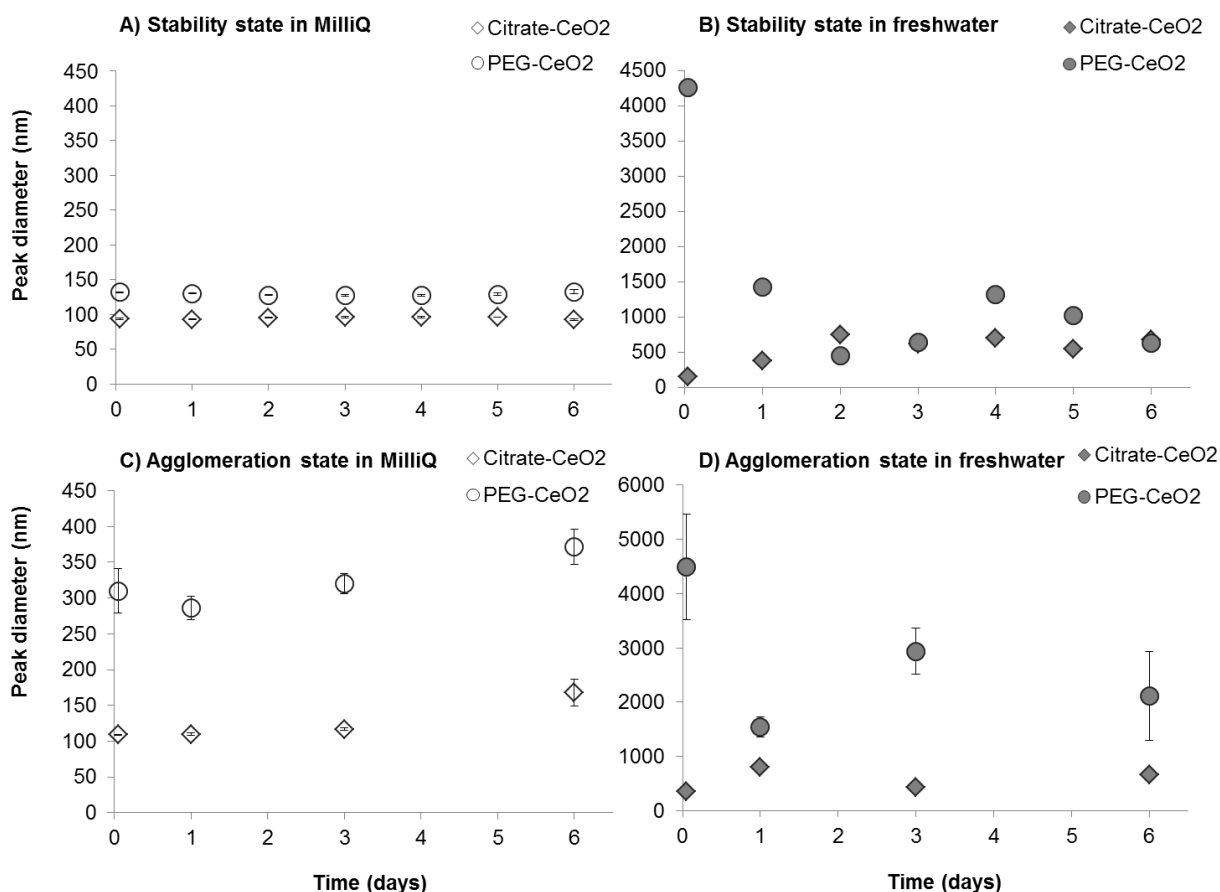
Figure 2.2: Hydrodynamic diameter of Citrate-CeO₂(diamonds) and PEG-CeO₂ particles (circles) remaining in suspension over 6 days aging in either MilliQ (A- open symbols) or freshwater (B- closed symbols). This is contrasted with the agglomeration state of these particles in either MilliQ (C) or freshwater (D). Hydrodynamic diameter is presented as the peak size through scattering intensity (nm).

Behaviour in ultrapure water:

Nanoparticle behaviour was measured over 6 days as this represents the 5 day biological exposure period, plus the 24 hours prior to exposure where sediments were allowed to settle. Both Citrate and PEG-CeO₂ were relatively stable over the 6 day period in ultrapure water (Figure 2.2.A and C). Stability state refers to dispersions that were not shaken before each sampling point, so as to only sample the stable particles remaining in suspension from the supernatant.There appeared to be some larger PEG-CeO₂ particles which sedimented in MilliQ. The mean peak size of these agglomerated particles after shaking the dispersions experienced a slight increase from 309 to 371 nm over

the 6 day incubation period (Figure 2.2.C), compared with the mean size of the particles which remained stable in dispersion of ~130 nm (Figure 2.2.A). Citrate-CeO_2 also experienced a slight increase in mean agglomerate size over the 6 days, from 109 to 168 nm in ultrapure MilliQ water (Figure 2.2.C). This suggests that there are a small proportion of larger particles which do sediment during the incubation period, whilst a population of particles with a peak size of ~95 nm remained stable in the dispersion. It should be noted both Citrate and PEG-CeO_2 in MilliQ were present in bimodal distributions. A secondary peak of 10.5 nm remained in dispersion for Citrate-CeO_2 and of 14.8 nm for PEG-CeO_2. These particles are more representative of the primary particle size stated by the manufacturer of 4-8 nm.

Behaviour in freshwater:

In freshwater, the behaviour of CeO_2 nanoparticles was markedly different. A stable population of Citrate-CeO_2 remained in suspension, trending towards larger particles over the 6 day incubation from 140 to 662 nm (Figure 2.2.B). PEG-CeO_2 on the other hand was lost from suspension within the first 24 hours, evidenced by the initial large size of aggregates >4000 nm in size which were lost resulting in a peak size of 1400 nm. This was accompanied by a drop in count rate and change in attenuator position as the time series progressed, indicating a loss of particles from suspension. Peak size then fluctuated across the rest of the period between 400 and 1300 nm. The max size of agglomerates found in the Citrate-CeO_2 samples ranged between 358 to 797 nm with a relatively low polydispersity index ranging between 0.173 to 0.257 (Figure 2.2.D). This indicates that these agglomerates were similar in size to the final size of particles remaining in suspension (Figure 2.2. C), but had sedimented out without agglomerating further to sizes >1000 nm, unlike PEG-CeO_2.

No secondary peak of primary sized particles ~14 nm were detectable in freshwater. Particles >200 nm in size will experience 1000 times greater scattering intensity than particles <20 nm when using DLS, which could mask the signal of these primary particles.

2.3.3 Producing two distinct phenotypes: feeding and non-feeding organisms
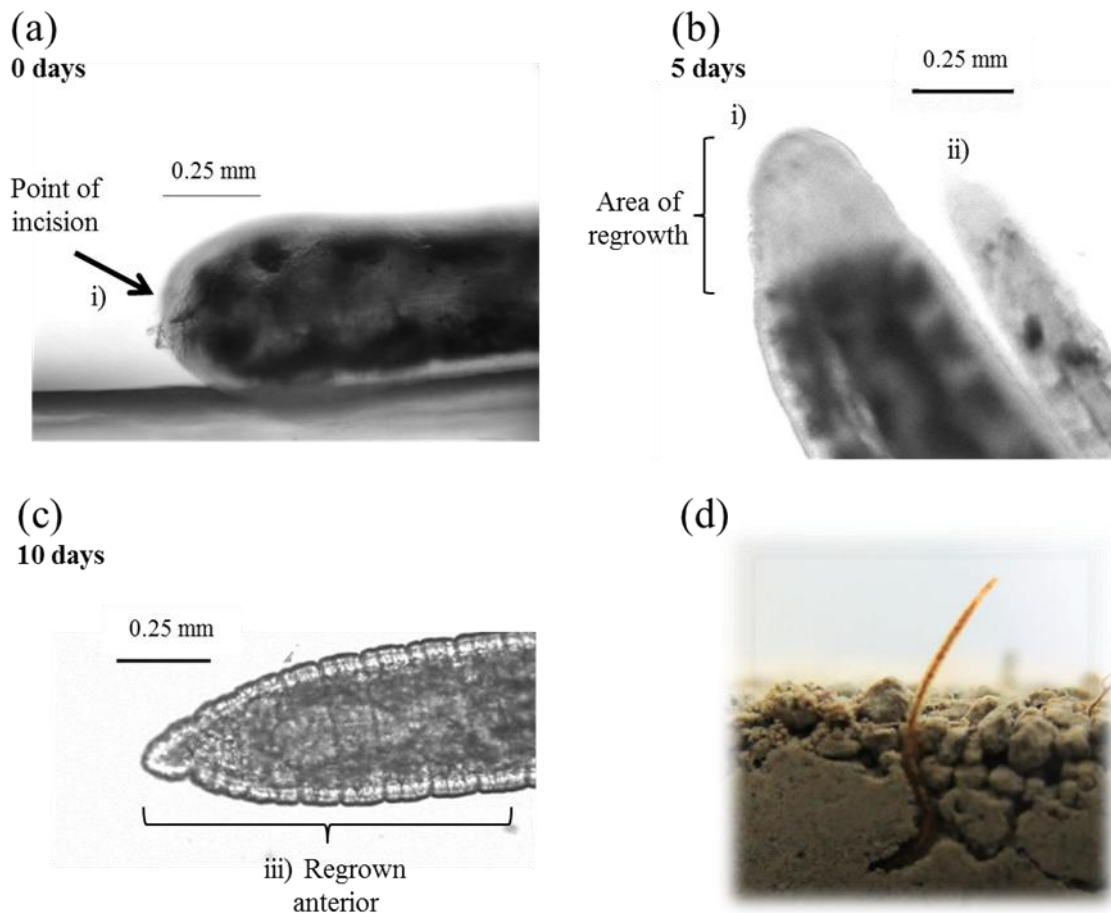
Figure 2.3: Grey scale light microscopy of various stages of regrowth after fractionation by incision at the organisms' mid-point. (a) is immediately after fractionation, (b) after 5 days regrowth and (c) after 10 days. (d) is an example of an individual with its anterior feeding within the sediment whilst the posterior is raised into the overlying water for gas exchange. i) identifies the blastema at the point of incision and its regrowth, ii) is the posterior end of the organism whilst iii) is the fully regrown anterior, identified by fully formed segmentation and the recommencement of feeding upon the sediment.

Light microscopy of the posterior fragment of organisms immediately after fractionation (Figure 2.3.a) demonstrates the rapid formation of the blastema to seal the incision. This is followed by epimorphosis (regeneration of lost body parts through the differentiation of stem cells in the blastema) and morphallaxis (re-organisation of the tissues behind the point of incision) over the next 7 – 10

days as the anterior regrows. Incomplete regeneration of a functioning anterior is confirmed after 5 days (Figure 2.3.b), supported by no visual evidence of feeding upon the sediment. This verifies that non-feeding organisms prepared for biological exposures are indeed incapable of feeding upon the sediment during the 5 day exposure period. Viability of organisms after artificially induced fractionation is confirmed by the full regrowth of the functioning anterior after 10 days (Figure 2.3.c) and recommencement of feeding upon the sediment. This validates the use of *L. variegatus'* ability to undergo asexual reproduction and regeneration of lost body segments to generate a non-feeding phenotype.

2.3.4 Route of uptake of dissolved cerium from waterborne exposures

Table 2.4: Percentage species distribution of Ce(III)NO$_3$ spiked to freshwater at either 11.3 mgL^{-1} or 11.3 µgL^{-1}, representing Ce^{III} water only exposures, calculated using visual MINTEQ modelling.

Species	Proportion of total Ce 11.3 mgL^{-1} (%)	Proportion of total Ce 11.3 µgL^{-1} (%)
CeCO$_3^+$	58.55	77.164
Ce^{+3}	22.13	6.449
CeSO$_4^+$	14.89	4.539
Ce(CO$_3$)$_2^-$	1.76	10.228
CeHCO$_3^{+2}$	1.27	0.423
CeOH^{+2}	0.94	1.096
Ce(SO$_4$)$_2^-$	0.18	0.055
CeCl^{+2}	0.16	0.047
CeNO$_3^{+2}$	0.12	na

The speciation of cerium after spiking Ce(III)NO$_3$ to freshwater at either a high concentration 11.3 mgL^{-1} or low concentration 11.3 µgL^{-1} is presented in Table 2.4. All species of cerium were below their saturation point and so persist as dissolved species in freshwater. CeCO3+ was the most abundant species for both high and low concentration exposures with 58.55 and 77.164 % of the total Ce respectively for 11.3 mgL^{-1} and 11.3 µgL^{-1} exposures. Dissolved Ce^{III} made up 22.13% of the high concentration exposure (11.3 mgL^{-1}) whilst in the low concentration exposures 6.449% of Ce was modelled as Ce^{III}.
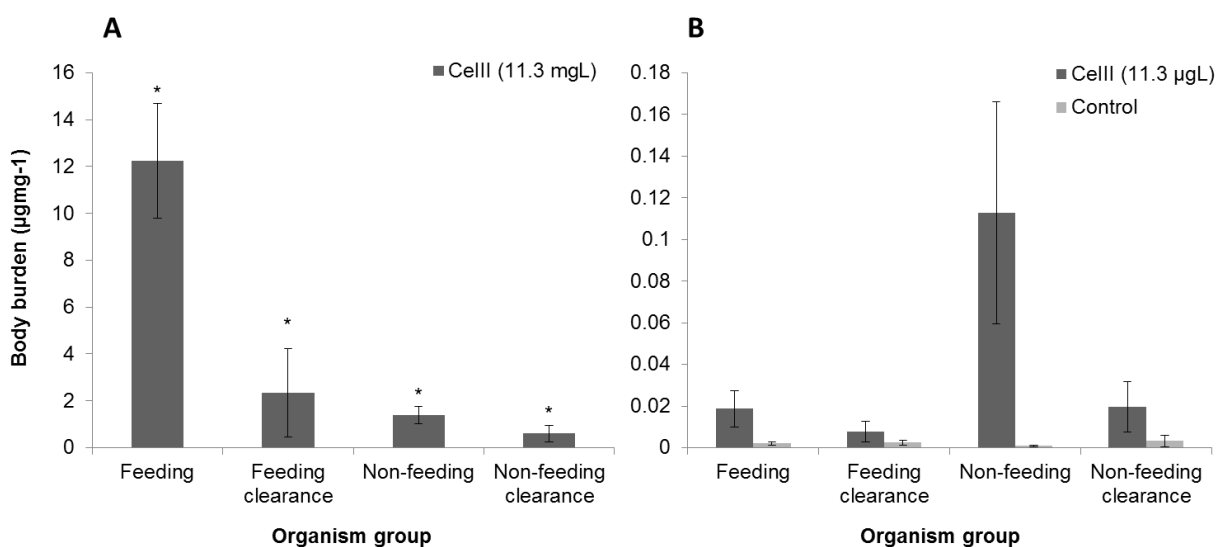
Figure 2.4: Body burdens (µgmg^{-1} Ce) in worms exposed to expected concentrations of 11.3 mgL^{-1} (A) or 11.3 µgL^{-1} Ce^{III}(B) dosed as cerium nitrate (Ce$^{(III)}$NO$_3$) in freshwater (n=3). Body burdens represent accumulation of Ce through different routes to uptake after acute 24 hour water only exposures. Significant accumulation of Ce compared with the corresponding controls is denoted by an asterisk (*) in (A).

Concentration of cerium measured for the two 24 hour, waterborneexposures was found to be 12.9^{+}/- 0.09 mgL^{-1} and 7.1^{+}/- 0.007 µgL^{-1}, in reasonable agreement with the expected doses. Neither data sets for 12.9 mgL^{-1} or 7.1 µgL^{-1} exposures conformed to the assumption of normality or homogeneity of variance and so were log transformed before analysis. There was significant accumulation of Ce in exposed organisms compared to controls at both exposure concentrations (p<0.001, Tukey's HSD). Due to the high variation within organism groups during the high 12.9 mgL^{-1} exposures (Figure 2.4.A), the only significant difference in accumulation between the various organism groups was between the feeding organisms and non-feeding clearance organisms (p=0.008, LSM Tukey's method). After a clearance phase body burdens were between 0.6 and 2.3 µgmg^{-1} for non-feeding and feeding organisms, but were not significantly different (p=0.669, LSM Tukey's method) suggesting this is the contribution of transdermal accumulation of Ce during these exposures. Corresponding control body burdens were <1 ngmg^{-1}.

In the presence of the low concentration of Ce^{III} (7.1 µgL^{-1}) the accumulation after 24 hours was lower and closer to the background body burdens in the

worms (Figure 2.4 B). However, Ce was still detectable above the limit of quantification of the ICP-MS and overall accumulated significantly above background concentrations in the controls (p = 0.0058, Tukey's HSD). There was no statistically significant difference between organism groups (p = 0.461, ANOVA). Feeding therefore did not contribute significantly towards body burdens, indicating transdermal uptake was responsible for accumulation of cerium in the low concentration Ce^{III} exposure. Non-feeding worms without a gut clearance phase experienced high but variablebody burdens, at 112.95 $^{+}$/- 53.3 ngmg^{-1}. All other organism groups experienced body burdens between 7.7 and 19.6 ngmg^{-1} whilst controls averaged at 2.3 ngmg^{-1} with a standard error of 0.68 ngmg^{-1}.

2.3.5 The relative importance of transdermal and dietary uptake of CeO_2inwaterborne exposures

Body burdens for worms exposed to various sized CeO_2 NPs in freshwater for 24 hours were non-normally distributed. Box-Cox analysis found log-transformations to be the most appropriate to ensure that the data conformed to the assumptions of normality and homogeneity of variance required for ANOVA. No interaction effect between nanoparticle treatment and organism group was found when included in the linear model, and so this interaction term was removed. Omnibus ANOVA upon this log-transformed data found no effect of either nanoparticle treatment or organism group (p>0.05, ANOVA). Therefore we cannot say that there was significant accumulation in any nanoparticle treatment as compared to the controls (Figure 2.5).
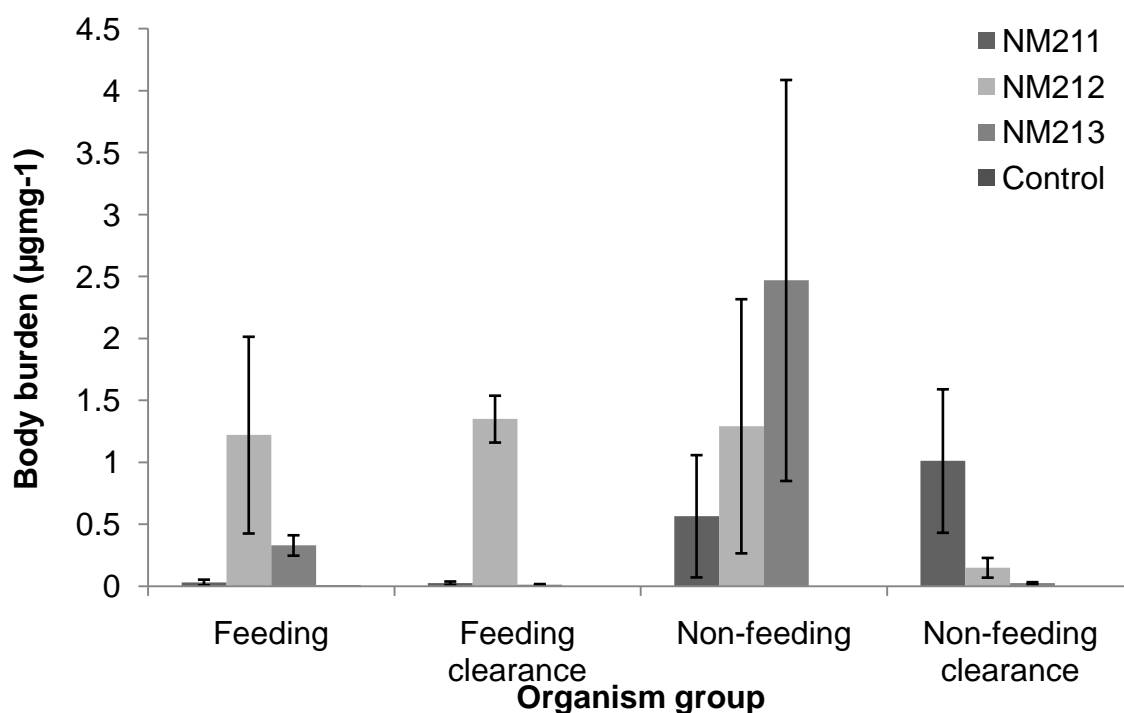
Figure 2.5: Body burdens (µgmg^{-1} Ce) in worms exposed to a calculated 11.3 mgL^{-1} Ce for NM211 and NM212 or 1.13 mgL^{-1} Ce for NM213 in freshwater (n=3). Body burdens represent accumulation of Ce through different routes to uptake after acute 24 hour water only exposures.

The image in Figure 2.6 is an example of the state of organisms in the water only exposures to NM-series CeO$_2$ spiked in the low mgL^{-1} concentration range after 24 hours. Survival was 100% in all treatments; however, in exposure units where organisms were exposed to engineered cerium, "casts" of mucus were apparent in all samples. These mucus casts appeared to be clumped around organisms (Figure 2.6.A) whilst in the process of being shed or were scattered within the water (Figure 2.6.B).

Pooled samples of this mucus were freeze dried, acid digested and measured using ICP-MS to give an indication of their Ce content. The results are displayed in the table in Figure 2.6 (note that mucus cast for NM213 was lost during storage and so this information could not be collected). Each treatment experienced a concentration in the µgmg^{-1} range in these mucus casts, greater than the body burdens in the exposed organisms. The contribution of these mucus layers at the organisms' surface towards body burdens may explain the high variability observed in the data in Figure 2.5, which mean that no statistically significant effect of either independent variable could be established.

Treatment	Exposure concentration (mgL^{-1} Ce)	Mucus concentration (µgmg^{-1} Ce)
NM211	9.66	46.20
NM212	9.78	17.81
NM213	1.04	n.a.
CeIII	12.92	8.04
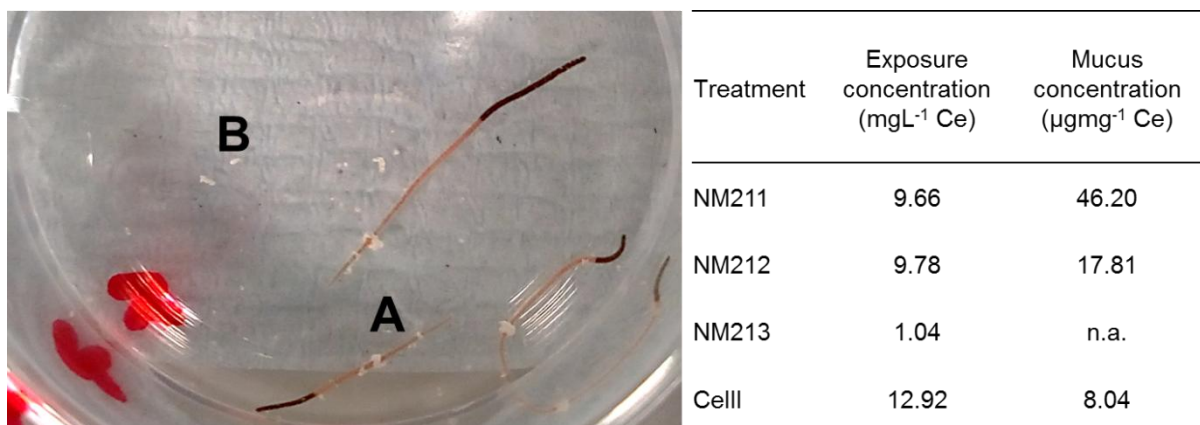
Figure 2.6: Worms exposed to NM-series CeO$_2$ during water only exposures. A) Demonstrates clumping of mucus around the organisms' surface whilst B) is shed mucus in the water. **The table gives reference to the initial spiked concentration of Ce and the concentration of Ce detected in pooled samples of the shed mucus for each treatment.**

2.3.6 The role of size and solubilityupon bioaccumulation of ceriumin sediments

Body burdens of Ce in worms exposed to NM-series CeO$_2$nanoparticles and Ce^{III} in sediments did not conform to the assumptions of normality and homoscedacity required for ANOVA. All data was log-transformed prior to building the model and exploring the data. A significant interaction was found between nanoparticle treatment and the organism group after data was log transformed (p = 0.0257, ANOVA), indicating that the pattern of accumulation in each organism group differed between cerium treatments. Therefore, *post hoc* testing comprised of least squares means (LSM) pairwise contrasts using Tukey's method to examine the significance of differences between body burdens at different levels of both cerium treatmentand organism group. In this experiment, control organisms experienced no significant difference in Ce body burdens within each exposure phenotype (i.e. within feeding or non-feeding groups, p>0.9, LSM Tukey's method), meaning that there was no loss of Ce from the background body burdens during either clearance phase.
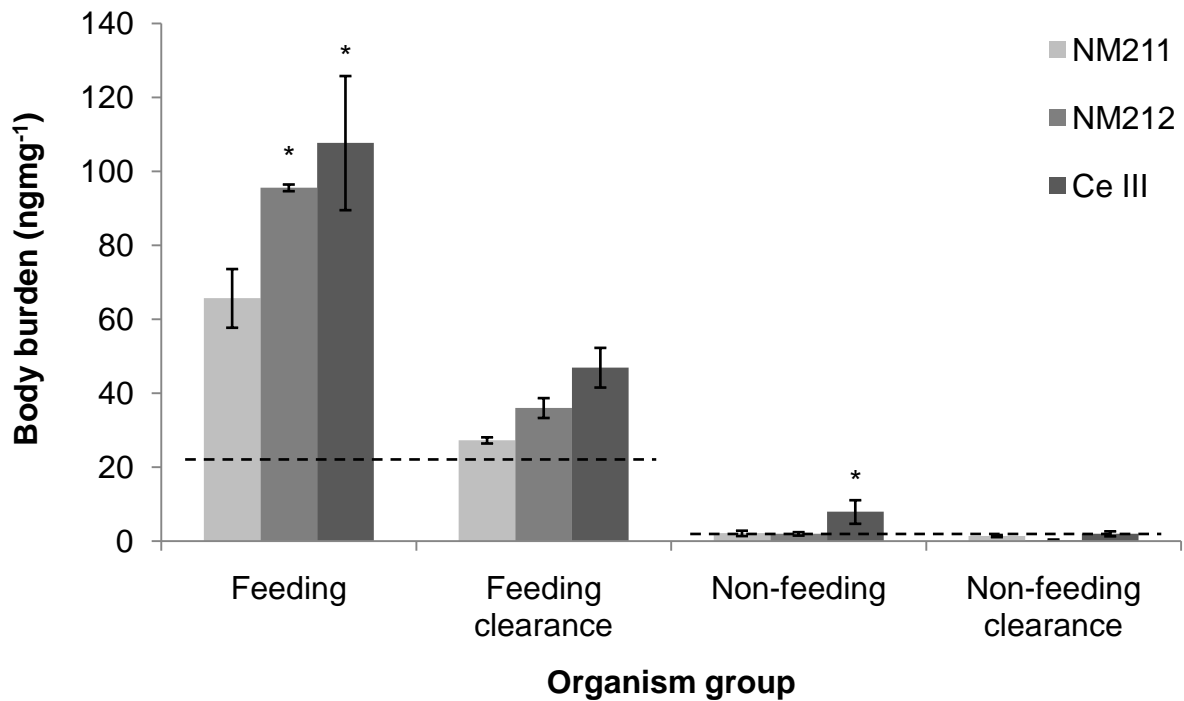
Figure 2.7:Body burdens (ngmg^{-1} Ce) in organisms exposed to CeO$_2$ NPs of varying size and to dissolved Ce^{III} (n=3). Dotted lines (---) represent the background Ce body burdens in control organisms. Significant accumulation of Ce greater than in control organisms is denoted by an asterisk (*).

Both NM212 (p = 0.006, LSM Tukey's method) and Ce^{III} (p = 0.0011,LSM Tukey's method) were internalised above the level of Ce in the controls through ingestion in feeding organisms before the gut clearance phase. However, after 6 hours evacuation of the guts, this was no longer significant for any Ce treatment. As there was no significant bioaccumulation in organisms above that of the controls in all groups other than Feeding organisms, BAF$_5$ was not calculated for this exposure.

Non-feeding worms exposed to nanoparticle treatments (NM211 or NM212) experienced no significant uptake of Ce compared to the controls (p>0.29, LSM Tukey's method). Therefore, there was no evidence of transdermal uptake of these uncoated CeO$_2$ nanoparticles under these exposure conditions (Figure 2.7). Ce^{III} on the other hand, is accumulated significantly above the control concentrations in non-feeding organisms to 7.9 ngmg^{-1} (p = 0.0031, LSM Tukey's method). This accumulated Ce is then lost during the clearance step (p = 0.0011, LSM, Tukey's comparison between non-feeding and non-feeding

clearance), with concentrations returning to the baseline level in the controls ~2 ngmg^{-1} (p = 0.94, LSM, Tukey's).

2.3.7 The effect of surface coatings on accumulation of CeO_2 dosed in sediments

Comparison between feeding versus non-feeding worms demonstrates the primacy of ingestion for accumulation of small 4-8 nm CeO_2 nanoparticles in the deposit feeding worm (Figure 2.8). Accumulation of Ce above control concentrations was detected for all nanoparticle treatments, so BAF_5 was also analysed. Body burdens and BAF_5 were not normally distributed so data were log transformed. The background BAF_5 for feeding control worms was significantly higher than any other control group (p<0.013, LSM Tukey's method) and so was plotted separately in Figure 2.8. No organism exposed to engineered CeO_2 experienced any transdermal uptake of Ce, with BAF_5 and body burdens in all non-feeding organisms being equal to or lower than the background level of the controls (p>0.05, LSM Tukey's method).
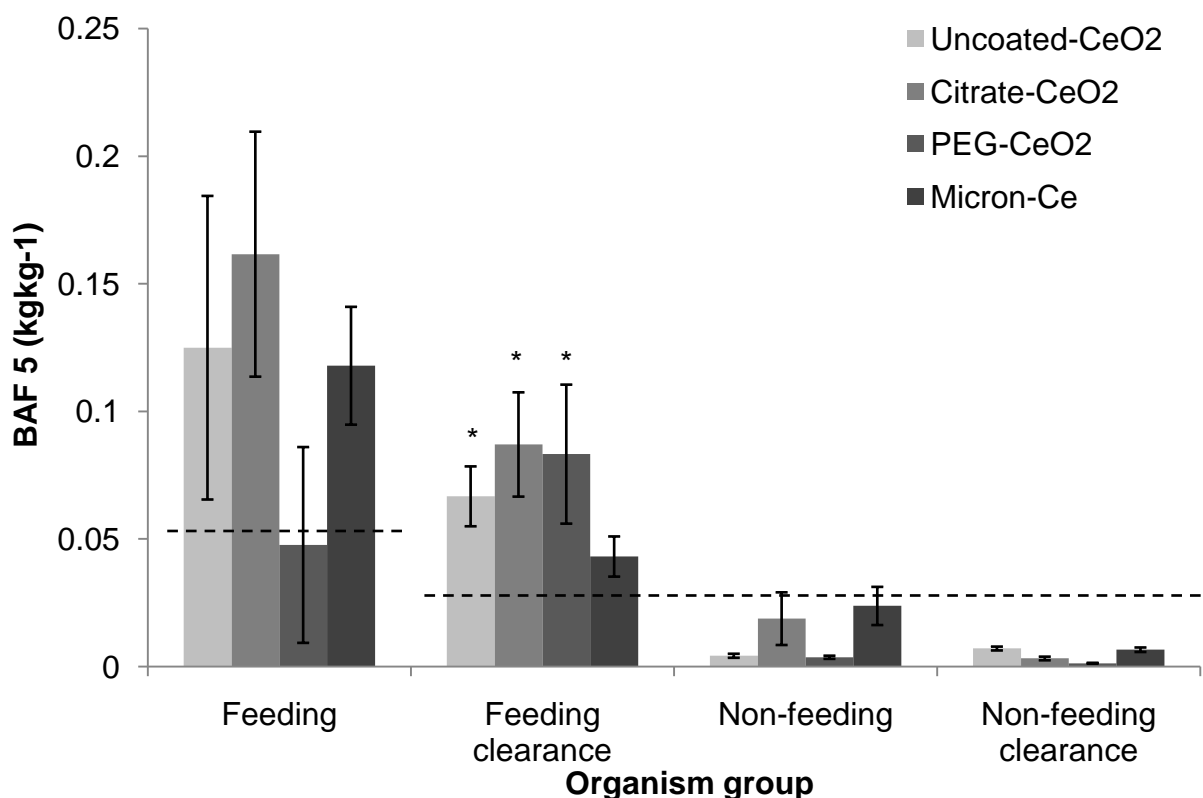
Figure 2.8: BAF_5 (kgkg^{-1}) for organisms exposed to uncoated, Citrate-CeO$_2$ or PEG-CeO$_2$ (n=5). Dotted line (---) represents Ce attributed to the background concentration in the controls. BAF_5 significantly higher than the control is denoted through the symbol (*).

If the gut contents were not purged with a 6 hour clearance phasethere was no difference in accumulation of Ce through ingestion in nanoparticle treatments compared to the control (p > 0.05, LSM Tukey's method). This group represents all Ce accumulated within the organism and that which is associated with material within the guts or loosely adsorbed material to external membranes. Therefore accumulation of engineered Ce could be masked by the relatively high concentration of natural Ce associated with sediments in the guts. Feeding organisms with a gut clearance phase on the other hand accumulated significantly more Ce during exposure to all nanoparticles, coated and uncoated (BAF$_5$),than in the controls (p<0.0045, Tukey's HSD). This was not the case for micron sized CeO$_2$where body burdens of Ce were no different tothe corresponding control concentrations (p = 0.379, LSM Tukey's method). As such, 4-8 nmuncoated, Citrate and PEG-CeO$_2$nanoparticles experienced significant accumulation of Ce through ingestion even after clearing of gut contents, whilst micron CeO$_2$ did not. This accumulation did not result in body burdens greater than external concentrations in the sediment, and so Ce is not consideredbiomagnified during this 5 day exposure period (all BAF$_5$<1).

2.4 Discussion

The results demonstrate the successful application of a method to generate two phenotypes: feeding and non-feeding worms, to assess both the route and extent of uptake of nanoparticles from sediments.This method can be applied to water only and sediment exposures provided concentrations are not sufficient to induce excessive mucus production in the worms. In water only exposures, the experiments address the contribution that either transdermal uptake or uptake through drinking make towards bioaccumulation of nanoparticles. Within sediments, experiments compare the relative importance of transdermal and dietary routes to nanoparticle uptake, through ingestion of sediment material. Examining the bioaccumulation of a range of CeO$_2$ nanoparticles varying in size and surface functionalisation, allowed us to assess the effect these particle characteristics have upon: a) how these particles present themselves to sediment dwelling organisms (their partitioning between sediment fractions and their size and stability in water) and b) the extent of uptake and the route through which they are accumulated.

2.4.1 The behaviour of stabilised CeO$_2$ nanoparticles in waterborne exposures

Stabilisation mechanisms of the coated particles

In simple freshwater media, representing particles in sediment pore waters independent of interactions with the solid fraction of the sediment, Citrate and PEG-CeO$_2$showed differences in their behaviour. Citric acid is a tricarboxylic acid, which behaves as a chelating ligand, adsorbing to Ce^{IV} at the surfaceof particles through bridging of the carboxylate group. This has been demonstrated for commercially available 10 nm Citrate-CeO$_2$, similar to those used in this study, using Attenuated Total Reflection-Fourier Transform Infraredspectroscopy [16]. Siriwardane 2012, in a masters' thesis described howadsorbed citrate molecules on 9 nm CeO$_2$ nanoparticles can form multiple layers increasing the surface charge of the particle-ligand complex and so improving electrostatic stability[17]. DLS demonstrated that Citrate-CeO$_2$ and PEG-CeO$_2$ have a primary particle size of 10.5 and 14.8 nm respectively. At this size citrate would be adsorbing to the particle surface largely through bridging and the formation of multiple stabilising layers of citrate.

PEG on the other hand forms a random hydrated hydrophilic coil at the particle surface, providing steric stabilisation to nanoparticles by preventing other particles from penetrating the PEG layer. The effectiveness of this layer at providing steric stability for solid nanoparticles is dependent on the size and surface coverage of the PEG[18] and whether the PEG is present as intertwined random coils or can extend to their full extent from the nanoparticle surface, thus increasing the thickness of this sterically stabilising layer[19]. It was hypothesised that these two differing stabilisation mechanisms would alter the fate and behaviour of CeO$_2$ NPs in sediments and as such, influence the route to uptake and extent of their bioaccumulation in sediment dwelling worms.

Particle behaviour in ultrapure water

In ultrapure MilliQ water coatings had a strong stabilising effect on the CeO$_2$, with negligible loss ofparticles from suspension over 6 days. This is evidenced by no change in attenuator position and no difference in the size of particlesdetected (~100 nm) between stability and agglomeration analysis (Figure 2.2 A and C). DLS inherently weights particle size towards larger

particles due to the exponential relationship between scattering signal and particle size. To account for this, as is discussed in Chapter 1, particle size is presented as the peak diameter rather than the Z-average. This still has its limitations as it remains a scattering intensity based value, however, it improves on the Z-average as it does not attempt to calculate an average diameter for particles which may be present as a multimodal distribution. This is the case for the Citrate and PEG coated CeO_2. A secondary peak (by intensity) exists for these particles that can be detected in MilliQ water, with an average hydrodynamic diameter of 10.5 nm for Citrate-CeO_2 and 14.8 nm for PEG-CeO_2. This fits well with the manufacturers stated primary particle size of 4-8 nm for both particles. The slightly larger size for the PEG-CeO_2 may correspond to the nature of the PEG association with the nanoparticle, where PEG molecules extend from the particle surface, providing steric stabilisation and so resulting in a larger hydrodynamic diameter. DLS of Uncoated-CeO_2 (4-8 nm) found particles aggregated so rapidly their Z-average upon dispersing in either ultrapure MilliQ or freshwater was >1000 nm, PDI >0.7 and after 24 hours there was almost total sedimentation of the samples, with no detectable signal in suspension. This was similar to the findings of the JRC for the uncoated NM-series CeO_2[9]. Uncoated-CeO_2 particles had a similar positive zeta potential of +12 mV as the uncoated NM-series particles and so will likely experience similar behaviour in freshwater. This may go some way to explaining the lack of bioaccumulation of uncoated NM-series nanoparticles compared to thestabilised Citrate and PEG-CeO_2 particles.

Particle behaviour in freshwater

In freshwater, both Citrate and PEG-CeO_2 experienced destabilisation to some extent, resulting in aggregation/agglomeration and subsequent sedimentation of particles. Citrate-CeO_2 particles remaining in suspension aggregated across the 6 days, fluctuating between 300 and 1000 nm after 48 hours (Figure 2.2 B), indicating dynamic aggregation and sedimentation as large particles are lost from suspension. PEG-CeO_2 was even less stable than Citrate-CeO_2. These particles experienced rapid aggregation immediately after dispersion in freshwater, the large peak diameter >4000 nm reflecting large particles acting under gravity and sedimenting rather than being driven by Brownian motion. As such, these sizes should be used as an indicator of the stability state of the

particles rather than definitive diameters.Particles which undergo gravitational settling cannot be accurately measured with DLS, resulting in the large, micron-sized readings, which mask any smaller particles in suspension. Whilst such data must be treated with caution as to the values calculated, this still provides important qualitative data concerning the stability of these particles in the freshwater media.

Overall, these results indicate that primary sized CeO_2 particles can exist (11-15 nm) in dispersion in water, however, the majority of the particles are likely to experience aggregation and sedimentation within the sediments, thus reducing their mobility and increasing the likelihood of attachment to the solid fraction of the sediment.

2.4.2 Nanoparticle size and surface functionalisation does not significantly alter the fate of CeO_2 nanoparticles within the sediment

All forms of CeO_2 were predominantly immobile within the sediment (~99% bound to the solid fraction of the sediment) and there was no dissolution of Ce from nanoparticles during the exposure irrespective of their size or surface coating (Table 2.3), a finding that is supported in previous studies [8, 20]. Ce^{III} did present a small fraction of dissolved Ce in the pore waters ~ 0.867 μgkg^{-1}but a colloidal concentration similar to that of nanoparticulate Ce of 10.6 μgkg^{-1}. For the NM-series particles, their positive surface charge (Table 2.1) is likely to lead to rapid association with negatively charged components of the sediment, including overall negatively charged clays and organic matter. In freshwater,coated CeO_2 nanoparticles also appear to aggregate, reaching sizes of >200 nm (Figure 2.2 B and D), which would exclude the majority from the colloidal fraction of the sediments we examined (<200 nm).

This immobility of the coated CeO_2could be due to heteroaggregation of the negatively charged Citrate and PEG-CeO_2nanoparticles (Table 2.1) with natural organic matter or to positively charged edges in lattice layer clays and on amorphous iron and aluminium oxides, especially at lower pH where there is increased protonation of hydroxyl groups [8]. In our sediments, the pH of the overlying water was 7.75 $^+$/- 0.03, whist pH of the pore waters separated from the sediment were 7.45 +/- 0.01. Clays such as montmorillonite undergo protonation of Al-OH groups only at pH <6.5, therefore during our exposure, such clays would be likely to largely retain their negative charge [21]. Whilst at low

ionic strength and at low nanoparticle concentrations, this can be sufficient to prevent heteroaggregation between negatively charged nanoparticles and clays, under higher ionic strengths this is not always the case. For example, 30 nm TiO_2 NPs at 4 mgL^{-1} under conditions of 0.1 M ionic strength and pH 8 have been shown to still experience heteroaggregation with a sodium montmorillonite clay [22]. Such relatively high ionic strength leads to a compression of the electric double layer extending from negatively charged surfaces, thus lowering the interaction energy barrier which attractive van der Waals forces must overcome for aggregation. This can then increase deposition of nanoparticles onto colloids in saturated porous media like sediments [23].

Conditions during our exposure were pH ~7.5, a relatively high ionic strength of ~0.01 M and with an initial spiking concentration of ~100 mgL^{-1}Ce. Surface charge as represented by zeta-potential was reduced for both coatednanoparticles in freshwater as compared with MilliQ water from -37.9 and -48.9 mV in MilliQ to -15.7 and -16.5 mV in freshwater for Citrate and PEG-CeO_2 respectively. This could reduce their stability against heteroaggregation with negatively charged constituents of the sediment. Interestingly, whilst zeta-potential for Citrate-CeO_2 in freshwater remained stable across the biological exposure period, the zeta-potential for PEG-CeO_2 was significantly reduced over time, to -6.3 mV. This could be due to the lower affinity that the PEG coating has for CeO_2, meaning there is loss of stabilising coating from the NP surface over time. This may have been responsible for the slightly lower persistence of colloidal Ce in the pore waters for PEG-CeO_2 exposures compared to the other forms of CeO_2(Table 2.3) and greater propensity for agglomeration (Figure 2.2B). Therefore, it is likely that the high association of CeO_2 with the solid fraction of the sediment is due to this deposition via van der Waals forces onto natural colloidal surfaces and incorporation of CeO_2 into larger flocs or heteroaggregates of natural organic matter which could not pass through the 0.2 μm filter. It would appear from these results that the heteroaggregation of Ce to the solid fraction of the sediment and lack of dissolution prevented direct transdermal uptake of the CeO_2 NPs by the sediment dwelling worms. This led to the size or form of surfactant having little influence over fate and bioavailability of CeO_2 NPs within the sediment, resulting in limited accumulation and only through dietary pathways. Instead,

sediment properties rather than particle characteristics determine the fate of nanoparticles during these exposures.

2.4.3 Dissolved species of Ce^{III} are accumulated through both ingestion and transdermal uptake from waterborne exposures

Worms were exposed in freshwater for 24 hours to two concentrations of Ce^{III} spiked as Ce(III)NO$_3$. The highest concentration was similar to the loading rate of Ce^{III} in subsequent sediment exposures, equivalent to a spiking concentration of 5 mgkg^{-1}. Both exposures resulted in significant uptake of Ce across all organism groups as compared to the controls. At the higher mgL^{-1} concentration, the presence of Ce also induced a physiological response from the organisms, resulting in the production of excess mucus. The lower concentration exposure was performed to confirm the transdermal accumulation of Ce observed in the higher concentration exposure.

Both exposures resulted in significant uptake of Ce compared to the controls. At the higher concentration, accumulation differed between both treatment (Ce^{III} versus controls) and organism groups. Feeding organisms with no gut clearance phase accumulated significantly more Ce than any other organism group when exposed to 12.9 mgL^{-1} Ce. This indicates there is some contribution of imbibed fluid towards overall body burdens which is then lost from these feeding organisms after gut clearance. As there was no significant difference between feeding clearance and non-feeding clearance organisms, we can conclude that this fluid in the gut does not contribute to body burdens through assimilation of Ce within the gut over this short time scale. As such, body burdens between 0.6 and 2.3 µgL^{-1} Ce can be attributed to transdermal uptake during these high concentration exposures.

Transdermal uptake is confirmed for Ce^{III} at the lower concentration exposure of 7.1 µgL^{-1} Ce. In this case, body burdens were lower and differences between organism groups were indistinguishable. Therefore, as there was no difference in body burdens of Ce between organism groups, all uptake of Ce is attributable to transdermal uptake.MINTEQ modelling (Table 2.4) found that a significant proportion of Ce is in the Ce^{III} form, 22.13% and 6.449% respectively for the high and low concentration exposures. The pharmacokinetics of dissolved cerium ions differs from that of nanoparticles. Dissolved Ce^{III} can act as a Lewis-acid, orientating towards Lewis-base OH$^-$ in cell plasma membrane

78

proteins. This has been demonstrated by the targeting of Ce^{III} to cell plasma membrane proteins in horseradish and uptake into cells exposed at high µM concentrations [24]. The Ce^{III} then forms a Lewis acid-base adduct, with the oxygen donating a lone electron pair to the Ce^{III} and resulting in a single reaction product with no secondary products. The effect of this within biological systems is that dissolved Ce ions experience slower elimination from the blood and accumulation in the skeleton, liver, kidneys and gastrointestinal tract of rats intravenously injected with cerium chloride[25]. This Lewis acid-base type reaction may be the mechanism for transdermal accumulation of dissolved Ce in non-feeding worms.

2.4.4 Mucus production in response to mgL^{-1} waterborne CeO_2 exposures limits interpretation of the role of size on nanoparticle uptake

Water only exposures were used to assess the influence of nanoparticle size upon uptake. Organisms were exposed to a calculated concentration of 11.3 mgL^{-1} Ce for NM211, NM212 and 1.13 mgL^{-1} NM213. These concentrations were chosen as they represent similar concentrations to the total Ce added to sediment exposures, but in the absence of solid sediment material. Whilst they are high relative to the expected diffuse concentrations in freshwater environments, predicted in the ngL^{-1} range [26], similar concentrations in the mgL^{-1} range are routinely tested in the literature. For example, investigations into the uptake and toxicity of CeO_2 to *D. magna* have been performed at concentrations between 0.1-10 mgL^{-1} [27], tens of mgL^{-1} [28] and 10 – 1000 mgL^{-1} [29].

Such high concentrations appear to be unsuitable for quantitative analysis of the bioaccumulation of CeO_2 from waterborne exposures in *L. variegatus*. Exposure to these concentrations of nanoparticles elicited a possible defence mechanism, where organisms shed a mucus layer in response to cerium exposure. This behaviour was only apparent in the engineered cerium treatments, not the controls and so is likely a response mechanism to either the abrasive effect of the nanoparticles or to the presence of cerium itself. An example of these mucus casts can be seen in Figure 2.6. Mucus casts were pooled per treatment type so as to collect sufficient mass to weigh a dry weight prior to ICP-MS, giving a single pooled sample for each exposure. Therefore, no statistical analysis of differences in Ce concentration in the mucus between treatments can be made. However, each treatment did induce production of

mucus casts containing a concentration of Ce in the μgmg^{-1} range. This supports the hypothesis that these mucus casts are a response or defence mechanism, incorporating engineered Ce and then shedding this mucus layer to reduce contact of nanoparticles with the organisms' epidermis.

This physiological response makes interpretation of the bioaccumulation data difficult. Organisms in waterborne exposures experienced body burdens as high as in the μgmg^{-1} range, an order of magnitude higher than is observed when engineered CeO_2 is spiked to sediments at a similar concentration (Figure 2.7).Organisms experienced large variation between exposure units, with no statistically significant effectof either nanoparticle treatment or organism group upon body burdens. As a result of this wide variation, nanoparticle treatments could not be distinguished from control concentrations, even though average body burdens were in some cases several orders of magnitude greater. We suggest that the wide variation measured is due to some of this mucus associated Ce being retained at the organisms' surface during sampling and so body burdens measured do not truly represent the accumulated metal concentrations. No such mucus production was observed when organisms were exposed to Ce^{III} at 7.1 μgL^{-1}.The high concentration of CeO_2 in these exposures appears to have induced a response in the organisms, producing layers of mucus which were sufficient in quantity to shed to the surrounding water.

Mucus production in other aquatic worms as a response to metal stressors has been documented, including *Tubifex tubifex*in the presence of aqueous cadmium and copper in exposures representing highly contaminated sediment sites with metal concentrations in the $mgkg^{-1}$ range [30]. Excessive mucus production has also been implicated in the toxicity of zinc and lead at mgL^{-1} concentrationsto *T. tubifex* and *Limnodrilus hoffmeisteri*[31]. It is conceivable that in exposing the organisms to such a high concentration of CeO_2 in the water, the CeO_2 nanoparticles themselves face an additional or less permeable barrier to uptake in the form of this mucus layer [32] than if the organisms were exposed at a lower concentration. The NM-series particles have a positive charge in ultrapure waters of between +28 and +33 mV.Positively charged nanoparticles may experience transport through mucus barriers 20-30 times slower than negatively charged particles[33] which would explain the effective incorporation of these particles in the mucus[34]. This is important as in much of the literature,

concentrations exceeding those used in this study are routinely examined to assess ecotoxicological effects of CeO_2 nanoparticles to aquatic organisms, often in the mgL^{-1} concentration range[35, 36].

Such high concentrations of CeO_2 may be eliciting similar responses in other organisms. In fact, an ancillary finding of the work by Conway *et al.* 2014 [37] was that the marine mussel *Mytilus galloprovincialis*produced double the mass of pseudofaeces when exposed to 3 mgL^{-1} uncoated CeO_2 nano-rods (dimensions $67 \pm 8 \times 8 \pm 31$ nm) than in controls. They propose that this was due to the mussels perceiving the CeO_2 as inedible and so increasing pseudofaeces production to limit intake of the nanoparticles. In our case, this may be more as a direct physiological response to the cerium contamination. As mucus cast production occurred in both nanoparticle and Ce^{III} exposures it is likely that this is a direct response to the elemental cerium itself rather than a response to the mechanical abrasion of the nanoparticles.This mucus production in by aquatic worms in response to high metal exposures has been documented as far back as in 1968 [31]. Still, the capacity for mucus production to be stimulated in the presence of metals and to act as a barrier to nanomaterial uptake is too rarely acknowledged in the nano-ecotoxicology literature, with some notable exceptions such as the review by Handy *et al.* 2008, into the mechanistic uptake of nanomaterials in fish [38].

Future exposures would need to be conducted at lower concentrations in the sub mgL^{-1} range to avoid inducing the formation of these mucus layers. This would allow the accumulation behaviour of these nanoparticles to be investigated as a function of their primary particle size and properties, rather than as a function of the defensive response the ceriumelicits from the organisms themselves. A move in the wider nano-ecotoxicology field towards lower concentrations is also encouraged in order to assess mechanisms of toxicity that have greater environmental relevance.

2.4.5 The role of size and dissolution on bioaccumulation of CeO_2 from sediments

In sediment exposures, size played no role in the extent of bioaccumulation of ceria for the uncoated NM-series CeO_2 particles. Whilst there was some contribution of sediment ingested CeO_2 towards body burdens for NM212 and Ce^{III}, after a gut clearance phase this was not sufficient to result in appreciable

accumulation of cerium compared to the controls (Figure 2.7). These NM-series particles were provided as dry powders with a positive Zeta potential when dispersed in ultrapure water of +28 and +33 mV for NM211 and NM212 respectively. As such we expect rapid and strong association of these nanoparticles to the largely negatively charged solid constituents of the sediment. Alumina clays are abundant in sediments and are largely negatively charged due to isomorphous substitution of a single Si^{4+} with Al^{3+} in the neutrally charged Si_2O_4 quartz crystal to form the clay $SiAlO_4^-$. Binding of the positively charged uncoated CeO_2 nanoparticles to these negative sites within the solid fraction of the sediment could prevent dissociation of CeO_2 within the gut and subsequent uptake across the gut epithelia. As no significant difference was calculated between exposed worms and controls after the gut clearance these CeO_2particles were not considered accumulated during the 5 day exposure period from the sediments.

Ce^{III} on the other hand experienced some transdermal accumulation of Ce, above that in controls. This supports the observation of transdermal accumulation in waterborne exposures (Figure 2.4), but in this case of uptake from sediments, accumulation was only significant for non-feeding organisms before the clearance phase in clean freshwater. Accumulation was less from sediments (7.9 $ngmg^{-1}$) compared to in waterborne exposures (2.3 μgmg^{-1}) when exposed to similar total concentrations of Ce^{III}. Sediments therefore reduced the bioavailability of dissolved cerium to the organism. However, these results indicate that dissolved and nanoparticulate forms of the metal experience very different routes to uptake, with Ce^{III} available for uptake across the skin, a pathway that was not possible for nanoparticulate CeO_2.

2.4.6Small stabilised nanoparticles are accumulated through diet from sediments, but surface functionalisation does not alter the extent of uptake

The size of uncoated NM-series nanoparticles did not alter the route or extent of uptake of CeO_2 from sediments. These particles were not accumulated in any feeding organism once their gut contents had been cleared. This was markedly different from the results forstabilizedCeO_2 nanoparticles. Exposure to 4-8 nmuncoated and coated nanoparticles resulted in accumulation of Ce above background levels of the controls in feeding organisms. After a gut clearance

phase, all three nanoparticles were accumulated significantly above the controls. Interestingly, this accumulation was not significant for micron sized CeO_2, indicating that translocation of CeO_2 within the gut of these worms is only possible for nanoparticulate CeO_2. Considering that no difference in this accumulation through ingestion was found between nanoparticle treatments, this confirms that sediment properties are responsible for the bioavailability of these nanoparticles, not the properties of the particles themselves. This was true for both the fate of the particles within the sediments and their subsequent bioaccumulation. Although there was some bioaccumulation of CeO_2 from these nanoparticle treatments, CeO_2 was not considered biomagnified during this exposure as BAF_5 were ~0.1 $kgkg^{-1}$ and so concentrations of Ce within the worms did not exceed that in the surrounding sediment.

Without a gut clearance, BAF_5 was no different in CeO_2 treatments than in the controls,most likely due to sediment associated Ce in the guts dominating body burdens.This means that after relatively short exposures, the accumulated Ce available for trophic transfer through the food chain (say through predation of these worms by fish) is not significantly higher for worms exposed to CeO_2nanoparticles than either micron sized CeO_2 or natural Ce in the sediments (Figure 2.8).

This poses an interesting question for researchers and regulators alike, as standard test guidelines for calculating BAF such as the OECD test number 315, recommend no gut clearance phase [4] as this should return the most conservative BAF. However, this experiment demonstrates that under shorter exposure periods (5 days) and for nanomaterials where accumulation is low, calculating BAF in this way does not capture the whole picture required to understand bioaccumulation of nanoparticles. Due to the low concentrations accumulated within the organisms between 5-20 $ngmg^{-1}$ compared to the naturally occurring concentration in the sediments (43.6 $ngmg^{-1}$), retaining sediment material within the gut when sampling masks the truly accumulated CeO_2 that is not simply associated with ingested sediment material in the gastrointestinal tract.When this ingested material is eliminated from the organisms during the gut clearance phase, it becomes apparent that there is indeed some additional accumulation of Ce when worms are exposed to nanoparticulate CeO_2 compared with natural Ce present in the sediments.

Therefore, careful consideration should be taken whether to measure and report BAF values that represent the concentration available for trophic transfer through food chains (feeding organisms including their gut contents) or that which remains accumulated within the organism after this material in the guts has been removed. This decision should be hypothesis driven and acknowledgement of this made when interpreting BAF values for engineered nanomaterials in the environment.

Conclusions

In this work we successfully exploit *L. variegatus'* remarkable capacity for regeneration of lost body segments to create two phenotypes: feeding and non-feeding worms to investigate the relative importance of ingestion and transdermal uptake for nanoparticle bioaccumulation. Persistence of cerium in either the colloidal or dissolved phases of the pore water successfully provided the context within which to interpret uptake of cerium in the worms. Dissolved Ce^{III} was available through ingestion and transdermal uptake in both waterborne and sediment based exposures. The mechanism for this transdermal uptake however, is not yet clear. Transdermal uptake in waterborne exposures far exceeded that from sediments (body burdens of 1.4 μgmg^{-1} in freshwater compared to 7.9 $ngmg^{-1}$ in sediments), likely owing to the lower persistence of dissolved Ce species in sediments. No nanoparticle treatment on the other hand experienced transdermal uptake from waterborne or sediment exposures. Waterborne exposures at mgL^{-1} must be treated with caution. These concentrations are high relative to predicted environmental concentrations but are routinely used in the literature. Future studies must acknowledge the potential for such exposures to elicit an increase in mucus production, observed in these experiments, which could act as a barrier to uptake and complicate the interpretation of bioaccumulation and toxicity of nanomaterials.

In sediments, no CeO_2 nanoparticle dissolved and their persistence in the colloidal fraction of the pore waters was <1% of the dosed concentration. 10 nm, 28 nm and micron sized CeO2 with no stabilising coatings (NM-series particles) were not bioaccumulated through either ingestion or transdermal uptake once gut contents had been evacuated. Small nanoparticles (primary particle size <10 nm) with stabilising coatings were accumulated from

sediments, but did not undergo biomagnification (BAF_5 0.087 and 0.083 $kgkg^{-1}$ for Citrate-CeO_2 and PEG-CeO_2 respectively). The form of coating (electrostatic or steric) did not alter the route or extent of accumulation of cerium from sediments, nor their fate within sediments. Therefore, whilst nanoparticle surface coatings may increase bioavailability of CeO_2 through feeding, we have demonstrated that in sediment environments the potential for biomagnification is low, with uptake of engineered CeO_2 not exceeding that in the surrounding sediment after 5 days exposure.

References

1   D. Nam, B. Lee, I. Eom and P. Kim, *Mol. Cell. Toxicol.*, 2014, **10**, 9–17.

2   A. M. Lohrer, S. F. Thrush and M. M. Gibbs, *Nature*, 2004, **431**, 1092–1095.

3   R. K. Cross, C. Tyler and T. S. Galloway, *Environ. Chem.*, 2015, **12**, 627.

4   OECD, *OECD Guidelines for the Testing of Chemicals 315: Bioaccumulation in Sediment-dwelling Benthic Oligochaetes*, OECD Publishing, 2008.

5   V. G. Martinez, P. K. Reddy and M. J. Zoran, *Hydrobiologia*, 2006, **564**, 73–86.

6   M. T. Leppänen and J. V. K. Kukkonen, *Environ. Sci. Technol.*, 1998, **32**, 1503–1508.

7   M. V. Karlsson, S. Marshall, T. Gouin and A. B. A. Boxall, *Environ. Toxicol. Chem.*, 2016, **35**, 836–842.

8   G. Cornelis, B. Ryan, M. J. McLaughlin, J. K. Kirby, D. Beak and D. Chittleborough, *Environ. Sci. Technol.*, 2011, **45**, 2777–2782.

9   C. Singh, S. Friedrichs, G. Ceccone, N. Gibson, K. A. Jensen, M. Levin, H. Goenaga Infante, D. Carlander and K. Rasmussen, *Cerium Dioxide, NM-211, NM-212, NM-213: Characterisation and Test Item Preparation*, 2014.

10   Prospect, 2010, 1–10.

11   B. K. Gaiser, A. Biswas, P. Rosenkranz, M. A. Jepson, J. R. Lead, V. Stone, C. R. Tyler and T. F. Fernandes, *J. Environ. Monit.*, 2011, **13**, 1227.

12   J. Hammes, University of Trier, 2012.

13   OECD, *Guidance on sample preparation and dosimetry for the safety testing of manufactured nanomaterials*, 2012.

14   D. R. Mount, T. D. Dawson and L. P. Burkhard, *Environ. Toxicol. Chem.*, 1999, **18**, 1244–1249.

15   RStudio Team, 2016.

16   M. Auffan, A. Masion, J. Labille, M. A. Diot, W. Liu, L. Olivi, O. Proux, F. Ziarelli, P. Chaurand, C. Geantet, J. Y. Bottero and J. Rose, *Environ. Pollut.*, 2014, **188**, 1–7.

17   I. W. Siriwardane, University of Iowa, 2012.

18   Y. Liu, M. K. Shipton, J. Ryan, E. D. Kaufman, S. Franzen and D. L. Feldheim, *Anal. Chem.*, 2007, **79**, 2221–2229.

19   S. Westrøm, *NTNU (Norwegian Univ. Sci. Technol.*

20   J. Liu, S. Legros, G. Ma, J. G. C. Veinot, F. von der Kammer and T. Hofmann, *Chemosphere*, 2012, **87**, 918–924.

21   E. Tombácz and M. Szekeres, *Appl. Clay Sci.*, 2004, **27**, 75–94.

22   J. Labille, C. Harns, J. Y. Bottero and J. Brant, *Environ. Sci. Technol.*, 2015, **49**, 6608–6616.

23   W. Sang, V. L. Morales, W. Zhang, C. R. Stoof, B. Gao, A. L. Schatz, Y. Zhang

and T. S. Steenhuis, *Environ. Sci. Technol.*, 2013, **47**, 8256–8264.

24 G. Yang, Z. Sun, X. Lv, Y. Deng, Q. Zhou and X. Huang, *Biol. Trace Elem. Res.*, 2012, **150**, 396–402.

25 R. A. Yokel, S. Hussain, S. Garantziotis, P. Demokritou, V. Castranova and F. R. Cassee, *Environ. Sci. Nano*, 2014, **1**, 406–428.

26 F. Gottschalk, T. Sun and B. Nowack, *Environ. Pollut.*, 2013, **181**, 287–300.

27 B. K. Gaiser, T. F. Fernandes, M. A. Jepson, J. R. Lead, C. R. Tyler, M. Baalousha, A. Biswas, G. J. Britton, P. A. Cole, B. D. Johnston, Y. Ju-Nam, P. Rosenkranz, T. M. Scown and V. Stone, *Environ. Toxicol. Chem.*, 2012, **31**, 144–154.

28 A. García, R. Espinosa, L. Delgado, E. Casals, E. González, V. Puntes, C. Barata, X. Font and A. Sánchez, *Desalination*, 2011, **269**, 136–141.

29 K. van Hoecke, J. T. K. Quik, J. Mankiewicz-Boczek, K. a C. De Schamphelaere, A. Elsaesser, P. van Der Meeren, C. Barnes, G. Mckerr, C. V. Howard, D. van De Meent, K. Rydzyn, K. a Dawson, A. Salvati, A. Lesniak, I. Lynch, G. Silversmit, B. De Samber, L. Vincze and C. R. Janssen, *Environ. Sci. Technol.*, 2009, **43**, 4537–4546.

30 L. Méndez-Fernández, M. Martínez-Madrid and P. Rodriguez, *Ecotoxicology*, 2013, **22**, 1445–1460.

31 S. L. Whitley, *Hydrobiologia*, 1968, **32**, 193–205.

32 S. Ma and D. Lin, *Environ. Sci. Process. Impacts*, 2013, **15**, 145–160.

33 J. S. Crater and R. L. Carrier, *Macromol. Biosci.*, 2010, **10**, 1473–1483.

34 Z.-J. Zhu, R. Carboni, M. J. Quercio, B. Yan, O. R. Miranda, D. L. Anderton, K. F. Arcaro, V. M. Rotello and R. W. Vachet, *Small*, 2010, **6**, 2261–2265.

35 B. Collin, E. Oostveen, O. V. Tsyusko and J. M. Unrine, *Environ. Sci. Technol.*, 2014, **48**, 1280–1289.

36 T. Marie, A. Mélanie, B. Lenka, I. Julien, K. Isabelle, P. Christine, M. Elise, S. Catherine, A. Bernard, A. Ester, R. Jérôme, T. Alain and B. Jean-Yves, *Environ. Sci. Technol.*, 2014, **48**, 9004–9013.

37 J. R. Conway, S. K. Hanna, H. S. Lenihan and A. A. Keller, *Environ. Sci. Technol.*, 2014, **48**, 1517–1524.

38 R. D. Handy, T. B. Henry, T. M. Scown, B. D. Johnston and C. R. Tyler, *Ecotoxicology*, 2008, **17**, 396–409.

Chapter 3

The role of surface functionalisation on the fate and route to uptake of partially soluble silver nanoparticles from sediments

Abstract

The epidermis provides the first barrier to the uptake of nanoparticles, but we know little of the role transdermal uptake upon nanoparticle bioaccumulation in sediment dwelling organisms. Using aquatic worms at different life stages we examined the uptake of 10 nm silver nanoparticles (Ag NPs) in feeding and non-feeding worms, comparing the relative importance of dietary versus transdermal uptake of particles with different stabilising coatings. Nanoparticle fate in sediment pore water was followed using centrifugation and ultrafiltration. We hypothesised that particle coatings would alter nanoparticle dissolution and partitioning within sediments, and so the route by which they are accumulated.

Particle coating altered the extent but not the route to uptake. Partially soluble Ag NPs, were accumulated predominantly through transdermal uptake to concentrations between 6.5 and 130 times greater than that in the sediment. The dissolved fraction of Ag in the sediment pore waters did not differ between nanoparticle coatings or between nanoparticles and a positive control of silver nitrate ($AgNO_3$). The extent of bioaccumulation did not differ between Citrate-Ag and $AgNO_3$, suggesting that all transdermal uptake of Citrate-Ag could be accounted for by the dissolved silver in the sediment pore waters. However, PEG-Ag exposed organisms experienced significantly more silver accumulation than either Citrate-Ag or $AgNO_3$, even though the total dissolved silver in the sediments did not differ. This suggests that only ~30% of Ag accumulated across the skin could be attributed to dissolved pore water Ag during exposures to PEG-Ag. This additional transdermal uptake of PEG-Ag may be due to either cellular uptake of the PEG-Ag nanoparticles themselves or due to increased surface associations of PEG-Ag to the epidermis of the worms, resulting in localised dissolution and transdermal uptake of soluble forms of silver.

Contents

3.1. Introduction

Silver nanoparticles (Ag NPs) are the focus of much research due to their rapidly expanding use in a variety of consumer goods and medical applications and their potential for release into freshwater environments in the effluent from waste water treatment plants for example[1]. Much research has been conducted on the toxicity of dissolved silver in the aquatic environment. Dissolved silver is largely accumulated in freshwater fish across the gills, where its toxic mechanism is through inhibition of sodium (Na^+) uptake, in particular through the universal membrane bound enzyme $Na^+/K^+/ATPase$ (or sodium-potassium pump)[2] and subsequent disruption of ionoregulation in the fish resulting in cardiovascular collapse. It is accumulated in the form of Ag^+ across epithelial cell membranes at the surface of the gill through these proton coupled Na^+ channels but may also experience passive uptake across membranes in freshwater when present as the neutral complex of $AgCl_0$ for example[3]. Nanoparticulate silver has also been recently implicated in this disruption of sodium regulation in Japanese medaka (*Oryziaslatipes*)larvae[4]. Therefore, the persistence of both dissolved and particulate silver during sediment based nanosilver exposures may lead to uptake of silver through both ingestion and transdermal accumulation.

The extent of dissolution of silver nanoparticles (Ag NPs) within sediments will depend upon the localised physicochemical properties they experience [5]. During water only exposures, the water flea *Daphnia magna* and the sediment dwelling worm *Lumbriculus variegatus* have been observed to experience very different biodynamic accumulation of silver whenexposed to Ag NPs for 48 and 96 hours respectively. Uptake and elimination of silver in *L. variegatus* appeared to be largely constrained by the bioavailability of dissolved silver species, released during each of the nanoparticle exposures, whilst *D. magna* exhibited an elimination profile that suggested a major contribution of ingested Ag NPs themselves towards silver bioaccumulation[6]. This is of interest as Chapter 2 concludes that for the case of cerium oxide nanoparticles (CeO_2 NPs) which prevail in the particulate form, ingestion was the only route available to bioaccumulation. The potential for dissolution of silver from Ag NPs within saturated porous media[7] indicates that whilst ingestion dominates bioaccumulation of ceria during CeO_2 NP exposures, this may not be the case

for silver. Transdermal uptake of dissolved forms of silver either through epithelial sodium channels or through passive diffusion of neutral species such as $AgCl_0$ may be possible within the sediment. Transdermal accumulation of silver nanoparticles themselves could also be possible, for example there is some evidence of cellular internalization of silver nanoparticles in epithelial cells in the gut of the estuarine worm *Nereisdiversicolor* through endocytotic pathways[8].

The fate of Ag NPs within sediment exposures will be influenced both by the physicochemical properties of the sediment and the characteristics of the nanoparticles themselves. For this study we examined two common commercial surfactants, citrate and polyethylene glycol (PEG) used to stabilise Ag NPs in dispersion. Negative citrate ions adsorb to the nanoparticle surface resulting in stabilisation of nanoparticles through electrostatic repulsion, whilst PEG strongly binds to Ag^+ at the nanoparticle surface through complexation of thiol groups to the silver, conferring steric stabilisation against aggregation[9]. Differences in surfactants have not only been demonstrated to alter aggregation kinetics of silver nanoparticles,[10] but also affect deposition and transport behaviour in sediments[11]. Various nanoparticle coatings have been demonstrated to alter silver dissolution within water only exposures. It is the extent of dissolution which has been proposed as responsible for the variation in toxicity of between silver nanoparticles to*D. magna*[12, 13]. Therefore we aim to assess the stabilising effect of two commercial surfactants on the partitioning of Ag NPs to the solid fraction of the sediments and between the colloidal and dissolved fractions of the pore waters during sediment based exposures using the sediment dwelling freshwater worm, *Lumbriculus variegatus.*

We hypothesise that modifying the nanoparticle surface with either citrate or PEG will alter the extent of dissolution or persistence of nano sized silver particles in the sediment pore waters (which may be available for transdermal uptake). A combination of centrifugation and filtration, established in Chapter 1was employed to examine the fate of these colloidal and dissolved transformation products of the NPs in the sediment pore waters. Bioaccumulation and the route to uptake of silver was also assessed using the freshwater worm *L. variegatus* using the procedure developed in Chapter 1. During these exposures feeding and non-feeding organisms are exposed to

nanoparticle spiked sediments for 5 days to investigate the relative importance of ingestion and transdermal uptake of silver from sediments.

By investigating the fate of silver during biological exposures we aim to assess whetherdifferences in silver accumulation during exposure to Citrate or PEG-Ag can be accounted for by changes in the dissolution of silver under the test conditions.

3.2. Methods

3.2.1 Materials

Two silver nanoparticles were investigated, electrostatically stabilised citrate coated Ag (Cit-Ag) and sterically stabilised PEG-mercaptopropionic ether (molecular weight 550 Da) coated Ag (PEG-Ag) each with a primary particle size of 3-15 nm according to the manufacturer (PlasmaChem, Germany). Nanoparticles were provided as dispersions in water and were prepared as detailed in Chapter 1.Silver nitrate ($AgNO_3$) was used as a representative ionic form of silver. Control exposures refer to Ag naturally present in the standard soil LUFA Speyer 2.4 (LUFA Speyer, Germany). Sample preparation to quantify silver concentrations in water, sediment and tissue samples followed the procedures outlined in Chapter 1. Samples were analysed using inductively coupled plasma mass spectrometry (ICP-MS).

3.2.2 Comparing size and stability of Ag NPs in MilliQ and freshwater

Detailed technical methods for this characterisation are presented in Chapter 1. Briefly, a combination of Dynamic Light Scattering (DLS) and Transmission Electron Microscopy coupled to Energy-dispersive X-ray Spectroscopy (TEM-EDS)was used to measure the characteristics of the primary particles as provided by the manufacturers in dispersion in MilliQ water. The stability and evolution of Ag NP size and aggregation state in both MilliQ water and freshwater over the 6 day bioaccumulation exposure period was assessed using DLS. Two experimental protocols were used to examine particle size, developed in Chapter 1.

Briefly, the first method involved particles left quiescent, from which aliquots of the supernatant were removed for DLS at each time point representing the evolution of particles which remained stable in suspension. This method is

referred to as the **stability analysis**. The second method differed by re-suspending agglomerates that sedimented during the incubation before each sampling point. This allowed characterisation of the full spectrum of agglomerates and aggregates that were developing during the biological exposures. This is referred to as **agglomeration analysis** and was performed for both DLS and TEM. Hydrodynamic size from DLS is reported as peak diameter. This refers to the mean diameter of the primary peak in the scattering intensity distribution, where generally 90% of the particles (by scattering intensity) fall.

Qualitative analysis of particle shape, agglomeration state and the persistence of distinct Ag NPs <100 nm is size at the end of the exposure period was carried out using TEM-EDS after 6 days incubation in freshwater. Samples were prepared as detailed in Chapter 1.

3.2.3 Investigating loss of particle coatings during dilution in different media

Using DLS, the effect of dilution upon nanoparticle stability was examined systematically across the first hour of preparation in freshwater and the dispersion vehicles (either Citrate or PEG vehicles) provided by the manufacturer. Dilutions were prepared of 10, 1 and 0.1 % of the original stock concentration to assess whether instability was due to a dilution effect of the nanoparticles themselves or the loss of the external excess citrate and PEG that occurs as Ag NPs were prepared for the biological exposures in freshwater. These dilutions lowered the Ag concentration nominally to 15.1, 1.51 and 0.151 μgml^{-1} when Citrate-Ag was diluted, whilst PEG-Ag resulted in nominal Ag concentrations of 12.6, 1.26 and 0.126 μgml^{-1}. The original concentration of excess citrate and PEG in the nanoparticle dispersions supplied by the manufacturer was 0.56 and 100 gL^{-1}respectively. Therefore, the total excess citrate concentration when diluted in MilliQ or freshwater was 56, 5.6 and 0.56 μgml^{-1} whilst the total excess PEG was nominally 10000, 1000 and 100 μgml^{-1}.

3.2.4 The relative importance of dietary versus transdermal uptake of silver

Feeding and non-feeding phenotypes were prepared in accordance with the rationale and methods set out in Chapter 1. The model system for investigating

the relative importance of dietary versus transdermal uptake of nanoparticles from sediments, developed in Chapter 1was used for this study.

Briefly, feeding and non-feeding organisms were prepared by synchronising organisms through inducing fractionation through a small incision to the mid-section of the worm. Sediments were prepared 24 hours prior to exposure, following the wet spiking protocol outlined in Chapter 1, to a desired concentration of 2.5 $mgkg^{-1}$ calculated from the nanoparticle stock concentrations provided by the supplier. Discrepancies between the stated concentrations and the measured Ag concentration in the stocks resulted in slight deviation from the desired concentration of 2.5 $mgkg^{-1}$ Ag.These worms were then exposed to either 0.76 $mgkg^{-1}$ Citrate-Ag, 0.12 $mgkg^{-1}$ PEG-Ag, 3.3 $mgkg^{-1}$ $AgNO_3$ or controls of uncontaminated sediment.

5 worms were randomly assigned per exposure unit and each organism group consisted of at least 5 replicates. In addition to the two main phenotypes of feeding and non-feeding worms, these groups were subdivided into those which experienced a gut clearance phase of 6 hours (e.g. **"Feeding gut clearance"**) and those which did not (e.g. "**Feeding**"). Organisms were exposed to the sediment for 5 days in the same fashion as in Chapter 1, before removal, gut clearance (where necessary) and finally snap freezing in liquid nitrogen to store at -80 °C.

3.2.5 Fate of Ag nanoparticles in sediment during the biological exposures

The rationale for determining the partitioning of Ag NPs to the solid, colloidal and dissolved fraction of the sediment is presented in Chapter 1. In this study, the dissolved fraction of the sediment was used to calculate the transdermal uptake of silver attributable to dissolved species of silver in the sediment pore waters.

3.2.6 Modelling the speciation of silver nitrate in the simulated pore waters

Using the open software water chemistry tool Visual MINTEQ (Visual MINTEQ v3.1, Sweden) the speciation of silver nitrate dissolved in the OECD freshwater used during these experiments was modelled. This modelling was based upon the working assumption that the chemical composition of the sediment pore waters was identical to the prepared freshwater media used to saturate the

95

sediments. This allows us to examine the speciation of silver between dissolved and precipitated phases in the absence of the solid fraction of the sediment. This acts as a conservative worst case scenario for the presence of dissolved species of Ag within sediment pore waters.

3.2.7 Data handling and statistics

Bioaccumulation factors after 5 days (BAF$_5$) were calculated as:

$$\text{BAF}_5 = \frac{C_{org}}{C_{sed}} \qquad \text{(Eq.1)}$$

C$_{org}$ refers to the body burden or elemental concentration of the relevant nanoparticle within the organism normalised to dry tissue mass (ng mg^{-1}) after 5 days exposure, whilst C$_{sed}$ refers to the elemental concentration of Ag within the sediment normalised to dry sediment mass (ng mg^{-1}). It should be noted that C_{sed} is the combined concentration of background elemental concentration and the additional spiked nanoparticle. BAF$_5$ has the units of kg dry weight organism per kg dry weight sediment (kg kg^{-1}).

To investigate the relationship between nanoparticle fate in the sediments and their bioaccumulation, body burdens normalised to the concentration of dissolved LMW species of the nanoparticles were also calculated for non-feeding organisms in exposures (Eq. 2). This assumes that all transdermal uptake is of dissolved LMW species. The rationale is that adjusting the Bioaccumulation Factor for Low Molecular Weight Species (BAF$_{LMW}$) will allow examination of whether LMW species explain the accumulation of nanomaterials during the investigation by comparing the capacity for BAF$_5$ and BAF$_{LMW}$ to explain variation in the accumulated body burdens.

$$\text{BAF}_{LMW} = \frac{C_{org}}{C_{LMW}} \qquad \text{(Eq.2)}$$

Once again, C$_{org}$ refers to the body burden or elemental concentration of the relevant ENM within the organism normalised to dry tissue mass (ng mg^{-1}) after 5 days exposure, whilst C$_{LMW}$ refers to the elemental concentration of dissolved LMW species within the sediment normalised to dry sediment mass (ng mg^{-1}). BAF$_{LMW}$ has the units of kg dry weight organism per kg dry weight sediment (kg kg^{-1}).

All statistical analysis was performed in R[14]. For the bioaccumulation study a minimum adequate model approach was taken to explain the data set using a factorial design two way analysis of variance. Examination of normality and homogeneity of variance through plotting of residuals and Q-Q plots found that body burdens of silver accumulated did not conform to the assumption of normality. Box-Cox analysis resulted in the choice of log-transforming both the body burdens and BAF_5 data for use in the ANOVA model. A linear model was only constructed for BAF_5 once the ANOVA confirmed that each silver treatment experienced significant accumulation of silver above the control body burdens (Dunnett contrasts, $p < 1e^{-10}$ for each silver treatment compared to the control). Control BAF_5 was not calculated or examined in the model as the low background concentration of Ag in the sediment one order of magnitude lower than the treated concentrations results in artificially high BAF_5 that are non-comparable with our treatment BAF_5. When analysing the BAF_{LMW} data for non-feeding organisms, descriptives of normality required square root transformation of the data to comply with the assumptions of the ANOVA.

Data where there was no interaction effect was examined using Tukey's HSD whilst data sets where an interaction effect was present used the least-squares means (LSM) pairwise contrasts using Tukey's method. Graphs present means, standard errors and statistically significant differences with significance taken as $p< 0.05$.

3.3. Results

3.3.1 Characterisation of pristine particles and the effect of dilution on stability

The pristine particles differed from the manufacturers stated characterisation in some respects. DLS found the primary peak size by scattering intensity of both Citrate and PEG-Ag to be greater than the stated size of 10 nm (Table 3.1). However, quantitative analysis of TEM images after incubation of nanoparticles for 6 days in freshwater found that some distinct primary particles could persist in this size range. The calculated primary particle diameters of 10.63 and 6.7 nm for Citrate and PEG-Ag respectively align closer with the manufactures stated size (~10 nm). The electrostatic nature of the citrate stabiliser was apparent in MilliQ water, with a surface zeta potential of -43.3 mV. PEG acts as

an electro-steric stabiliser presenting a zeta potential of -28.96 mV in MilliQ at the start of the incubation.

Table 3.1: Characteristics of the pristine particles in ultrapure MilliQ water(5.67 μgml⁻¹). TEM size calculated from primary sized particles which persisted as individual particles and loose agglomerates in freshwater after 6 days incubation (+/- standard deviation).

Treatment	Primary peak inMilliQ water (nm)	Primary particle size TEM, freshwater (nm)	Zeta-potential MilliQ (mV)	Sediment concentration (mgkg⁻¹)
Citrate-Ag	45.2	10.63 +/- 3.35	-43.3	0.76
PEG-Ag	130.9	6.7 +/- 2.59	-28.96	0.12

The stability of particles immediately after dispersion in different media was examined using DLS to assess the effect of dilution upon nanoparticle aggregation. Diluting the Ag NPs in their respective ligand vehicles allowed us to test the effect of diluting of nanoparticles whilst maintaining the excess ligand concentration (of citrate or PEG) and so to infer whether stability is lost for either AgNP as the concentration of excess surfactant decreases and whether this behaviour differs between dilution in MilliQ or in freshwater (Figure 3.1).
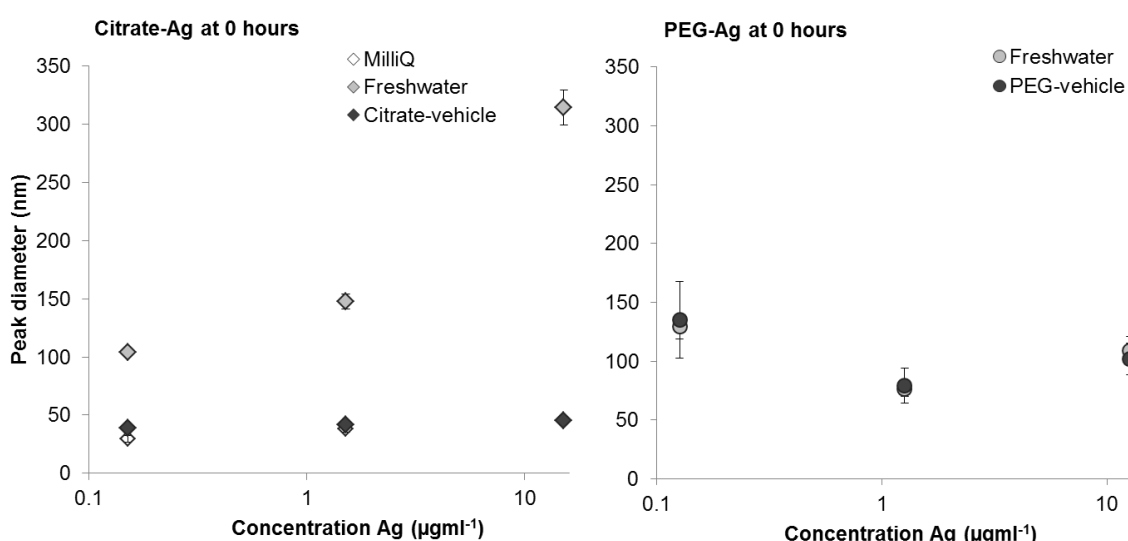
Figure 3.1: Effect of dilution upon particle stability and size immediately after dispersion in MilliQ (open symbols), freshwater (light grey symbols) and the nanoparticle vehicle (dark grey symbols).

Citrate-Ag was stable in MilliQ and the citrate vehicle at all dilutions (Figure 3.1), though at the lowest concentration, Citrate-Ag diluted in MilliQ was significantly smaller, with a peak size of 29.55 nm compared with 38.95 nm in the citrate vehicle (p = 0.006, Tukey's least significant means). DLS measures the hydrodynamic diameter of the particle, including its surface coating; therefore this could be due to the loss of some citrate from the nanoparticle surface in MQ resulting in an apparent reduction in size. In freshwater these particles were less stable, aggregating to 314 nm when at a concentration of 15.1 μgml^{-1}. These particles appeared to aggregate to a smaller size at lower concentrations, suggesting that the number of particles may have a limiting effect on aggregation. A secondary smaller size cohort of particles between 9 and 34 nm were also detected at lower concentrations (0.151 and 1.51 μgml^{-1}), similar in size to primary particles measured using TEM (Table 3.1). PEG-Ag on the other hand experienced no difference in behaviour in freshwater than when diluted in the PEG-vehicle (p= 0.969, ANOVA) indicating that at least during the first hour of preparation, the PEG is not lost from the nanoparticle surface to the surrounding media. At the lowest concentration of 0.126 μgml^{-1} the peak size of particles was significantly greater at ~130 nm than the ~78 nmof those at 1.26 μgml^{-1} (p=0.003, Tukey's HSD). However, the count rate at 0.126 μgml^{-1} in both media had dropped to <50 kcps, reducing the sensitivity of the measurements.

3.3.2 Qualitative examination of nanoparticle size, shape and chemical transformations after 6 days incubation in freshwater.
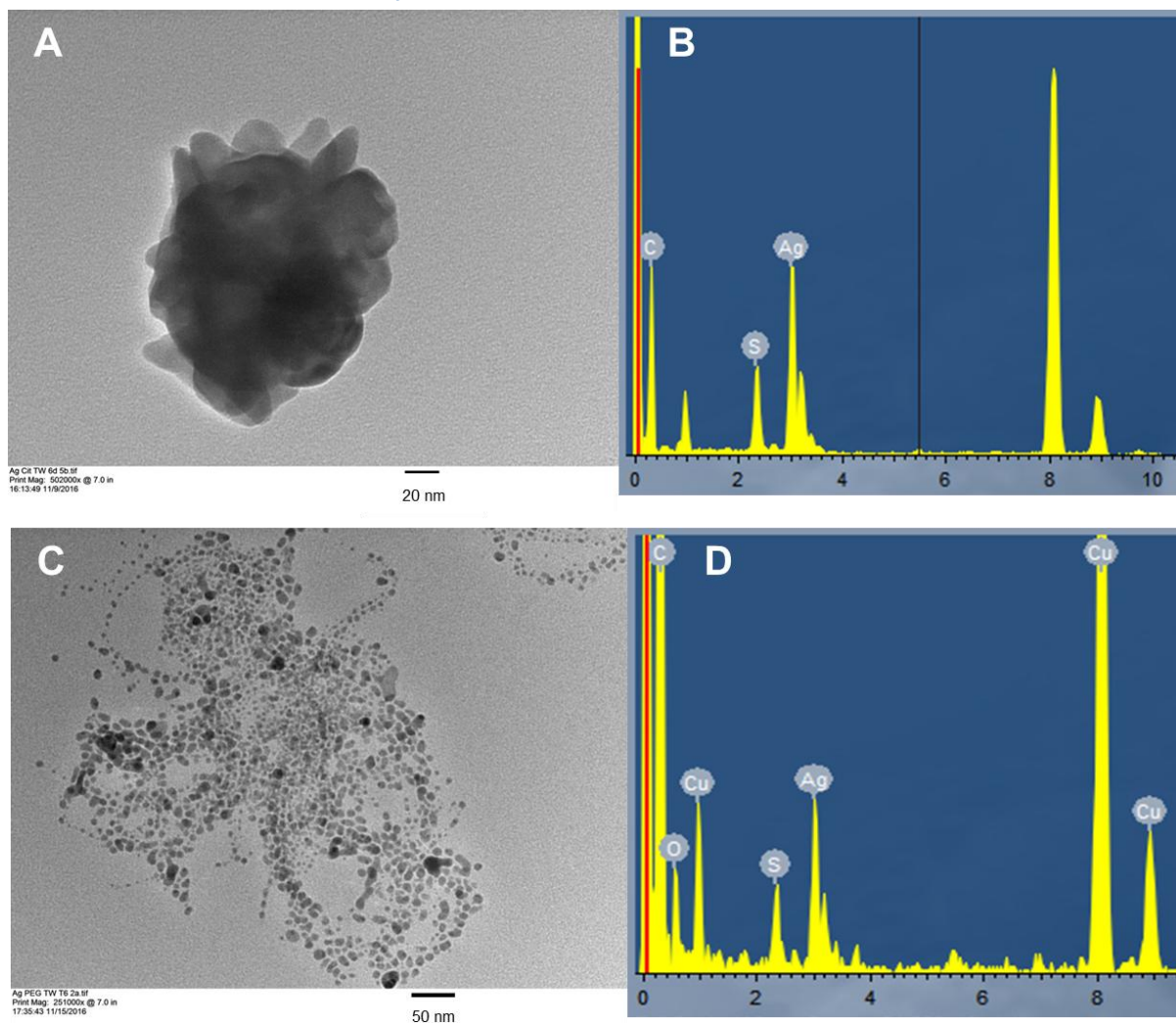
Figure 3.2: Qualitative analysis of representative Ag NPs incubated in freshwater for 6 days using TEM-EDS. A) Citrate-Ag particle demonstrating evidence of sintering between particles and the sulfidation of the particles indicated by the presence of sulphur in the EDS spectra (B). PEG-Ag NPs could still be detected as single particles or loose agglomerates on the grid (C) with the presence of sulphur in the EDS indicating sulfidation of the particles to some extent, but also oxygen, indicative of the formation of Ag_2O (D).

Qualitative examination of the Citrate and PEG-Ag after 6 days incubation in freshwater was conducted using a combination of TEM-EDS. The low concentrations examined meant quantitative examination of the particle size distributions was limited. Higher concentrations were not prepared for TEM due to the potential for concentration dependent aggregation of Citrate-Ag in

freshwater (Figure 3.1) and so TEM grids were prepared at the same spiking concentration as for sediment exposures. The TEM images presented in Figure 3.2 are representative examples of the particles observed for the two Ag NPs, specifically, examples of the two forms of particles which were distinct to each treatment. For Citrate-Ag, the majority of observed particles were present as these small aggregates of what appear to be sintered Ag NPs between 100 and 300 nm in size (Figure 3.2.A). Such particles were not observed for PEG-Ag.EDS spectra confirm that the aggregates comprise of silver, with an additional peak of sulphur suggesting sulfidation occurring over the 6 days (Figure 3.2.B). For PEG-Ag, no such sintered aggregates of this size and shape were observed. Instead large, loose agglomerations of single primary particles were observed with a mean diameter of 6.7 nm. In this case, EDS found not only the peaks associated with silver and sulphur, but also oxygen. An oxidised Ag_2O shell around some of the nanoparticles could explain this and perhaps contribute to the prevalence of Ag NPs in their primary particle form, unlike Citrate-Ag. Agglomerates similar to those detected for PEG-Ag were also found for Citrate-Ag, however, in this instance the majority of particles experienced bridging between adjacent particles. The defining difference between the two coatings appeared to be the prevalence of bridged or sintered dense aggregates >100 nm in size for Citrate-Ag compared to the persistence of loose agglomerates of PEG-Ag where the individual particles appeared to be still distinct from one another.

3.3.3 Modelling silver speciation in freshwater

Outputs from the Visual MINTEQ modelling software find 6.86% of silver spiked to the freshwater to be present as dissolved Ag^+ (Table 3.2) Our spiking concentration was 5.67 mgL^{-1}Ag (to attain a total of 2.5 mgkg^{-1} Ag spiked to the sediment) and so we could expect ~0.389 mgL^{-1} of Ag^+ in the pore waters in the absence of the solid phase. This provides a worst case scenario of 0.171 mgkg^{-1} Ag^+ in our sediments, if we were to assume that the sediments do not alter the pore water chemistry and that no silver binds to the solid fraction of the sediment.

Table 3.2: Species distribution and concentration of silver modelled in freshwater media at a spiked concentration of 5.67 mgL^{-1}(2.5 mgkg^{-1}).

Species name	Concentration (μML^{-1})	% of total concentration
Ag^{+}	3.602	6.855
AgCl (aq)	33.054	62.9
(AgCl$_2$)$^{-}$	15.678	29.835
(AgCl$_3$)$^{2-}$	0.109	0.208
(AgSO$_4$)$^{-}$	0.106	0.201

3.3.4 Stability and agglomeration of Ag nanoparticles in dispersion over time
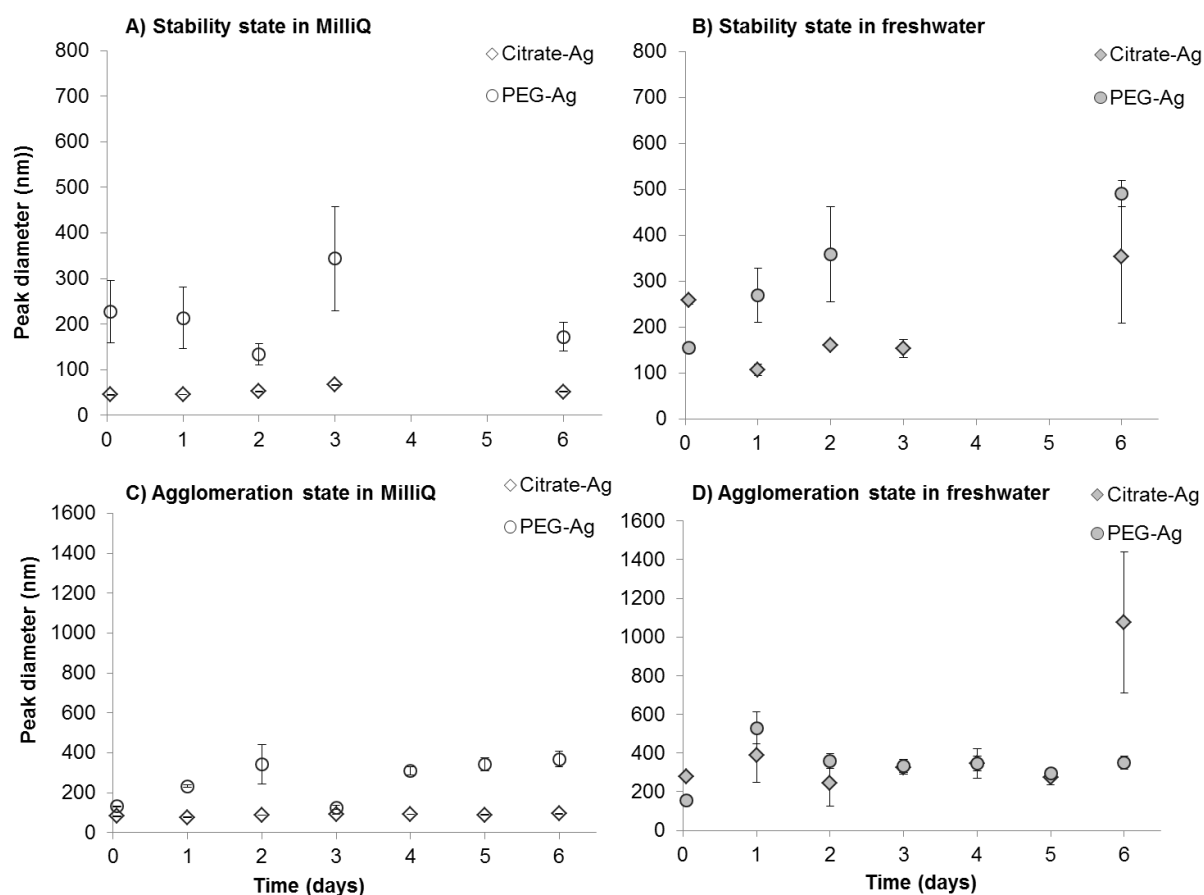
Figure 3.3: Comparing hydrodynamic diameter of Citrate-Ag(diamonds) and PEG-Ag particles (circles) remaining in suspension over 6 days aging in either MilliQ (A- open symbols) or freshwater (B- closed symbols). This is contrasted with the agglomeration state (refer to methods) of these particles again in either MilliQ (C) or freshwater (D). Hydrodynamic diameter is presented as the peak size through scattering intensity (nm).

Figure 3.3 compares DLS measurements of peak size for particles which remained stable across the exposure period (those which remained suspended in the supernatant) and the agglomerates which settled during the exposure (by re-suspending all particles before each measurement). This was performed in

both MilliQ and freshwater to contrast aggregation behaviour of particles in ultrapure water with a simple freshwater proxy for the sediment pore waters. Suspended Citrate-Ag was detected in relatively stable populations in the supernatant of both media across the 6 day incubation period (Figure 3.3 A and B) averaging 52.05 nm +/- 1.6 in MilliQ and 209.2 nm +/- 32.4 in freshwater. For these stable particles in MilliQ, a secondary peak with a mean size of 5.03 nm +/- 1.4 nm was detectable, which is in close agreement with the manufacturers' stated primary size of the particles of 3-15 nm. This population was only detectable for the stability analysis in MilliQ, possibly due to the presence of larger particles in other incubations masking the low signal of these smaller nanoparticles.

In fresh water there was some sedimentation of both Citrate and PEG-Ag, as the attenuator position moved from position 5 to 11 across the incubation period, suggesting fewer counts each day. For the agglomeration analysis, two consistent populations of Citrate-Ag were detected of 87 nm +/- 1.09 (in MilliQ, Figure 3.3 C) and 308.6 nm +/- 29.7 (in freshwater, Figure 3.3 D). In freshwater at the 6 day time point Citrate-Ag appeared to aggregate >1000 nm (Figure 3.3 D). However, this peak size should be treated with caution as it only accounted for ~70% of the scattering intensity measured and the count rate was below 300 kcps, reducing the accuracy of such measurements. Indeed, a secondary peak, measuring ~150 nm and accounting for 20-35% of the scattering intensity was observed at this time point, which may be more representative of the true particle size of Citrate-Ag remaining in suspension in freshwater after 6 days.

The relationship between PEG-Ag and stability over time was more complex. These particles did experience some sedimentation during the course of the incubation in both media. In MilliQ water, PEG-Ag particles which remained in suspension during the stability analysis fluctuated between 134-343 nm (Figure 3.3 A). Peak size after 3 days was significantly greater than at the start of the incubation (p = 0.0011, Dunnett contrasts). The same was true in freshwater, where only peak size at day 3 was significantly greater than the original size at the start of the experiment (p < 0.001, Dunnett contrasts). At this time point, a significant secondary peak (between 15 – 30 % of the total scattering intensity) existed, averaging at 350 nm +/- 34.9. This is within the expected range of other peak sizes stable in the freshwater (Figure 3.3 B), suggesting a few large or

103

sediminting particles masking the intensity peak of the smaller stable particles. Agglomeration analysis confirmed the majority of particles reached a peak size of 264 +/- 22 nm in MilliQ and 331 nm +/- 22 in freshwater.
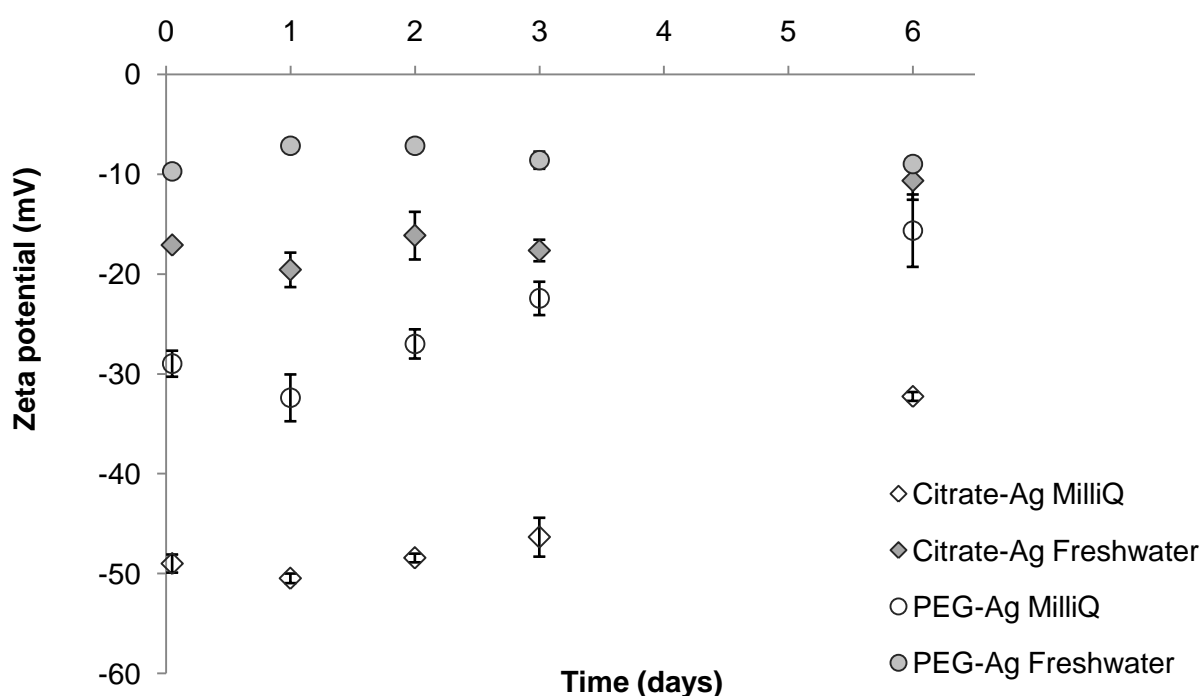
Figure 3.4: Zeta potential of silver nanoparticles which remained in suspension over 6 days incubation in ultrapure MilliQ water or freshwater media.

Both Citrate and PEG-Ag experienced a reduction in zeta potential, in freshwater compared with in MilliQ and over time. This may be due either to a loss of coating molecules from the particle surface, or through attraction of counter ions from the freshwater surrounding the particles and compressing the electric double layer, reducing the measured zeta potential. The continued stability of Citrate-Ag in MilliQ reflects the zeta potential remaining more negative than -30 mV throughout the incubation. In freshwater, the reduced, but stable zeta potential between -10 and -20 mV is consistent with the slight agglomeration observed alongside the persistence of a stable population of particles ~200 nm. PEG acts as a steric stabiliser and so the reduction in zeta potential is not of such importance in determining stability. PEG-Ag particles experienced fluctuating sizes in both MilliQ and freshwater consistent with the TEM images of loose agglomerates of distinguishable particles (Figure 3.2) with a primary size of 6.7 nm (Table 3.1).

3.3.5 Route to uptake of Ag NPs with different surface functionalisation

Silver was bioaccumulated above sediment concentrations during all exposures to AgNP and $AgNO_3$, with body burdens ranging between 1.2 and 100 times greater in the organisms than in the surrounding sediment. All treatments experienced significant accumulation of Ag compared to controls ($p<1e^{-10}$, Dunnett contrasts). Due to the low concentration of background silver in the sediments (0.08 mgkg^{-1}) and the control worms, BAF_5 were not calculated for control worms as they would be artificially inflated and so non-comparable to the silver treatments. Therefore, subsequent analysis of the silver treatment BAF_5 was performed only on the treatment groups and used $AgNO_3$ as a positive control for the accumulation of silver from a source of dissolved LMW-Ag. BAF_5 were non-normally distributed so data was square root transformed to improve the fit of the data Q-Q plot and so allow for examination with ANOVA.

Only in Citrate-Ag exposed worms did sediment associated Ag in the gut contribute significantly towards BAF_5 ($p = 0.0074$, LSM Tukey's method). Thisindicates there is onlya slight contribution of ingested sediment associated Agtowards body burdens, provided no clearance step is performed. For each silver treatment, there was no significant difference between BAF_5 in feeding clearance organisms and non-feeding organisms ($p>0.31$, LSM Tukey's method). Therefore, the majority of bioaccumulation of Ag in all worms occurred through transdermal uptake (Figure 3.5). The extent of transdermal uptake of Ag represented by BAF_5 differed between each form of Ag treatment. BAF_5 in non-feeding organisms after clearance could be ranked in descending order from most bioavailable as PEG-Ag (88.3 kgkg^{-1}) > Citrate-Ag (6.5 kgkg^{-1}) ≥ $AgNO_3$ (1.2 kgkg^{-1}). Transdermal uptake of Ag by non-feeding organisms after gut clearance during PEG-Ag exposures was significantly higher than in either Citrate-Ag or $AgNO_3$ treatments ($p <0.0001$, Tukey's least significant means), but did not differ between Citrate-Ag or $AgNO_3$ ($p = 0.4549$,LSM Tukey's method). Only transdermal uptake is possible in these non-feeding organisms suggesting that the mechanism for transdermal uptake is similar in Citrate-Ag and $AgNO_3$ exposures, but differs for PEG-Ag. This can be explored in more detail through examination of the fate of the NPs during the exposure period.
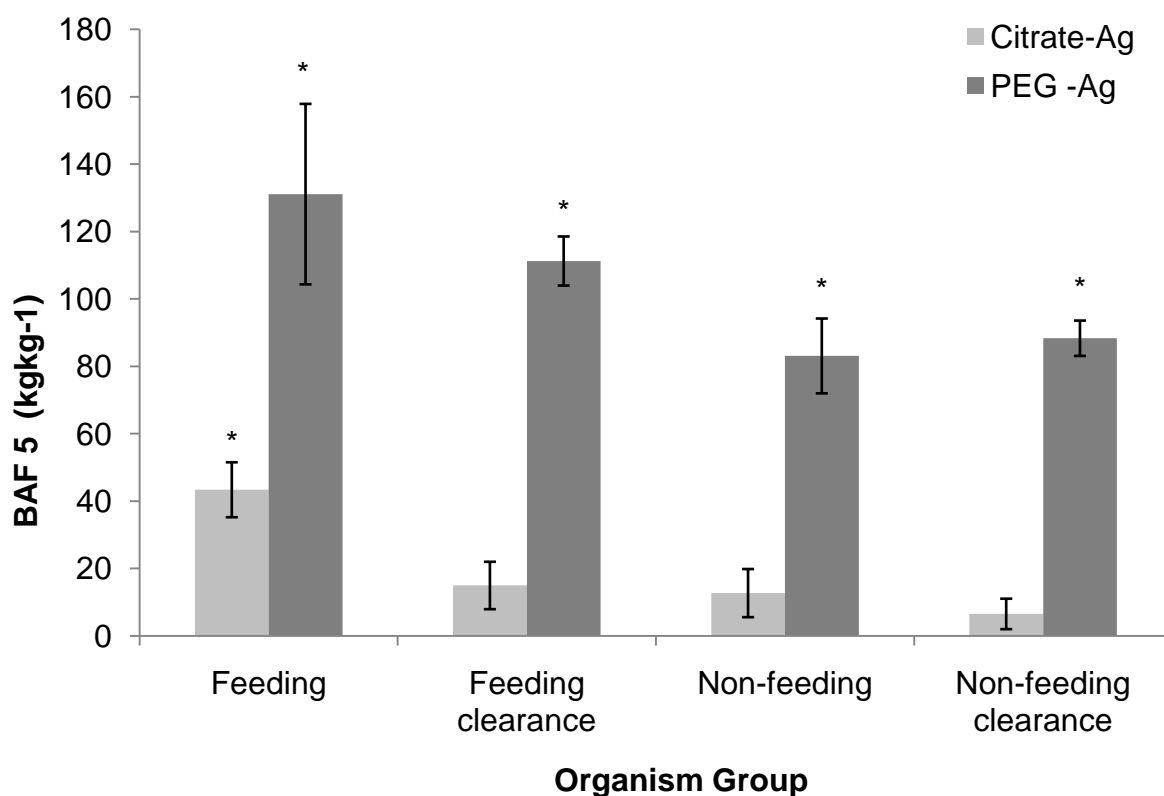
Figure 3.5: Bioaccumulation factors (BAF$_5$) for organisms exposed to Ag NPs coated with either citrate or PEG. Organism groups which experienced significantly greater accumulation of silver than those exposed to the positive control of AgNO$_3$ are identified by the asterisk (*).

3.3.6 Explaining differences in route to uptake of nanoparticles through investigation into the fate of Ag NPs in sediment pore waters

AgNP exposures did experience dissolution in the sediments (Table 3.3). Both Citrate-Ag and PEG-Ag NPs experienced similar concentrations of silver in both the colloidal and LMW fractions of the sediment as AgNO$_3$ (p=0.153, ANOVA), irrespective of their initial spiked concentrations which varied from 0.12 mgkg^{-1} (PEG-Ag) to 3.3 mgkg^{-1} (AgNO$_3$). As there was no significant difference in LMW-Ag for any treatment, the mean concentration of ~0.02 mgkg^{-1} soluble Ag would appear to be an apparent maximal concentration of soluble Ag that can persist in these sediments. This suggests that persistence of soluble forms of silver in the pore waters is limited by conditions within the sediment.

Table 3.3: Partitioning of Ag NPs between the solid, colloidal and low molecular weight fraction of the sediment at the end of the biological exposure period.

Ag+

$AgCl_x$ (aq)

Ag(I)-complexes

Treatment	Total sediment concentration mgkg^{-1}	Colloidal fraction <200 nm mgkg^{-1} (s.e.)	LMW fraction <1kDa mgkg^{-1} (s.e.)
Citrate-Ag	0.76	0.049 (0.004)	0.0214 (0.003)
PEG-Ag	0.12	0.032 (0.005)	0.0281 (0.009)
AgNO$_3$	3.25	0.019 (0.009)	0.0107 (0.001)

We hypothesised that dissolution of LMW soluble species from a nanoparticle within the sediments would alter the route to uptake, potentially allowing for transdermal uptake of the metal as a secondary product of nanoparticle transformations in the sediment. To test this, BAF$_{LMW}$ was calculated for non-feeding organisms, normalising body burdens to the average LMW-Ag concentration in the pore waters. This made the assumption that all transdermal uptake was of LMW-Ag. Once again, BAF$_{LMW}$ was square root transformed to comply with assumptions of normality and homogeneity of variance for ANOVA. This found that only nanoparticle coating had a significant effect upon BAF$_{LMW}$ ($p = 0.0006$, ANOVA). Figure 3.6demonstrates that Citrate and AgNO$_3$ experience no difference in BAF$_{LMW}$ ($p= 0.968$, Tukey HSD). This reflects the fact that they experienced no significant difference between either total body burdens or LMW-Ag concentration in the sediment pore waters. BAF$_{LMW}$ for PEG-Ag on the other hand remained significantly higher than the corresponding AgNO$_3$ treatment ($p<0.001$, Tukey's HSD) and Citrate-Ag ($p= 0.00225$, Tukey's HSD). This suggests whilst LMW-Ag may account for all transdermal uptake of Ag during exposures to Citrate-Ag and AgNO$_3$, it cannot account for all transdermal uptake of Ag during PEG-Ag exposures.
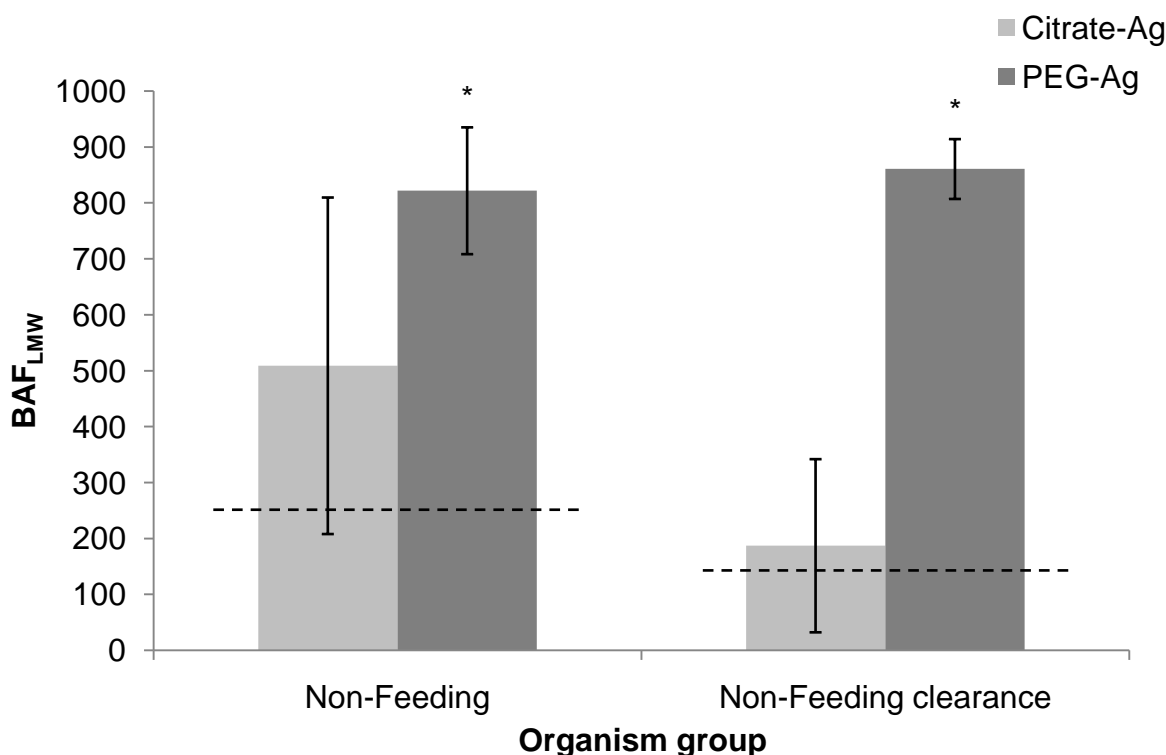
Figure 3.6: Bioaccumulation factors representing transdermal uptake of dissolved low molecular weight species of Ag (BAF$_{LMW}$) during nanoparticle exposures contrasted with BAF$_{LMW}$ for a positive control of dissolved AgNO$_3$, presented as the dotted line (- - -). Accumulation of Ag significantly greater than during exposures to AgNO$_3$ is denoted by an asterisk (*).

3.4 Discussion

3.4.1 Nanoparticles remain relatively stable throughout biological exposures

The fate of nanoparticles in suspension was examined across the full 6 day exposure period using a combination of TEM and DLS. The DLS results are semi-quantitative due to the inherent difficulties with interpreting results from this technique for the polydisperse and multimodal distributions, which these particles displayed. The primary output from DLS is the Z-average and it is this result that is often reported. This diameter is calculated using the scattering intensity of nanoparticles, but this intensity is proportional to the square of the molecular weight of the particles. Therefore the presence of even a few large aggregates can have a disproportionate effect on the analysis, skewing the Z-average and leading to an overestimation of the hydrodynamic size of particles.

108

As such, we present the average hydrodynamic diameter of the primary peak in the scattering intensity distribution. This is the intensity peak within which generally >90% of the signal falls. This is termed "peak diameter" when reported in this study.

Citrate and PEG-Ag were relatively stable in both media, ultrapure MilliQ water and artificial freshwater. Both nanoparticles had a population of particles which remained stable and in suspension throughout the 6 day exposure period. For Citrate-Ag this ranged between 45 and 87 nm in MilliQ water and between 106 and 350 nm in freshwater (Figure 3.3). Other nanoparticles including CeO_2, titanium dioxide and zinc oxide aggregating to ~300 nm in diameter have also been demonstrated to remain stable in suspension and not experience significant sedimentation [15]. Interestingly, in MilliQ water, where the majority of particles were <100 nm, a bimodal distribution was detectable, with a secondary peak in intensity with an average size of 5 +/- 1.4 nm. This fits well with the primary particle size of Citrate-Ag (10.63 nm) and for PEG-Ag (6.7 nm) measured using TEM (Table 3.1). The hydrodynamic diameter for PEG-Ag particles in MilliQ water was 130.9 nm, which may explain why this smaller peak ~10 nm was not so consistently detected for PEG-Ag, due to the greater scattering intensity of the larger particles masking the signal of these smaller particles. TEM images qualitatively support the DLS findings in freshwater too. Citrate-Ag particles appeared predominantly as small, sintered aggregates <1000 nm in size, whilst several loose agglomerates of distinct individual particles were observed for PEG-Ag (Figure 3.2). Less electron dense bridging structures between AgNPs similar to those observed in the Citrate-Ag samples have been identified as Ag_2S nano-bridges when PVP-Ag was aged for 24 hours in micro molar concentrations of Na_2S solutions [16]. This may have implications for bioavailability as it is these particles which remain stable in suspension which may present themselves to organisms through contact with the skin whilst in dispersion in the pore waters.

Some sedimentation was observed for the two coated nanoparticles over time, coinciding with a reduction in the surface zeta potential, in particular in freshwater (Figure 3.5). One hypothesis for this reduction in the surface potential may be caused by loss of stabilising citrate and PEG molecules from the nanoparticle surface to the surrounding media. To test this, nanoparticles

were dispersed at a range of concentrations in both freshwater media and in the surfactant vehicle in which the nanoparticles were originally supplied in dispersion. If molecules from the particle coating were lost to the surrounding media, we would expect the particles to aggregate as the external concentration of excess citrate or PEG decreased. For PEG-Ag, there was no difference in particle size between those dispersed in the PEG vehicle or in artificial freshwater at any of the concentrations measured immediately after dispersal. This confirms thestrong association of PEG to the Ag nanoparticle, where the thiol group of themercaptopropionic acid-PEG forms a covalent bond with the positively charged Ag^+ at the particle surface[9].

This was not the case in freshwater for Citrate-Ag. The citrate ligand forms a bidentate chelate complex with the metal, and so can be more easily replaced than the strong silver-thiol bond. Diluting Citrate-Ag in MilliQ and in the citrate, vehicle did not alter the peak diameter measured immediately after dispersion for these particles. This suggests that Citrate is not lost from the nanoparticle surface simply due to the reduction in external citrate concentration, provided no competing ions or biotic ligands are present. In freshwater, a very different pattern is observed. There is rapid aggregation to 314 nm at the highest concentration of 15.1 µgml^{-1} silver. At lower concentrations closer to the range spiked to the sediments (5.6 µgml^{-1}) this aggregation is still apparent, but reaches a lower size (147 nm at 1.51 µgml^{-1} and 104 nm at 0.51 µgml^{-1}).This suggests that citrate may be lost from the particle surface as the excess concentration in the surrounding media is lost or that the electrostatic stability of these particles is reduced by the presence of counter ions in the water. It also demonstrates that there is a concentration dependant element to this aggregation behaviour. The distinct methods of binding of these two coatings to the silver may in part explain the difference in particles observed using TEM after 6 days in freshwater. Imaging found some PEG-Ag particles still present as individual particles, whilst Citrate persisted as small dense aggregates <300 nm (Figure 3.2) or as branching agglomerates where particles appeared fused together. Interestingly these branched aggregates observed for Citrate-Ag (but not for PEG-Ag) were visually very similar to branching uncoated Ag particles in the literature [17], suggesting loss or degradation of the citrate coating during incubation in freshwater.

110

3.4.2 Transdermal uptake accounts for the majority of Ag uptake from the sediments

Worms exposed to all three forms of silver experienced bioconcentration of Ag after 5 days exposure, with BAF_5 ranging from 1.1 to 131.1 kgkg^{-1}.It is generally thought that nanoparticles will not reach equilibrium when assessing accumulation, due to their dynamic nature over time altering their partitioning and fate in sediments. This is not always the case, as Coleman *et al.* 2013 demonstrated, a time to steady state in water only exposures could be calculated for accumulation of 24 nm PVP stabilised Ag NPs and bulk Ag in *L. variegatus* as 4 and 13 days respectively[18]. Interestingly, the steady state body burden of Ag after 4 days exposed to PVP-Ag NPs in Coleman's study was 14.6 ngmg^{-1}. This is of a similar magnitude as the 12.7 and 22.8 ngmg^{-1} detected for feeding worms exposed to Citrate and PEG-Ag respectively, suggesting that body burdens during this study may also be close to steady state. This would have to be confirmed in future investigations to examine this kinetic uptake of Ag over longer time periods.

There is some contribution of ingested material towards bioaccumulation of silver, with significantly higher body burdens of Ag in feeding organisms exposed to Citrate-Ag before the gut clearance,compared to after this material is evacuated. However, after a clearance phase, there was no significant difference in body burdens between the two worm phenotypes, feeding and non-feeding organisms, for any of the silver treatments. This indicates the majority of the Ag body burden was accumulated through transdermal uptake rather than through ingestion. This presents two possible explanations for the accumulation of Ag:

1. The nanoparticles themselves were taken up across the epidermis through processes at the cellular level.
2. Dissolved low molecular weight species of silver, either in the pore waters, or dissolving from NPs associated with the organisms' external surfaces were responsible for transdermal uptake of Ag.

3.4.3 Dissolved species of LMW-Ag contribute to transdermal accumulation of Ag

Dissolved species of ceria were implicated in the transdermal uptake of Ce from sediments, discussed in Chapter 2. CeO_2 nanoparticles which did not dissolved were only bioaccumulated through ingestion, whilst sediments spiked with $Ce(NO_3)_3$ as a source of dissolved Ce^{III} experienced slight transdermal uptake of Ce. This is an important difference in the fate of Ag nanoparticles within sediments compared to CeO_2. Citrate-Ag, PEG-Ag and $AgNO_3$ all experienced similar levels of dissolution within the sediments. Many studies have implicated dissolution products of nanoparticles in both toxicity of Ag NPs [12] and bioaccumulation of other metal NPs [19] to a range of aquatic species. Although such toxicity is often attributed to the dissolved ion of Ag^+, during these exposures it is unlikely that this positively charged ion will persist in the predominantly negatively charged sediment environment. In light of this, and the confirmation of transdermal uptake of dissolved Ce from sediments, we hypothesised that transdermal uptake of silver could be attributable to the dissolved LMW-Ag which persisted in the sediment pore waters (Table 3.3).

Transformation products of Ag nanoparticle dissolution can persist in the environment as a variety of soluble Ag species and complexes, including silver chloride ions [20] such as $AgCl_{(aq)}$ and $AgCl^{2-}$, Ag-complexes with thiosulfate or complexes with any LMW natural organic matter such as smaller fulvic acids [21]. These dissolved forms of silver may be accumulated across the epidermis through sodium transport channels or if neutrally charged, passively across membranes [22]. Transport through sodium channels may occur in particular across the posterior which acts as a surface for gas exchange, as this has been demonstrated to be the mechanism for uptake of dissolved Ag in the gills of fish and is implicated in their resultant toxicity [3]. For the purposes of this study, these species of soluble Ag are operationally defined as low molecular weight Ag (LMW-Ag), which can pass through a modified polyethersulfone 1 kDa ultracentrifugation filter.

Irrespective of the initial spiked concentration of Ag to the sediment, LMW-Ag in the pore water at the end of the exposure did not differ between treatments (p=0.153, ANOVA). The concentration of LMW-Ag in the pore waters at the end of the exposure was 0.02 (+/- 0.0037) mgkg^{-1} sediment, or 0.045 mgL^{-1} pore

water across Ag treatments. Therefore, it is not the form of silver (nanoparticle versus dissolved, electrostatically stabilised versus sterically stabilised) that determines the extent of dissolution in these sediments in this instance. Rather, properties of the sediment itself dictate the persistence of LMW-Ag in pore waters.

To assess the contribution that dissolved LMW-Ag made towards transdermal uptake of silver, nanoparticle treatments were contrasted with exposures to $AgNO_3$, used as a positive control representing uptake of silver from a source of dissolved Ag^+. If we make the assumption that all transdermal uptake of Ag is of dissolved LMW species, we can adjust the bioaccumulation factors to represent uptake across the skin only of the LMW fraction of Ag (BAF_{LMW}) from the sediment pore waters.Correcting accumulation factors in this way in water only exposures has been performed in other studies investigating ZnO NPs [19] and Ag NPs and has been demonstrated to explain the differences in accumulation observed between different coated Ag nanoparticles in *D. magna*[12].As all treatments experienced the same concentration of LMW-Ag in the sediment pore waters we would expect BAF_{LMW} to be the same across NP treatments, provided the assumption that transdermal uptake of Ag is only possible for LMW-Ag is correct.BAF_{LMW} did not differ between $AgNO_3$ and Citrate-Ag, suggesting that transdermal uptake of Ag in the Citrate-Ag NP treatment could be attributed solely to dissolved LMW-Ag released during this exposure. The same could not be said for PEG-Ag. BAF_{LMW} was still significantly greater in PEG-Ag exposures than for the positive control of $AgNO_3$, which represented transdermal uptake only of LMW-Ag. Therefore, only around 30% of all transdermal uptake of Ag during PEG-Ag exposures could be attributed to LMW-Ag in the sediment pore waters.

3.4.4 PEG-Ag NPs experience transdermal accumulation of Ag not wholly accounted for by dissolved species of Ag

The additional transdermal bioaccumulation of Ag during the PEG-Ag exposures could be through two possible routes examined in Figure 3.7.
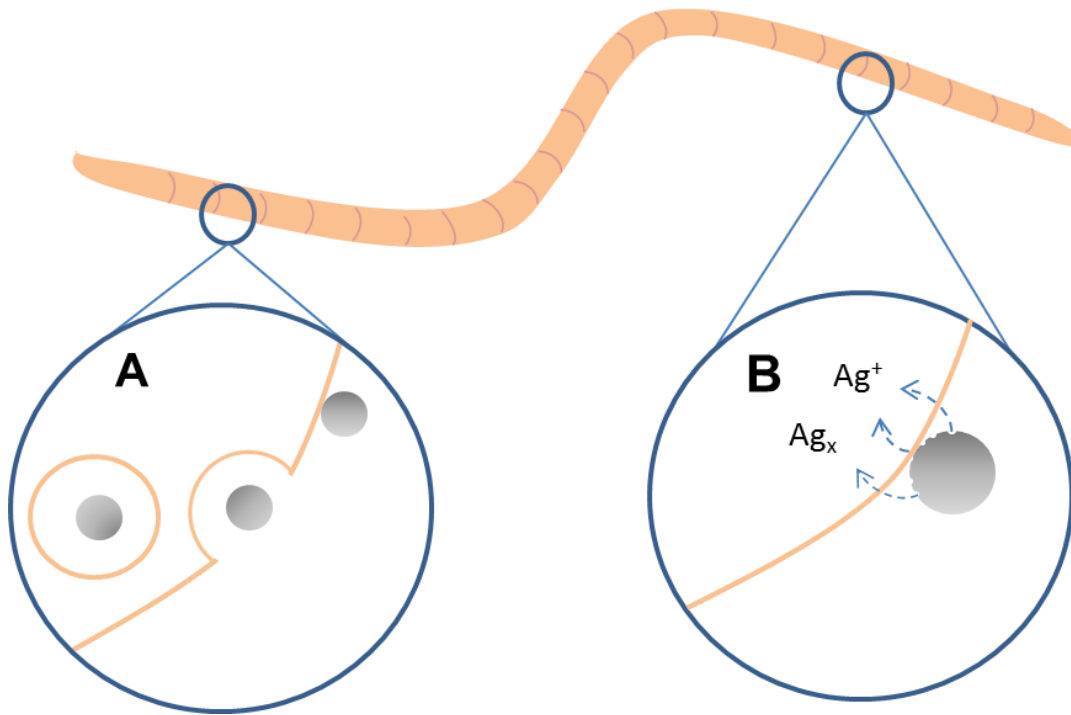
Figure 3.7: Schematic of the two hypothesised mechanisms explaining the increased accumulation of Ag during PEG-Ag exposures A) endocytic pathways and B) localised dissolution.

A. The nanoparticles themselves, or small heteroaggregates which persist in the <200 nm colloidal fraction of the pore water are directly accumulated through cellular mechanisms such as endocytosis at the organisms surface.

B. PEG-Ag nanoparticles associate with external membranes, possibly through interaction with the surface mucus layer. Localised dissolution of LMW-Ag at these points of association is then responsible for additional transdermal uptake of dissolved Ag through membrane transport channels.

To understand why PEG-Ag appears to be experiencing behaviour distinct from the other silver treatments, it is important to understand the process by which these particles are stabilised. Citrate only loosely adsorbs to the surface of Ag nanoparticles through Van der Waals forces [23], meaning it may rapidly dissociate if the external concentration of free citrate decreases, for example upon spiking into the sediment.Figure 3.1 provides evidence of this instability of the citrate coating in freshwater, with particle peak diameter increasing to over doublethe size compared to when diluted in the citrate vehicle or ultrapure water. Surface zeta potential also decreased to below -20 mV in freshwater,

which could cause nanoparticles initially coated with citrate to rapidly associate with solid constituents of the sediment, removing the possibility of individual Citrate-Ag particles coming into contact with organisms external membranes.

PEG on the other hand covalently binds through a sulphur containing thiol group, which forms a particularly strong bond with Ag^+ at the surface of Ag NPs, thus resulting in a highly stable surfactant [9]. Other studies have also found PEG to provide greater stability to Ag nanoparticles than Citrate in various aquatic media [23]. This could explain the increased potential for transdermal uptake of PEG-Ag compared to Citrate-Ag. There was no statistical difference in the total concentration of Ag in the colloidal fraction of the pore waters for the two Ag nanoparticle treatments.This suggests that it is the form of these colloidal particles which is responsible for the difference in accumulation observed. For example, PEG-Ag may have remained either singly dispersed or as small homoaggregates of PEG-Ag whilst Citrate-Ag persisted in a less bioavailable form due to the greater stability of the PEG coating.

TEM-EDS images confirm that both Citrate and PEG-Ag particles incubated in test water can persist in this <200 nm colloidal fraction across the exposure period predominantly in association with sulphur, suggesting sulfidation of the NP surfaces to some extent (Figure 3.2). Interestingly, qualitative examination of the particles found far greater sintering between Citrate-Ag than PEG-Ag NPs. Citrate-Ag was predominantly found in large, spiky and deformed sintered aggregates (Figure 3.2 A) whilst PEG-Ag could still be found in large, loose agglomerates where distinct individual 5 - 30 nm particles were still visible (Figure 3.2 C). Due to the relatively low concentrations examined (~5 µgml^{-1} Ag), quantitative analysis of these images was not possible. However, it provides indirect evidence of a difference in aggregation behaviour of these two coated Ag NPs in the test water over the exposure period. This feature could contribute towards transdermal uptake of NPs themselves through cellular mechanisms such as endocytotic pathways, which has been observed in the gut epithelial cells of the marine worm *Nereisdiversicolor*[8].

If it were PEG-Ag nanoparticles themselves which were taken up across the skin, we would expect this to be a function of their relative stability and persistence as primary particles 5-30 nm in size which could come into contact

with the external surfaces of the worm. However, we saw in Chapter 2 that Citrate-CeO_2 particles which experienced a similar aggregation pattern to PEG-Ag were not available for transdermal uptake. These Citrate-CeO_2 particles reached a peak size of ~300 nm and in ultrapure water were demonstrated to have a primary particle size of 10.5 nm (measured by DLS) similar to PEG-Ag particles which had an area equivalent diameter of 6.7 nm (measured by TEM). Therefore, it does not appear to be the primary size of these particles which is responsible for increased Ag uptake in PEG-Ag treatments. Likewise, if it were due to the biocompatibility of the PEG coating allowing for transdermal uptake of nanoparticles, we would also expect to see transdermal uptake of the 14.8 nm PEG-CeO_2 particles in Chapter 2. No such uptake was observed. These two findings make it unlikely that the PEG-Ag particles were directly accumulated across the skin through transdermal uptake of the particles themselves. In addition to this, whilst silver nanoparticles may be taken up through receptor mediated endocytosis this uptake appears to be greatest at an optimal size of 50 nm[24] and be reduced in the presence of more complex protein containing matrices such as foetal calf serum[25]. The small primary size of the PEG-Ag particles (6.7 nm) and the complex mix of natural organic matter present in the sediment therefore reduce the likelihood of direct uptake of PEG-Ag nanoparticles through receptor mediated endocytosis.

An alternative explanation for the increased bioavailability of PEG-Ag through transdermal uptake could be that the colloidal particles observed by TEM become entrapped within the worms' surficial mucus layer, and this allows for localised dissolution to then contribute to the transdermal uptake of dissolved Ag during these exposures.PEG coated particles in the micron size range experience a gentle repulsive interaction when in contact with mucus, which it has been suggested could allow for smaller particles such as the PEG-Ag NPs <200 nm to diffuse within mucus pores [26]. This would allow for direct contact between PEG-Ag and the worms epidermal cells. Two factors could then lead to an increase in dissolution for these PEG-Ag particles at the worms epidermis compared to Citrate-Ag. The PEG-Ag appeared to persist as loose agglomerates where the distinction between individual 10 nm particles was still visible, whilst Citrate-Ag appeared to have experienced greater sintering and sulfidation. Studies have demonstrated that smaller Ag nanoparticles<15 nm

dissolve at a faster rate through oxidation of the metallic Ag at the particles surface, in part due to their larger surface area to volume ratio [27]. Therefore, PEG-Ag particles which persisted as individual 10 nm particles may experience greater dissolution in close proximity to the worms' surface than the Citrate-Ag.

Another important factor emerging in the recent literature is the role of naturally occurring thiol containing ligands upon nanoparticulate silver dissolution. Cysteine is an important component of the more complex organic structures such as proteins and natural organic matter that make up mucus layers and biological exudates. It is a thiol containing ligand that has a strong affinity to silver and has been demonstrated to increase the solubility of 20 nm Citrate-Ag particles [28]. Nanoparticles entering the mucus layer at the bio-interface between the organism and the surrounding media may become trapped, possibly interacting electrostatically and binding to mucoproteins[29]. This could in turn increase the contact time nanoparticle have in close proximity to aquatic organisms surfaces, increasing the potential for dissolution and uptake of dissolved Ag species through transport channels in epithelial cells. Detailed research is needed into the chemical transformations that nanoparticles undergo within more complex organic matrices representing mucus and biological exudates in order to confirm whether localised dissolution will be increased for nanoparticles associating with mucus membranes at organisms' surfaces.

Three strands of evidence from our work suggest that the increased uptake of silver during PEG-Ag exposures is not of nanoparticles directly, but of dissolved species of silver:

i. Transdermal uptake of silver was the major route to silver bioaccumulation in all treatments

ii. Particles were soluble in the sediments and the extent of dissolution was similar in each silver treatment irrespective of particle coating or initial spiked concentration

iii. Direct transdermal uptake of PEG-Ag nanoparticles is unlikely as no such transdermal uptake was observed for CeO_2 particles of a similar size and stability (Citrate-CeO_2) or of similar coating (PEG-CeO_2).

117

Therefore we hypothesise that the increased transdermal accumulation of PEG-Ag compared to Citrate-Ag and $AgNO_3$ is the result of localised dissolution of silver from these nanoparticles at the organisms' surface. A combination of persistence of small discreet PEG-Ag NPs in the pore waters, the potential for PEG-Ag NPs to migrate through the surficial mucus layer and the more rapid dissolution experienced by smaller particles, in particular in the presence of natural thiol containing ligands, could be responsible for the increased transdermal accumulation of Ag during PEG-Ag exposures we observed in *L. variegatus*.

Conclusions

Following biologically relevant aspects of nanoparticle fate alongside biological exposures allowed us to examine the impact of different stabilising coatings upon the route and extent of uptake of silver nanoparticles from sediments. Silver was predominantly accumulated through transdermal uptake of dissolution products from the nanoparticle exposures. The extent of dissolution of LMW-Ag did not differ between nanoparticle treatments or a positive control of dissolved $AgNO_3$. Total accumulation of silver did not significantly differ between electrostatically stabilised Citrate-Ag and $AgNO_3$ suggesting all transdermal uptake of silver during Citrate-Ag exposures could be attributed to uptake of dissolved LMW-Ag. Sterically stabilised PEG-Ag on the other hand experienced greater bioaccumulation of Ag than either Citrate-Ag or $AgNO_3$, even though the persistence of dissolved LMW-Ag in these treatments was the same. Therefore, not all of the uptake of silver by worms during exposures to PEG-Ag could be attributed to dissolved LMW-Ag in the sediment pore waters. With reference to the existing literature and characterisation of these particles stability in freshwater, we conclude that the additional transdermal uptake of silver during PEG-Ag exposures was unlikely to be direct transdermal uptake of the particles themselves. Rather, the persistence of small individual PEG-Ag nanoparticles in freshwater could allow these particles to come into direct contact with external membranes. Unlike the Citrate-Ag particles which appeared to form dense, partially sulfidized aggregates >100 nm in size, the small size of the PEG-Ag would lead to increased localised dissolution of these particles upon contact with the organisms skin. Thiswould then lead to additional transdermal uptake of dissolved species of silver across the

118

organisms' epidermis. To elucidate this mechanism, future work should focus upon visualisation of nanoparticles at the organisms' surface, to prove or discount direct uptake of silver nanoparticles across the skin.

References

1   A. C. Johnson, M. D. Jürgens, A. J. Lawlor, I. Cisowska and R. J. Williams, *Chemosphere*, 2014, **112**, 49–55.

2   M. Grosell, C. Nielsen and A. Bianchini, *Comp. Biochem. Physiol. - C Toxicol. Pharmacol.*, 2002, **133**, 287–303.

3   N. R. Bury and C. M. Wood, *Am. Physiol. Soc.*, 1999, R1385–R1391.

4   K. W. H. Kwok, W. Dong, S. M. Marinakos, J. Liu, A. Chilkoti, M. R. Wiesner, M. Chernick and D. E. Hinton, *Nanotoxicology*, 2016, **10**, 1306–1317.

5   R. K. Cross, C. Tyler and T. S. Galloway, *Environ. Chem.*, 2015, **12**, 627.

6   F. R. Khan, K. B. Paul, A. D. Dybowska, E. Valsami-Jones, J. R. Lead, V. Stone and T. F. Fernandes, *Environ. Sci. Technol.*, 2015, **49**, 4389–4397.

7   G. Cornelis, C. DooletteMadeleine Thomas, M. J. McLaughlin, J. K. Kirby, D. G. Beak and D. Chittleborough, *Soil Sci. Soc. Am. J.*, 2012, **76**, 891.

8   J. García-Alonso, F. R. Khan, S. K. Misra, M. Turmaine, B. D. Smith, P. S. Rainbow, S. N. Luoma and E. Valsami-Jones, *Environ. Sci. Technol.*, 2011, **45**, 4630–4636.

9   R. A. Sperling and W. J. Parak, *Philos. Trans. R. Soc. A Math. Phys. Eng. Sci.*, 2010, **368**, 1333–1383.

10   A. M. El Badawy, K. G. Scheckel, M. Suidan and T. Tolaymat, *Sci. Total Environ.*, 2012, **429**, 325–331.

11   A. M. El Badawy, A. Aly Hassan, K. G. Scheckel, M. T. Suidan and T. M. Tolaymat, *Environ. Sci. Technol.*, 2013, **47**, 4039–4045.

12   C. M. Zhao and W. X. Wang, *Nanotoxicology*, 2012, **6**, 361–370.

13   H. J. Jo, J. W. Choi, S. H. Lee and S. W. Hong, *J. Hazard. Mater.*, 2012, **227–228**, 301–308.

14   RStudio Team, 2016.

15   A. A. Keller, H. Wang, D. Zhou, H. S. Lenihan, G. Cherr, B. J. Cardinale, R. Miller and J. I. Zhaoxia, *Environ. Sci. Technol.*, 2010, **44**, 1962–1967.

16   C. Levard, B. C. Reinsch, F. M. Michel, C. Oumahi, G. V. Lowry and G. E. Brown, *Environ. Sci. Technol.*, 2011, **45**, 5260–5266.

17   C. Coutris, E. J. Joner and D. H. Oughton, *Sci. Total Environ.*, 2012, **420**, 327–333.

18   J. G. Coleman, A. J. Kennedy, A. J. Bednar, J. F. Ranville, J. G. Laird, A. R. Harmon, C. A. Hayes, E. P. Gray, C. P. Higgins, G. Lotufo and J. A. Steevens, *Environ. Toxicol. Chem.*, 2013, **32**, 2069–2077.

19   F. R. Khan, A. Laycock, A. Dybowska, F. Larner, B. D. Smith, P. S. Rainbow, S. N. Luoma, M. Rehkämper and E. Valsami-Jones, *Environ. Sci. Technol.*, 2013, **47**, 8532–8539.

20   E. Lombi, E. Donner, K. G. Scheckel, R. Sekine, C. Lorenz, N. Von Goetz and B. Nowack, *Chemosphere*, 2014, **111**, 352–358.

21   WHO, *Concise international chemical assessment document 14- Silver and silver compounds: Environmental aspects*, 1997.

22   B. Zhou, J. Nichols, R. C. Playle and C. M. Wood, *Toxicol. Appl. Pharmacol.*, 2005, **202**, 25–37.

23   M. Tejamaya, I. Römer, R. C. Merrifield and J. R. Lead, *Environ. Sci. Technol.*, 2012, **46**, 7011–7017.

24   K. Kettler, K. Veltman, D. van de Meent, A. van Wezel and A. J. Hendriks, *Environ. Toxicol. Chem.*, 2014, **33**, 481–492.

25   K. Kettler, P. Krystek, C. Giannakou, A. J. Hendriks and W. H. de Jong, *J. Nanoparticle Res.*, 2016, **18**, 1–11.

26   J. C. Swavola, T. D. Edwards and M. A. Bevan, *Langmuir*, 2015, **31**, 9076–9085.

27   T. S. Peretyazhko, Q. Zhang and V. L. Colvin, *Environ. Sci. Technol.*, 2014, **48**, 11954–11961.

28   A. P. Gondikas, A. Morris, B. C. Reinsch, S. M. Marinakos, G. V. Lowry and H. Hsu-Kim, *Environ. Sci. Technol.*, 2012, **46**, 7037–7045.

29   R. D. Handy, T. B. Henry, T. M. Scown, B. D. Johnston and C. R. Tyler, *Ecotoxicology*, 2008, 17, 396–409.

Chapter 4

The role of exposure history on nanoparticle fate and bioaccumulation in sediments

Abstract

Greater recognition is being given to the potential effects of aging upon nanoparticle transformations, changing their partitioning or the extent of dissolutionwithin sedimentsover time. Hypothesised lifecycle histories of silver nanoparticles (AgNPs) identify several major emission routes into the aquatic environment, each of which may involve a series of transformations before particles reach freshwater sediments. This study assesses how three different exposure scenarios will alter the fate and behaviour of 50 nm AgNPs within sediments (all AgNPs stabilised with PVP) and the implication for silver bioaccumulation. The exposure scenarios represent: accidental release (Fresh-Ag), historic contamination (Aged-Ag) and silver sulphide particles transformed during waste water treatment (Ag_2S). The kinetic uptake and elimination of silver under these three scenarios was compared tosoluble silver ($AgNO_3$) in feeding and non-feeding *Lumbriculus variegatus*, a sediment ingesting worm.

None of the nanoparticles were accumulated significantly by the worms. Nanoparticles representing accidental release (Fresh-Ag) and entry to sediments after waste water treatment (Ag_2S)were bound to the solid fraction of the sediment >200 nm in size and did not dissolve, resulting in no uptake of silver in either feeding or non-feeding worms.A mobile colloidal fraction of silver <200 nm emerged in the pore waters after 3 months ageing PVP-Ag, but this was still not accumulated by the worms, indicating that for this study, the persistence of colloidal silver in the pore waters was not a good indicator of bioavailability. Significant bioaccumulation was only recorded for $AgNO_3$,for which a dissolved fraction persisted in the sediment pore waters. This was found to be accumulated through transdermal uptake. This study demonstratesthat insoluble AgNPs were not accumulated, even after aging within sediments. Future studies should utilise AgNPs that experience dissolution to assess whether a dissolved fraction in the pore water may

emerge over time and contribute towards bioaccumulation of silver from sediments in the longer term.

Contents

4.1 Introduction

The fate of nanoparticles released into the environment is by its very nature dynamic, both spatially but also across time. Nanoparticle transformationsareTransformations such as complexation with organic matter [1] and sulfidation [2] have been demonstrated to alter the fate or bioavailability of nanoparticles to aquatic organisms and are driven by their surrounding conditions.If nanoparticles are transported between different environmental compartments, it is conceivable that transformations which occur under one set of conditions will go onto affect the fate and behaviour of these particles as they enter new environments[3]. For example, the protein corona formed around nanoparticles in biological media has been demonstrated to remain intact upon cellular uptake, protecting cells from damage induced by cationic polystyrene nanoparticles until they are transported to and degraded in the lysosomes [4]. As our understanding of the dynamic nature of nanoparticle behaviour improves, there is an emerging call for a life-cycle based approach towards investigating the effect of nanoparticle aging upon their ecotoxicity[5]. The majority of ecotoxicological studies examine the effect of nanoparticles which are dosed immediately prior to the introduction of organisms. This tests for a very specific exposure scenario: the release of "as manufactured" nanoparticles into an otherwise uncontaminated environment and the acute effects of these "fresh" particles upon organisms which have not been exposed to this contaminant before. In freshwater environments, this would represent scenarios such as the accidental spillage or release of particles during production, use or storage and transport. Whilst this is an important potential exposure scenario, it does not acknowledge the effect thatnanoparticle transformations may incur over extended periodsof time.

Silver nanoparticles have been observed to persist both as particles distinct from the solid fraction of sediments [6] and to some extent as dissolved silver in soil suspensions, which are similar in composition to saturated sediments [7]. This dissolution reaction may bedynamic. Reformation of nanoparticulate silver through reduction of dissolved Ag^+ in the presence of humic acids from river andsediment sources is possible and has been detected under environmentally relevant conditions [8]. As such, dissolved silver in sediment pore waters may be in flux through constant cycling of silver between the nanoparticle and dissolved

form. In previous chapters we have demonstrated that when dissolved low molecular weight species of silver persist in sediment pore waters, transdermal uptake of silver is possible in the sediment dwelling oligochaete *Lumbriculus variegatus* (Chapter 3). However, our knowledge of nanoparticle fate and its impact upon bioavailability over longer timescales from months to years is currently limited. In some cases, significant or even complete degradation of the coatings can occur when aged in water. For example, 10 nm Citrate-CeO_2 nanoparticles experienced complete degradation and loss of citrate from the particle surface when aged in MilliQ water under artificial light for 122 days [9]. In soils, electrostatically stabilised silver nanoparticles appeared to become less mobile over time, with 20% of 5 nm Citrate-Ag spiked to soils being water extractable over the first 2 days, then decreasing to trace levels over 10 weeks [10]. Interestingly, uncoated 19 nm AgNPs were initially associated mainly with the solid fraction of the sediment (1-3% water extractable) however, after 10 weeks aging, 7.2% of the uncoated silver was now in the bioaccessible fraction of the sediment, defined as water extractable and ion exchangeable silver. As such, aging may result in increased or decreased bioavailability of silver nanoparticles, depending upon their surface coating. Whilst changes to bioaccessibility have been hypothesised by assessing the behaviour and fate of AgNPs in soils, to the author's knowledge no published literature exists wherein measurements of bioaccumulation of sediment aged AgNPs has been attempted.

To begin to address this knowledge gap, this chapter will assess the kinetic uptake of silver from sediments over 14 days, spiked with "fresh" as manufactured polyvinylpyrrolidone coated silver nanoparticles (PVP-Ag, 50 nm). This will be compared to the accumulation of silver from sediments spiked with the same particles, but allowed to age for 3 months prior to the introduction of the aquatic worms (Aged-Ag). To assess the effect of aging upon nanoparticle fate within sediments and their subsequent bioaccumulation, the partitioning of silver between those bound to the solid fraction of the sediment and those which persist in either the colloidal (<200 nm) or dissolved (<1kDa) fraction of the sediment pore water will also be investigated using a combination of microfiltration and centrifugal ultrafiltration.

PVP-Ag nanoparticles are widely used in the literature due to the efficacy of PVP as a stabilising coating. Tejamaya *et al.* 2012 recommend their use after systematically testing the stability of Citrate, PEG and PVP-Ag (all 10 nm) in OECD *Daphnia* culture media [11] as they were the most stable, experiencing low sedimentation, and little changes in shape or dissolution. Therefore, using these particles should test the capacity for predominantly silver nanoparticle uptake rather than uptake of dissolution products from the nanoparticle exposures. Existing literature also suggests that endocytotic mechanisms of uptake are a likely route to cellular internalisation of nanoparticles and that nanoparticle size alters the efficiency of this accumulation pathway, with particles ~50 nm experiencing the greatest uptake[12]. It is these factors which have determined our choice of 50 nm PVP-Ag particles as a representative AgNP for this study.

Another importantreal world example of the life-cycle specific aging of nanoparticles is that of the transfer of silver nanoparticles in textiles through the process of repeated washing into both terrestrial and aquatic environments via the waste water treatment process. Transformations which occur during earlier stages of the nanoparticles life cycle, for example during washing or processing of waste water would mean that the particles entering aquatic environments are likely to have very different properties than those pristine particles usually used for ecotoxicity testing. Nano-enabled textilescontaining silver nanoparticles release silver during machine washing. The speciation of this silver varies dramatically with the textile in question, but a range of transformations occur including transformation of the Ag into nano-AgCl, nano-Ag_2S or into dissolved silver nitrate and sulphatespecies [13]. This released silver may then enter waste flows, with 7.09 metric tons of Ag NPs expected to enter waste water treatment plants in European Unionper year,~22% of the total annual production in 2012 of 32.4 tons [14]. The estimated release rate of silver from treatment plants into the aquatic environment varies widely and is dependent on pH and the elemental composition of coagulants used during the flocculation step, ranging between 20 and 100% removal efficiencies [15]. However, the consensus is that silver sulphide species will be the most prevalent form of silver to pass out of such treatment processes, and indeed such particles have been detected and characterised in sewage sludge products at the end of this process [16].

Therefore, we used manufactured silver sulphide (Ag_2S) nanoparticles (50 nm) as a representative form of transformedsilver, eluted from waste water treatment plants and entering freshwater environments. Ag_2S is highly stable and insoluble under most environmental conditions. Following the fate of each of these particle/exposure scenarios and the partitioning of silver over time between the solid, colloidal and dissolved fractions of the sediment will also examine the role of dissolution products upon silver accumulation during nanoparticle exposures.

4.2 Methods

4.2.1 Materials

To investigate the effect of aging on AgNP bioaccumulation, 50 nmpolyvinylpyrrolidone coated silver (PVP-Ag) and silver sulphide nanoparticles (Ag_2S NPs), both dispersed in 0.02 mM PVP, were provided by the Catalan Institute of Nanoscience and Nanotechnology (ICN, Spain).Silver nitrate ($AgNO_3$) was used as a representative soluble form of silver. Control exposures refer to the standard soil LUFA Speyer 2.4 with no additional engineered silver added. Preparation of nanoparticle exposures, reagents and samples was performed in accordance with the methods presented in Chapter 1.

4.2.2 Aging of PVP coated silver nanoparticles

PVP-Ag was spiked to the sediment using the wet spiking procedure established in Chapter 1 to a calculated loading concentration of 2.5 mgkg^{-1} Ag based upon the stock concentrations provided by the manufacturer. Prior to spiking, the sediment was autoclaved to prevent microbial growth during the aging period. This spiked sediment was saturated and left quiescent in a sealed, acid washed, airtight glass container for 3 months (93 days) at 20˚C before the start of the exposures. The container was wrapped in foil for the duration to prevent photodegradation of the silver. Such quiescent aging has been used to age silver nanoparticles in soils [10]. At the end of the aging period, sediment was homogenised by overhead mixing for 24 hours, before dividing between exposure units and addition of the overlying water. This was allowed to settle for 24 hours before organisms were added to the system.

4.2.3 Characterising the nanoparticles in ultrapure and freshwater

A combination of transmission electron microscopy (TEM), Ultraviolet and visible light spectrophotometry (UV-vis) and dynamic light scattering (DLS) was used to characterise the properties of the pristine particles before addition to the exposure units and in freshwater. Image-J software was used to analyse TEM images. Detailed methods for these three techniques can be found in Chapter 1.

4.2.4 Kinetic uptake and elimination of silver during exposure to fresh, aged and transformed PVP-Ag nanoparticles

Three nanoparticle exposure scenarios were examined in this experiment, Fresh-Ag, Aged-Ag and Ag_2S each using silver nanoparticles 50 nm in diameter. $AgNO_3$ represented comparable exposures to a source of soluble silver. Silver was wet spiked at a calculated loading concentration of 2.5 $mgkg^{-1}$ into sediments, following the protocol outlined in Chapter 2. Each sediment was spiked with Ag dispersion equal to the water holding capacity of the sediment to achieve the desired loading rate. This was then mixed thoroughly for 24 hours on an overhead rotating platform at 5 rpm (VELP ScientificaRotax 6.8). At the end of this mixing period, sediment was divided between exposure units to equate to approximately 10 g per test unit. Feeding and non-feeding organisms were prepared as outlined in Chapter 2. Exposure units comprised of 10 g sediment under 40 ml freshwater and water quality was followed throughout according to OECD test guidelines TG315 (DOI: 10.1787/2074577x). Growth, mortality and qualitative data concerning worm health and behaviour were recorded throughout the exposures.

Uptake period:

Bioaccumulation of Ag was followed across 14 days for each silver treatment with 5 time points at which organisms were sampled (n=5 for each time point). These sampling points were after 1, 3, 5, 7 and 14 days, and each test unit comprised of a pooled sample of 3 worms, randomly assigned to their exposure units. The exposure period was limited to 14 days to prevent further fractionation of feeding organisms during the test period as this would prevent organisms from feeding and so complicate the interpretation of bioaccumulation of silver over time. For the 5 day time point, non-feeding worms were also sampled (n=5) so as to be comparable with the exposures conducted in

Chapter 3. Conductivity of the freshwater was 633 $^+/-$ 5 µScm^{-1} and pH 7.77 $^+/-$ 0.03 across the biological exposures.

Upon extracting worms from their sediment exposures at each time point, pooled tissue samples were gently rinsed with clean freshwater media and were snap frozen immediately in liquid nitrogen and stored at -80 ᵒC until they could be freeze dried and weighed to measure dry mass. This was so that body burdens would reflect the total uptake of silver in the organisms including that in transit within the gut so as to provide a conservative bioaccumulation factor. These dried tissues and sediments were microwave digested in an *aqua regia* acid mix of HNO_3 (~70%) and HCl(>30%).

Elimination period:

The elimination period followed a similar sampling procedure to that of the uptake phase but this time at 7 time points: 0, 6, 12, 24, 72, 120 and 168 hours after an initial uptake phase of 14 days. Organisms were exposed to their respective silver treatment for 14 days in a single large spiked housing unit per treatment ensuring all organisms were exposed to the same sediment to achieve the same starting body burdens of Ag for elimination. These larger exposure units complied with the OECD test guidelines with the same water to sediment ratio of 1:4 as the individual test units and an organic matter to worm tissue mass ratio of >50:1. At the start of the elimination phase (after 14 days exposure to AgNP contaminated sediments) organisms were removed from the spiked housing units and 0 hours organisms were sampled immediately after gentle rinsing. All organisms were then randomly assigned to clean sediment exposure units for the elimination period. 5 test units were sampled per treatment at each sampling time point, resulting in 5 pooled replicates of 3 organisms per time point, rinsed briefly in clean test water, before snap freezing in liquid nitrogen and storage at -80℃. Controls consisted of worms on clean sediment sampled at the start and end of the uptake and elimination phases in accordance with OECD recommendations [17]. Once again, samples were then desiccated in a freeze drier before weighing to measure the dry tissue mass for calculation of body burdens of silver. All samples were treated as outlined in Chapter 1 for preparation for analysis by ICP-MS.

4.2.5 Examining the fate of silver in sediments

The fate and partitioning of silver between the solid bound, colloidal (<200 nm) and dissolved (<1kDa) fractions of the sediment over the uptake period of 14 days was followed using the methodology outlined in Chapter 1. Total sediment concentrations were measured at the start of the exposure. Colloidal Ag present in the water extractable fraction of the sediments (<200 nm) was measured at three time points across the exposure period (1, 5 and 14 days) whilst the dissolved low molecular weight fraction of silver (LMW-Ag <3kDa) was measured at the end of the uptake exposure after 14 days.

4.2.6 Data handling and analysis

Concentrations for many of the samples during these experiments were close to the limit of quantification (LOQ) of the ICP-MS. The LOQ was defined as:

$$LOQ = B + (10 * RSD) \qquad \text{Eq.1}$$

Where B refers to the concentration of silver in the blanks from the respective digest run and RSD refers to the relative standard deviation calculated internally during analysis by ICP-MS for the measurements of the blank.

Where accumulation was greater than the controls and reached a steady state across the uptake period, bioaccumulation factors were calculated. These represented the concentration of silver within the organisms relative to the external concentration of silver in the sediment.

BAF_{ss} (bioaccumulation factor at steady state) was calculated as:

$$BAF_{ss} = \frac{C_{org}}{C_{sed}} \qquad \text{Eq.2}$$

C_{org} refers to the steady state body burden or elemental concentration of the relevant nanoparticle within the organism normalised to dry tissue mass ($ngmg^{-1}$), whilst C_{sed} refers to the elemental concentration of Ag within the sediment normalised to dry sediment mass ($ngmg^{-1}$). It should be noted that C_{sed} is the combined concentration of background elemental concentration naturally present in the sediment and the additional spiked nanoparticle. BAF_{ss} has the units of kg dry weight organism per kg dry weight sediment ($kgkg^{-1}$).

Statistical analysis of the uptake and elimination phases of the exposure were conducted in the open source software R studio[18]. Multiple regression analysis

was used to examine the kinetic uptake and elimination of silver in exposed worms. The work flow for statistical analysis followed a systematic approach to test *a priori* planned contrasts. First the quality of the data was assessed. These experiments examined body burdens at the limits or our detection capabilities using ICP-MS and as such, variation in the LOD between ICP-MS runs means some samples were at or below the limits of quantification. The LOQ for the raw ICP-MS signal was ~0.06 ngml^{-1} which was the equivalent to ~0.4 ngmg^{-1} body burdens based upon the mean weight of worms during the experiment. Samples where 2 or more cases out of 5 were below the LOQ (Eq. 1) were deemed to be on or below the sensitivity of the experiment. These data points were scored simply as <LOQ and so were coded as n.a. for statistical analysis. Data was then checked for homogeneity of variance using Levene's test for homoscedasticity and Cook's distances were calculated to detect outliers.Two outliers were detected through these diagnostic tests and so were removed from the data set.

Construction of the model and regression analysis started with examination of the uptake and elimination in control organisms to test whether there was any change in body burdens over time for these groups. A linear model was then constructed to assess the effect of treatment and time upon uptake of silver. Planned contrasts were used to compare the rate of uptake in each of the silver treatments against the control. Results from the regression analysis are presented as Beta values (the gradient of the linear relationship between silver uptake and time) whilst statistical significance was considered where p values <0.05. For treatments where body burdens were greater than that of the controls, a separate regression analysis was performed to calculate the rate of uptake or elimination of silver across the exposure period.

4.3 Results

4.3.1 Characterisation of pristine particles and their stability in freshwater over time
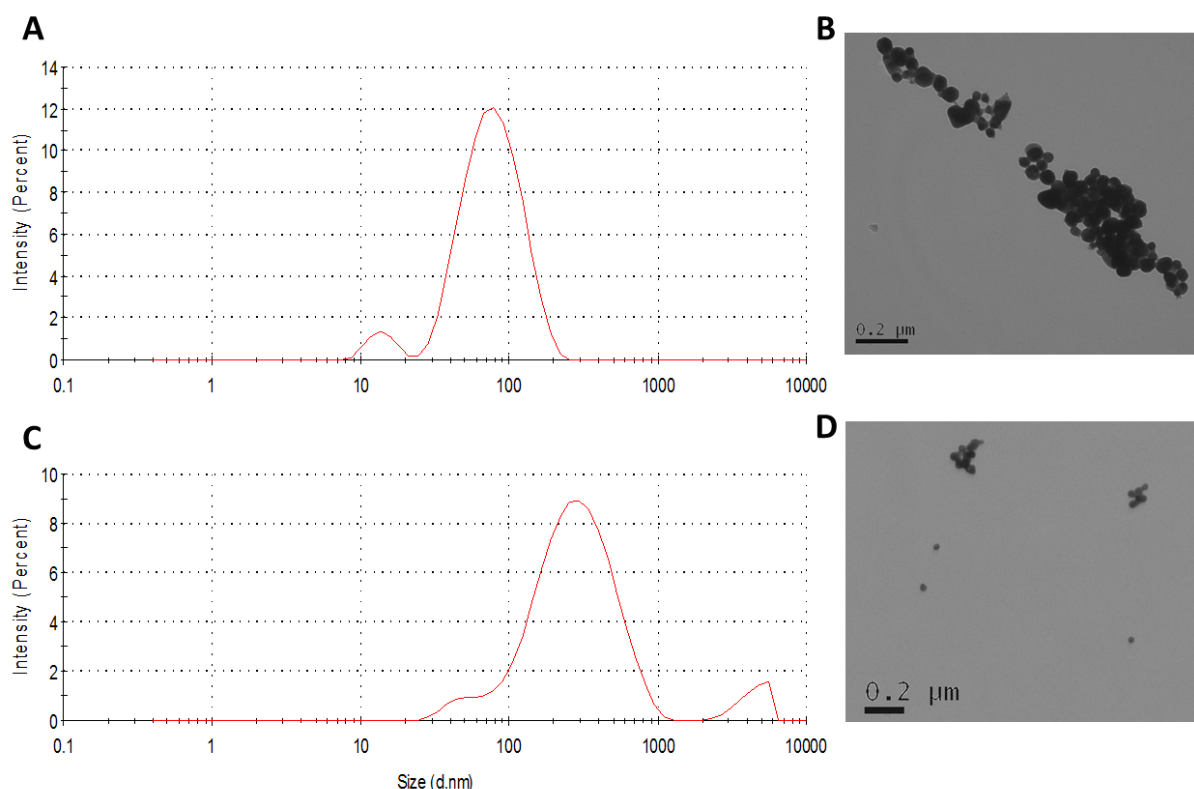
Figure 4.1: Particle size frequency distributions (Z-average, nm) measured by DLS of 50 nm PVP-Ag (A) and Ag$_2$S (C) in MilliQ. TEM images correspond to PVP-Ag (B) and Ag$_2$S (D) in freshwater after 24 hours.

Characterisation by DLS of the dispersed nanoparticles in ultrapure water produced results in close agreement with those provided by the supplier (Figure 4.1 A and C). PVP-Ag had a hydrodynamic diameter (Z-average) of 60.24 nm compared to the stated Z-average of 68.94 nm, whilst Ag$_2$S had a Z-average of 231.1 nm compared with 234.9 nm measured by the manufacturer. A number based size distribution of the Ag$_2$S found the peak size to be ~58 nm, in close agreement with the stated primary particle size of 50 nm. Qualitative examination of the particles confirmed that the particles were spherical in shape and discreet particles were visible in the expected size range ~50 nm. Quantitative measurement of particle size from the TEM images was not possible due to the proximity of particles to each other in small aggregates (Figure 4.1 B and D) preventing accurate water-shedding between individual nanoparticles in the Image-J software.
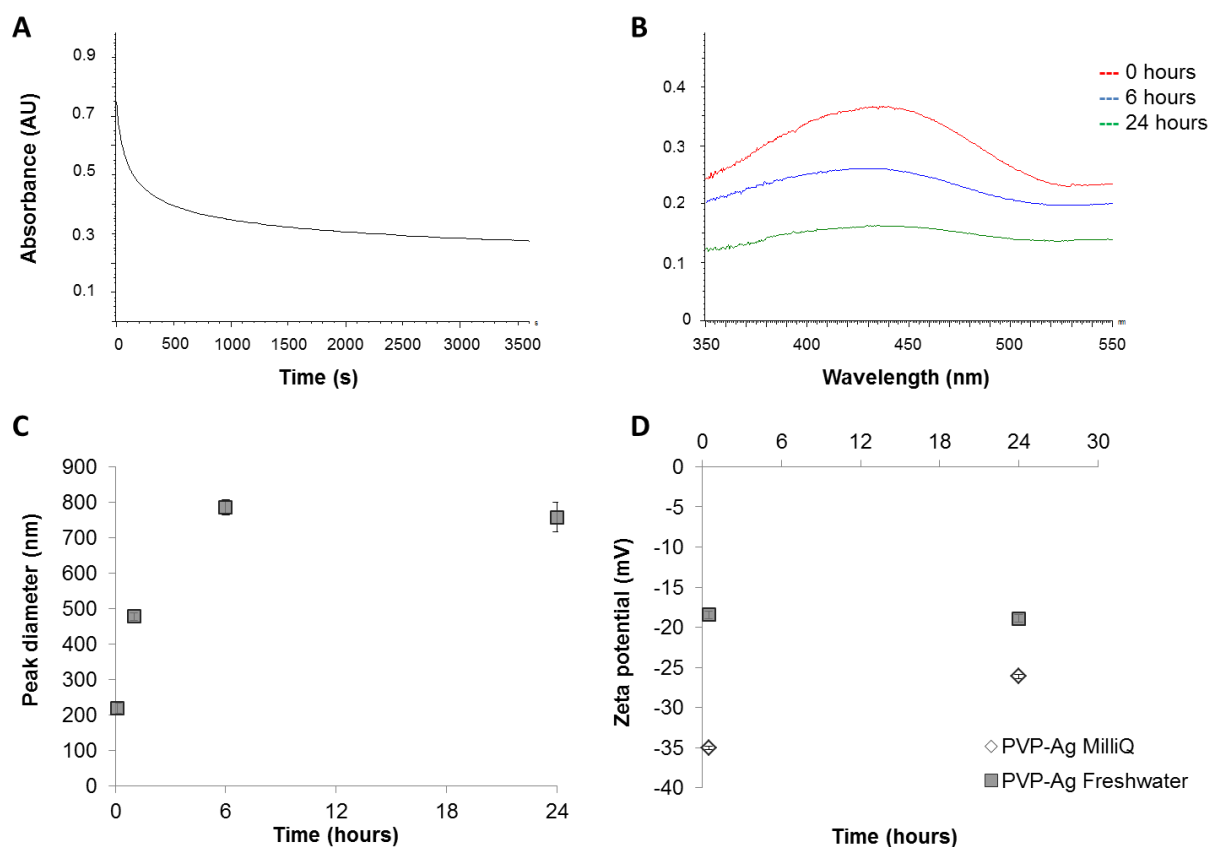
Figure 4.2: Characterisation of PVP-Ag in ultrapure and freshwater over time. A)demonstrates the loss of absorbance in PVP-Ag dispersions in freshwater at λ 420 nm over the first hour after preparation. B)is the full spectrum scan from 350 – 550 nm wavelengths over 24 hours of the same PVP-Ag dispersion in freshwater. The change in peak diameter (nm) of PVP-Ag in freshwater over 24 hours is presented in C) whilst the change in surface zeta potential in both ultrapure MilliQ and freshwater at the start and end of the 24 hour incubation is presented in D).

In freshwater, PVP-Ag experiencedsedimentation within the first 24 hours, with a loss in absorbanceat λ 420 nm within the first hour (Figure 4.2 A) followed by a steady loss in absorbance across the full spectrum detected by UV-vis (Figure 4.2 B). The aggregation over the first 24 hours to a stable suspended population of particles with a peak size of ~800 nm (Figure 4.2 C) is also evidenced in the peak broadening detected by UV-vis (Figure 4.2 B). This corresponded to a loss in Zeta potential over 24 hours in both media. Reduction in Zeta potential in freshwater was immediate (-18.46 mV) whilst in ultrapure water was characterised by a slower reduction from -35.02 mV to -26.12 mV over 24 hours (Figure 4.2 D).

134

4.3.2 Fate of fresh and aged PVP-Ag, Ag$_2$S and AgNO$_3$ within sediments
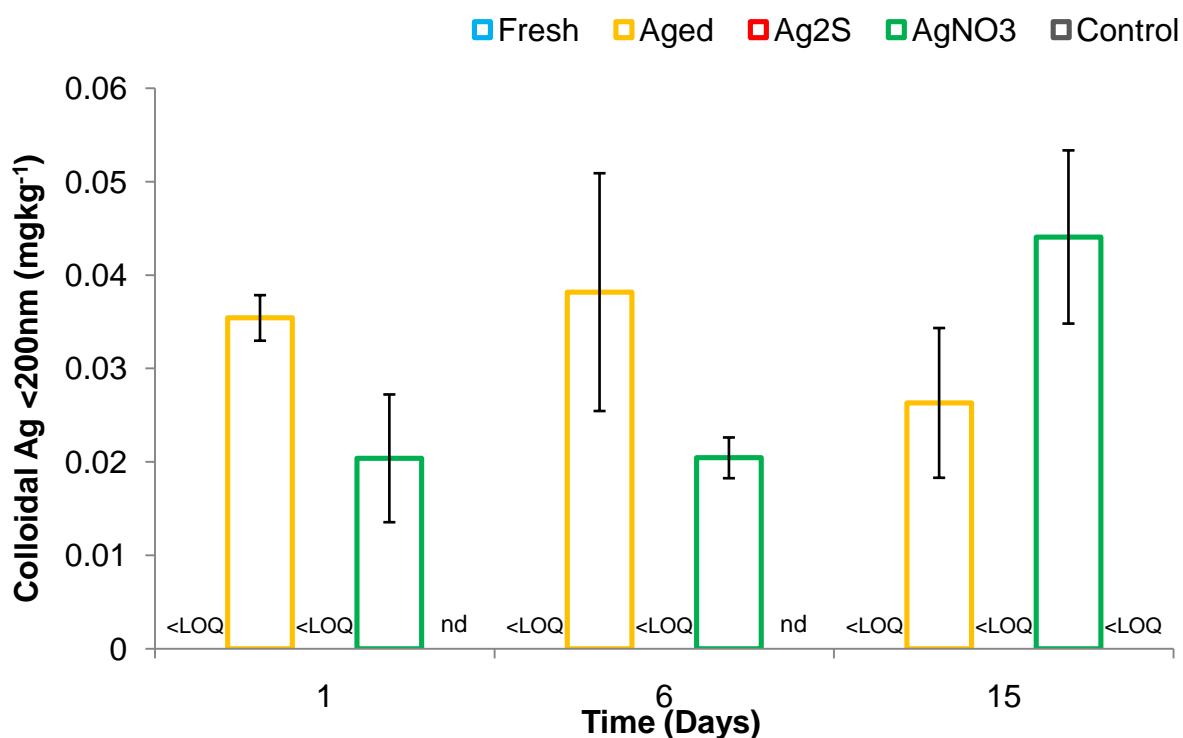
Figure 4.3: Fate of silver in the pore water colloidal fraction (<200 nm) over 14 days. <LOQ refers to samples below the limit of quantification of the ICP-MS for these runs (LOQ = 0.13 ngml^{-1}), nd = no data.

Sediment samples were taken 1, 6 and 15 days after spiking the sediments, corresponding to day 0, 5 and 14 of the biological uptake phase due to the 24 hour settling period at the start. Fresh-Ag, Ag$_2$S and controls all had no detectable Ag in the colloidal fraction of the pore water across the exposure period (Figure 4.3). Aging of the PVP-Ag nanoparticles re-mobilised silver in the pore waters after 3 months, with a stable population of Ag in the colloidal fraction of the pore waters (<200nm) of 0.033 $^+$/- 0.014 mgkg^{-1}. The data was normally distributed (p=0.1028, Shapiro-Wilks test) and homoscedastic (p=0.9627, Levene's test) fulfilling both assumptions for ANOVA. Modelling for the effect of treatment and day upon the colloidal concentration of silver found that Aged-Ag was not statistically different from that in the AgNO$_3$ exposures of 0.029$^+$/- 0.018 mgkg^{-1} (p = 0.534, ANOVA). Nor was there any change in concentration of silver in the colloidal fraction of the pore waters over time (p = 0.389, ANOVA). Conditions in the pore water remained stable across the exposure period, with a pH of 7.52 $^+$/- 0.02 and conductivity of 651 $^+$/- 5 µScm^{-1}.

Table 4.1: Partitioning of Ag NPs between the solid, colloidal and low molecular weight (LMW) fraction of the sediment. Colloidal fraction represents the average concentration of three time points whilst the LMW fraction is the concentration at the end of the 14 day exposure period.

Ag+

$AgCl_x$ (aq)

Ag(ɪ)-complexes

Treatment	Sediment concentration mgkg^{-1} (s.e.)	Colloidal fraction <200 nm mgkg^{-1} (s.e.)	LMW fraction <1kDa mgkg^{-1}
Fresh-Ag	1.36 (0.04)	<LOQ	<LOQ
Aged-Ag	2.83 (0.13)	0.033 (0.0048)	<LOQ
Ag_2S	1.11 (0.16)	<LOQ	<LOQ
$AgNO_3$	2.45 (0.08)	0.029 (0.0055)	0.005 (0.001)
Control	0.083 (0.012)	<LOQ	<LOQ

The form of silver treatment had a significant effect upon the fate of silver within the sediments. Neither Fresh-Ag nor Ag_2S were present in detectable quantities in the colloidal fraction of the sediment, and the same was true of control sediments (Table 4.1). The limit of quantification for the ICP-MS of the colloidal fraction was 0.003mgkg^{-1}. Aged-Ag (PVP-Ag aged for 3 months in sediment) and $AgNO_3$ on the other hand were detected in the colloidal fraction <200 nm at similar concentrations to those found for Citrate-Ag, PEG-Ag and $AgNO_3$ in Chapter 3 (0.049, 0.032 and 0.019 mgkg^{-1} respectively).>66% of $AgNO_3$ samples had detectable LMW-Ag, averaging at 0.005 mgkg^{-1} whilst all other Ag treatments experienced no detectable LWM-Ag. Controls, Fresh-Ag and Ag_2S <1kDa LMW-Ag fractions experienced contamination in preliminary trials and so these samples were repeated and the results of this repeat experiment are presented in Table 4.1.

4.3.3 Survival and growth of worms in response to silver exposures

No mortality was observed in any treatment across the uptake period. To ensure that exposure to any of the forms of silver was not indirectly affecting bioaccumulation, for example through sediment avoidance or causing a halt to feeding, growth across the exposure period was assessed (Figure 4.4). All

organisms from silver treatments experienced an increase in tissue mass across the exposure period equal to or greater than the growth observed in controls. *A priori* contrasts found Fresh-Ag and Aged-Ag worms to experience no difference in tissue mass compared to controls (Beta = 0.5 and 1.2, p = 0.44 and 0.059 respectively) whilst Ag_2S and $AgNO_3$ experienced slightly higher tissue mass at the end of the exposure than controls (Beta = 1.9, p < 0.05). Therefore, feeding did not appear to be inhibited in the presence of silver.
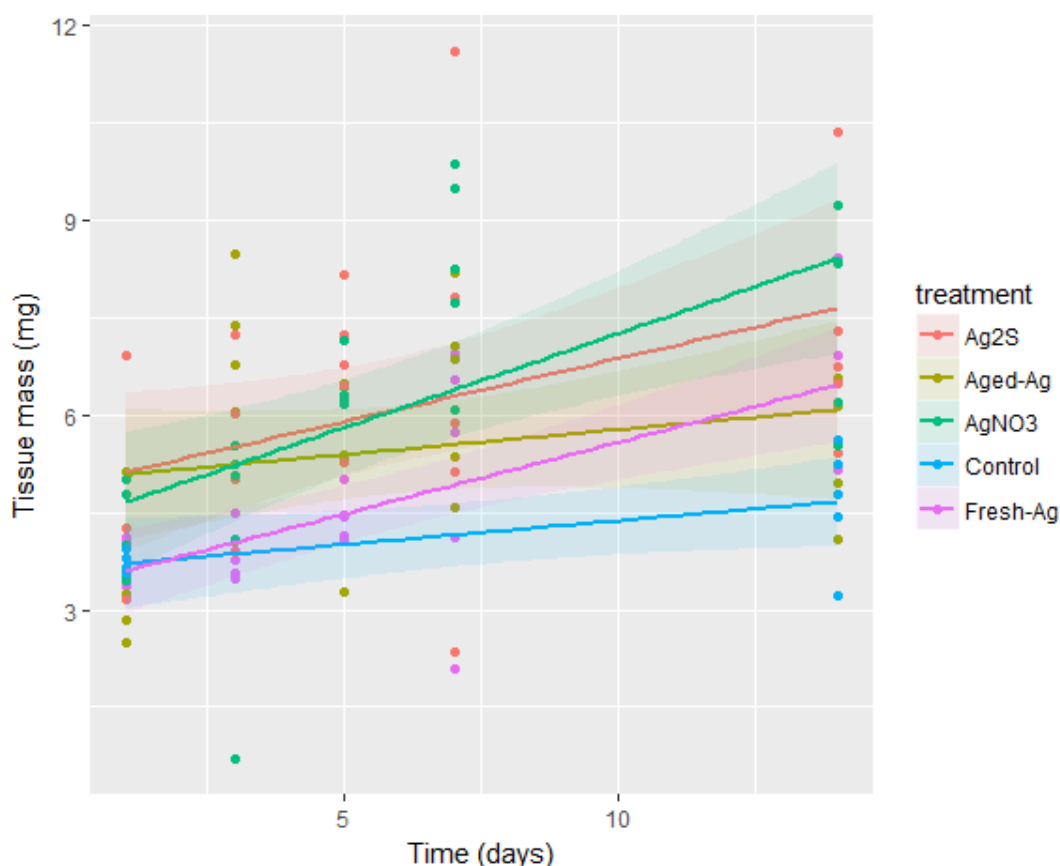
Figure 4.4: Regression analysis of organism growth over the uptake period. Regression lines are plotted along with 95% confidence intervals (shaded areas).

4.3.3 Kinetic uptake of silver from treated sediments over 14 days

For treatments and time points where 2 or more of the 5 cases per data point were below the limit of quantification, the mean for that population was deemed to be on or below the LOQ. In light of this, no quantifiable uptake of Ag was recorded for Fresh-Ag or Ag_2S exposed worms for the first 5 days (Figure 4.4). Regression analysis was employed to assess the kinetic uptake of silver in each treatment over time. During diagnostic analysis of preliminary linear models of the whole data set, two outliers were identified which could have a significant effect on the predictive capacity of the model (Cook's distance of >0.5). These

137

cases were removed from subsequent analysis. Summary statistics contrasting silver treatments with the control treatment in the new regression model found only AgNO$_3$ to be significantly different from the control (Beta = 7.98, p < 0.001).
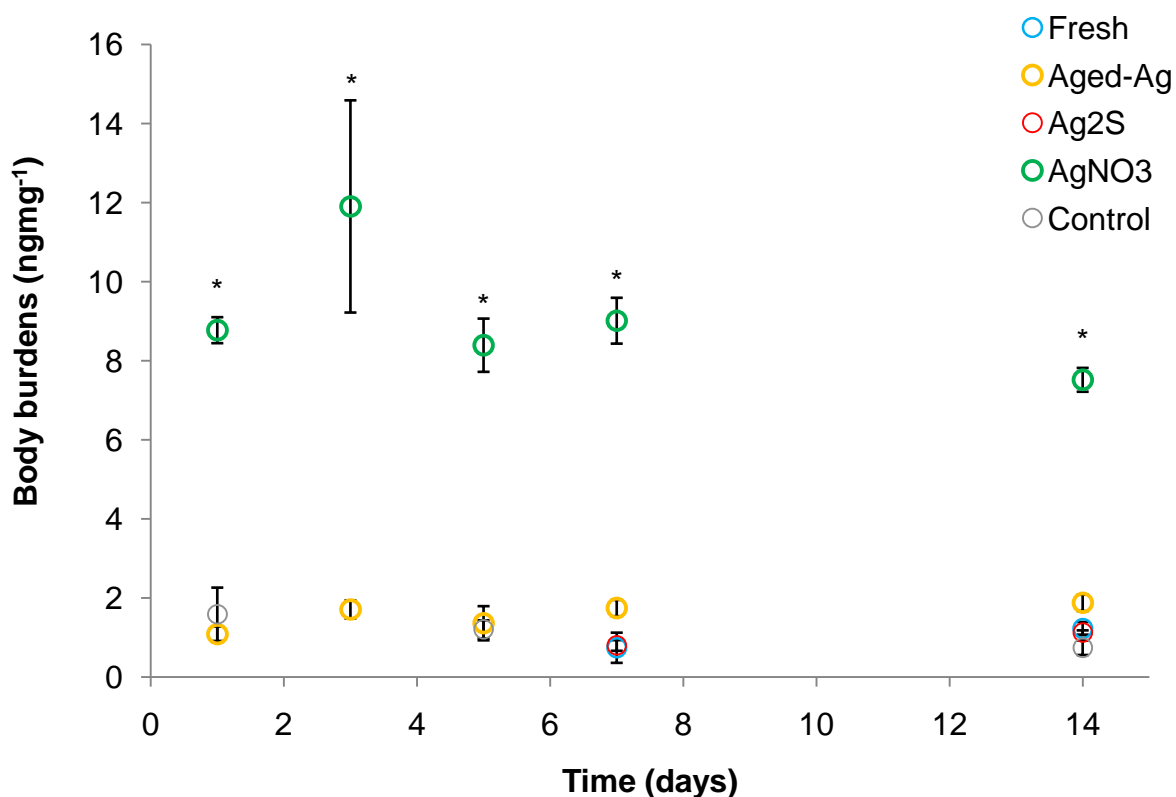
Figure 4.5: Uptake of silver over 14 days from sediments in feeding organisms. Significantly greater body burdens of silver than in controls are denoted by (*).

For control organisms, internal background concentrations of Ag did not change significantly over the exposure period (Figure 4.5), ranging between0.7 and 1.5 ngmg^{-1}(Beta = -0.063, p = 0.15). Silver was >LOQ for Fresh-Ag and Ag$_2$S exposures after 7 days exposure. Once silver had reached quantifiable levels, neither Fresh-Ag, nor Ag$_2$S were accumulated to concentrations above that of the controls (p=0.89 and p = 0.87, planned contrasts between controls and Fresh-Ag and Ag$_2$S respectively).

Ag was above the limit of quantification throughout the whole exposure in Aged-Ag treatments. Regression analysis found a small trend upwards in body burdens of 0.045 µgg^{-1}day^{-1}.This was close to being consideredstatistically significant (Beta = 0.045, p = 0.054) and multiple regression on the whole data set found no significant difference between Aged-Ag and controls (Beta = 1.15,

p = 0.205, planned contrasts).$AgNO_3$ was the only other silver treatment that experienced body burdens above the LOQ across theentire exposure. Data conformed to the assumption of homoscedasticity for linear regression. There was a slight decrease in concentration across the exposure period of 0.107 µgg^{-1}day^{-1}, however, the significance of this trend was close to the alpha of 0.05 (p= 0.0496). Overall this indicates that body burdens of Ag in $AgNO_3$ exposed organisms reached a steady state of ~9 ngmg^{-1} within the first 24 hours of exposure.This equated to a BAF$_{ss}$ of 3.73 +/- 0.25 kgkg^{-1}. As only $AgNO_3$ was bioaccumulated above that of the controls calculation of BAF$_{ss}$for nanoparticle treatments and comparison between exposures was not suitable.

4.3.4Kinetic elimination of silver after accumulation from sediment exposures

Concentration of Ag in Fresh-Ag, Aged-Ag and $AgNO_3$ exposed organisms was reduced to <LOQ within the first 6 hours of elimination and did not experience significantly higher starting body burdens than the controls (after 14 days exposure) so were not analysed for elimination kinetics. Only $AgNO_3$ is plotted in Figure 4.6.
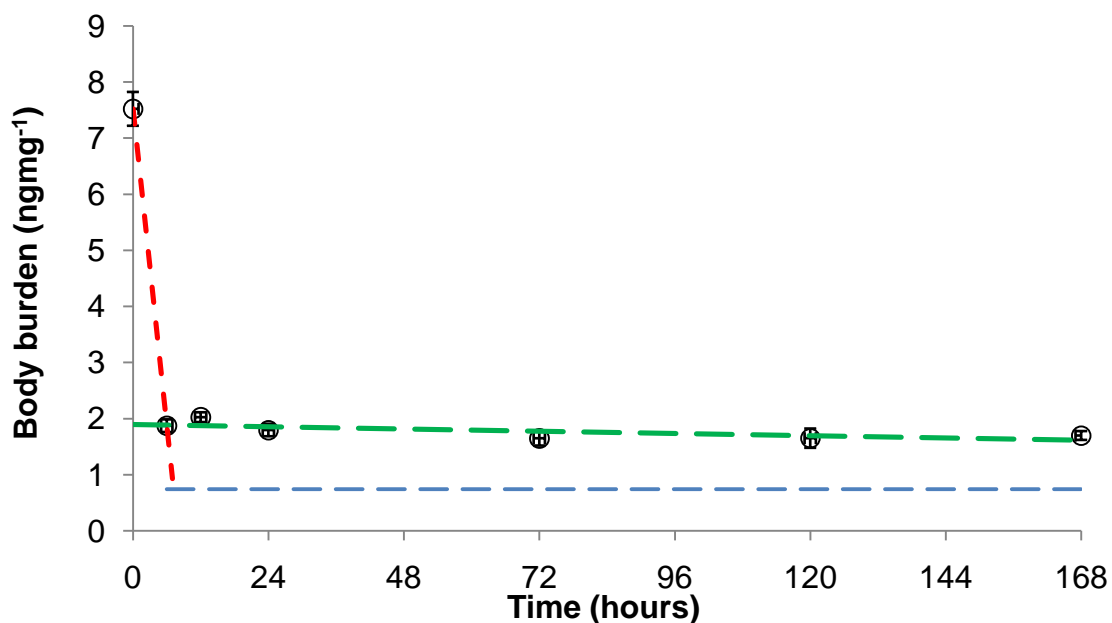
Figure 4.6: Elimination of Ag from worms over 7 days after 14 days exposure to AgNO$_3$ contaminated sediment (2.45 mgkg^{-1}). Red dashed line represents the rapid elimination rate during first phase elimination whilst the green dashes represent elimination constant for the second slow phase elimination. Blue dashes represent the background Ag in controls after 14 days uptake.

AgNO$_3$ is contrasted with the final body burdens in controls at the end of the exposure (0.74 ngmg^{-1}). Regression analysis showed AgNO$_3$ was significantly greater than the baseline of controls (Beta = 1.47, p < 0.001). Elimination of Ag occurred in a biphasic manner, with the first phase between 0 and 6 hours consisting of rapid loss of Ag at a rate of 0.942 ngmg^{-1}hour^{-1} (Beta -0.942, p < 0.001). This was the equivalent of losing 12.5% of the starting body burden of Ag per hour during the first 6 hours of elimination. The second slower elimination phase for the remainder of the 7 day elimination period occurred at a rate of 0.0395 ngmg^{-1} day^{-1}. This loss of 0.526% per day was on the cusp of statistical significance (Beta -0.0016, p = 0.0504) and so should be treated with caution. To conclude, the second period of elimination can be characterised as a very slow period of elimination with residual body burdens remaining ~1.7 ngmg^{-1} Ag, over double that of the baseline in the controls of 0.74 ngmg^{-1} for at least 7 days.

4.3.5 The relative importance of transdermal versus ingestion for uptake of silver after 5 days exposure
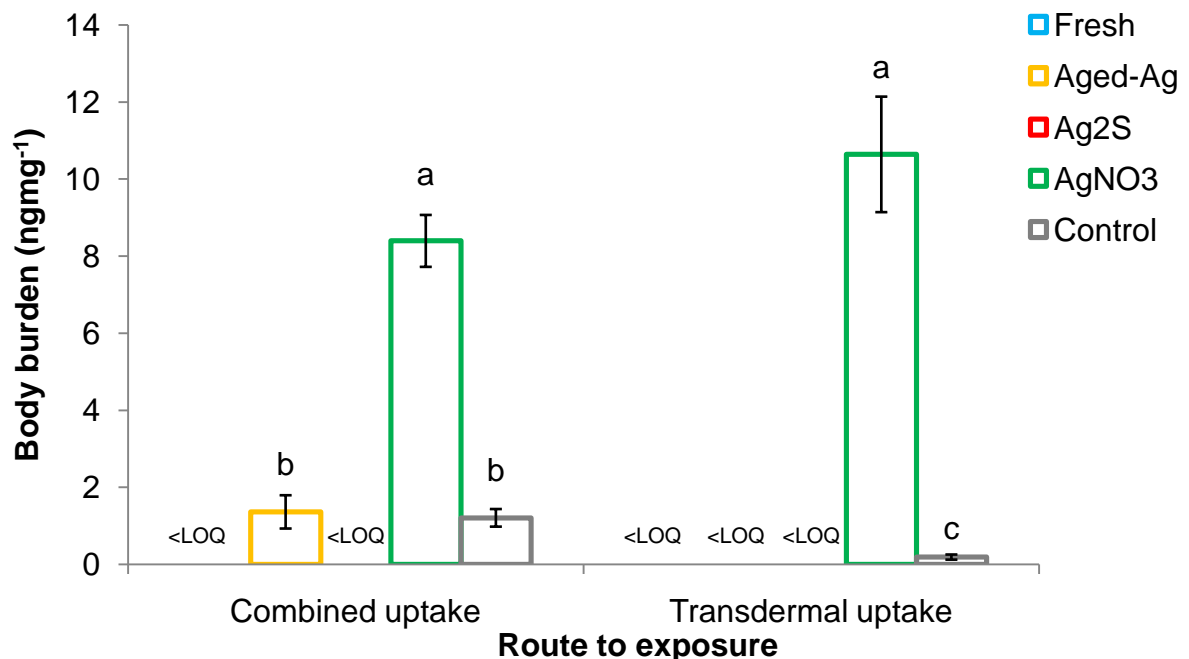
Figure 4.7: The route to uptake of Ag after 5 days exposure to dissolved AgNO$_3$ andthree Ag NP exposure scenarios (Fresh and Aged PVP-Ag and Ag$_2$S) and controls. Like for like letters represent no significant difference between cases.

Statistical analysis into the relative importance of ingestion and transdermal uptake was only undertaken on treatments where accumulation was considered >LOQ after 5 days exposure (Figure 4.7). As such Fresh-Ag and Ag_2S treatments were discounted from the analysis as they experienced 2 or more of the 5 cases making up each data point <LOQ for the ICP-MS. The remaining data did not conform to the assumption of normality required by ANOVA and so was square root transformed to address this. A significant interaction effect was detected between treatment and the route to exposure (p = 0.01213, ANOVA). *Post hoc* testing found that there was no difference between Aged-Ag and controls in feeding organisms (p = 0.9886, LSM Tukey's method). $AgNO_3$ exposed organisms on the other hand had significantly greater body burdens of Ag than controls in both feeding and non-feeding organisms (p <0.001, LSM Tukey's method), and the uptake of Ag in these two organism groups did not differ significantly (p = 0.1332, LSM Tukey's method). There was a significant difference between feeding and non-feeding control organisms representing the slight contribution of naturally occurring sediment associated silver in the sediments in organisms exposed to combined routes to uptake compared to transdermal uptake alone (p = 0.0305, LSM Tukey's method).

4.4 Discussion

4.4.1 Exposures representing accidental release or transformations during waste water treatment led to no detectable dissolution or accumulation of silver over 14 days

Dissolved low molecular weight species of silver have been implicated in contributing towards the uptake and toxicity of silver nanoparticles towards aquatic organisms[19,20]. Our own work has demonstrated that exposure to AgNPs that are to some extent soluble, results in transdermal uptake of silver (Chapter 3). The rationale for using Ag_2S during this experiment was twofold. Primarily, Ag_2S represents a transformed form of AgNP which we would expect to form during nanoparticlepassage through the waste water treatment network. For example, Whitley *et al.* 2013, found ~70% of silver in nanoparticle treatmentswas converted to Ag_2S in sediment pore waters amended with sewage sludge, irrespective of the nature of the particle coatings including citrate, PVP and uncoated Ag^{21}.An ancillary motive for using Ag_2S as a representative transformed AgNP is that it is an insoluble particle, and so allows

for investigation of the accumulation of silver nanoparticles in the absence of dissolved silver.

Ag_2S was not accumulated in worms above that of the controls across the entire exposure period (Figure 4.5). Indeed silver did not reach a quantifiable level in the organisms until 7 days into the exposure. Control organisms experienced a steady background concentration of Ag of between 0.7 and 1.5 $ngmg^{-1}$ throughout the uptake and elimination phases. Stock worms from the housing tanks prior to acclimation on clean sediment had body burdens <LOD for ICP-MS. This suggests that this background was reached during the 10 day acclimation period on clean sediment (background silver of 0.083 $mgkg^{-1}$) that all organisms experienced before the start of the exposure. The fact that worms exposed to Fresh-Ag and Ag_2S appear not to experience detectable body burdens of Ag for the first 5 days whilst control organisms did is a reflection of how the concentrations measured for this experiment are at the analytical limits of the ICP-MS set-up. Ag was detectable in some cases from Fresh-Ag and Ag_2S in these first few days, however for each of these treatments >40% of cases were below the LOQ for the ICP-MS. Inter-run variability in baseline signals measured by the ICP-MS results in a slightly different LOQ for each run, which resulted in more of the Fresh-Ag and Ag_2S samples <LOQ than controls. These data points were treated as <LOQ as there were too few cases to calculate an accurate mean or standard deviation.

Reduced or interrupted feeding in the presence of nanoparticulate Ag could explain the inconsistent body burdens observed for Fresh-Ag and Ag_2S exposed worms compared to the more consistent concentrations detected for controls. To test for this, regression analysis was performed on the tissue masses of each treatment over time. This tests for the rate of growth of worms across the exposure period and so is an indirect indicator of reduced feeding. All treatments including the control experienced an increase in tissue mass over the 14 day uptake period, starting from the same initial tissue mass. Final tissue massin all silver treatments was equal to or higher than in the controls (Figure 4.4).This indicates that feeding and growth was not significantly impaired by the silver exposures.

Therefore, we confirm that the lack of accumulation in feeding worms when exposed to either Fresh-Ag or Ag_2S is not due to inhibition in feeding, but due to the fate and behaviour of these particles in the sediment. Neither Fresh-Ag nor Ag_2S spiked to the sediment was present in the LMW-Ag or colloidal phase of the pore waters. This could explain the complete lack of transdermal or dietary uptake observed for either of these particles (Figure 4.7).In particular, work in Chapter 3 implicated dissolved species of silver, dissociating from the nanoparticle surface upon contact with the organism as a potential mechanism for transdermal uptake. Previous studies have calculated the BAF after 28 days for Ag_2S as 0.18 kgkg^{-1} in *L. variegatus*[22]. However, that study was conducted at far higher concentrations than our experiments, with sediments spiked at 444 mgkg^{-1}. This demonstrates the importance of understanding BAF in context of the exposure concentration and how that relates to expected environmental concentrations. At these more realistic concentrations of 2.5 mgkg^{-1}there was no evidence that Fresh-Ag or Ag_2S particles could dissolve and we saw no accumulation of silver, either through transdermal or dietary uptake. This suggests that these particles were simply unavailable to the organisms under these conditions.This is in agreement with emerging literature indicating that transformations of silver nanoparticles in waster waters effluents reduce their bioavailability [1].

4.4.2 The changing fate of silver under different exposure scenarios

Freshly spiked 50 nm PVP-Ag rapidly associated with the solid fraction of the sediment. This is counter to what was expected from studies investigating the fate of PVP-Ag nanoparticles in simplified media. Several studies have reported lower attachment efficiencies of PVP-Ag compared to other coated Ag NPs. PVP is a water soluble homopolymer that binds to AgNPs through the strong affinity of the N and O atoms of its polar imide group to silver, conferring steric stabilisation [23]. This is expected to prevent deposition of PVP-Ag on solid surfaces. For example, even at a high ionic strength of 100 mM of $CaCl_2$ and pH 10, PVP-Ag experienced no deposition onto a quartz crystal microbalance [24]. Under these conditions, electrostatic attraction was expected to lead to deposition as the zeta potential of the PVP-Ag was +17 mV and for the deposition surface of the microbalance -7.4 mV. The lack of deposition demonstrates that steric stabilisation is provided by the PVP. However,

increasing the complexity of the surface for deposition, for example by coating quartz sand "sediment" columns with kaolinite clay or ferrihydrite-coated sand still reduces the transport of PVP-Ag through the sand column [25]. Other common iron and clay soil minerals have been found to heteroaggregate with both sterically and electrostatically stabilised 20 – 30 nm AgNPs resulting in >85% of silver aggregating to >450 nm [26]. This extensive heteroaggregation also appeared to be the case in our study, with no colloidal Ag present in the <200 nm fraction of the pore waters during the Fresh-Ag treatment. This highlights the difficulties with extrapolating results from simplified mobility experiments such as silica sand transport columns or quartz microbalance deposition to complex media, more closely representing real world conditions.

In our test system, the high retention of silver by the solid fraction of the sediment may be through heteroaggregation with natural colloids >200 nm in size, or integration of PVP-Ag within flocs of natural organic matter within the sediment. Even in the absence of natural colloids, the peak hydrodynamic diameter of PVP-Ag increased within the first 24 hours to ~800 nm (Figure 4.2 C). This explains the lack of detectable levels of silver in the colloidal (<200 nm) fraction of the Fresh-Ag pore water. Likewise, the Z-average for Ag_2S after 24 hours in freshwater was 252 nm with a peak diameter of 408 nm (Figure 4.1 C), again resulting in no detectable Ag in the colloidal fraction of the pore waters. Colloidal silver from $AgNO_3$ treatments on the other hand could be detected in the sediment pore waters throughout the 14 day uptake phase. The persistence of colloidal silver in the pore waters (0.029 +/- 0.005 mgkg^{-1}) did not differ significantly from that found in Chapter 3 (0.019 +/- 0.009 mgkg^{-1}). This is likely to be dissolved species of silver associated with natural colloids <200 nm in size, or nanoparticulate silver formed from the reduction of dissolved silver in the presence of organic matter, as was discussed in Chapter 3.

Aging the PVP-Ag resulted in a labile fraction of silver emerging in the sediment pore waters after the 3 months incubation. In keeping with the results presented in Chapter 3, the concentration of silver in the colloidal fraction did not differ significantly from that of $AgNO_3$. This indicates that conditions within the sediment are limiting the concentration of silver possible in this colloidal fraction, rather than properties of the silver itself. This hypothesis is strengthened by the absence of a time effect upon silver concentration in this fraction. There was no

144

change in colloidal Ag in either $AgNO_3$ or Aged-Ag treatments over the 14 day exposure period (Figure 4.3), suggesting that colloidal silver had reached a stable concentration. The formation of colloidal silver, mobile in the pore water during the 3 month aging period may occur in two ways. PVP-Ag particles themselves may dissociate from the solid fraction of the sediment over time. This is usually under dynamic conditions of flow, where sheering of particles from larger homo/heteroaggregates is possible[27, 28], but may also occur theoretically where particles only weakly deposited at collector surfaces can overcome this interaction through random variations in kinetic energy and diffuse from the surface [29, 30]. Such re-mobilisation of silver nanoparticles has been observed in work by Coutris *et al.* 2012, where 19 nm uncoated AgNPs initially associated strongly with the solid fraction of the sediment, but were re-entrained into the "bioavailable" water extractable and ion exchangeable fraction of the pore waters over a 10 week period [10]. It should be noted however thatdetermining the exact cause for this re-mobilisation of silver was not within the scope of the study.

The second mechanism for the establishment of a labile colloidal phase of Ag in the sediment pore waters during 3 months aging may be through chemical weathering of the particles and subsequent reduction and formation of AgNPs and colloids from these dissolution products in the pore water. Characterisation of 16 nm NM300K reference Ag NPs aged in soils at 155 $mgkg^{-1}$over timescalesfrom 4 weeks to 10 months, found that particles bound to soil grains under saturated conditions acted as a constant source of dissolved Ag, increasing the concentration in the pore waters over time [31]. The authors proposed that dissolved species of silver were released from the particles into the pore waters, and, where exposure concentrations were high, dissolution from these particles could exhaust the supply of complexing anions (e.g. pore water chloride) resulting in this increasing fraction of mobile silver in the pore waters. Our spiking concentration was much lower than this, so exhaustion of pore water chloride for complexing dissolved silver from the nanoparticles is unlikely. However, reduction of dissolved silver to form small nanoparticles in the presence of humic acids has also been detected under environmentally relevant conditions [8]. Our sediments contain 2.26% organic carbon by dry weight. Therefore, a combination of dissolution and complexation of low

molecular weight species of silver and reduction of this silver to form nanoparticles in the presence of natural organic matter could be responsible for the appearance of silver in the colloidal fraction of the pore water after 3 months aging.

4.4.3 Implications of aging for nanoparticle bioavailability in sediments

This study assessed the impact of quiescent aging upon Ag NP bioavailability. It should be noted that this is simply one of a range of potential aging processes that may occur for nanoparticles in freshwater environments. It does not aim to define a rule from which to extrapolate the effect of aging on other nanoparticles or under different environmental conditions, rather it presents a novel case study using silver, which aims to measure changes in nanoparticle fate during aging and how this effects bioaccumulation.

During this study, quiescent aging of PVP-Ag nanoparticles did appear to change the fate of these particles in the sediment. A labile colloidal fraction of silver emerged for PVP-Ag treated sediments after aging for 3 months which was not apparent for the Fresh-Ag particles spiked to the sediment (Figure 4.3). This did not translate to a significant increase in bioavailability of the silver as these Aged-Ag particles were not accumulated to concentrations greater than the controls. Body burdens of silver in all nanoparticle treatments were close to the sensitivity of the experiment, with body burdens being <LOQ for Fresh-Ag and Ag_2S until the seventh day of the exposure. Whilst accumulation of Aged-Ag appeared qualitatively different from Fresh-Ag or Ag_2S (body burdens were measureable from the first sampling time point) we cannot conclude that Aged-Ag nanoparticles were more bioavailable as they were not accumulated significantly above the background concentration in the worms.

Importantly, whilst the emergence of a colloidal fraction of silver in the pore waters was statistically significant, this did not translate to a persistent dissolved fraction of silver in the pore waters or an appreciable increase in silver uptake from the sediments of these aged particles in the worms. Further work comparing feeding organisms with and without a gut clearance phase may be able to distinguish between Ag in transit in the gut and that which translocated into tissues after ingestion. This was employed successfully to distinguish between the sediment associated Ce in the guts (which was masking

differences in accumulation between CeO_2 exposed worms and controls) and the contribution of ingestion engineered CeO_2NPs to accumulation in Chapter 2.

4.4.4 Different exposure scenarios did not alter the route to uptake of insoluble silver

Non-feeding worms were generated to quantify the contribution of transdermal uptake of silver towards nanoparticle bioaccumulation under the three exposure scenarios. In our previous work, this has demonstrated that transdermal uptake of silver can account for the bioaccumulation of silver from Citrate-Ag and PEG-Ag treated sediments and that dissolved species of silver in turn can account for most of this transdermal uptake (Chapter 3). Differences in final body burdens of silver between Citrate-Ag and PEG-Ag treatments was most likely due to differences in persistence of these particles and contact between the particles and the worms' epidermal surfaces. Localised dissolution of the nanoparticle at this point of contact could lead to transdermal uptake of dissolved low molecular weight species of silver through established cellular uptake mechanisms, for example through sodium ion transport channels[32]. In this study, neither PVP-Ag nor Ag_2S experienced measurable dissolution within the sediments. Therefore, uptake of silver in non-feeding worms, in particular those exposed to Ag_2S, an insoluble particle, tests the capacity for transdermal uptake of nanoparticles themselves rather thanof localised dissolution at the organisms' surface.

After 5 days exposure, no transdermal uptake was observed for any of the nanoparticle treatments (Figure 4.7). Only $AgNO_3$ was accumulated across the skin. There was no difference in body burdens between feeding and non-feeding worms exposed to $AgNO_3$, indicating that ingestion made negligible contributions towards silver accumulation. The final body burdens in these worms were between 8.4 and 10.6 ngmg^{-1}. This is in good agreement with the $AgNO_3$ exposed worms in Chapter 3, which had body burdens of 7.4 and 5.6 ngmg^{-1} in feeding and non-feeding groups respectively, also after 5 days exposure to 2.5 mgkg^{-1} $AgNO_3$. This confirms that the test method provides reproducible and consistent results. The lack of transdermal uptake of Ag in any of the nanoparticle treatments demonstrates that within these model freshwater sediments, nanoparticles themselves are not accumulated across the skin, it is dissolved low molecular weight species of silver, only present in $AgNO_3$ treatmentswhich are responsible for transdermal uptake.

It was expected from the literature that if the PVP-Ag particles could persist as 50 nm nanoparticles, some cellular uptake through endocytosis would be possible. Cellular uptake of 30 nm Citrate-Ag nanoparticles through endocytic pathways has been confirmed in the gut epithelial cells of the marine worm *Nerisdiversicolor*[33] whilst Khan *et al.* 2014, used inhibitory drugs to demonstrate the uptake of dissolved silver through sodium (Na^+) channels and of ~20 nm Citrate-Ag through clathrin and caveolae-mediated endocytosis [34]. If our 50 nm PVP-Ag or Ag_2S could persist in the pore waters as distinct, individual particles we might expect to see some contribution of ingestion towards body burdens. In sub-oxic conditions, similar 50 nm PVP-Ag has been demonstrated to be resistant to aggregation in the presence of either Na_2S, or humic acids [35], however, in the freshwater media used during this study, PVP-Ag aggregated within 24 hours to >800 nm. This demonstrates the importance of characterisation of all nanoparticles under conditions used in exposures as even with the same core and surface properties, extrapolation of nanoparticle behaviour from the literature to a biological system can still be un-representative. Small, individual particles may persist for Aged-Ag in the pore waters. However, uptake was too low to be distinguished against the background of the controls without a gut clearance phase, resulting in a final concentration of 1.9 ngmg^{-1} Ag in worms exposed to Aged-Ag compared to 0.75 ngmg^{-1} in controls at the end of the exposure (Figure 4.5).

After 5 days exposure, any contribution of Ag translocated across the gut epithelia was masked by the contribution of sediment associated silver in the gut contents, resulting in similar body burdens of Ag in Aged-Ag and control worms. No clearance step was performed for these organisms in accordance with OECD TG315 which recommends no clearance phase in order to measure a conservative BAF (DOI: 10.1787/2074577x). Also our previous work in Chapter 3suggested that if transdermal uptake was possible then the 6 hour clearance step in freshwater did not significantly reduce body burdens, contributing towardsour decision not to include a clearance step for these organisms. However, the inclusion of a clearance step may have been able to distinguish between Ag associated with sediment in the guts and that which had been accumulated through ingestion, as was possible for the CeO_2 NPs studied in Chapter 2.In light of this, we recommend that for nanomaterials which

experience significant accumulation above controls, a gut clearance phase can be used on a case by case basis, basing the decision on the hypothesis being tested. For nanoparticles where there is limited accumulation or where transdermal uptake is not possible, we recommend a gut clearance phase so as to remove any sediment associated nanomaterials. When exposure concentrations are close to the background concentration in the uncontaminated sediments, this material may mask the true accumulation of the nanoparticle as we found for 4-8 nm cerium oxide nanoparticles in Chapter 2. As such, investigation of transdermal uptake should be the priority for nanoparticles which undergo dissolution, but the contribution of ingestion towards uptake of insoluble nanoparticles must not be overlooked.

4.4.5 The kinetics of accumulation and elimination of dissolved silver from spiked sediments

None of the silver nanoparticle treatments resulted in body burdens significantly greater than the controls and so assessment of the bioaccumulation kinetics for these particles was not possible. $AgNO_3$ on the other hand reached a steady state within the first day of exposure. Across the whole exposure period BAF_{ss} was 3.73 +/- 0.25 $kgkg^{-1}$, which was in good agreement with the BAF_5 of feeding organisms exposed to $AgNO_3$ in Chapter 3 of 2.23 +/- 0.24 $kgkg^{-1}$.There was a slight decrease in uptake of 0.045 $\mu gg^{-1}day^{-1}$,but this was not statistically significant (Figure 4.5). The steady state concentration of silver from dissolved silver uptake was therefore between 7.5 and 12 $ngmg^{-1}$. Identical exposures in Chapter 3 resulted in the similar body burdens of Ag (7.4 $ngmg^{-1}$) and a dissolved fraction of silver of 0.01 $mgkg^{-1}$ in the sediment pore waters.This suggests that uptake of dissolved silver through proton coupled Na^+ channels or passive uptake across membranes in freshwater when present as the neutral complex of $AgCl_0$ for example, is in equilibrium with the external concentration of dissolved silver in the sediment pore waters between 0.005 - 0.01$mgkg^{-1}$. This accumulation was predominantly though transdermal uptake rather than uptake across the gut, as there was no difference in accumulation between feeding and non-feeding worms (Figure 4.7).

The elimination profile of $AgNO_3$ fitted a two compartment loss model. The majority of silver was lost within the first 6 hours of elimination on clean sediment (Figure 4.6) at a rate of 0.942 $ngmg^{-1}hour^{-1}$. This was followed by a

slower elimination phase which over 6 days was not significant, resulting in non-eliminated residues of 1.78 $^+$/- 0.05 ngmg^{-1} or ~24% of the body burden at steady state, compared to the control background of 0.74 $^+$/- 0.2 ngmg^{-1}. Interestingly, this differed from our previous work where a 6 hour clearance step in freshwater resulted in no significant loss of silver from the tissues (Chapter 3). Elimination of silver in Chapter 3 was performed in freshwater only, based on work by Mount *et al.* 1999, where they found that 6 hours elimination was sufficient to eliminate >98% of the gut contents of the worms whilst limiting depuration of non-ionic organic contaminants from tissues [36]. Khan *et al.* 2015 found similar slow elimination of silver from *L. variegatus* in freshwater as that demonstrated in Chapter 3[37]. After exposure to AgNO$_3$, silver was eliminated at a rate of ~13% per day or 3.24% in 6 hours, which is in agreement with the lack of significant elimination of Ag from non-feeding worms after 6 hours clearance in freshwater in Chapter 3.

4.4.6 Elimination profiles for dissolved silver differed between water only and sediment based elimination

Elimination differed between clearance occurring in freshwaterfrom our previous work and on sediment in this chapter. There was no significant loss of Ag accumulated across the skin from either nanoparticles or AgNO$_3$ after 6 hours gut clearance in freshwater (Chapter 3), compared to clearance on clean sediment resulting in a loss of >70% of the accumulated Ag within the first 6 hours (Figure 4.6). Insufficient literature exists to systematically identify for the worm *L. variegatus*whether these two different profiles of elimination exist for other nanomaterials or for silver more generally when organisms are depurated on either clean sediment or in water only. Future work is necessary to investigate whether such different elimination profiles under the two conditions are foundfor other nanomaterials or species.

The process of elimination of accumulated silver upon transfer of the worms into clean freshwater or sediment could in part be simply movement of silver along a diffusion gradient, from high concentrations in the worms out into the low background of the sediments.However, this would not account for the markedly different elimination profiles we observed between these two methods. There may also be active elimination of silver from the gut. For example, goblet cells in the intestinal tract of mice have been demonstrated to internalise carbon

nanoparticles in vesicles and excrete these through exocytosis into the gastrointestinal cavity [38].Similar waste processing within cells may be responsible for the elimination of silver after internalisation and could explain the difference we observe between clearance phases conducted in freshwater and sediments.

Detoxification ofmetal ions occurs through several mechanisms in cells, including incorporation into metallothionein or metallothionein like proteins and through biomineralisation and the formation of insoluble metal granules [39]. Metallothioneins are a cysteine containing protein with a strong affinity to silver which hold two main biological roles: the first in the routine handling of excess essential metals such as zinc and copper in the cell, and the second in the detoxification of non-essential metals including cadmium, silver and mercury. Recent studies suggest that although $AgNO_3$ and Ag NPs may experience different routes to cellular uptake and internalisation they can experience similar toxicodynamic responses[40]. For example, silver dissolving from Citrate-Ag and PVP-Ag particles within hepatocytes diffuse out of vesicles and complex with sulphur containing glutathione and metallothionein in much the same fashion as $AgNO_3$ [41]. These studies indicate that *in vivo*, whilst the molecular pathways to internalisation may differ between nanoparticulate and dissolved silver, they may experience some of the same processes within cells upon uptake. This could explain why there was no difference in elimination of silver irrespective of the silver treatment worms were exposed to, with no significant loss of Ag from tissues after 6 hours clearance in water (Chapter 3).

Silver bound to metallothionein or insoluble metal granules would be stored or eliminated from the cell during the natural cell cycle, as metallothioneins, like all proteins have limited lives and are transported to and broken down in lysosomes[42]. Detoxified metals can then be eliminated from the cell in residual bodies (vesicles containing non-digested material) [43]. It is possible that transport and elimination of these waste metals to the worm gut may be faster under conditions where the organism is feeding and themetabolism of the worm is higher. This could lead to a more rapid elimination of lysosomal residual bodiesin worms allowed to purge their guts on clean sediment than in water only. Active metabolism and an increase in ventilation and filtration rates are well documented in the presence of a food source in other invertebrates such

as the mussel *Mytilus edulis*[44]. Similar processes could be activated for these worms.Alternatively, any metal removal and elimination into the guts during the elimination phase could be more effective in clean sediments, where exocytosedmetal granules or deposits could be entrained by the constant supply of passing sediment and so removed more rapidly from the gut lining than if sediment material is simply being eliminated from the gut and replaced with water, as was the case during water-only elimination. However, currently this is speculative. Future work is needed to establish the exact cause behind the increased rate of elimination of silver in the presence of sediment than in water only and whether this difference is due to differences between an active motile and inactive gut.

Attempts to mechanistically model elimination rates for a range of metals have found that whilst metals with a high affinity to sulphur ligands experience higher absorption efficiencies, all metals studied in a meta-analysis experience comparable elimination rates across a range of species when adjusted to body mass of the organisms[45]. Therefore, although nanoparticles may experience differing uptake rates, this relationship between slower elimination in water only clearance phases could hold true both for a range of nanoparticles and may also prove ubiquitous across many species. Future efforts should address the relationship between the medium and the rate of elimination of nanomaterials and assess its ubiquity in other species, as it has great implications for developing standardised testing and for the metrics we use to define nanomaterial risk.

Conclusions

We examined the fate of dissolved and colloidal silver in the sediment pore waters throughout three different exposure scenarios to assess whether these fate parameters could explain patterns of uptake of nanoparticulate silver. The hypothesis was that the effect of aging upon these dynamic fate processes would alter either the route or extent of bioaccumulation. Both Fresh-Ag representing accidental releases and Ag_2S representing AgNPs transformed during the waste water treatment process were entirely bound to the solid fraction of the sediment, with no silver detected in the colloidal or dissolved fraction of the pore waters. Neither of these particles were accumulated in the

worms. We found that aging 50 nm PVP-Ag did result in the release of a mobile colloidal (<200 nm) fraction of silver in the pore waters after 3 months, but that this was not soluble and was not accumulated significantly by the organism. Only AgNO$_3$ exposures representing a soluble form of silver resulted in significant uptake of silver by the worm *L. variegatus*. As such, dissolved silver in the pore waters was a better predictor of bioavailability than colloidal silver. Future studies should focus upon silver nanoparticles which can experience dissolution within sediments, and investigate how aging affects fluxes of dissolved silver to the pore waters and its subsequent impact upon bioaccumulation.

References

1   A. Azimzada, N. Tufenkji and K. J. Wilkinson, *Environ. Sci. Nano*, 2017, **4**, 1339–1349.

2   M. Baalousha, K. P. Arkill, I. Romer, R. E. Palmer and J. R. Lead, *Sci. Total Environ.*, 2015, **502**, 344–353.

3   G. V. Lowry, K. B. Gregory, S. C. Apte and J. R. Lead, *Environ. Sci. Technol.*, 2012, **46**, 6893–6899.

4   F. Wang, L. Yu, M. P. Monopoli, P. Sandin, E. Mahon, A. Salvati and K. A. Dawson, *Nanomedicine Nanotechnology, Biol. Med.*, 2013, **9**, 1159–1168.

5   D. M. Mitrano and B. Nowack, *Nanotechnology*, 2017, **28**, 1–23.

6   F. Van Koetsem, T. T. Geremew, E. Wallaert, K. Verbeken, P. Van der Meeren and G. Du Laing, *Ecol. Eng.*, 2015, **80**, 140–150.

7   G. Cornelis, C. DooletteMadeleine Thomas, M. J. McLaughlin, J. K. Kirby, D. G. Beak and D. Chittleborough, *Soil Sci. Soc. Am. J.*, 2012, **76**, 891.

8   N. Akaighe, R. I. MacCuspie, D. A. Navarro, D. S. Aga, S. Banerjee, M. Sohn and V. K. Sharma, *Environ. Sci. Technol.*, 2011, **45**, 3895–3901.

9   M. Auffan, A. Masion, J. Labille, M. A. Diot, W. Liu, L. Olivi, O. Proux, F. Ziarelli, P. Chaurand, C. Geantet, J. Y. Bottero and J. Rose, *Environ. Pollut.*, 2014, **188**, 1–7.

10   C. Coutris, E. J. Joner and D. H. Oughton, *Sci. Total Environ.*, 2012, **420**, 327–333.

11   M. Tejamaya, I. Römer, R. C. Merrifield and J. R. Lead, *Environ. Sci. Technol.*, 2012, **46**, 7011–7017.

12   K. Kettler, K. Veltman, D. van de Meent, A. van Wezel and A. J. Hendriks, *Environ. Toxicol. Chem.*, 2014, **33**, 481–492.

13   E. Lombi, E. Donner, K. G. Scheckel, R. Sekine, C. Lorenz, N. Von Goetz and B. Nowack, *Chemosphere*, 2014, **111**, 352–358.

14   T. Y. Sun, F. Gottschalk, K. Hungerbühler and B. Nowack, *Environ. Pollut.*, 2014, **185**, 69–76.

15   Q. Sun, Y. Li, T. Tang, Z. Yuan and C. P. Yu, *J. Hazard. Mater.*, 2013, **261**, 414–420.

16   B. Kim, C.-S. Park, M. Murayama and M. F. Hochella, *Environ. Sci. Technol.*, 2010, **44**, 7509–7514.

17   OECD, *OECD Guidelines for the Testing of Chemicals 315: Bioaccumulation in Sediment-dwelling Benthic Oligochaetes*, OECD Publishing, 2008.

18   RStudio Team, 2016.

19   B. J. Shaw and R. D. Handy, *Environ. Int.*, 2011, **37**, 1083–1097.

20   H. J. Jo, J. W. Choi, S. H. Lee and S. W. Hong, *J. Hazard. Mater.*, 2012, **227–228**, 301–308.

21   A. R. Whitley, C. Levard, E. Oostveen, P. M. Bertsch, C. J. Matocha, F. Von Der

Kammer and J. M. Unrine, *Environ. Pollut.*, 2013, **182**, 141–149.

22   M. P. Hirsch, *Environ. Toxicol. Chem.*, 1998, **17**, 605–609.

23   P.-Y. Silvert, R. Herrera-Urbina and K. Tekaia-Elhsissen, *J. Mater. Chem.*, 1997, **7**, 293–299.

24   B. J. R. Thio, O. M. Montes, M. A. Mahmoud, D. W. Lee, D. Zhou and A. A. Keller, *Environ. Sci. Technol.*, , DOI:10.1021/es203596w.

25   A. M. El Badawy, A. Aly Hassan, K. G. Scheckel, M. T. Suidan and T. M. Tolaymat, *Environ. Sci. Technol.*, 2013, **47**, 4039–4045.

26   M. Hoppe, R. Mikutta, S. Kaufhold, J. Utermann, W. Duijnisveld, E. Wargenau, E. Fries and G. Guggenberger, *Eur. J. Soil Sci.*, 2016, **67**, 573–582.

27   F. He, M. Zhang, T. Qian and D. Zhao, *J. Colloid Interface Sci.*, 2009, **334**, 96–102.

28   I. Chowdhury, Y. Hong, R. J. Honda and S. L. Walker, *J. Colloid Interface Sci.*, 2011, **360**, 548–555.

29   C. Shen, B. Li, Y. Huang and Y. Jin, *Environ. Sci. Technol.*, 2007, **41**, 6976–6982.

30   S. A. Bradford, S. Torkzaban and J. Simunek, *Water Resour. Res.*, 2011, **47**, 1–12.

31   M. J. C. van der Ploeg, R. D. Handy, P. L. Waalewijn-Kool, J. H. J. van den Berg, Z. E. Herrera Rivera, J. Bovenschen, B. Molleman, J. M. Baveco, P. Tromp, R. J. B. Peters, G. F. Koopmans, I. M. C. M. Rietjens and N. W. Van den Brink, *Environ. Toxicol. Chem.*, 2014, **33**, 743–752.

32   N. R. Bury and C. M. Wood, *Am. Physiol. Soc.*, 1999, R1385–R1391.

33   J. García-Alonso, F. R. Khan, S. K. Misra, M. Turmaine, B. D. Smith, P. S. Rainbow, S. N. Luoma and E. Valsami-Jones, *Environ. Sci. Technol.*, 2011, **45**, 4630–4636.

34   F. R. Khan, S. K. Misra, N. R. Bury, B. D. Smith, P. S. Rainbow, S. N. Luoma and E. Valsami-Jones, *Nanotoxicology*, 2015, **9**, 493–501.

35   C. J. Milne, D. J. Lapworth, D. C. Gooddy, C. N. Elgy and É. Valsami-Jones, *Environ. Sci. Technol.*, 2017, **51**, 6063–6070.

36   D. R. Mount, T. D. Dawson and L. P. Burkhard, *Environ. Toxicol. Chem.*, 1999, **18**, 1244–1249.

37   F. R. Khan, K. B. Paul, A. D. Dybowska, E. Valsami-Jones, J. R. Lead, V. Stone and T. F. Fernandes, *Environ. Sci. Technol.*, 2015, **49**, 4389–4397.

38   B. Zhao, L. Sun, W. Zhang, Y. Wang, J. Zhu, X. Zhu, L. Yang, C. Li, Z. Zhang and Y. Zhang, *Nanomedicine Nanotechnology, Biol. Med.*, 2014, **10**, 839–849.

39   J. C. Amiard, C. Amiard-Triquet, S. Barka, J. Pellerin and P. S. Rainbow, *Aquat. Toxicol.*, 2006, **76**, 160–202.

40   M. Novo, E. Lahive, M. Díez-Ortiz, M. Matzke, A. J. Morgan, D. J. Spurgeon, C. Svendsen and P. Kille, *Environ. Pollut.*, 2015, **205**, 385–393.

41   G. Veronesi, A. Deniaud, T. Gallon, P.-H. Jouneau, J. Villanova, P. Delangle, M.

Carrière, I. Kieffer, P. Charbonnier, E. Mintz and I. Michaud-Soret, *Nanoscale*, 2016, **8**, 17012–17021.

42   C. D. Klaassen, S. Choudhuri, J. McKim-JM, M. L. D. Lehman and W. C. Kershaw, *Environ.Health Perspect.*, 1994, **102 Suppl**, 141–146.

43   J. A. Viarengo, A.; Nott, *Comp. Biochem. Physiol.*

44   B. L. Thompson, R J; Bayne, *J. Exp. Mar. Bio. Ecol.*, 1972, **9**, 111–124.

45   J. Veltman, Karin; Huijbergts, Mark A. J.; van Kolck, Maurits; Wang, W.; Hendriks, *Environ. Sci. Technol.*, 2008, **42**, 852–858.

Chapter 5

General discussion: Prioritising future research using engineered nanosilver as an example

Abstract

Nano-ecotoxicology faces a fundamental challengewith the enormity of understanding the dynamic fate of materials that may vary both by core composition and surface functionalisation. Not only this, but the fate and toxicity of these particles may change between environmental compartments and across time. Research into the fundamental chemistry and biotic interactions of these materials at the nanoscale is ongoing, in attempts to quantitatively link intrinsic properties of nanomaterials to their effects in different environments. This thesis addresses an important aspect of engineered nanomaterials risk assessment, that of their accumulation into aquatic species. In this discussion I present a targeted approach toaid in prioritising nanomaterials and exposure scenarios for further study, using the example of nanosilver. The results from the experimental chapters are presented in the context of this targeted approach and their contribution towards the case for nanosilver as a nanomaterial of concern is discussed. The contribution of this knowledge to our understanding of the differences in fate and bioaccumulation of soluble forms of silver compared with nanosilver is also critically discussed.

Contents

5.1 A targeted approach to nanomaterial study prioritisation: the case for nanosilver

The production of engineered nanomaterials (ENMs) for a variety of applications is an emerging global industry. This has prompted calls for the risk assessment of these materials to human and environmental health so that the industry can develop sustainably into the future. Whilst much research effort has been undertaken to this end, systematic evaluation of the risks ENMs present to the environment has had varied success due to the disparate nature of the many institutions, researchers and funding bodies, each with their own focus and priorities. Below, we present the rationale used to inform the experimental decisions made throughout this thesis, discussing in the process the wider context within which these results should be viewed. This takes the form of a series of perspectives, from which to inform decisions as to how we could prioritise nanomaterials and experimental designs, using our work on nanosilver as an example. The focus is upon emissions, environmental fate and biological relevance as key influencing factors to helpprioritise and develop nanomaterial studies in the future.

5.1.1 Silver nanoparticles in the context of wider silver emissions

Several attempts have been made to predict the emissions of engineered nanomaterials (ENMs) into the environment at national [1], regional [2] and global scales[3]. Silver nanoparticles (AgNPs) have been subject to much research in the field of nanoecotoxicology due to the wide range of applications for the particles, including medical uses, paints, cosmetics, textiles and consumer electronics, each of which presents a different route to entry to the environment during its production, use and disposal. This has informed the choice of particles for the experimental work presented in this thesis. To understand the implications of our findings in the wider context of nanomaterial releases at a range of scales, it is necessary to understand the emissions flows of these materials .Production volumes and material reactivity are crucial for predicting environmental concentrations of ENMs. However, there are various sources of uncertainty when making such predictions. For example, Piccinno*et al.* 2012 suggest the production capacities reported by industry, often used in modelling attempts, can lead to overestimations of emissions as these reflect the total production capacity at the time rather than current production [4]. Assumptions must also be made as to release rates and the fate of ENMs in the environment, for which empirical data remains sparse.

Considering these potential sources of uncertainty, it is expected that the actual production volume of nanosilver in Europe in 2012 was ~30 metric tons (Mg) [2] and globally between 5.5 and 550 Mgin 2011 [4].Whilst this is an expanding industry, these emissions of AgNPs must be put in the context of the production of other forms of silver. Global production of silver was 31.3 Gg in 2016 according to the World Silver Survey 2017, authored by the industry group, The Silver Institute (http://www.silverinstitute.org/site/WSS2017.pdf). Even under the maximum emissions scenario proposed by Piccinno*et al.* 2012 of 550 Mg of AgNPs produced worldwide [4], nanoparticulate silver would still only represent ~1.7% of the total silver produced annually. Therefore, a focus for nano-ecotoxicologists should be to determine the relative toxicity of nano-forms of silver compared to positive controls of silver compounds for which we already regulate and have extensive toxicity data. Our work contributes to this effort, using silver nitrate($AgNO_3$) as a representative soluble form of silver.Targeting environmental compartments and conditions for which we can expect the

highest contamination from ENMs is another way in which we can prioritize such testing.

5.1.2 Risk quotients for silver nanoparticles in the aquatic environment

Predicted environmental concentrations (PECs) of ENMs, an output from ENM emissions modelling efforts, can be used to target environmental compartments and geographical regions of concern. These values are currently subject to many sources of uncertainty, including uncertainty in models over production volumes, characterisation of the materials in production and their environmental fate[5]. In particular, our inability to validate PECs with quantitative measurements of ENMs in environmental samples,hinders attempts to use a traditional risk assessment framework to assess ENMs [6] or incorporate them into exiting regulatory frameworks such as the EU Water Framework Directive [7]. Research efforts are continuing to develop instruments and techniques capable of detecting and quantifying ENMs in complex environmental matrices [8], but performing these measurements is at the very limits of our current capabilities and such techniques are not yet routine. However, PECs are still an important component for ENM risk assessment and may be used alongside predicted no effect concentrations (PNECs) to calculate a risk quotient (RQ), provided these uncertainties are understood and acknowledged,as described in Equation 1.

$$RQ = \frac{PEC}{PNEC} \qquad \text{(Eq. 1)}$$

Thresholds can then be defined, above which an RQ is considered to be of concern. For the RQ defined in Eq. 1, the level of concern for aquatic organisms is generally defined as being a chronic risk if the RQ > 1.0 [9]. PNECs are also susceptible to sources of uncertainty. My work has aidedefforts to reduce this uncertainty by contributing towards a systematic evaluation of the quality of nanotoxicity literature[10]. This aims to allowdata taken from the literature for setting environmental safety values to be weighted according to the quality of the study.

Previous estimates of RQs for ENMs in surface waters range from 0.7 – 16 for titanium dioxide (TiO$_2$ NPs) to 0.0008 – 0.002 for AgNPs [11]. A more recent exemplary environmental risk assessment of the JRC reference silver nanomaterial NM300k, calculated RQ for these AgNPs applied in textiles in various environmental compartments [12]. This resulted in RQ for NM300k in

sediments ranging between 0.017 and 0.24. This higher RQ for sediments than surface waters is due to their fate in the aquatic environment.

5.1.3 Prioritising sediments as a compartment of concern for AgNP exposure

As we identified in the published review presented in Appendix 1[13], ENMs entering the aquatic environment predominantly experience rapid sedimentation due to a combination of homo- and heteroaggregation. A range of ENMs, aged quiescently in the presence of natural colloids under 6 different water chemistries experienced sedimentation rates between 0.0001 to 0.14 m day^{-1}[14]. Indeed, in our own work, we demonstrated qualitatively that both cerium oxide (CeO_2 NPs) and AgNPs experienced some aggregation and subsequent sedimentation of these larger particles within the first 24 hours dispersion in freshwater (Chapter 2 and 3). This is in good agreement with modelled estimates that sediments across the European Union and Switzerland are expected to receive 2.6 µgkg^{-1} year^{-1} of AgNPs, four orders of magnitude higher than PECs for AgNPs in surface waters of 0.66 ngL^{-1}[2]. These models, much like the RQs calculated by Voelkeret $al.$ 2015 rely on the assumption of homogenous distributions in the environment[12]. However, we know that many of the emissions of AgNPs are from point sources such as outflows of waste water treatment plants [15]. Therefore, whilst on average, RQs may be below the threshold of 1.0 which would normally trigger a cause for concern and the need for further investigation, it is conceivable that for some areas this threshold would be surpassed.

Money et $al.$ 2012 assess the probability that RQs for a range of ENMs would be surpassed in different environmental compartments, using Bayesian networks to incorporate expert opinion and evidence into risk assessments [16]. They found that the probability of RQ for AgNPs being > 1.0 was 65.5% for sediments and only 13.9% for surface waters. This led them to conclude that further study of the risk AgNPs present to sediments is warranted, and that this data should be fed back into the Bayesian network model to update and reduce uncertainty. The investigations presented in this thesis into the effect of surface properties and aging of AgNPs upon bioaccumulation and the route to uptake contribute towards this goal. To target geographical areas at most risk from

AgNPs, a more nuanced approach calculating spatially resolved PECs could identify areas in which the RQ threshold of 1.0 is surpassed.

Gottschalk *et al.* 2011 performed such an analysis, predicting concentrations of TiO$_2$NPs, zinc oxide (ZnO NPs) and AgNPs in rivers across Switzerland from emissions from waste water treatment plants[1]. Their predictions examined two scenarios, a conservative scenario in which there is no removal of ENMs during waste water treatment and an optimistic scenario under which ENMs transform/sediment rapidly. Such models may be improved by introducing values for stability and sedimentation measured empirically. To address this issue, Hammes*et al.* 2013 used principle component analysis to categorize freshwaters from 808 sampling points across Europe into 6 water types [17]. They then used this to predict the stability of model nanoparticles in surface waters across Europe as a function of these water classifications. Combining the approaches taken in these two studies could be successfully employed in the future to define sediment classes at either national or regional scales. Such information could then be combined with emissions flow maps to target areas for future monitoring or to help define a set of sediment conditions that could then be replicated in the laboratory for hazard testing of ENMs.

5.2 The importance of different routes to uptake for nanomaterial bioaccumulation

Bioaccumulation is an important component of contaminant risk assessment as it provides the baseline data for understanding the entry points of contaminants into ecosystem food webs. This is particularly true of contaminants such as AgNPs which are currently close to the RQ threshold for concern. Throughout this thesis, the focus is on how investigating the bioaccumulation of nanomaterials can tell us something as to how they will enter food webs once within the aquatic environment. Using a model sediment dwelling species,the role that different particle properties play in determining this route to uptake is addressed and in turn, how this affects the extent of bioaccumulation. Such work can provide context for nanomaterial engineers and manufacturers to inform directions for producing "safe by design" particles.If particles can be designed to be unavailable to benthic prey organisms occupying lower trophic levels then this will limit their impact upon benthic communities. Not only this,but

it will also limit transfer between benthic and pelagic zones through predation by pelagic fish for example, thus preventing a route to re-entry of nanomaterials from sediment sinks into surface water communities. Developing our understanding of the routes to uptake of ENMs into organisms will also give us insight into likely biological targets and sites of action for toxicity.

5.2.1 The accumulation of insoluble cerium oxide nanoparticles

This thesis validates the use of *Lumbriculus variegatus* as a model sediment ingesting freshwater worm to investigate both the route and extent of uptake of NPs from sediments. Using insoluble cerium oxide nanoparticles (CeO_2) we examined the contribution of ingestion and transdermal uptake towards bioaccumulation of ENMs in the absence of dissolution products from the particles. CeO_2 NPs predominantly partitioned to the solid fraction of the sediment >200 nm in size, and surface coating and form of the NP made little difference to their fate within the sediment. This reduced their availability compared to water only exposures, which elicited mucus production as a stress response from the worms, not apparent in the sediment exposures. We found that ingestion of small 10 nm particles could result in bioaccumulation of Ce above that of controls after relatively short exposure periods of 5 days (Chapter 2). Whilst this accumulation was relatively low (body burdens were ~10% of the external concentration of CeO_2 NPs in the sediment) it demonstrated that small 10 nm particles could be accumulated through ingestion, irrespective of their surface coatings (uncoated, citrate or PEG).Whilst CeO_2 was not biomagnified in any sediment exposure, it provided a useful model for the fate of insoluble ENMs, demonstrating the potential for ingestion to contribute towards uptake, whilst also finding no evidence of transdermal uptake of these particles.

5.2.2 The accumulation of partially soluble silver nanoparticles

Silver on the other hand did experience transdermal uptake across external surfaces of the worm. The key difference between the fate of silver nanoparticles (AgNPs) compared with CeO_2 NPs was the persistence of a small dissolved fraction of silver in the sediment pore waters ~0.1 mgkg^{-1} for citrate and PEG coated particles (Citrate-Ag and PEG-Agrespectively). Our rationale was that measuring this dissolved fraction of low molecular weight silver (LMW-Ag) during the exposure could provide context for any differences we found in bioaccumulation between nanoparticles and dissolved forms of silver.

Interestingly, the concentration of LMW-Ag in the sediment pore waters did not differ between any silver treatmentwhere dissolution was possible. This indicates that the fate of nanomaterials in sediments may be more strongly determined by the properties of the surrounding media than those of the particle itself. Chapter 3 concludes that LMW-Ag in the pore waters could account for all transdermal uptake of silver in silver nitrate ($AgNO_3$) and Citrate-Ag exposures, however it did not account for all the uptake of silver observed in PEG-Ag treatments. 50 nm silver sulphide (Ag_2S) and PVP coated Ag (PVP-Ag) experienced no dissolution into the sediments and no uptake in worms after 5 days (Chapter 4) indicating that it is unlikely that the additional accumulation of PEG-Ag in Chapter 3 was due to direct transdermal uptake of PEG-Ag across the epidermis. Rather, we propose that PEG-Ag NPs persisted as loose agglomerates of individual 10 nm particles rather than binding and sintering into larger denser aggregates as occurred for Citrate-Ag. This potentially resulted in increased localised dissolution of PEG-Ag NPs at the worms' surface. We propose that increased localised dissolution was responsible for the additional uptake of PEG-Ag from sediments.

5.2.3 The effect of aging upon AgNP bioaccumulation

The dynamic behaviour of nanoparticles over time, has led to discussion as to whether ENMs could increase in bioavailability or toxicity as particles age within the environment and how best to experimentally test this [18]. Chapter 4 begins to address this concern through a simple quiescent aging technique to assess the impact of aging particles within sediments for 3 months upon their kinetic uptake. This had the additional benefit of addressing three potential exposure scenarios for AgNPs: direct release, particles aging within sediments, and transformed particles eluted from waste water treatment processes. Neither PVP coated AgNPs (PVP-Ag) nor "transformed" sulfidized particles (Ag_2S) were soluble throughout the exposures, resulting in no transdermal uptake of silver. Aging did qualitatively alter the fate of the PVP-Ag in the sediments, resulting in the emergence of a colloidal fraction of Ag <200 nm in the pore waters after 3 months, but once again, these were not soluble and led to no statistically significant increase in bioavailability. Whilst comparative literature is scant, similar findings have been demonstrated for 20-40 nm ZnO NPs in a range of soils, where aging for 6 months led to an increase in pore water Zn (<450 nm)

but could not explain all changes in bioaccumulation or toxicity in the earthworm*Eiseniaandrei*[19]. AgNPs have also been demonstrated to be rapidly immobilised within soil, followed by an increase in pore water silver over a timescale of months [20]. A comparison between the fate of 60 nm Citrate-Ag and PVP-Ag with $AgNO_3$ in soils found aging for 2 months reduced the total Ag in pore waters for all forms of Ag[21].However, the two AgNPs remained significantly more mobile than $AgNO_3$ which could lead to greater bioavailability over longer periods than soluble forms of Ag such as $AgNO_3$. As such, future work should focus on AgNPs which are partially soluble in sediments and address the effect of aging upon this soluble fraction over time.

5.3 Areas of divergence between soluble and nanosilver: the implications for regulation

This discussion has identified sediments as an environmental compartment at risk of contamination from AgNPs. An important question for regulators will be whether AgNPs present a greater risk to this compartment than other silver compounds currently accounted for in regulation.There is some consensus over certain nanospecific behaviours which distinguish nano-silver from dissolved forms, but we need to also appreciate those areas in which fate and toxicity of dissolved and AgNPs are aligned, as this will allow current regulation and environmental protection efforts to be adapted more easily for the incorporation of nanosilver. Whilst this thesis cannot hope to answer this question in full, we have identified three areas of convergence between the fate and bioavailability of AgNPs compared to $AgNO_3$, which we have used as a proxy for other soluble silver compounds.

1. Transdermal uptake was responsible for silver accumulation in this sediment.Dietary uptake of silver did not contribute significantly towards bioaccumulation for any AgNP or $AgNO_3$.
2. The dissolved fraction of silver in the pore waters was the same for all partially soluble forms of silver (Citrate-Ag, PEG-Ag and $AgNO_3$). This indicates that sediment properties dictate the persistence of a dissolved fraction of silver in the pore waters for silver which is at least partially soluble.

3. Neither exposures to AgNPs nor AgNO$_3$ resulted in BAF above the recommended threshold of 1000, which would trigger concern for its bioaccumulative potential.

In light of this, under the conditions tested in this work, Ag$_2$S and PVP-Ag present a lower hazard to sediment dwelling species than AgNO$_3$ whilst partially soluble particles (Citrate-Ag and PEG-Ag) experience the same route to uptake as soluble AgNO$_3$, with transdermal uptake accounting for all bioaccumulation of silver (Chapter 3). Strategies for the safe design of AgNPs therefore could focus on limiting this dissolution within sediments.

An important divergence between the fate and bioaccumulation of AgNPs and AgNO$_3$ was identified for PEG-Ag. This electro-sterically stabilised particle experienced greater accumulation in *L. variegatus* than AgNO$_3$ even when bioaccumulation was adjusted to assume all uptake was of the dissolved fraction of silver in the sediment pore waters. This indicates that for 10 nm PEG-Ag, not all accumulation could be attributed to this dissolved pore water silver. PEG-Ag particles appeared to persist as distinct individual 10 nm particles when aged in freshwater for the exposure period. We propose that this persistence was responsible for the increased accumulation of silver compared to AgNO$_3$, through contact of these particles with external surfaces and subsequent localised dissolution.We suggest this mechanism as there was no direct evidence of transdermal uptake of particles themselves either of a similar size and coating (10 nm PEG-CeO$_2$) or similar core composition (50 nm PVP-Ag). There is also tentative supporting evidence for this emerging in the literature. For example Tsyusko*et al.* 2012 found AgNPs and AgNO$_3$ to elicit similar molecular-level responses in the earthworm *Eiseniafetida*even through<15% of AgNPs were oxidized during the exposure, which they suggest indicates that dissolution of AgNPs is likely to happen during or after uptake and it is these dissolved species of Ag which are responsible for the similar pattern of molecular response[22]. Future work should focus on the implications of particle coatings and surfactants which increase the persistence of ENMs as discreet nanoparticles and how this may increase the potential for direct uptake of these particles or increased contact at the nano-bio interface, leading potentially to localised dissolution and uptake.

Conclusions

This thesis aimed to assess some of the key factors which influence the bioaccumulation of engineered nanomaterials in sediment dwelling species. To this end, experimental work prioritised two common metal nanoparticles, cerium oxide and silver. This work has contributed towards our understanding of the complex interplay between nanoparticle properties, sediment conditions and the nano-bio interface and how these determine the route and extent of bioaccumulation from sediments.Several themes have emerged and can be summarised thus:

1) Sediments act as a sink for ENMs in the aquatic environment in which unique transformations and interactions with both the biotic and abiotic components of the sediment will influence nanomaterial fate, bioavailability and ultimately the risk they present to benthic organisms.

2) Measuring biologically relevant fate processes such as dissolution and the persistence of a nano-sized fraction of material during exposures is essential to provide the context in which traditional endpoints such as bioaccumulation can be interpreted.

3) Bioaccumulation of engineered metal nanoparticles from sedimentswas primarily dependent upon the core properties of the material (solubility) and to a lesser extent surface properties (mechanism of stabilisation using surfactants).

4) Transdermal accumulation of metals from nanoparticle exposures was shown to be exclusively from dissolved metals from the particle, and in the case of these experiments was only observed for nanosilver, not CeO_2.

5) Particle surface properties may influence the extent of this uptake indirectly by either increasing the potential for contact/dissolution at the organism surface (PEG coating) or reducing particle solubility (PVP coating).

Whilst nanoparticle core properties and their mechanism of stabilisation did result in detectable differences in the route and extent of uptake of cerium and silver from sediments, under current regulatory guidelines, these particles tested would not be considered bioaccumulative. It should be noted that whilst BAF and BCF are useful metrics for comparisons between treatments within a

study with a consistent design, they are less suitable when comparing the bioaccumulative potential of different materials under different exposures and conditions due to their inherent sensitivity to differences in exposure concentration. Therefore, alternatives to BAF should be considered for defining nanomaterial bioaccumulation in the future. The potential for biomagnification through trophic transfer was beyond the scope of these studies and so remains to be addressed. Future studies should examine the potential for nanosilver to act as a source of dissolved silver within sediments over longer time periods. It will also be important to address the molecular mechanism of cellular uptake of nanoparticles in complex systems such as sediments, as nanomaterials have been recorded to experience direct cellular uptake during cell-line experiments, but such uptake was not in evidence under these more complex conditions. Sediments will act as a sink for nanomaterials released to the aquatic environment. The focus of future work should be whether the greater concentrations expected in the benthos will be sufficient to result in environmental toxicity in the face of the reduced bioavailability of these particles in sediments compared with in the water column.

References

1   F. Gottschalk, C. Ort, R. W. Scholz and B. Nowack, *Environ. Pollut.*, 2011, **159**, 3439–3445.

2   T. Y. Sun, F. Gottschalk, K. Hungerbühler and B. Nowack, *Environ. Pollut.*, 2014, **185**, 69–76.

3   A. A. Keller, S. McFerran, A. Lazareva and S. Suh, *J. Nanoparticle Res.*, , DOI:10.1007/s11051-013-1692-4.

4   F. Piccinno, F. Gottschalk, S. Seeger and B. Nowack, *J. Nanoparticle Res.*, , DOI:10.1007/s11051-012-1109-9.

5   M. Baalousha, G. Cornelis, T. A. J. Kuhlbusch, I. Lynch, C. Nickel, W. Peijnenburg and N. W. van den Brink, *Environ. Sci. Nano*, 2016, **3**, 323–345.

6   B. Nowack, *NanoImpact*, 2017, **8**, 38–47.

7   A. Baun, N. B. Hartmann, K. D. Grieger and S. F. Hansen, *J. Environ. Monit.*, 2009, **11**, 1774.

8   M. Baalousha, B. Stolpe and J. R. Lead, *J. Chromatogr. A*, 2011, **1218**, 4078–4103.

9   S. Luoma and P. Rainbow, *Metal contamination in aquatic environments: science and lateral management*, 2008.

10   M. L. L. Fernandez-Cruz, D. Hernandez-Moreno, J. Catalan, R. Cross, H. Stockmann-Juvala, J. Cabellos, V. R. Lopes, M. Matzke, N. Ferraz, J. J. Izquierdo, J. M. Navas, M. V. Park, C. Svendsen and G. Janer, *Environ. Sci. Nano*, , DOI:10.1039/C7EN00716G.

11   N. C. Mueller and B. Nowack, *Environ. Sci. Technol.*, 2008, **42**, 44447–53.

12   D. Voelker, K. Schlich, L. Hohndorf, W. Koch, U. Kuehnen, C. Polleichtner, C. Kussatz and K. Hund-Rinke, *Environ. Res.*, 2015, **140**, 661–672.

13   R. K. Cross, C. Tyler and T. S. Galloway, *Environ. Chem.*, 2015, **12**, 627.

14   J. T. K. Quik, I. Velzeboer, M. Wouterse, A. A. Koelmans and D. van de Meent, *Water Res.*, 2014, **48**, 269–279.

15   A. C. Johnson, M. D. Jürgens, A. J. Lawlor, I. Cisowska and R. J. Williams, *Chemosphere*, 2014, **112**, 49–55.

16   E. S. Money, K. H. Reckhow and M. R. Wiesner, *Sci. Total Environ.*, 2012, **426**, 436–445.

17   J. Hammes, J. A. Gallego-Urrea and M. Hassellöv, *Water Res.*, 2013, **47**, 5350–5361.

18   D. M. Mitrano and B. Nowack, *Nanotechnology*, 2017, **28**, 1–23.

19   A. Romero-Freire, S. Lofts, F. J. Martín Peinado and C. A. M. van Gestel, *Environ. Toxicol. Chem.*, 2017, **36**, 137–146.

20   C. Coutris, E. J. Joner and D. H. Oughton, *Sci. Total Environ.*, 2012, **420**, 327–333.

21   A. R. Whitley, C. Levard, E. Oostveen, P. M. Bertsch, C. J. Matocha, F. Von Der

Kammer and J. M. Unrine, *Environ. Pollut.*, 2013, **182**, 141–149.

22   O. V. Tsyusko, S. S. Hardas, W. A. Shoults-Wilson, C. P. Starnes, G. Joice, D. A. Butterfield and J. M. Unrine, *Environ. Pollut.*, 2012, **171**, 249–255.

Supplementary Files

Supplementary File1

Recipe for the artificial hard water (freshwater) used throughout experiments (reproduced from OECD Test Guideline 315 "Bioaccumulation in Sediment-dwelling Benthic Oligochaetes", DOI: 10.1787/2074577x)

(a) Calcium chloride solution Dissolve 11.76 g $CaCl_2$ x 2 H_2O in deionised water; make up to 1 L with deionised water

(b) Magnesium sulphate solution Dissolve 4.93 g $MgSO_4$ x 7 H_2O in deionised water; make up to 1 L with deionised water

(c) Sodium bicarbonate solution Dissolve 2.59 g $NaHCO_3$ in deionised water; make up to 1 L with deionised water

(d) Potassium chloride solution Dissolve 0.23 g KCl in deionised water; make up to 1 L with deionised water

All chemicals must be of analytical grade. The conductivity of the distilled or deionised water should not exceed 10 μScm^{-1}.

25 ml each of solutions (a) to (d) are mixed and the total volume made up to 1 L with deionised water.

The sum of the calcium and magnesium ions in this solutions is 2.5 mmol/L. The proportion Ca:Mg ions is 4:1 and Na:K ions 10:1. The acid capacity KS4.3 of this solution is 0.8 mmol/L.

Supplementary File2

Properties of the LUFA Speyer natural soil substrate

Property	LUFA Speyer soil 2.4
Organic carbon (%C)	2.26 +/- 0.5
Nitrogen (% N)	0.2 +/- 0.04
pH (0.01 M CaCl2)	7.2 +/- 0.2
Cation exchange capacity (meq)/100g	31.4 +/- 4.6
Water holding capacity (g/100g)	44.1 +/- 1.2
Water holding capacity (g/1000ml)	1288 +/- 36

Particle size distribution (mm) according to German DIN (%)	
<0.002	26.3 +/- 2.1
0.002 - 0.006	8.3 +/- 1.0
0.006 - 0.02	14.5 +/- 1.1
0.02 - 0.063	23.1 +/- 1.1
0.063 - 0.2	19.1 +/- 0.3
0.2 - 0.63	7.0 +/- 2.5
0.63 - 2.0	1.7 +/- 0.2
Soil type	Clayey loam

Particle size distribution (mm) according to USDA (%)	
<0.002	25.9 +/- 2.1
0.002 - 0.05	40.5 +/- 1.0
0.05 - 2.0	33.6 +/- 1.8
Soil type	Loam

Appendix 1

Transformations that affect fate, form and bioavailability of inorganic nanoparticles in aquatic sediments

Abstract

Inorganic nanoparticles are at risk of release into the aquatic environment owing to their function, use and methods of disposal. Aquatic sediments are predicted to be a large potential sink for such engineered nanomaterial (ENM) emissions. On entering water bodies, ENMs can undergo a range of potential transformations dependent on the physicochemical nature of the immediate environment, as they pass from the surface waters, to sediments and into sediment-dwelling organisms. This review assesses the current state of research on transformations of metal-based ENMs in the aquatic environment, and considers the implications of these transformations for the fate and persistence of ENMs and their bioavailability to organisms within the benthos. We identify the following factors of key importance in the fate pathways of ENMs in aqueous systems: (1) extracellular polymeric substances, prevalent in many aquatic systems create the potential for temporal fluxes of ENMs to the benthos that is currently unaccounted for in predictive models. (2) Weak secondary deposition onto sediment grains may dominate sediment-ENM interactions for larger aggregates >500 nm, potentially granting dynamic long term mobility of ENMs within sediments. (3) Sulfurization, aggregation and reduction in the presence of humic acid is likely to limit the presence of dissolved ions from soluble ENMs within sediments. (4) Key benthic species are identified based on their ecosystem functionality and potential for ENM exposure. On the basis of these findings, we recommend future research areas which will support prospective risk assessment by enhancing our knowledge of the transformations ENMs undergo and the likely effects these will have.

Contents

Introduction

The use and application of Engineered Nanomaterials (ENM) is rapidly expanding, with a global industry estimated to be worth US$ 3 trillion by 2020 [1]. This growth is reflective of their wide ranging applications, spanning environmental remediation [2, 3], commercial products [4-7] and medicine [8]. The expansion of commercial uses for ENMs is fuelled by the unique properties materials display at the nano-scale compared with the larger (bulk) form of the material, principally due to their high surface area to volume ratio [9]. It is this high reactivity at the nanoscale that has established ENMs as a contaminant separate from their bulk form. The commonly used definition of a nanomaterial is a material with at least one dimension <100 nm [10, 11]. Nanoparticles (NP) have all three dimensions <100 nm, whereasnanosheets and nanorods exist with one or two dimensions <100 nm. In terms of regulation, the European Commission has a working definition of engineered nanomaterials as "containing particles, in an unbound state or as an aggregate or as an agglomerate and where, for 50% or more of the particles in the number size distribution, one or more external dimensions is in the size range 1-100 nm" [12].

Attempts have been made to model the release of ENMs into the environment at both national and global scales [13-15] however, a lack of data on production [16] and emission rates, inhibitsaccurate prediction of the release potential of ENMs [17]. Recent estimates predicted 1,100 – 29,200 metric tons of the global ENM production in 2010 was released directly into water bodies [18]. Most of these ENMs will pass through some form of water treatment process before entering the aquatic environment, which can be highly effective at removing ENMs such as silver (AgNPs)[19].In one study, silver in the effluent from a model waste water treatment plant accounted for only 2.5% of the original dosed concentration [20]. However, some ENMs may also be released directly to aquatic systems. Coatings and cosmetics comprise the largest share of commercial products containing ENMs [21] and are the two largest potential sources of ENM release into the environment [18]. Most ENMs utilized in coatings and cosmetics are inorganic metal or metal oxide NPs (MeO) [22, 23]such as titanium dioxide (TiO_2), zinc oxide (ZnO), silicon dioxide (SiO_2) and cerium oxide (CeO_2) whichhave high production and release volumes [14, 16, 18]. These may be released from painted exterior facades and other consumer

products directly into the aquatic environment [23, 24]with uncertainecological consequences [25]. There is little regulation in place for their production or disposal, making the area of nano-ecotoxicology one of vital importance for prospective risk assessment [25-27].

Water bodies receiving ENMs present a diverse range of environments, from fast flowing rivers, to lakes, high in natural organic matter (NOM) or oceans of high ionic strength. Differences in both physical and chemical conditions of the immediate environment may drastically alter the fate and behaviour of ENMs. Both naturally occurring NPs[28, 29] and ENMs [30, 31] have been shown to aggregate and sediment on transport into saline environments as occurs when entering estuarine waters. In the Gironde estuary, France, silver from anthropogenic sources contributes 24-90% of particulate Ag fluxes into sediments [32, 33]. In some instances,for example TiO_2 in the Rhine river,modelled sediment concentrations exceed that in the overlying water by up to six orders of magnitude [34]. ENMs have also been observed to move in run-off from terrestrial soil into aquatic sediments [35]. Therefore, sediments are predicted as amajor sink for ENM emissions [11].

The transformations that an ENM may experience on entering the aquatic and benthic environment can be subdivided into four main categories:

- Physical transformations, including aggregation processesand deposition onto sediment grains.
- Chemical transformations, including dissolution, exchange of surfactants, influence of other inorganic chemicals and redox reactions.
- Interactions with macromolecules external to organisms such as NOM and extra-cellular polymeric substances produced in the water column or by biofilms at sediment surfaces.
- Biologically mediated transformations involving partitioning among benthic communities bioturbation and transformations associated with ingestion-egestion dynamics.

Each of these transformations may influence the toxicity,bioaccessibilityand bioavailability of ENMs. Bioaccessible ENMs can be taken up by an organism, but their potential for cellular internalisation may be physically or temporally constrained, whereas bioavailable ENMs may be readily internalised by cells

and tissues. As such, transformations of ENMs and their effect on bioavailability in sediments are an important component of ENM hazard prediction. There has been recent progress in standardizing approaches to measuring the toxicity of chemicals in sediment environments [36], butthe existing framework for chemical contaminants may not be suitable for ENMs owing to the fundamental differences between solute and colloidal chemistry. International efforts are working towardsachieving the same quality of standardisation and environmental realism for nano as for traditional chemical ecotoxicology [25, 37,38]. To do this a firm understanding of the transformations that occur through the products lifecycle is of utmost importance [39].

The present review critically analyses knowledge concerning the hazard potential ofinorganic ENMs in the benthic environment. We distinguish between organic and inorganic ENMs for the purposes of the current review owing tounique fate processes of inorganic ENMs concerning dissolution and the presence of ions, and the differences in the specific challenges for investigators that organic and inorganic ENMs present, which must be dealt with separately. The reviews focus is on the interactions that occur between inorganic ENMs with both biotic and abiotic components of the benthic environment and the implications of these transformations for the fate and bioavailability of ENMs to benthic species. Investigatingthese processes and transformations will help identify the form of inorganic ENMs likely to be present within the benthos. In doing so, this information can be used in support of standardised testing for predictive risk assessment of ENMs in sediments.

1.Transformations in the water column

Many transformations occur in the water column on release of ENMs into the aquatic environmentand as they pass from suspension in the water column, to their incorporation into sediments (Figure 1). These transformations facilitate the flow of ENMs from the water column into sediments and may persist within the benthos. Transformations include physiochemical transformations such as the dynamic interplay between aggregation and dissolution, as well as interactions with NOM and aggregates of biogenic exudates known as "marine snow"all of which may have lasting implications for ENM fate within the benthos.

NP coated with NOM may prevent homoaggregation, which can lead to enhanced stability.

Homoaggregation occurs in waters of low NOM and high IS. Results in sedimentation.

Large heteroaggregates formed with biologically derived organic matter, particularly under high IS conditions. Increases sedimentation.

Ingestion of suspended NPs by pelagic species or the pelagic phase of some sediment dwellers.

Dynamic cycling of NP within the sediments with bioturbation and egestion burying and re-suspending NPs.

Larger aggregates targeted by filter feeders, increasing uptake of NP in epibenthos.

Contact with mucus on external membranes resulting in floculation of these and other excretory products and subsequent sedimentation.

Epibenthic Organisms

Endobenthic Organisms

Sedimentation and association with sediment grains gives access to sediment ingesting benthic dwellers.

NPs suspended in the pore water can be transported through saturated sediments.

Figure 1: Conceptualization of the aggregation processes resulting in the accumulation of ENMs in sedimentsand their exposure to benthic dwelling organisms.

1.1 Aggregation

On release into water bodies, metal ENMs exhibit behaviour similar to other colloids, with their fate dominated by aggregation and dissolution [39-41]. In principle, this follows Derjaguin-Landau-Verwey-Overbeek (DLVO) theory, where aggregation behaviour is the product of attractive van der Waals forces and repulsive electrostatic forces. The balance of these opposing forces is highly dependent on the physical and chemical properties of the ENM in question and the properties of the media in which the ENM is suspended. Most materials suspended in water have a negative surface charge, attracting counter ions from the solution and inducing the repulsive Electric Double Layer (EDL), which on close interaction with other negatively charged colloids results in electrostatic repulsion. This prevents aggregation and results in a material becoming stabilized in suspension. Ionic strength of the surrounding water influences aggregation behaviour, with high ionic strength typical of saline

marine waters, resulting in a compression of the EDL reducing electrostatic repulsion and therefore increasing homoaggregation[42-46]. A similar effect has been seen as the pH approaches the pH point of zero charge (pH_{zpc}) for the particle [47, 48]. This reduced stability of the ENM and subsequent increase in homoaggregationresults in faster rates of sedimentation under conditions of high IS or where the pH of the surrounding water is close to the pH_{zpc} of the ENM [43, 49, 50]. The capacity of ionic strength to influence aggregation can be limited by particle shape.Changing ionic strength had minimal influence upon aggregation of rod shaped ZnO (aspect ratio 10:1) owing to the lower interaction energies involved between rod shaped NPs, whilst dramatically increasing aggregation for 20 nm spherical ZnO until aggregation was no longer limited by ionic strength [42].Increasing ionic strength not only facilitateshomoaggregation, but also heteroaggregation with large natural colloids (>0.2 μm diameter). Heteroaggregation has been demonstrated as the main cause behind sedimentation of ENMs in river water [51] a process exacerbated in waters of high ionic strength. CeO_2, and AgNPs, coated with either polyvinylpyrrolidone (PVP) or SiO_2, experiencedhigher rates of heteroaggregation with larger natural colloids in saline water and faster sedimentation [52]. Therefore sediments are a likely reservoir of these particles upon release into surface waters, particularly if they move along a salinity gradient such as that in an estuarine environment, into waters of higher ionic strength [53].

The aggregation behaviour of ENMs depends not only on the physiochemical characteristics of the water but also the physical properties of the ENMs themselves. Both concentration and initial particle size have a pronounced effect on aggregation behaviour. At higher concentrations, MeOs such as TiO_2, ZnO and CeO_2 sediment at afasterrate than when dosedat lower concentrations [50, 51]. Higher concentrations result in a greater number of particle-particle interactions and so a greater potential for homoaggregation. This relationship is dynamic. Evidence of aged TiO_2 from commercially available sunscreens showed two distinct size distributions formed after 48 hours, one <700 nm in diameter and the other group of larger low density heteroaggregates >10 μm of TiO_2 with other components of the sun creams [53]. Such bimodal size distributions may arise because rapid aggregation reduces the overall number

of particles in suspension, reducing the frequency of particle interactions, thus a second group of smaller or individual ENMs remain in suspension [51, 53]. Such aggregation during aging can be irreversible. Dry powders of 85 nm hematite ENMs, did not disaggregate below 100 nm when stored for 1 month [46]. Additionally, ENMs of a smaller initial size have been observed in several cases to result in larger aggregates [45, 46, 54], for example 10 nm citrate capped AgNPs aggregated to 300 nm after 3 days, compared with the 100 nm particles which formed 200 nm aggregates in saline water [55]. Overall, it is likely that a significant proportion of ENMs released into the aquatic environment will persist as larger aggregates.

The dynamic nature of ENM aggregation behaviour makes characterisation of ENMs in natural matrices difficult, owing to the propensity for NPs to change during the process of characterisation. Much of the past literature quotes the primary particle size when presenting results. However, as can be seen these reported sizes may bear little resemblance to the actual size distributions of ENMs in the laboratory exposures. As such, the current research efforts to improve separation and sizing techniques such as field flow fractionation and single particle inductively coupled plasma mass spectrometryarevital in order for progress to be made in our understanding of ENM aggregation and its implications for environmental fate.

1.2 Dissolution

Dissolution also plays a significant role in the fate of MeO NPs on release into water bodies. Evidence suggests that there is a relationship between particle size and dissolution rate at the nanoscale [56], though it is not the exponential predicted by solely using thermodynamic theory [44, 57]. This may be due to a number of factors, including the larger surface area relative to volume increasing the number of "hotspots" for dissolution [57], surface morphology [42] and NP concentration [58]. In general, smaller NPs have a greater rate ofdissolution, however, other factors can reverse this general rule. For example, 78 nm CeO_2 NPs had a greater concentration of Ce(III) impurities than smaller, 33 nm NPs, and so experienced greater dissolution at low pH <5 [59]. Other factors that may suppress the rate of dissolution include ligand exchange in the presence of phosphate [59] and aggregation [44, 56, 60]. In fact, aggregation has been observed to reduce dissolution rates of ZnO[61], in one case to values

180

similar to the bulk form [62]a finding that has been attributed to an increase in the thickness of the diffusion layer with size [63]. A slower rate of aggregation in lower ionic strength media has been demonstrated to increase ZnO aggregate density [49], which could also reduce diffusion efficiency of solutes from the interior of the aggregate to the bulk solution [63]. Both transformations involved in dissolution and aggregation are likely to continue in tandem alongside sediment specific processes such as interactions with sediment grains and biofilms upon reaching the benthos. It is this dynamic interplay of dissolution and aggregation that is a fundamental difference between traditional solute chemistry and ENMs colloidal behaviour.

1.3 Interaction with natural organic matter

In waters containing high NOM such as lakes, rivers and estuaries, NP-NOM complexes dominate particle behaviourbecause NOM concentrations are likely to be orders of magnitude higher than ENM concentrations. This co-aggregation of NOM with ENM may grant either steric [64-68] and/or electrostatic stability [44, 65, 69, 70] to the ENM, reducing sedimentation [50, 71]. Keller *et al.* (2010) found that in the presence of ~5 mMhumic acid, TiO_2 (27 nm), ZnO (24 nm) and CeO_2 (67 x 8 nm) formed stable heteroaggregates of ~300 nm in size, which then remained in suspension[50]. This can be compared with the same ENMs in the absence of NOM, where aggregates formed across the 400 minute time period, ranged from ~400-1200 nm and settled out of suspension. At low concentrations of NOM, typical of groundwater (between 0.1 and 2 mg/L), the stabilizing effect of NOM becomes concentration dependent.An exposure ratio of 2% NOM to ENM concentrations caused bridging and flocculation of TiO_2NPs, whereasNOM concentrations of ~20% stabilized 25% of the ENM as suspended colloids ~300 nm [72] in agreement with Keller *et al.* (2010) [50]. Suspended ENMs can still have an effect on benthic communities by disrupting the life cycle of the planktotrophic larvae produced by many sediment dwellers that feed in the water column. To the authors knowledge no published data explores the effects of ENMs on planktotrophic stages of otherwise benthic dwelling species. Such tests would be of particular use as there is little acknowledgment of this benthic-pelagic coupling in current regulatory frameworks.

1.4 Interaction with extracellular polymeric substances

Clusters and films of aggregated organic and inorganic matter are prevalent in both marine and freshwaters.Much of this forms from exudates of extra-cellular polymeric substances (EPS) from a diverse range of microbes [73]that attach to these agglomerates [73, 74]. These microgels provide an efficient transport mechanism for the movement of organic and inorganic matter from surface waters to the benthos known as "marine snow" [75, 76], with sedimentation rates from 1 – 368 m d^{-1} [77]. MeOs are rapidly incorporated into EPS, with a 95% incorporation efficiency for TiO_2 after 168 hours [78]. Such marine snow events are likely to occur after phytoplankton blooms and are not restricted solely to marine environments, with fluxes of particulate organic matter in sediments coinciding with the disappearance of EPS in the surface waters of Lake Constance, Germany [79]. Waste water treatment plants also act as an important source of EPS. ENMs come into contact with an array of microbes and EPS associated with sewage sludge and so may become complexed with such EPS upon release in the effluent into water bodies[80]. The presence of ENMs has been suggested to enhance aggregation and assembly of EPSmicrogels in marine waters. In the absence of ENMs, EPS aggregated to <0.5 μm, whereas the presence of a high concentration (100 μg L^{-1}) of 23 nm polystyrene NPs resulted in EPS-NP aggregates of 4-6 μm [81]. This could mean that in the presence of ENMs, marine snow may flocculate and sediment at a faster rate than usual, which may have wider ecosystem implications, through alteringlocal dynamics of this process.

When EPS flocculate and sediment, not only is there an increased exposure of ENMs to the benthos, but therecan also be other transformations of ENMs, impactingon aggregation and dissolution [82]. EPS was shown to increase heteroaggregation for both positively and negatively charged cadmium selenide (CdSe)quantum dots (used as a representative inorganic ENM). The size of aggregates differed under illumination, with ~800-3800 μm aggregates formed under dark conditions and ~700-1300 μm under a light:dark regime of 14h:10h. Interestingly, aggregation should suppress dissolution through reducing the surface area from which ions can dissolve.However, in this study, particularly under lit conditions, dissolution of the CdSe was actually increased. Proteins in the EPS acted as a source for CdSephotocatalyzed production of reactive

oxygen species (ROS), thus destabilizing the CdSe. This effect increased dissolution and degradation of the quantum dots. Although UV is attenuated by waters and so does not reach the benthos in many cases, in natural lake waters with low dissolved organic carbon, ultra violet penetration can reach a depth of 10 m[83] and so photoactive properties of some MeOs may still play an important role in ENM transformations. Flocs of EPS may remain in surface waters for 5-16 days [84] allowing time for significant degradation of photocatalytic ENMs such as CdSe quantum dots or TiO_2 close to the water's surface. Thispotentially increases exposure of pelagic species to dissolved ions from the ENM, while reducing the amount of particles that could sediment out to the benthos. However, during windy conditions[84] and when concentrations of EPS are great (for example after algal blooms) [79]rapid sedimentation can occur. This could result in seasonal fluxes of high ENM concentrations in the benthos. This is a hazard that is not recognized in current predictions of sediment concentrations of ENMs. Marine snow is not acknowledged in predictive models and sedimentation rates are assumed to be constant across the year [14, 85].As such, ENM interactions with EPS need to be better understood and are expected to be an important factor in predictive modelling of the environmental fate of ENMs.

2.Transformations at the surface of sediments

At the sediment-water interface,deposition onto natural colloids appears to be the main mode of sedimentation and incorporation into sediments [51]. This is of particular importance in turbulent, colloid rich systems e.g. rivers, estuaries and coastal systems. Heteroaggregation of CeO_2, PVP-Ag, and silica-coated silver (SiO_2-Ag) NPs with suspended sediment flocks has been observed 12 orders of magnitude higher in turbulent waters than in quiescent conditions. This resulted in sedimentation rates one to two orders of magnitude higher than in still or stagnant waters [86]. In lakes, scavenging of ENMs from the water column by suspended sediment particles dominates ENM sedimentation in shallow waters,in particular in the diffusive benthic boundary layer, or "fluff layer" just above the sediment surface [87]. Therefore, for many MeOs, persistence in the benthos will involve aggregated ENMs deposited onto sediment grains and natural colloids. Further transformations will then alter the composition and form

that ENMs take at the surface of sediments. These include interactions with epibenthic species, bio-resuspension and EPS derived from plants and microbes inhabiting the surface of aquatic sediments.

2.1 Effects of animal species on composition and distribution of ENMs at the sediment-water interface

The species composition of epibenthic communities will have a profound effect upon the size distribution and form of ENMs before settling to the sediment surface.*Daphnids*(water fleas) have an average filter mesh size of 400-700 nm and may only feed on suspended particles greater than this size [88]. As a consequence, *Daphniahyalina*alters the size distribution of natural colloids, simultaneously reducing the number of aggregates larger than their filter mesh size and increasing the number of smaller aggregates <400 nm [89]. A similar effect was observed for 30 nm mercaptoundecanoic acid- capped AuNPsin the presence of *D. magna* and the freshwater shrimp,*Gammaruspulex,* [90]. Such increases in smaller inorganic colloids in the presence of filter feeders have been suggested as a combination of selective ingestion of larger aggregates and break-down of these aggregates during digestion and egestion [91]. Although these studies concede that population densities in the investigations were too low to have asignificanteffect on the natural systems they represented, in areaswith a high density of filter feeding organisms, significant change to the size distribution of ENMs reaching the benthos may be possible.

Selective feeding by epibenthic species will expose some NPs to mucus in both the gut and gills which will determine particle interactions much like EPS. Surface mucus represents a significant barrier to uptake of ENMs across dermal pathways [92]. Studies on the mussel *Mytilusgalloprovincialis*, showed most CeO_2 and ZnO NPs dispersed in suspension were rejected in pseudofaeces before ingestion could occur[93]. Pseudofaeces are produced in the gills at a much higher rate compared with normal faeces and so act as an efficient mechanism for sorting unwanted NPs during filtration [93, 94].This results indeposition of mucus-NP complexes onto sediment surfaces, similar in composition to the EPS-ENM complexes discussedpreviously.

On ingestion, the gastrointestinal mucus is the first barrier for uptake of ENMs into the organisms' tissues and acts as another biological compartment for mucus-ENM interactions. Negatively charged ENMs may cross this barrier

184

faster than their cationic counterparts [95, 96]. Hydrophobic ENMs are also expected to experience far greater uptake, bioaccumulation and cellular internalization than their hydrophilic counterparts [96, 97]. However, even those ENMs that reach intestinal epithelial cells and are internalised may still be ejected back into the gastrointestinal mucus to be eliminated from the organisms. Goblet cells have been recorded to internalize activated carbon NPs into intracellular vacuoles, which are then secreted at the gut lumen through exocytosis [98]. These excreted ENMs will have undergone mechanical and chemical transformations due to changes in pH throughout the digestive process, for example, 45 nm gold (Au) NPs excreted by the clam *Corbicula flumine* were far less spherical and uniform in size than pre-exposure [99].

This transformation of NPs in faeces and mucus exudates represents an important process in benthic-pelagic coupling. In areas with high population densities of burrowing and sediment ingesting organisms, bioresuspension of nanomaterials in faecal pellets bring a significant volume of sediments and their associated contaminants to the sediment surface [100]. For example, bioresuspension through release of faecal pellets of the burrowing mud shrimp *Callinassa subteranea* has been estimated to equal an annual sediment turnover budget of 11 kg dry sediment m^{-2} $year^{-1}$ [101]. Although to date there has been no published direct investigation into the effect this bioresuspension has on ENMs, the importance of bioturbation and resuspension in other nutrient and chemical cycles [102] suggests these processes are likely to play an important role in benthic-pelagic coupling of ENM cycles.

2.2 Interactions with EPS at the sediment-water interface

EPS exuded from bacteria will also affect the distribution of ENMs at the sediment surface. Induced aggregation of biogenic ZnS NPs to sizes of 1-10 µm by proteins exuded from microbes has been demonstrated to limit their transport in subsurface waters, and in turn incorporate excess Zn ions from pore waters [103]. This demonstrates how EPS from microbial communities can alter the form of ENM at the sediment surface, reducing the concentration of Zn ions in interstitial pore waters within sediments, whilst increasing the nanoparticulate fraction. Such EPS may not only originate from bacteria. Bone *et al.* (2012), prepared different exposure stocks of 50 nm PVP-AgNPs and 12 nm Gum Arabic (GA) capped AgNPs by preparing them in the presence of

sediment, plants or both sediments and plants[104]. EPS produced by the plants as a detoxification response to the presence of the NPs caused the ENMs to aggregate and sediment, reducing the ENM concentration suspended in the water, and so reducing toxicity to these organisms feeding in the water column.Therefore, in shallow waters where there are likely to be aquatic flora, EPS production will be higher and significantly increase sedimentation of ENMs. Whether this decrease in exposure and toxicity to feeders in the water column would be mirrored by an increase in toxicity to sediment dwelling specieswas not assessed, becauseno benthic species was included in the exposure. This highlights the importance of including a sediment ingesting benthic organism as part of the base set of organisms for the standardized testing ofNP aquatic hazards, becausereduced toxicity to pelagic species due to sedimentation across the exposure period could be negated by an increase in toxicity to benthic species.

Incorporation of MeOs into larger aggregates may also increase exposure to some epibenthicorganisms. For example, the mussel *Mytilus edulis* and oysters, *Crassostreavirginica* both experienced rapid uptake and accumulation of 100 nm fluorescently labelled polystyrene NPs when they were embedded into laboratory generated aggregates (>100 μm), whereas the freely suspended particles (<1 μm) experienced no uptake over a 45 minute exposure [105]. The aggregated ENMs were bioaccessiblewhereas the untransformed ENMs were not, due to this species greater capture efficiency of particles > 1 μm in size. Research now needs to address whether this transformed,bioaccessible fraction of ENMs is also bioavailable to benthic-dwelling species.

3.Subsurface transformations in the benthos

Onincorporation into sediments, the ENM will interact with two distinct environments: the pore waters, and the sediment grain surfaces. These interactions are highly dependent upon the physiochemical transformations that the ENM has undergone and will determine the particles bioavailability to benthic dwelling organisms. Geochemical heterogeneities in the sediment such as mineral form, distribution and concentration also add complexity to the task of understanding subsurface transformations and greatly influence deposition and transport behaviour of ENMs in saturated porous media[106]. There is a lack

of information on the fate and processes acting upon ENMs in aquatic sediments, thusmany processes are inferred through the use of our knowledge on ENM behaviour in similar matrices such as saturated soils, for which there has been greater research effort.

3.1 Physical transformations will determine deposition and transport of ENMs within sediments

The balance between attractive van der Waals forces and repulsive electrostatic forces are the main interactions that determine the form of deposition of ENMs onto sediment grain surfaces. These two forces create a primary "energy minimum" close to the sediment grain surface (< ~1 nm) where a strong net attraction occurs and beyond which an energy barrier exists to deposition [107]. The strength of this barrier to deposition depends upon the ionic strength of the media, with greater ionic strength resulting in a smaller EDL and so smaller energy barrier [108]. Under cases of high ionic strength or low pH this energy barrier can be entirely overcome, allowing deposition in this primary energy minima [109]. Surface charge of different minerals within sediments may also alter deposition, with more negatively charged silica and iron oxide experiencing greater deposition of CeO_2 NPs than on alumina [110]. Alternatively, as electrostatic repulsion decreases at an exponential rate with distance, a zone of weak attraction can exist further from the NP surface, known as the secondary energy minima [111]. Under less favourable conditions for primary deposition, secondary deposition in this weaker zone of attraction can still occur. The factors that determine deposition of an ENM can thus be conceptualised as those that increase interactions between ENMs and sediment grains and those that increase the attachment efficiencies of these interactions.

Ionic strength plays an important role in determining the attachment efficiency between NPs and sediment grains in the benthos. An increase in ionic strength has been demonstrated to increase deposition of TiO_2 [112, 113], CeO_2 [114], copper oxide (CuO), ZnO[115] and aluminium oxideAl_2O_3[116] in saturated porous media. The form this deposition takes depends on the size and surface charge of the NP in question. As negatively charged aggregates become larger, their surface potential becomes more negative [47, 69]. As such, secondary deposition would dominate the fate of larger NPs >500 nm because they induce a stronger interaction barrier and deeper secondary energy minimum, preventing

deposition in primary energy minima but encouraging secondary deposition [111, 117]. However, pH and ionic strength can significantly reduce these energy barriers for example, at pH 7,a value close to the $pH_{zpc}$of both ZnO and iron oxide(Fe_3O_4),these particles aggregate to > 1 μm and no energy barrier is present soconditions are favourable for primary deposition [115]. This has wide implications for the longer term fate of ENMs in sediments because primary deposition is generally irreversible whereas deposition in the secondary energy minimais reversible. This can occur through Brownian motion [117, 118] or if there is a change in flow rate [119], or ionic strength [107, 111] which would be periodical in estuarine systems. Under some conditions the secondary energy minimum will play the dominant role in NP deposition, primarily for aggregated particles approximately >500 nm, where an increase in size may result in greater deposition in the secondary energy minimum [111] but also in some cases for smaller NPs ~30 nm [118, 120]. However for the majority of NPs <100 nm[30], or for rod shaped NPs where the interaction energies are reduced, the secondary minima are expected to play a far smaller role in ENM deposition [121]. Towards the larger end of the scale where ENM aggregates are > 1 μm, physical straining dominates ENM removal from the interstitial water [108, 109]. This is where the pores become too small for the ENM to pass through (Figure 2) and so the particles are trapped and no longer mobile.

Interstitial Water
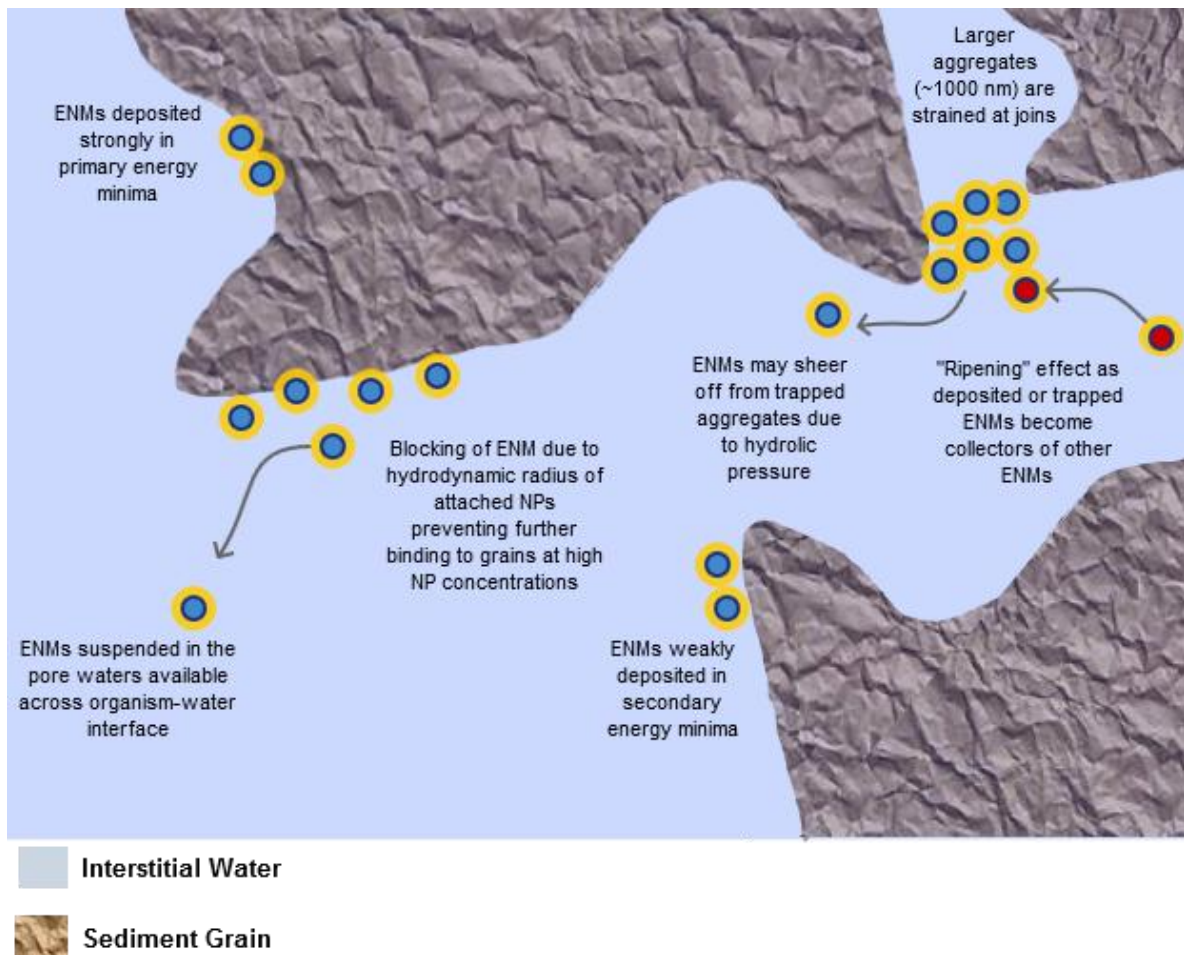
Sediment Grain

Figure 2: physical interactions of ENMs with sediment grains and potential for ENM transport within pore waters.

Over time, deposition and straining can result in a "ripening" effect where deposited and strained aggregates act as collecting surfaces themselves, allowing further deposition of the ENM as has been shown to occur for TiO_2[112]. Such deposition can be enhanced by particle shape, for example the higher deposition and ripening effectobserved of rod shaped latex NPs (aspect ratio 4:1) that was not seen with spherical latex NPs under unfavourable conditions [121]. This ripening effect has now been found to occur also for mixtures of ENMs; with fullerene(C_{60}) NPs showing reduced transport in the presence of TiO_2NPs as the C_{60} become retained by pre-deposited TiO_2[122]. Although straining initially reduces transport of ENMs through sediments, these strained aggregates may act as a longer term source of NPs into the pore waters as hydraulic forces shear particles from the surface of these aggregates [109]. Interestingly, favourable conditions for aggregation and deposition can actually result in greater transport of NPs in the pore waters.If, for instance,larger aggregates avoid straining, their size would allowmovement only in wider pores

with a greater flowrate and so they will travel greater distances[113]. This is known as size exclusion. Another scenario in which conditions favourable for deposition can result in greater concentrations of ENM suspended in pore waters is where there are high concentrations of the ENM. In these instances, the surface of a sediment grain may become saturated with deposited, negatively charged NPs, creating an electrostatic barrier preventing further deposition [116, 121]. This process of "blocking" is particularly effective under lower ionic strength as the EDL of the ENMs expand, thus blocking an area of the grain surface much larger than the NPs actual size. As such, point sources of high ENM concentrations could result in high deposited and strained concentrations close to the source, which may then act as a constant release of NPs over time through shearing from aggregates, size exclusion and blocking (Figure 2).

ENMs such as Ag and CeO_2 are likely to be more mobile than their ionic counterparts [123]which are unlikely to persist as free ions in sediments due to strong partitioning to organic matter [124]. In areas of high ENM concentrations, shearing of strained aggregates, blocking and size exclusion all result in increased transport and suspension of ENMs in the interstitial waters in fresh water sediments. However,in pore waters of high ionic strength, such as marine or estuarine sediments, penetration of ENMs deep into the sediment is still likely to be limited [125], and retention profiles of TiO_2have shown most of the retained ENMs are concentrated in the top 4 cm of the saturated sand columns [122, 126, 127]. This reduced transport may be exacerbated, as has been found for AgNPs, by heteroaggregation with clay particles [124, 128] and other natural colloids such as maghemite or montmorillonite [106].However, bioturbation in areas with high densities of burrowing organisms may overcome these factors which limitENM mobility.For example, bioturbation may lower the bulk density and rigidity of the surficial sediment layer [129], thus making it more prone to erosion processes and resuspension of any sediment and associated NPs into the overlying waters.

3.2 Bioavailability of ENMs within sediments

The different forms of deposition in sediments and the relative distribution of ENMs between sediment grains and pore waters will affect the bioavailability of the ENMs to benthic dwelling organisms and in turn their toxicity. Ingestion has

been established as an important pathway for ENM uptake in aquatic organisms.Association to food material increased both uptake and toxicity of CdSe/ZnS quantum dots and AgNPs to *Daphnia magna* compared with those simply exposed in a water suspension [130, 131].Deposition into the primary or secondary energy minima of sediment grains therefore could increase exposure through ingestion for Oligochaetes and other sediment ingesting organisms. The limited penetration of MeOs into surface sediments also makes them bioaccessible to those organisms living within the surface layer of sediments. This was in evidence in a study where TiO_2 spiked into the surface sediment at a depth of 1 mm,resulted in greater uptake and toxicity to *Hyalellaazteca* and *Chironomusdilutus*than when spiked deeper into the sediment (7 mm) [132]because these organisms feed primarily at the surface sediments. Coutris*et al.* (2012), found that uncoated 19 nm AgNPs, although rapidly retained in soils through deposition, were increasingly re-entrained in the pore water over time[133].These uncoated NPs reached concentrations in the pore waters 8-9 times higher than for citrate stabilized AgNPs or ionic $AgNO_3$.This re-entrainment of NPs into pore waters means that ENMs deposited onto sediment grains may still act as a reasonably stable and continuous source of ENMs suspended in the pore waters which are available for dermal uptake into sediment dwellers.

3.3 Chemical transformationsand thepersistence of ENMs in sediments

Surfactants can dramatically increase the persistence and mobility [134] of MeOs in sediments. ENMs coated with surfactants that confer steric stabilityare more resistant to aggregation and deposition. PVP capped AgNPs had an attachment efficiency to quartz sand grains two orders of magnitude lower than that of pristine AgNPs[135]. Likewise, polyelectrolyte coated zerovalent iron (Fe^0) remained mobile in sediments even after 8 months aging, demonstrating the slow rate of degradation of some surfactants [136]. Although many studies are investigating fateand toxicity of coated or stabilized NPs [137-139],limited data on the production volumes or nature of the surfactants used by manufacturers means it is not yet possible to accurately predict which coatings of NPs will be most prevalent in the environment.

Several studies have looked at the longer term chemical transformations of MeO NPs within sediments. Inorganic chemicals in particular appear to have a

significant and long term effect upon the transformation products of ENMs and their bioavailability and toxicity. Manufactured surfactants have been demonstrated to make ENMs highly persistent in the benthos and inorganic constituents of the sediment can act in a similar way. Such chemical transformations can dominate surface properties to the point where different ENMs behave uniformly, irrespective of ENMs'original surface properties. Dale *et al.* (2013), highlight that sulfurisation plays a dominant role in Ag fate within sediments [140], overriding any difference between surfactants, with ~70% of citrate-capped, PVP-capped and pristine AgNPs persisting as Ag_2S in sediment pore waters when amended with sewage sludge [141]. This sulfidation also limits the prevalence of dissolved ions in the pore waters. AgNPs dosed into saturated soils and bound to sediment grains were shown to release a constant supply of AgNPs into the interstitial waters over a 4 week exposure period. Particulate Ag underwent some degree of dissolution before sulfidationoccurred and the resulting ionic Ag was rapidly complexed with pore water chloride. This formed NPs smaller than the original particles, 50-70 nm in diameter with an Ag_2S shell [142]. Although the formation of a highly insoluble Ag_2S shell [143]reduces toxicity caused by the release of Ag^+ ions it does grant it a half-life in sediments between 10 and >100 years depending on the organic carbon content [140]. Where we draw the boundary for what can still be described as the primary contaminant is uncertain. From an ecotoxicologistsperspective, discerning between dissolved free ions and the primary NP is key to understanding if there is a nano-specific toxic effect, or if NPtoxicity is simply due to the release of free ions [62, 144-147]. Alternatively, both of these modes of toxicity can be considered under the toxic capacity of the NP, as the NP may act as a source or store for the later release of toxic ions. This question of persistence needs to be addressed using long term studies investigating aging and its effect on toxicity.

Phosphate and nitrate also influence the chemical transformations of MeOs in the benthos.In the presence of phosphate there is a rapid reduction in the rate of dissolution of ZnO[148]. The presence of phosphate also altered themorphology of ZnOfrom structurally uniform spheres to a mixture of amorphous and crystalline phases of ZnO and zinc phosphate ($Zn_3(PO_4)_2$), which in turn could increase its persistence and alter reactivity or bioavailability.

Nitrate is also observed to increase persistence of some ENMs, for example itincreased the stability of Fe^0 to such an extent that after 6 months aging in sediments, the Fe^0 and mineral content of aged samples differed little from fresh samples of Fe^0 [149]. A major route of ENM discharge into waters is via sewage treatment plants and the high levels of sulphur, nitrate and phosphate in these effluentsare likely to increase the stability and persistence of ENMs in the benthos.

3.4 NOM affectsENM mobility and the prevalence of dissolved ions within sediments

Dissolution may occur in the water column or on uptake within organisms [150, 151],but within sediments,the rate of ENM dissolution is reduced. Ions such as Ag^+ are transformed into NPs within 4-14 days through reduction in the presence of humic acid [152]. The presence of both humic and fulvic acids rapidly reduce ion release from AgNPs, even at low NOM concentrations of 5 mg L^{-1}, resulting in negligible dissolution at concentrations of 50 mg L^{-1} [153]. This strongly suggestsa low prevalence of dissolved ions derived from metal ENMswithin the benthos.

NOMwill not only reduce the prevalence of dissolved ions from AgNPsin pore waters, but will also increase transport distances for many ENMs through saturated porous media. Humic acids in particular have been shown toincrease the mobility ofnanoparticulate Fe_3O_4 and ZnO[115], TiO_2[126], Cu^0[154] and Ag [106] within pore waters. At low concentrations,NOM-ENM complexation may provide electrostatic stability, reducing the rate of deposition by making the NP surface charge more negative [126].At higher concentrations of between 1-20 mg/L NOM can also provide steric stabilization [134, 155, 156]preventing close proximity between the NP and the grain surface,makingdeposition in the primary energy minima impossible [157]. This steric repulsion is not affected by changing ionic strength, pH or electrolyte composition [158]. Fulvic acids on the other hand have a smaller molecular size and so when coating ENMs confer less steric stability thus less resistance to deposition [156].

Other components of NOM can reduce mobility of ENMs in sediments. Examples of this include oxalic and adipic acids,which have been shown to reduce the stability of TiO_2 when adsorbed to the NPs, promoting aggregation [159] and straining of these aggregates. The process of adsorption of organic

193

acids to the NP was unchanged by either initial or aggregated particle size, suggesting attachment was uniform, irrespective of the size of NP coming into contact with these organic acids. Another example of where NOM can reduce ENM mobility is for polysaccharide NOM present in waste water sludge and EPS which increased the retention of C_{60}NPs in saturated porous media [160]. Whether such a reduction in mobility also occurs for MeO ENMs has not yet been established. Many interactions with NOM initially reduce the mobility of ENMs in sediments, through formation of aggregates leading to physical straining.Although most ENMs will experience reduced transport in sediments, the potential for re-entrainment of ENMs into pore waters under some conditions from weak secondary deposition onto sediment grain surfaces means a significant percentage may still experience longer term mobility.

Table 1 presents a summary of some of the key transformations and processes affecting ENMs as they pass from pelagic to benthic systems, representing a range of metal nanoparticles with reference to the available literature.

Table 1: Important surface and sub-surface transformations of ENMs and our understanding of their impact upon fate of ENMs in aquatic sediments

Transformation	Environmental compartment	ENM composition (primary particle size)	Outcome	Reference
Natural organic matterforms heteroaggregateswhich can stabilise ENMs	Surface waters	ZnO (4 nm)	Dissolved Suwamee River humic acid at 7.3 mg/L resulted in Zeta potential below -30 mV and reduced sedimentation over 120 min. Lower levels of HA (1.7 mg/L) caused greater sedimentation,through chargeneutralisationby the HAof theNPs positive charge, resulting in greater aggregation.	Bianet $al.$ 2011 [44]
		ZnO (24 nm), TiO2 (27 nm)and CeO2 (8 nm)	All NPs formed aggregates ~300 nm in diameter that were stable and experienced no sedimentationover 7 h in mesocosmfreshwater with total organic carbon of 5.3 mM.	Keller et $al.$ 2010 [50]
		TiO2 (30 nm)	Suwamee River humic acid at 10 mg/L stabilised TiO2 NPs through both electrostatic and steric repulsion, particle Zeta potential being between -30 and -40 mV at 0.1 - 100 mMNaCl (Na+ cation dominates marine waters). Ca+, the cationwhich is prevalent in freshwaters was foundto be more effective at causing aggregation at lower concentrations than NaCl, this effect wasnegated by the presence of the humic acid.	Thioet $al.$ 2011 [71]
		TiO2 nanorod core, coated withAl(OH)3 and poly-dimethylsiloxane (PDMS) layers(10 x 50 nm TiO2 core)	A TiO2 nanocomposite used in sunscreens. 35 % of the particles remained in suspensionas aggregates ~300 nm after 48 h. Humic acid at 2% w/w (< 1 mg/L) causedfloculation through bridging between NPs, whilst at 20% w/w the NP was stabilised, experiencing nosedimentation over 48 h.	Labilleet $al.$ 2010 [72]
Filter feeders may alterthe size distribution ofENMs reaching the benthos	Surface waters andSediment-waterboundary	Mercaptoundecanoic acid-cappedAu NPs (30 nm)	Particles aggregated to 10x primary particle size, averaging ~300 nm. In presence of *Daphnia magna* this reduced to <200 nm within 10 h. In the presence of *Gammaruspulexa* size stabilised at ~150 nm over the 100 h exposure.	Park et $al.$ 2014 [90]
		Natural inorganic colloids in lake water (50 - 2000 nm)	After 310 min in the presence of *Daphnia magna,* inorganic colloids <400 nm increased to between 100-130% of their original concentration before the organisms were added. Colloids >400 nm decreased to a minimum of ~40% of their original concentration.	Filella et $al.$ 2008 [89]
Natural organic mattercan reduce presence ofdissolved ions	Sediment	AgNO3 (ionic)	Silver Nitrate solutions were exposed to 1-100 mg/L Suwamee River humic acid and three sedimentary humic acids, all of which reduced the Ag+	Akiagheet $al.$ 2011 [152]

195

			ions, forming AgNPs within 2 to 4 days at	
		Citrate stabilised Ag NPs (2-8 nm)	22 C. NPs had a wide size distribution but with similar means between 70-90 nm found by dynamiclight scattering. 5 mg/L of both Suwarmee River humic and fulvic acid reduced dissolved Ag by 1 order of magnitude, from ~15% of total Ag to ~1%.	Liu *et al.* 2010 [153]
Sulfurization increases persistance but reduces dissolution	Sediment	Modelled Ag NPs	Modelled half-life of Ag NPs (both Ag0 and AgS2) varied with organic carbon (OC) with low OC half-life of 6.6 years, mid OC 77 years and high OC 280 years.	Dale *et al.* 2013 [140]
		PVP-Ag NPs (60 nm) Citrate Ag NPs (60 nm)	When aged in the presence of sewage sludge, 70 and 78% of the PVP and citrate coated NPs respectively formed AgS2. Aging reduced Ag ions in the pore water to < 2% of total Ag.	Whitley *et al.* 2013 [141]
Natural organic matter increases ENM transport in saturated porus media	Sediment	Fe3O4 (<50 nm), TiO2 (<100 nm), CuO (<100 nm) and ZnO (<50 nm)	All ENM were aggregated in test water > 100 nm. Mobility decreased in order of TiO2 > CuO > ZnO > Fe3O4. 62% of TiO2 were initially eluted from the bead column, but in the presence of 60 mg/L humic acid this increased to 98% for both TiO2 and CuO.	Ben-Moshe *et al.* 2010 [115]
		TiO2 (10 x 40 nm) ~90 nm in test conditions	At pH 5.7, humic acid (1 mg/L) reduced deposition onto sediment grains, increasing transport through electrostatic and steric effects. At pH 9, the effect of NOM was limited as humic acid did not adsorb well to the TiO2 NPs.	Chen *et al.* 2012 [126]
Co-transport of suspended colloids and ENMs	Sediment	TiO2 (25 nm) 200 nm in test conditions and C60 (135-505 nm in test conditions)	At pH 7, transport of TiO2 increased with increasing C60 concentration, as the C60 competed for deposition sites on quartz sand grains.TiO2 NPs which did deposit acted as additional sites for deposition, reducing transport of C60 when in the presence of TiO2.	Cai*et al.* 2013 [122]
		PVP capped AgNPs (10 nm) 40 nm in test conditions	Ag NPs experienced rapid heteroaggregation with maghemite or montmorillonite. In soils with a higher porosity this leads to size exclusion and greater heteroaggregate transport. In most soils this reduced mobility due to primary deposition, resulting in a maximum transport depth of 12 cm.	Cornelis *et al.* 2013 [106]

4. Uptake of ENMs into benthic organisms

Sediment ecosystems have historically acted as a buffer against extinction events. As an example in the late Permian mass extinction event, globally only one functional group (based on mode of life and functional morphology) was lost from the benthos [161]. However, at the local and regional scale, perturbations to the functional diversity of benthic ecosystems can have a profound effect on processes such as bioturbation [162]that are essential for global nutrient cycling and the productivity of aquatic ecosystems [163, 164]. The importance of this linking between the benthos and the overlying waters, known as the benthic-pelagic coupling is rarely referred to explicitly within the nano-ecotoxicology literature. Freshwater sediments act as a zone for diapause for zooplankton, an essential survival mechanism that increases the resilience of zooplankton throughout periods of unfavourable environmental conditions [165]. Benthic dwellers themselves act as ecosystem engineers and as such their composition and diversity determine the functioning of entire aquatic ecosystems [166-168]. Given this, understanding the risk that ENMs pose to the benthos is important, not only to predict the localized effects of ENMs, but also to understand the effects on the wider aquatic ecosystem.

Organisms exposed to ENMs within the benthos vary from sedentary organisms, to endobenthic, sediment ingesting Oligochaetes, to the juvenile stages of some pelagic species [169]. Biofilms are the major biological compartment for partitioning of ENMs when sedimenting to the benthos [24]. In a study on positively charged cetyltrimethylammonium bromide (CTAB) stabilized Au nanorods 61% were shown to partition into biofilms [170] reducing ENM mobility within sediments [171]. ENM toxicity towards these biofilms is of importance because they act as sediment biostabilizers, performing an essential role in the structure and functioning of the benthos [172]. Biofilms and other microbes also act as an important food source for many benthic grazers. Association with algae may increase the assimilation efficiency of MeOs and so bioavailability. In *D. magna* ~70% of accumulated Ag was attributable to AgNPs associated with algal food [131]. Some particles appear to become toxic only when associated with phytoplankton or biofilms. For example SiO_2 and CeO_2 NPs associated with algal food reduced sea urchin larvae survival [173]. This was

197

also demonstrated with CdSe/ZnSquantum dots, which were toxic when ingested in association with algal food in *D. magna* but not when freely suspended, even though bioaccumulation occurred for both exposure routes [130].

Feeding patterns of organisms will also determine the bioavailability of ENMs to benthic dwellers via dietary uptake. The grazing aquatic snail *Physaacuta*, selectively grazeson biofilms based on palatability. In stream mesocosm studies, various biofilms were exposed to a range of concentrations of TiO_2 and the greatest accumulation of the NP in *P. acuta* was when feeding on biofilms of the diatom *Synedra ulna* [174]. *S. ulna* produced the lowest biomass of all the mesocosms tested and so total TiO_2 available through ingestion should have been lower. However, in this mesocosm, the *P. acuta* ingested >50% of the total *S. ulna* biofilm, far more than any other biofilm and so ingestion and accumulation of TiO_2 was greater. Patterns of behaviour can also reduce exposure of ENMs to organisms. The larva of the nematoceran fly *Chironomus dilutes* creates a tube of sand around itself in sediments, totally preventing surface attachment of TiO_2NPs [132]. These studies highlight how the toxicity of an ENM is dependent not only on the inherent toxicity of the NP itself, but also on biological parameters defined by organism behaviour and how it partitions among benthic communities.

The characteristics of some exemplar benthic species of great importance for hazard prediction for ENMs in the benthos are identified in Table 2, by defining their functional role within ecosystems and the route through which they will be exposed to ENMs. The five groups outlined include a range of organisms that play important roles in ecosystem engineering within the benthos and include groups that represent the benthic-pelagic coupling. Routes of exposure are suggested, based on the evidence collected in the present review. Examples of species used to investigate the question of NP hazard in the benthos are included in Table 2 along with the corresponding standardised chemical ecotoxicity testing methods that are currently in use. Owing to the differences between solute and colloidal chemistry, thorough characterisation of NPs in the test media and their transformations is necessary to determine the suitability of these tests when using NPs, and in order to accurately interpret any results.

Table 2: Exemplar species for ecotoxicity testing of ENMs in the benthos including their potential exposure route, grouped by their role in ecosystem functioning.

Species Group	Functional Role	Species Examples	Expected Route to Exposure?	Standardised test protocols available
Microbes and bacteria	Biostabilization of sediments through EPS [172]	Epipsammic diatom species in sandy sediments; epipelic in clay based sediments	Adsorption in the "fluff layer" and settling to the sediment surface	None available to date
Deposit feeding oligochaete and polychaete	Bioturbation [102, 162] and bioresuspension [100, 101]	*Lumbriculus variegauts,Tubifex tubifex*	Ingestion of sediment deposited ENMs, some exposure possible through pore-waters	OECD TG 225 OECD TG 315 EPA 600-R-99-064
Epibenthic filter feeders	Determine size distribution of ENM reaching the sediment [89, 90]	*Scrobiculariaplana,Crassostreagigas*	Filter feeding out of suspension in the "fluff layer" incorporation pseudofaeces	Recommended by OECD ASTM E2455 - 06(2013)
Aquatic plants	Sediment stabilization and release of EPS [104]	*Potamogetondiversifolius, Egeria densa, Myriophyllum spicatum*	Potential exposure through root systems	OECD TG 239
Dormancy/juvenile organisms	Benthic-Pelagic Coupling [165]	Dormancy phase zooplankton, *Chronomidae*larvae	Through water column forplanktotrophic benthic larvae or sediment forpelagic species larvae	OECD TG 233

5. Conclusions and future recommendations

The various processes and transformations ENMs undergo upon their release into the environment have the potential to drastically alter their fate, form and toxicity. Realism in ecotoxicological testing of ENMs requires a better understanding of these processes to inform on their fate and nature and in turn to better understand which compartments and organisms are most at risk of exposure. From our analysis of the available literature, we identify that the following factors are critical in understanding the fate and form of transformed ENMs within the benthos.

- The presence of NOM and other biogenic exudates such as EPS will dominate inorganic ENM behaviour in the aquatic environment through heteroaggregation or by conferring steric stability. EPS can derive from both biofilms and free floating bacteria in the water column but can also arise as a response to stress in aquatic plants and so ENMs will interact with EPS both in the water column and at the sediment surface.

- The formation of "marine snow" from EPS and its potential to act as a vehicle for sedimentation of ENMs out of the water column may present a seasonal flux of ENMs to the benthos in both fresh and marine waters. This is not currently accounted for in attempts to model environmental concentrations of ENMs in the benthos.

- Aggregation, complexation with NOM and EPS and chemical transformations such as sulfidation, all reduce rates of dissolution and the release of toxic metal ions from ENMs. Therefore ENMs within the sediments are likely to be in the particulate form, prevailing as large aggregates or complexed with NOM and EPS.

- Complexation with NOM and EPS results in deposition into the weaker secondary energy minimum dominating nanoparticle interactions with sediment grains, increasing the mobility of many inorganic ENMs within saturated porous media. Therefore sediment dwelling organisms will be at risk from a variety of routes to exposure including ENMs in suspension in the interstitial waters, bound to sediment grains and at the sediment surface where they may be re-circulated into the water column through bioturbation.

- Biofilms at the sediment surface have the capacity to adsorb ENMs effectively and play an important role both in the cycling of nutrients within aquatic ecosystems and as primary producers. As such, the high incorporation of ENMs into biofilms could both disrupt local nutrient cycling and act as a source for trophic transfer of ENMs between benthic dwelling organisms, as many benthic organisms graze on these microbial biofilms.

We would argue that better understanding of the complex nature of the transformations of ENMs within the aquatic environment is essential for developing standardized (and appropriate) testing methods for the ecotoxicity of ENMs. Transformations within sediments represent a significant gap in our knowledge and our recommendations for the immediate future of research needs in this field are:

- Studies into bioaccumulation and toxicity of ENMs to benthic species should include sufficient characterization of the ENMs in the test water and where possible in the sediment matrix to examine the processes and transformations which dictate patterns of ENM fate and bioavailability.
- Studies using manufactured "transformed" ENMs such as AgNPs after sulfidation are needed to understand how such transformations affect ENM fate, behaviour and toxicity to benthic organisms compared with "pristine" particles.
- Assessment of the potential for fluxes of ENMs carried in "marine snow" to act as a vector for nanoparticle sedimentation to the benthos and to include such transport systems in predictive modelling of environmental concentrations of ENMs.
- Toxicity and bioaccumulation tests on a range of the benthic dwelling species identified in this review (Table 2) as being of particular risk of exposure, including aquatic plants and biofilms.

References

[1]   Roco MC, Mirkin CA, Hersam MC. *Nanotechnology research directions for societal needs in 2020: retrospective and outlook* 2011 (Springer Science & Business Media).

[2]   Cundy AB, Hopkinson L, Whitby RL. Use of iron-based technologies in contaminated land and groundwater remediation: a review. The Science of the total environment. **2008**, 400(1-3), 42-51.

[3]   Zhang Y, Li Y, Li J, Hu L, Zheng X. Enhanced removal of nitrate by a novel composite: Nanoscale zero valent iron supported on pillared clay. Chemical Engineering Journal. **2011**, 171(2), 526-31.

[4]   Lagaron JM, Lopez-Rubio A. Nanotechnology for bioplastics: opportunities, challenges and strategies. Trends in Food Science & Technology. **2011**, 22(11), 611-7.

[5]   Van Devener B, Anderson SL. Breakdown and Combustion of JP-10 Fuel Catalyzed by Nanoparticulate CeO2and Fe2O3. Energy & Fuels. **2006**, 20(5), 1886-94.

[6]   Lee J, Mahendra S, Alvarez PJ. Nanomaterials in the construction industry: a review of their applications and environmental health and safety considerations. ACS nano. **2010**, 4(7), 3580-90.

[7]   Mu L, Sprando RL. Application of nanotechnology in cosmetics. Pharmaceutical research. **2010**, 27(8), 1746-9.

[8]   Salata O. Applications of nanoparticles in biology and medicine. Journal of nanobiotechnology. **2004**, 2(1), 3.

[9]   Klaine SJ, Koelmans AA, Horne N, Carley S, Handy RD, Kapustka L, et al. Paradigms to assess the environmental impact of manufactured nanomaterials. Environmental toxicology and chemistry / SETAC. **2012**, 31(1), 3-14.

[10]   BSI. Terminology for nanomaterials PAS 136:2007 British Standards Institution. **2007**.

[11]   Klaine SJ, Alvarez PJJ, Batley GE, Fernandes TF, Handy RD, Lyon DY, et al. Nanomaterials in the Environment: Behavior, Fate, Bioavailability, and Effects. Environmental Toxicology and Chemistry. **2008**, 27(9), 1825.

[12]   Potocnik J, COMMISSION RECOMMENDATION of 18 October 2011 on the definition of nanomaterial (2011/696/EU), 2011 http://eur-lex.europa.eu/LexUriServ/LexUriServ.do?uri=OJ:L:2011:275:0038:0040:en:PDF (verified 10/04/2014 2014).

[13]   Mueller NC, Nowack B. Exposure Modeling of Engineered Nanoparticles in the Environment. Environmental science & technology. **2008**, 42(12), 4447-53.

[14]   Gottschalk F, Sonderer T, Scholz RW, Nowack B. Modeled environmental concentrations of engineered nanomaterials (TiO(2), ZnO, Ag, CNT, Fullerenes) for different regions. Environmental science & technology. **2009**, 43(24), 9216-22.

[15]   Gottschalk F, Sonderer T, Scholz RW, Nowack B. Possibilities and limitations of modeling environmental exposure to engineered nanomaterials by

probabilistic material flow analysis. Environmental toxicology and chemistry / SETAC. **2010**, 29(5), 1036-48.

[16] Hendren CO, Mesnard X, Droge J, Wiesner MR. Estimating production data for five engineered nanomaterials as a basis for exposure assessment. Environmental science & technology. **2011**, 45(7), 2562-9.

[17] Arvidsson R, Molander S, Sandén BA, Hassellöv M. Challenges in Exposure Modeling of Nanoparticles in Aquatic Environments. Human and Ecological Risk Assessment: An International Journal. **2011**, 17(1), 245-62.

[18] Keller AA, McFerran S, Lazareva A, Suh S. Global life cycle releases of engineered nanomaterials. Journal of Nanoparticle Research. **2013**, 15(6).

[19] Hou L, Li K, Ding Y, Li Y, Chen J, Wu X, et al. Removal of silver nanoparticles in simulated wastewater treatment processes and its impact on COD and NH(4) reduction. Chemosphere. **2012**, 87(3), 248-52.

[20] Kaegi R, Voegelin A, Sinnet B, Zuleeg S, Hagendorfer H, Burkhardt M, et al. Behavior of metallic silver nanoparticles in a pilot wastewater treatment plant. Environmental science & technology. **2011**, 45(9), 3902-8.

[21] Meyer DE, Curran MA, Gonzalez MA. An Examination of Existing Data for the Industrial Manufacture and Use of Nanocomponents and Their Role in the Life Cycle Impact of Nanoproducts. Environmental science & technology. **2009**, 43(5), 1256-63.

[22] Piccinno F, Gottschalk F, Seeger S, Nowack B. Industrial production quantities and uses of ten engineered nanomaterials in Europe and the world. Journal of Nanoparticle Research. **2012**, 14(9).

[23] Kaegi R, Ulrich A, Sinnet B, Vonbank R, Wichser A, Zuleeg S, et al. Synthetic TiO2 nanoparticle emission from exterior facades into the aquatic environment. Environmental pollution. **2008**, 156(2), 233-9.

[24] Cleveland D, Long SE, Pennington PL, Cooper E, Fulton MH, Scott GI, et al. Pilot estuarine mesocosm study on the environmental fate of Silver nanomaterials leached from consumer products. The Science of the total environment. **2012**, 421-422, 267-72.

[25] Bernhardt ES, Colman BP, Hochella MF, Cardinale BJ, Nisbet RM, Richardson CJ, et al. An Ecological Perspective on Nanomaterial Impacts in the Environment. Journal of Environment Quality. **2010**, 39(6), 1954.

[26] Colvin VL. The potential environmental impact of engineered nanomaterials. Nature biotechnology. **2003**, 21(10), 1166-70.

[27] Beketov MA, Cedergreen N, Wick LY, Kattwinkel M, Duquesne S, Liess M. Sediment Toxicity Testing for Prospective Risk Assessment—A New Framework and How to Establish It. Human and Ecological Risk Assessment: An International Journal. **2013**, 19(1), 98-117.

[28] Stolpe B, Hassellöv M. Changes in size distribution of fresh water nanoscale colloidal matter and associated elements on mixing with seawater. Geochimica et Cosmochimica Acta. **2007**, 71(13), 3292-301.

[29] Wen L-S, Santschi PH, Gill GA, Paternostro CL, Lehman RD. Colloidal and Particulate Silver in River and Estuarine Waters of Texas. Environmental science & technology. **1997**, 31(3), 723-31.

[30]   Petosa AR, Jaisi DP, Quevedo IR, Elimelech M, Tufenkji N. Aggregation and deposition of engineered nanomaterials in aquatic environments: role of physicochemical interactions. Environmental science & technology. **2010**, 44(17), 6532-49.

[31]   Chinnapongse SL, MacCuspie RI, Hackley VA. Persistence of singly dispersed silver nanoparticles in natural freshwaters, synthetic seawater, and simulated estuarine waters. The Science of the total environment. **2011**, 409(12), 2443-50.

[32]   Lanceleur L, Schafer J, Chiffoleau JF, Blanc G, Auger D, Renault S, et al. Long-term records of cadmium and silver contamination in sediments and oysters from the Gironde fluvial-estuarine continuum - evidence of changing silver sources. Chemosphere. **2011**, 85(8), 1299-305.

[33]   Lanceleur L, Schäfer J, Bossy C, Coynel A, Larrose A, Masson M, et al. Silver fluxes to the Gironde Estuary – Eleven years (1999–2009) of monitoring at the watershed scale. Applied Geochemistry. **2011**, 26(5), 797-808.

[34]   Praetorius A, Scheringer M, Hungerbuhler K. Development of environmental fate models for engineered nanoparticles--a case study of TiO2 nanoparticles in the Rhine River. Environmental science & technology. **2012**, 46(12), 6705-13.

[35]   Lowry GV, Espinasse BP, Badireddy AR, Richardson CJ, Reinsch BC, Bryant LD, et al. Long-term transformation and fate of manufactured ag nanoparticles in a simulated large scale freshwater emergent wetland. Environmental science & technology. **2012**, 46(13), 7027-36.

[36]   Diepens NJ, Arts GHP, Brock TCM, Smidt H, Van Den Brink PJ, Van Den Heuvel-Greve MJ, et al. Sediment Toxicity Testing of Organic Chemicals in the Context of Prospective Risk Assessment: A Review. Critical Reviews in Environmental Science and Technology. **2014**, 44(3), 255-302.

[37]   Kuhnel D, Nickel C. The OECD expert meeting on ecotoxicology and environmental fate - towards the development of improved OECD guidelines for the testing of nanomaterials. The Science of the total environment. **2014**, 472, 347-53.

[38]   Moore MN. Do nanoparticles present ecotoxicological risks for the health of the aquatic environment? Environ Int. **2006**, 32(8), 967-76.

[39]   Lowry GV, Gregory KB, Apte SC, Lead JR. Transformations of nanomaterials in the environment. Environmental science & technology. **2012**, 46(13), 6893-9.

[40]   Gustafsson O, Gschwend PM. Aquatic colloids: concepts, definitions and current challenges. Limnology and Oceanography,. **1997**, 42(3), 519-28.

[41]   Ju-Nam Y, Lead JR. Manufactured nanoparticles: an overview of their chemistry, interactions and potential environmental implications. The Science of the total environment. **2008**, 400(1-3), 396-414.

[42]   Zhou D, Keller AA. Role of morphology in the aggregation kinetics of ZnO nanoparticles. Water research. **2010**, 44(9), 2948-56.

[43]   French RA, Jacobson AR, Kim B, Isley SL, Penn RL, Baveye PC. Influence of Ionic Strength, pH, and Cation Valence on Aggregation Kinetics of

Titanium Dioxide Nanoparticles. Environmental science & technology. **2009**, 43(5), 1354-9.

[44]   Bian SW, Mudunkotuwa IA, Rupasinghe T, Grassian VH. Aggregation and dissolution of 4 nm ZnO nanoparticles in aqueous environments: influence of pH, ionic strength, size, and adsorption of humic acid. Langmuir : the ACS journal of surfaces and colloids. **2011**, 27(10), 6059-68.

[45]   Romer I, White TA, Baalousha M, Chipman K, Viant MR, Lead JR. Aggregation and dispersion of silver nanoparticles in exposure media for aquatic toxicity tests. Journal of chromatography A. **2011**, 1218(27), 4226-33.

[46]   Zhang Y, Chen Y, Westerhoff P, Hristovski K, Crittenden JC. Stability of commercial metal oxide nanoparticles in water. Water research. **2008**, 42(8-9), 2204-12.

[47]   Guzman D. KA, Finnegan MP, Banfield JF. Influence of Surface Potential on Aggregation and Transport of Titania Nanoparticles. Environmental science & technology. **2006**, 40(24), 7688-93.

[48]   Cumberland SA, Lead JR. Particle size distributions of silver nanoparticles at environmentally relevant conditions. Journal of chromatography A. **2009**, 1216(52), 9099-105.

[49]   Jassby D, Farner Budarz J, Wiesner M. Impact of aggregate size and structure on the photocatalytic properties of TiO2 and ZnO nanoparticles. Environmental science & technology. **2012**, 46(13), 6934-41.

[50]   Keller AA, Wang H, Zhou D, Lenihan HS, Cherr G, Cardinale BJ, et al. Stability and aggregation of metal oxide nanoparticles in natural aqueous matrices. Environmental science & technology. **2010**, 44(6), 1962-7.

[51]   Quik JT, Stuart MC, Wouterse M, Peijnenburg W, Hendriks AJ, van de Meent D. Natural colloids are the dominant factor in the sedimentation of nanoparticles. Environmental toxicology and chemistry / SETAC. **2012**, 31(5), 1019-22.

[52]   Quik JT, Velzeboer I, Wouterse M, Koelmans AA, van de Meent D. Heteroaggregation and sedimentation rates for nanomaterials in natural waters. Water research. **2014**, 48, 269-79.

[53]   Botta C, Labille J, Auffan M, Borschneck D, Miche H, Cabie M, et al. TiO(2)-based nanoparticles released in water from commercialized sunscreens in a life-cycle perspective: structures and quantities. Environmental pollution. **2011**, 159(6), 1543-50.

[54]   Zhao CM, Wang WX. Size-dependent uptake of silver nanoparticles in Daphnia magna. Environmental science & technology. **2012**, 46(20), 11345-51.

[55]   Park K, Tuttle G, Sinche F, Harper SL. Stability of citrate-capped silver nanoparticles in exposure media and their effects on the development of embryonic zebrafish (Danio rerio). Archives of pharmacal research. **2013**, 36(1), 125-33.

[56]   Meulenkamp EA. Size Dependence of the Dissolution of ZnO Nanoparticles. The Journal of Physical Chemistry B. **1998**, 102(40), 7764-9.

[57]   Mudunkotuwa IA, Rupasinghe T, Wu CM, Grassian VH. Dissolution of ZnO nanoparticles at circumneutral pH: a study of size effects in the presence

and absence of citric acid. Langmuir : the ACS journal of surfaces and colloids. **2012**, 28(1), 396-403.

[58]   Zook JM, Long SE, Cleveland D, Geronimo CL, MacCuspie RI. Measuring silver nanoparticle dissolution in complex biological and environmental matrices using UV-visible absorbance. Analytical and bioanalytical chemistry. **2011**, 401(6), 1993-2002.

[59]   Dahle JT, Livi K, Arai Y. Effects of pH and phosphate on CeO nanoparticle dissolution. Chemosphere. **2014**.

[60]   Li X, Lenhart JJ. Aggregation and dissolution of silver nanoparticles in natural surface water. Environmental science & technology. **2012**, 46(10), 5378-86.

[61]   Majedi SM, Lee HK, Kelly BC. Role of water temperature in the fate and transport of zinc oxide nanoparticles in aquatic environment. Journal of Physics: Conference Series. **2013**, 429, 012039.

[62]   Franklin NM, Rogers NJ, Apte SC, Batley GE, Gadd GE, Casey PS. Comparative Toxicity of Nanoparticulate ZnO, Bulk ZnO, and ZnCl2to a Freshwater Microalga (Pseudokirchneriella subcapitata): The Importance of Particle Solubility. Environmental science & technology. **2007**, 41(24), 8484-90.

[63]   Borm P, Klaessig FC, Landry TD, Moudgil B, Pauluhn J, Thomas K, et al. Research strategies for safety evaluation of nanomaterials, part V: role of dissolution in biological fate and effects of nanoscale particles. Toxicological sciences : an official journal of the Society of Toxicology. **2006**, 90(1), 23-32.

[64]   Saleh NB, Pfefferle LD, Elimelech M. Influence of biomacromolecules and humic acid on the aggregation kinetics of single-walled carbon nanotubes. Environmental science & technology. **2010**, 44(7), 2412-8.

[65]   Diegoli S, Manciulea AL, Begum S, Jones IP, Lead JR, Preece JA. Interaction between manufactured gold nanoparticles and naturally occurring organic macromolecules. The Science of the total environment. **2008**, 402(1), 51-61.

[66]   Pallem VL, Stretz HA, Wells MJM. Evaluating Aggregation of Gold Nanoparticles and Humic Substances Using Fluorescence Spectroscopy. Environmental science & technology. **2009**, 43(19), 7531-5.

[67]   Chen KL, Elimelech M. Influence of humic acid on the aggregation kinetics of fullerene (C60) nanoparticles in monovalent and divalent electrolyte solutions. Journal of colloid and interface science. **2007**, 309(1), 126-34.

[68]   Deonarine A, Lau BL, Aiken GR, Ryan JN, Hsu-Kim H. Effects of humic substances on precipitation and aggregation of zinc sulfide nanoparticles. Environmental science & technology. **2011**, 45(8), 3217-23.

[69]   Pelley AJ, Tufenkji N. Effect of particle size and natural organic matter on the migration of nano- and microscale latex particles in saturated porous media. Journal of colloid and interface science. **2008**, 321(1), 74-83.

[70]   Illes E, Tombacz E. The effect of humic acid adsorption on pH-dependent surface charging and aggregation of magnetite nanoparticles. Journal of colloid and interface science. **2006**, 295(1), 115-23.

[71] Thio BJ, Zhou D, Keller AA. Influence of natural organic matter on the aggregation and deposition of titanium dioxide nanoparticles. Journal of hazardous materials. **2011**, 189(1-2), 556-63.

[72] Labille J, Feng J, Botta C, Borschneck D, Sammut M, Cabie M, et al. Aging of TiO(2) nanocomposites used in sunscreen. Dispersion and fate of the degradation products in aqueous environment. Environmental pollution. **2010**, 158(12), 3482-9.

[73] DeLong EF, Franks DG, Alldredge AL. Phylogenetic diversity of aggregate-attached vs. free-living marine bacterial assemblages. Limnology and Oceanography. **1993**, 38(5), 924-34.

[74] Alldredge AL, Passow U, Logan BE. The abundance and significance of a class of large, transparent organic particles in the ocean. Deep Sea Research Part I: Oceanographic Research Papers. **1993**, 40(6), 1131-40.

[75] Asper VL. Measuring the flux and sinking speed of marine snow aggregates. Deep Sea Research Part A Oceanographic Research Papers. **1987**, 34(1), 1-17.

[76] Passow U. Transparent exopolymer particles (TEP) in aquatic environments. Progress in Oceanography. **2002**, 55(3-4), 287-333.

[77] Alldredge AL, Silver MW. Characteristics, dynamics and significance of marine snow. Progress in Oceanography. **1988**, 20(1), 41-82.

[78] Doyle JJ, Palumbo V, Huey BD, Ward JE. Behavior of Titanium Dioxide Nanoparticles in Three Aqueous Media Samples: Agglomeration and Implications for Benthic Deposition. Water, Air, & Soil Pollution. **2014**, 225(9).

[79] Logan BE, Passow U, Alldredge AL, Grossartt H-P, Simont M. Rapid formation and sedimentation of large aggregates is predictable from coagulation rates (half-lives) of transparent exopolymer particles (TEP). Deep Sea Research Part II: Topical Studies in Oceanography. **1995**, 42(1), 203-14.

[80] Limbach LK, Bereiter R, Müller E, Krebs R, Gälli R, Stark WJ. Removal of Oxide Nanoparticles in a Model Wastewater Treatment Plant: Influence of Agglomeration and Surfactants on Clearing Efficiency. Environmental science & technology. **2008**, 42(15), 5828-33.

[81] Chen CS, Anaya JM, Zhang S, Spurgin J, Chuang CY, Xu C, et al. Effects of engineered nanoparticles on the assembly of exopolymeric substances from phytoplankton. PloS one. **2011**, 6(7), e21865.

[82] Zhang S, Jiang Y, Chen CS, Spurgin J, Schwehr KA, Quigg A, et al. Aggregation, dissolution, and stability of quantum dots in marine environments: importance of extracellular polymeric substances. Environmental science & technology. **2012**, 46(16), 8764-72.

[83] Morris DP, Zagarese H, Williamson CE, Balseiro EG, Hargreaves BR, Modenutti B, et al. The attenuation of solar UV radiation in lakes and the role of dissolved organic carbon. Limnology and Oceanography. **1995**, 40(8), 1381-91.

[84] Riebesell U. Factors controlling the formation of marine snow and its sustained residence in surface waters. Limnology and oceanography. **1992**, 37(1), 63-76.

[85]   Sun TY, Gottschalk F, Hungerbuhler K, Nowack B. Comprehensive probabilistic modelling of environmental emissions of engineered nanomaterials. Environmental pollution. **2014**, 185, 69-76.

[86]   Velzeboer I, Quik JT, van de Meent D, Koelmans AA. Rapid settling of nanoparticles due to heteroaggregation with suspended sediment. Environmental toxicology and chemistry / SETAC. **2014**.

[87]   Koelmans AA, Quik JTK, Velzeboer I. Lake retention of manufactured nanoparticles. Environmental Pollution. **2015**, 196, 171-5.

[88]   Gophen M, Geller W. Filter mesh size and food particle uptake by Daphnia. Oecologia. **1984**, 64(3), 408-12.

[89]   Filella M, Rellstab C, Chanudet V, Spaak P. Effect of the filter feeder Daphnia on the particle size distribution of inorganic colloids in freshwaters. Water research. **2008**, 42(8-9), 1919-24.

[90]   Park S, Woodhall J, Ma G, Veinot JG, Cresser MS, Boxall AB. Regulatory ecotoxicity testing of engineered nanoparticles: are the results relevant to the natural environment? Nanotoxicology. **2014**, 8(5), 583-92.

[91]   Quik JT, Vonk JA, Hansen SF, Baun A, Van De Meent D. How to assess exposure of aquatic organisms to manufactured nanoparticles? Environ Int. **2011**, 37(6), 1068-77.

[92]   Ma S, Lin D. The biophysicochemical interactions at the interfaces between nanoparticles and aquatic organisms: adsorption and internalization. Environmental Science: Processes & Impacts. **2013**, 15(1), 145.

[93]   Montes MO, Hanna SK, Lenihan HS, Keller AA. Uptake, accumulation, and biotransformation of metal oxide nanoparticles by a marine suspension-feeder. Journal of hazardous materials. **2012**, 225-226, 139-45.

[94]   Foster-Smith RL. The effect of concentration of suspension on the filtration rates and pseudofaecal production for Mytilus edulis L., Cerastoderma edule (L.) and Venerupis pullastra (Montagu). Journal of Experimental Marine Biology and Ecology. **1975**, 17(1), 1-22.

[95]   Crater JS, Carrier RL. Barrier properties of gastrointestinal mucus to nanoparticle transport. Macromolecular bioscience. **2010**, 10(12), 1473-83.

[96]   Zhu ZJ, Carboni R, Quercio MJ, Jr., Yan B, Miranda OR, Anderton DL, et al. Surface properties dictate uptake, distribution, excretion, and toxicity of nanoparticles in fish. Small. **2010**, 6(20), 2261-5.

[97]   Verma A, Stellacci F. Effect of surface properties on nanoparticle-cell interactions. Small. **2010**, 6(1), 12-21.

[98]   Zhao B, Sun L, Zhang W, Wang Y, Zhu J, Zhu X, et al. Secretion of intestinal goblet cells: a novel excretion pathway of nanoparticles. Nanomedicine : nanotechnology, biology, and medicine. **2014**, 10(4), 839-49.

[99]   Hull MS, Chaurand P, Rose J, Auffan M, Bottero JY, Jones JC, et al. Filter-feeding bivalves store and biodeposit colloidally stable gold nanoparticles. Environmental science & technology. **2011**, 45(15), 6592-9.

[100] Graf G, Rosenberg R. Bioresuspension and biodeposition: a review. Journal of Marine Systems. **1997**, 11(3-4), 269-78.

[101]   Rowden AA, Jones MB, Morris AW. The role of Callianassa subterranea (Montagu) (THALASSINIDEA) in sediment resuspension in the North Sea. Continental Shelf Research. **1998**, 18(11), 1365-80.

[102]   Krantzberg G. The influence of bioturbation on physical, chemical and biological parameters in aquatic environments: A review. Environmental Pollution Series A, Ecological and Biological. **1985**, 39(2), 99-122.

[103]   Moreau JW, Weber PK, Martin MC, Gilbert B, Hutcheon ID, Banfield JF. Extracellular proteins limit the dispersal of biogenic nanoparticles. Science. **2007**, 316(5831), 1600-3.

[104]   Bone AJ, Colman BP, Gondikas AP, Newton KM, Harrold KH, Cory RM, et al. Biotic and abiotic interactions in aquatic microcosms determine fate and toxicity of Ag nanoparticles: part 2-toxicity and Ag speciation. Environmental science & technology. **2012**, 46(13), 6925-33.

[105]   Ward JE, Kach DJ. Marine aggregates facilitate ingestion of nanoparticles by suspension-feeding bivalves. Marine environmental research. **2009**, 68(3), 137-42.

[106]   Cornelis G, Pang L, Doolette C, Kirby JK, McLaughlin MJ. Transport of silver nanoparticles in saturated columns of natural soils. The Science of the total environment. **2013**, 463-464, 120-30.

[107]   Johnson WP, Li X, Assemi S. Deposition and re-entrainment dynamics of microbes and non-biological colloids during non-perturbed transport in porous media in the presence of an energy barrier to deposition. Advances in Water Resources. **2007**, 30(6-7), 1432-54.

[108]   Sang W, Morales VL, Zhang W, Stoof CR, Gao B, Schatz AL, et al. Quantification of colloid retention and release by straining and energy minima in variably saturated porous media. Environmental science & technology. **2013**, 47(15), 8256-64.

[109]   Chowdhury I, Hong Y, Honda RJ, Walker SL. Mechanisms of TiO2 nanoparticle transport in porous media: role of solution chemistry, nanoparticle concentration, and flowrate. Journal of colloid and interface science. **2011**, 360(2), 548-55.

[110]   Liu J, Legros S, Ma G, Veinot JG, von der Kammer F, Hofmann T. Influence of surface functionalization and particle size on the aggregation kinetics of engineered nanoparticles. Chemosphere. **2012**, 87(8), 918-24.

[111]   Hahn MW, Abadzic D, O'Melia CR. Aquasols: On the Role of Secondary Minima†. Environmental science & technology. **2004**, 38(22), 5915-24.

[112]   Chen G, Liu X, Su C. Transport and retention of TiO2 rutile nanoparticles in saturated porous media under low-ionic-strength conditions: measurements and mechanisms. Langmuir : the ACS journal of surfaces and colloids. **2011**, 27(9), 5393-402.

[113]   Solovitch N, Labille J, Rose J, Chaurand P, Borschneck D, Wiesner MR, et al. Concurrent aggregation and deposition of TiO2 nanoparticles in a sandy porous media. Environmental science & technology. **2010**, 44(13), 4897-902.

[114] Li Z, Sahle-Demessie E, Hassan AA, Sorial GA. Transport and deposition of CeO2 nanoparticles in water-saturated porous media. Water research. **2011**, 45(15), 4409-18.

[115] Ben-Moshe T, Dror I, Berkowitz B. Transport of metal oxide nanoparticles in saturated porous media. Chemosphere. **2010**, 81(3), 387-93.

[116] Rahman T, George J, Shipley HJ. Transport of aluminum oxide nanoparticles in saturated sand: effects of ionic strength, flow rate, and nanoparticle concentration. The Science of the total environment. **2013**, 463-464, 565-71.

[117] Hahn MW, O'Melia CR. Deposition and Reentrainment of Brownian Particles in Porous Media under Unfavorable Chemical Conditions: Some Concepts and Applications. Environmental science & technology. **2004**, 38(1), 210-20.

[118] Shen C, Li B, Huang Y, Jin Y. Kinetics of Coupled Primary- and Secondary-Minimum Deposition of Colloids under Unfavorable Chemical Conditions. Environmental science & technology. **2007**, 41(20), 6976-82.

[119] He F, Zhang M, Qian T, Zhao D. Transport of carboxymethyl cellulose stabilized iron nanoparticles in porous media: column experiments and modeling. Journal of colloid and interface science. **2009**, 334(1), 96-102.

[120] Tufenkji N, Elimelech M. Breakdown of colloid filtration theory: role of the secondary energy minimum and surface charge heterogeneities. Langmuir : the ACS journal of surfaces and colloids. **2005**, 21(3), 841-52.

[121] Seymour MB, Chen G, Su C, Li Y. Transport and retention of colloids in porous media: does shape really matter? Environmental science & technology. **2013**, 47(15), 8391-8.

[122] Cai L, Tong M, Ma H, Kim H. Cotransport of titanium dioxide and fullerene nanoparticles in saturated porous media. Environmental science & technology. **2013**, 47(11), 5703-10.

[123] Van Koetsem F, Geremew TT, Wallaert E, Verbeken K, Van der Meeren P, Du Laing G. Fate of engineered nanomaterials in surface water: Factors affecting interactions of Ag and CeO2 nanoparticles with (re)suspended sediments. Ecological Engineering. **2014**.

[124] Cornelis G, DooletteMadeleine Thomas C, McLaughlin MJ, Kirby JK, Beak DG, Chittleborough D. Retention and Dissolution of Engineered Silver Nanoparticles in Natural Soils. Soil Science Society of America Journal. **2012**, 76(3), 891.

[125] Buffet PE, Amiard-Triquet C, Dybowska A, Risso-de Faverney C, Guibbolini M, Valsami-Jones E, et al. Fate of isotopically labeled zinc oxide nanoparticles in sediment and effects on two endobenthic species, the clam Scrobicularia plana and the ragworm Hediste diversicolor. Ecotoxicology and environmental safety. **2012**, 84, 191-8.

[126] Chen G, Liu X, Su C. Distinct effects of humic acid on transport and retention of TiO2 rutile nanoparticles in saturated sand columns. Environmental science & technology. **2012**, 46(13), 7142-50.

[127] Jiang X, Tong M, Lu R, Kim H. Transport and deposition of ZnO nanoparticles in saturated porous media. Colloids and Surfaces A: Physicochemical and Engineering Aspects. **2012**, 401, 29-37.

[128] Fang J, Shan XQ, Wen B, Lin JM, Owens G. Stability of titania nanoparticles in soil suspensions and transport in saturated homogeneous soil columns. Environmental pollution. **2009**, 157(4), 1101-9.

[129] Rowden AA, Jago CF, Jones SE. Influence of benthic macrofauna on the geotechnical and geophysical properties of surficial sediment, North Sea. Continental Shelf Research. **1998**, 18(11), 1347-63.

[130] Jackson BP, Bugge D, Ranville JF, Chen CY. Bioavailability, toxicity, and bioaccumulation of quantum dot nanoparticles to the amphipod Leptocheirus plumulosus. Environmental science & technology. **2012**, 46(10), 5550-6.

[131] Zhao CM, Wang WX. Biokinetic uptake and efflux of silver nanoparticles in Daphnia magna. Environmental science & technology. **2010**, 44(19), 7699-704.

[132] Li S, Wallis LK, Diamond SA, Ma H, Hoff DJ. Species sensitivity and dependence on exposure conditions impacting the phototoxicity of TiO(2) nanoparticles to benthic organisms. Environmental toxicology and chemistry / SETAC. **2014**, 33(7), 1563-9.

[133] Coutris C, Joner EJ, Oughton DH. Aging and soil organic matter content affect the fate of silver nanoparticles in soil. The Science of the total environment. **2012**, 420, 327-33.

[134] Petosa AR, Brennan SJ, Rajput F, Tufenkji N. Transport of two metal oxide nanoparticles in saturated granular porous media: role of water chemistry and particle coating. Water research. **2012**, 46(4), 1273-85.

[135] El Badawy AM, Hassan AA, Scheckel KG, Suidan MT, Tolaymat TM. Key factors controlling the transport of silver nanoparticles in porous media. Environmental science & technology. **2013**, 47(9), 4039-45.

[136] Kim H-J, Phenrat T, Tilton RD, Lowry GV. Fe0Nanoparticles Remain Mobile in Porous Media after Aging Due to Slow Desorption of Polymeric Surface Modifiers. Environmental science & technology. **2009**, 43(10), 3824-30.

[137] Blinova I, Niskanen J, Kajankari P, Kanarbik L, Kakinen A, Tenhu H, et al. Toxicity of two types of silver nanoparticles to aquatic crustaceans Daphnia magna and Thamnocephalus platyurus. Environmental science and pollution research international. **2013**, 20(5), 3456-63.

[138] Buffet PE, Pan JF, Poirier L, Amiard-Triquet C, Amiard JC, Gaudin P, et al. Biochemical and behavioural responses of the endobenthic bivalve Scrobicularia plana to silver nanoparticles in seawater and microalgal food. Ecotoxicology and environmental safety. **2013**, 89, 117-24.

[139] Cho WS, Cho M, Jeong J, Choi M, Cho HY, Han BS, et al. Acute toxicity and pharmacokinetics of 13 nm-sized PEG-coated gold nanoparticles. Toxicology and applied pharmacology. **2009**, 236(1), 16-24.

[140] Dale AL, Lowry GV, Casman EA. Modeling nanosilver transformations in freshwater sediments. Environmental science & technology. **2013**, 47(22), 12920-8.

[141] Whitley AR, Levard C, Oostveen E, Bertsch PM, Matocha CJ, von der Kammer F, et al. Behavior of Ag nanoparticles in soil: effects of particle surface coating, aging and sewage sludge amendment. Environmental pollution. **2013**, 182, 141-9.

[142] van der Ploeg MJ, Handy RD, Waalewijn-Kool PL, van den Berg JH, Herrera Rivera ZE, Bovenschen J, et al. Effects of silver nanoparticles (NM-300K) on Lumbricus rubellus earthworms and particle characterization in relevant test matrices including soil. Environmental toxicology and chemistry / SETAC. **2014**, 33(4), 743-52.

[143] Kim B, Park CS, Murayama M, Hochella MF. Discovery and characterization of silver sulfide nanoparticles in final sewage sludge products. Environmental science & technology. **2010**, 44(19), 7509-14.

[144] Shaw BJ, Handy RD. Physiological effects of nanoparticles on fish: a comparison of nanometals versus metal ions. Environ Int. **2011**, 37(6), 1083-97.

[145] Matranga V, Corsi I. Toxic effects of engineered nanoparticles in the marine environment: model organisms and molecular approaches. Marine environmental research. **2012**, 76, 32-40.

[146] Hanna SK, Miller RJ, Zhou D, Keller AA, Lenihan HS. Accumulation and toxicity of metal oxide nanoparticles in a soft-sediment estuarine amphipod. Aquatic toxicology. **2013**, 142-143, 441-6.

[147] Yin L, Cheng Y, Espinasse B, Colman BP, Auffan M, Wiesner M, et al. More than the ions: the effects of silver nanoparticles on Lolium multiflorum. Environmental science & technology. **2011**, 45(6), 2360-7.

[148] Lv J, Zhang S, Luo L, Han W, Zhang J, Yang K, et al. Dissolution and microstructural transformation of ZnO nanoparticles under the influence of phosphate. Environmental science & technology. **2012**, 46(13), 7215-21.

[149] Reinsch BC, Forsberg B, Penn RL, Kim CS, Lowry GV. Chemical transformations during aging of zerovalent iron nanoparticles in the presence of common groundwater dissolved constituents. Environmental science & technology. **2010**, 44(9), 3455-61.

[150] Park EJ, Yi J, Kim Y, Choi K, Park K. Silver nanoparticles induce cytotoxicity by a Trojan-horse type mechanism. Toxicology in vitro : an international journal published in association with BIBRA. **2010**, 24(3), 872-8.

[151] Xia T, Kovochich M, Liong M, Madler L, Gilbert B, Shi H, et al. Comparison of the mechanism of toxicity of zinc oxide and cerium oxide nanoparticles based on dissolution and oxidative stress properties. ACS nano. **2008**, 2(10), 2121-34.

[152] Akaighe N, Maccuspie RI, Navarro DA, Aga DS, Banerjee S, Sohn M, et al. Humic acid-induced silver nanoparticle formation under environmentally relevant conditions. Environmental science & technology. **2011**, 45(9), 3895-901.

[153] Liu J, Hurt RH. Ion release kinetics and particle persistence in aqueous nano-silver colloids. Environmental science & technology. **2010**, 44(6), 2169-75.

[154] Jones EH, Su C. Fate and transport of elemental copper (Cu0) nanoparticles through saturated porous media in the presence of organic materials. Water research. **2012**, 46(7), 2445-56.

[155] Deshiikan SR, Eschenazi E, Papadopoulos KD. Transport of colloids through porous beds in the presence of natural organic matter. Colloids and Surfaces A: Physicochemical and Engineering Aspects. **1998**, 145(1-3), 93-100.

[156] Amirbahman A, Olson TM. The Role of Surface Conformations in the Deposition Kinetics of Humic Matter-Coated Colloids in Porous-Media. Colloid Surface A. **1995**, 95(2-3), 249-59.

[157] Hotze EM, Phenrat T, Lowry GV. Nanoparticle Aggregation: Challenges to Understanding Transport and Reactivity in the Environment. Journal of Environment Quality. **2010**, 39(6), 1909.

[158] El Badawy AM, Luxton TP, Silva RG, Scheckel KG, Suidan MT, Tolaymat TM. Impact of environmental conditions (pH, ionic strength, and electrolyte type) on the surface charge and aggregation of silver nanoparticles suspensions. Environmental science & technology. **2010**, 44(4), 1260-6.

[159] Pettibone JM, Cwiertny DM, Scherer M, Grassian VH. Adsorption of organic acids on TiO2 nanoparticles: effects of pH, nanoparticle size, and nanoparticle aggregation. Langmuir : the ACS journal of surfaces and colloids. **2008**, 24(13), 6659-67.

[160] Espinasse B, Hotze EM, Wiesner MR. Transport and Retention of Colloidal Aggregates of C60in Porous Media: Effects of Organic Macromolecules, Ionic Composition, and Preparation Method. Environmental science & technology. **2007**, 41(21), 7396-402.

[161] Foster WJ, Twitchett RJ. Functional diversity of marine ecosystems after the Late Permian mass extinction event. Nature Geoscience. **2014**, 7(3), 233-8.

[162] Solan M, Cardinale BJ, Downing AL, Engelhardt KA, Ruesink JL, Srivastava DS. Extinction and ecosystem function in the marine benthos. Science. **2004**, 306(5699), 1177-80.

[163] Lohrer AM, Thrush SF, Gibbs MM. Bioturbators enhance ecosystem function through complex biogeochemical interactions. Nature. **2004**, 431(7012), 1092-5.

[164] Snelgrove PV. The importance of marine sediment biodiversity in ecosystem processes. Ambio. **1997**, 578-83.

[165] Gyllstrom M, Hansson L-A. Dormancy in freshwater zooplankton: Induction, termination and the importance of benthic-pelagic coupling. Aquatic Sciences. **2004**, 66(3).

[166] Meadows PS, Meadows A, Murray JMH. Biological modifiers of marine benthic seascapes: Their role as ecosystem engineers. Geomorphology. **2012**, 157-158, 31-48.

[167] Meysman FJ, Middelburg JJ, Heip CH. Bioturbation: a fresh look at Darwin's last idea. Trends in ecology & evolution. **2006**, 21(12), 688-95.

[168] Palmer MA, Covich AP, Lake SAM, Biro P, Brooks JJ, Cole J, et al. Linkages between Aquatic Sediment Biota and Life Above Sediments as

Potential Drivers of Biodiversity and Ecological Processes. BioScience. **2000**, 50(12), 1062.

[169] Baker TJ, Tyler CR, Galloway TS. Impacts of metal and metal oxide nanoparticles on marine organisms. Environmental pollution. **2014**, 186, 257-71.

[170] Ferry JL, Craig P, Hexel C, Sisco P, Frey R, Pennington PL, et al. Transfer of gold nanoparticles from the water column to the estuarine food web. Nature nanotechnology. **2009**, 4(7), 441-4.

[171] Lerner RN, Lu Q, Zeng H, Liu Y. The effects of biofilm on the transport of stabilized zerovalent iron nanoparticles in saturated porous media. Water research. **2012**, 46(4), 975-85.

[172] Gerbersdorf SU, Wieprecht S. Biostabilization of cohesive sediments: revisiting the role of abiotic conditions, physiology and diversity of microbes, polymeric secretion, and biofilm architecture. Geobiology. **2014**.

[173] Gambardella C, Gallus L, Gatti AM, Faimali M, Carbone S, Antisari LV, et al. Toxicity and transfer of metal oxide nanoparticles from microalgae to sea urchin larvae. Chemistry and Ecology. **2014**, 30(4), 308-16.

[174] Kulacki KJ, Cardinale BJ, Keller AA, Bier R, Dickson H. How do stream organisms respond to, and influence, the concentration of titanium dioxide nanoparticles? A mesocosm study with algae and herbivores. Environmental toxicology and chemistry / SETAC. **2012**, 31(10), 2414-22.

Appendix 2
Awards, conferences and impact

Listed are awards, conference details and impact resulting from the work conducted as part of this PhD. This is followed by short abstracts for a selection of the presentations given on this topic throughout the PhD.

Research grants:
· **FENAC grant: £15,000 (2015).** Successful in attaining a competitive grant (graded 8 by the FENAC steering committee) for a full study at the FENAC facility as the researcher for the proposal for "Imaging the evolution of ceria nanoparticles in sediment pore waters over time".
· **FENAC grant**: **£16,000 (2014).** Successful at attaining a competitive grant (graded 8 by the FENAC steering committee) as the researcher for a pilot study "Investigating the aggregate size distribution of Ceria nanoparticles within sediment and tissue samples".

Travel grants:
· **SETAC Registration Grant: (May 2017).** Registration fee waiver.
· **Syngenta Student Travel Grant: (May 2017).** Coveringtravel costs for attending SETAC Europe AM17.

Awards:
· **SETAC Europe's ECETOC Young Scientist Award (SETAC Europe, Brussels: May 2017).** Awarded in recognition of the best platform presentation at SETAC Europe's 27[th]Anual Meeting, Brussels, Belgium.
· **Oral presentation award (ExeBioCon, Exeter: June 2016):** awarded best platform presentation during the ExeBioCon 2016.

Conferences & seminars:
· **SETAC Europe (Brussels, UK: May 2017).** Platform presentation "Routes of uptake and bioaccumulation of silver nanoparticles depend on their fate in sediments".
· **Leadership and Diversity in Organisations (Kent, UK: July 2016):** Platform presentation entitled"Empowering early career researchers through a student led press team".
· **ExeBioCon Postgraduate Conference (Exeter, UK: June 2016):** "The importance of characterisation when examining the murky world of nanoparticles in sediments" (platform presentation- awarded best presentation).
· **SETAC Europe (Nantes, France: May 2016).** Platform presentation entitled **"**Bioavailability of metal nanoparticles in a sediment dwelling organism: a study of transdermal and oral routes of uptake".
· **FENAC 1st FENAC Academic Workshop: Biological and Environmental Impacts of Nanomaterials (Birmingham, UK: March 2016).** Platform presentation "Investigating the bioaccumulation and route to uptake of metal nanoparticles from sediments".
· **ExeBioCon Postgraduate Conference (Exeter, UK: June 2015):** "Understanding transformations of nanoparticles in aquatic environments" (oral presentation).
· **FENAC workshop presentation (Birmingham, UK: December 2015).** Platform presentation "Combining fractionation and imaging techniques with biological exposures to investigate the route of nanoparticle uptake in sediment dwelling species".

SETAC Europe (Nantes, France: May 2016).

Bioavailability of metal nanoparticles in a sediment dwelling organism: a study of transdermal and oral routes of uptake

R. K. Cross[1], C. R. Tyler[1], T. S. Galloway[1]

Metal engineered nanomaterials (ENMs) are an emerging pollutant considered to be of risk to aquatic environments due to their inherent reactivity and high global production volumes. The behaviour of metal ENMs in aquatic sediment systems is dominated by transformations including aggregation, complexation with organic matter and in some cases dissolution of metal ions. Investigating ENM behaviour in sediments requires novel combinations of separation and microscopy techniques. This will allow us to correctly interpret the results from studies into the bioaccumulation of ENMs in benthic species.

Using a combination of centrifugal ultrafiltration and Asymmetric flow Field Flow Fractionation (AF4) the size distribution and dissolution of both ceria (CeO_2NPs) and silver (AgNPs) nanoparticles was followed in a model sediment system over 6 days. The aim was to compare uptake through transdermal or oral routes.

Two commercially relevant Ag NPs were chosen as test materials: one stabilised sterically with PEG (mono mPEGphosphonic acid ester), the other with an electrostatic stabiliser, citrate. The NPs had a primary particle size of 4-10 nm. A 5 day bioaccumulation exposure was conducted using the sediment dwelling oligochaete worm Lumbriculus variegatus. Organisms were either actively feeding (uptake through transdermal and oral ingestion) or non-feeding, achieved by utilising the species' natural mode of reproduction by clonal fragmentation, to yield non-feeding clones. Centrifugal ultrafiltration examined partitioning of CeO_2 and AgNPs between the solid and liquid phases of the sediment and NP dissolution. AF4 was used to investigate the size distribution and preferential heteroaggregation between the CeO_2 and AgNPs and other natural colloids present in the sediment pore waters.

Results demonstrate that for CeO_2 NPs, dissolution does not occur and there was no uptake of nanoparticles across transdermal pathways. Coating type (electrostatic or steric) also made no difference to bioavailability of these particles through ingestion. All three NP treatments were significantly more bioavailable than either the geogenic Ce present naturally in the sediments or micron sized CeO_2. Results for Ag NPs are ongoing and will be reported in full during the presentation. Results will be discussed in the context of the transformations that the nanoparticles have undergone and their interactions with other natural colloidal materials in the sediments.

ExeBioCon Postgraduate Conference (Exeter, UK: June 2016):

The importance of characterisation when examining the murky world of nanoparticles in sediments

R. K. Cross[1], C. R. Tyler[1], T. S. Galloway[1]

[1]Biosciences, College of Life and Environmental Sciences, University of Exeter, Geoffrey Pope, Stocker Road, Exeter, Devon, EX4 4QD, UK

Engineered nanomaterials (ENMs) have myriad uses and their ubiquity in common but often unexpected household products is growing (think nano silver lined socks). As their use increases, the potential for release into the wider environment also grows and the scientific community is still uncertain whether these particles could present a significant risk to ecosystems. Properties of nanoparticles such as size and shape have been shown to determine their potential for toxicity. Unfortunately for researchers, as ENMs enter aquatic environmentsthese properties change as ENMs undergo transformations. These transformations in turn depend both upon the particles properties and the physicochemical characteristics of the surrounding media. This makes predicting their potential risks tricky as not only do we need to know what the original particles looked like, but also how they change as they move through the environment, and what these transformations mean for their availability or toxicity to organisms.

Sediments present a potential sink for accumulation of ENMs released into the aquatic environment, but little is known about their fate once in these sediments. Our work is about linking these two aspects of nanoparticle research: the fate of these particles in the environment, and their potential for accumulation or toxic effects in aquatic organisms. How do the particles behave in sediments? What does this mean for the risk they pose to organisms? Can imaginative combinations of cutting edge tools finally shine a light onto the behaviour of these particles in this important ecosystem?

SETAC Europe (Brussels, Belgium: May 2017).

Routes of uptake and bioaccumulation of cerium oxide and silver nanoparticles depend on their fate in sediments

R. K. Cross[1], C. R. Tyler[1], T. S. Galloway[1]

[1]Biosciences, College of Life and Environmental Sciences, University of Exeter, Geoffrey Pope, Stocker Road, Exeter, Devon, EX4 4QD, UK

Keywords: nanotoxicity, nanoparticle fate, sediment ecotoxicology, bioaccumulation.

Engineered nanoparticles (NPs) undergo myriad transformations upon entering the aquatic environment, depending not only upon the composition of the particles but also the physicochemical properties of the surrounding media. Sediments are predicted to be a major sink of NPs released into the aquatic environment due to processes of aggregation and sedimentation occurring over relatively short timescales of a matter of hours to days in freshwaters. What is less understood is if NPs entering sediments will have the same capacity for toxicity as particles in suspension in the overlying water? Will transformations in sediments reduce or enhance nanoparticle bioavailability? Will these transformations be the same for NPs of different core or surface properties?

This work aims to address some of these questions. Specifically we hypothesise that persistence of dissolution products or a colloidal fraction of NPs in sediment pore waters will allow for transdermal uptake of NPs into sediment ingesting species. We generated two viable phenotypes of the sediment dwelling aquatic worm, *Lumbriculus variegatus* through fragmentation to produce feeding and non-feeding worms. These were exposed to cerium oxide (CeO$_2$ NPs) or silver nanoparticles (Ag NPs) stabilised either electrostatically with citrate or sterically with PEG (mono mPEGphosphonic acid ester). A combination of centrifugation and ultrafiltration techniques were employed alongside the biological exposures to examine the fate of nanoparticles in the sediment pore waters, quantifying the colloidal fraction containing CeO$_2$ or Ag NPs (<200 nm in size) and low molecular weight dissolution products (<1 kDa in size).

Results indicate that NPs which associate with the solid fraction of the sediment and do not dissolve within the sediments (CeO$_2$ NPs) were only available through ingestion. These particles were also less bioavailable than Ag NPs and neither their fate nor accumulation differed between the two forms of stabilisation. PEG coated Ag NPs experienced significantly greater accumulation of Ag through transdermal uptake than either Citrate-Ag or silver nitrate and not all of this transdermal uptake of Ag could be accounted for by dissolution. The cause for this is the focus of ongoing experiments to be discussed in more detail during the presentation, alongside ongoing investigations into Ag NP transformations during the gut transition in these aquatic worms and their kinetic uptake from sediments over time.

Freshwater sediments as an environmental reactor: defining biologically relevant fate parameters to provide context for nanomaterial bioaccumulation

R. K. Cross[1], C. R. Tyler[1], T. S. Galloway[1]

[1]Biosciences, College of Life and Environmental Sciences, University of Exeter, Geoffrey Pope, Stocker Road, Exeter, Devon, EX4 4QD, UK

Keywords: nanotoxicity, nanoparticle fate, sediment ecotoxicology, bioaccumulation.

Track: 3. Environmental chemistry and exposure assessment: analysis, monitoring, fate and modelling

Session: 3.24. The environment as a reactor determining fate and toxicity of nanomaterials

As the field of nanotoxicology matures there is a call for the research focus to progress from hazard identification to more ecologically relevant assessments of the risk that engineered nanomaterials (ENMs) pose as they undergo a range of transformations in the environment. This will require test designs prioritising environments most at risk of contamination, and which not only measure ecologically relevant endpoints, but also characterise the fate, transformations and behaviours of particles within the test system, providing the context for differences observed between treatments. Freshwater sediments present an ecosystem in need of further research, as these are predicted to be major sinks of ENMs entering the aquatic environment though waste water treatment and terrestrial pathways during material production, use and disposal.

Whist freshwater sediments have been identified as an ecological compartment at risk of contamination, very little is known about the fate of ENMs entering these sediments. We present a simple separation method to isolate the colloidal (<200 nm) and dissolved (<1kDa) fractions of the sediment pore water, which can be run alongside biological exposures. This provides the context for how these biologically accessible fractions of ENMs in the sediments may relate to intrinsic particle properties such as size, core composition and coatings. Using cerium oxide (CeO_2 NP) and silver nanoparticles (AgNP) we investigate the routes of bioaccumulation of these materials in the freshwater sediment dwelling worm *Lumbriculus variegatus*. By following the fate of these particles in the solid bound, colloidal and dissolved fractions of the sediment, we provide context to explain differences in both the route and extent of uptake of these materials by the worm.

This poster presents the successful application of this method to investigate the implications different stabilisation mechanisms (electrostatically stabilised citrate and sterically stabilised PEG coatings) have upon the route of uptake of CeO_2 and AgNPs and transformations they undergo during sediment exposures. Accumulation of CeO_2 through dietary uptake is linked to their strong associations to the solid fraction of the sediment and lack of dissolution (<1% of spiked cerium was extractable with water). Transdermal uptake of AgNP was attributed to dissolved silver in the pore waters and uptake of soluble silver, potentially through localised dissolution of particles at the worms' surface.

"He rocked in the swells, floating like the first germ of life adrift on the earth's cooling seas, formless macule of plasm trapped in a vapour drop and all creation yet to come"

Cormac McCarthy, Sutree